Role of MAF in bone metastasis

Anna Bellmunt i Tarragó

Barcelona, 2017

Role of MAF in bone metastasis

Memòria presentada per *Anna Bellmunt i Tarragó*
per optar al grau de doctora per la Universitat de Barcelona

Doctoranda
Anna Bellmunt i Tarragó

Director
Dr. Roger Gomis i Cabré

Tutor
Dr. Joan Josep Guinovart i Cirera

UNIVERSITAT DE BARCELONA
Facultat de Biologia
Programa de doctorat
en Biomedicina

UNIVERSITAT DE BARCELONA

INSTITUT DE RECERCA
BIOMÈDICA
DE BARCELONA

INSTITUTE FOR RESEARCH IN BIOMEDICINE
IRB BARCELONA

A la Sally i a la Masip,

"A person who never made a mistake never tried anything new"

Albert Einstein

Table of contents

Summary

The identification of genes that mediate metastasis is pivotal to better understand the mechanism, to develop novel drugs and to stratify patients with highest risk and consecutively administrate them preventive treatments. Despite significant advances on knowledge, diagnosis and treatment of cancer, metastasis remains the major cause of cancer-associated deaths.

Bone is one of the most common organs affected by metastatic lesions for its permeability and favorable conditions for cellular growth. Constant remodeling in bone homeostasis implies an incessant degradation of the bone that release high concentrations of growth factors into the microenvironment. Thereby, growth factors benefit both, formation of new bone and/or tumor cell growth. Although the importance of bone metastatic lesions in cancer patients and the advances on the knowledge of this process, few treatments are currently administrated to patients that suffer this disease, specifically Denosumab and Zoledronic acid (ZOL). Importantly, these treatments can improve the symptoms of bone lesions but cannot cure or reverse metastasis. This fact reflects the need to detect and tackle new targetable elements to reduce bone metastatic lesions.

Many molecular mechanisms have been described in bone metastasis, but only one predictor gene has been identified, *MAF*. MAF is a transcription factor that has been previously involved in carcinogenesis, specially in multiple myeloma (MM) and human angioimmunoblastic T-cell lymphomas (AITLs). Recently, MAF contribution has been associated for the first time with breast cancer bone metastasis.

In this thesis, we determined the role of MAF in several contexts. As a first approach we demonstrated that *MAF* is also a predictive marker of bone metastasis in prostate cancer (PC) patients. However, regarding androgen-independent PC cell lines, an overexpression of *MAF* was not enough to drive colonization of the mouse bone. Secondly, we report the beneficial effect of *MAF* downregulation on preventing skeletal metastasis in BoM2, a highly bone metastatic MCF7-derived cell line. MAF impinged bone colonization in a higher degree that other treatments against bone metastasis, such as PTHrP antagonist or recombinant OPG. This fact identifies MAF as a new potential target to focus on the generation of new drugs. Finally, MAF showed a tendency to redirect metastases to other organs than bone in the presence of ZOL treatment *in vivo*. Thus, we validated the

association between MAF overexpression and an increase on extraskeletal metastases after ZOL preventive treatment in non-postmenopausal BC patients.

Moreover, a mouse model was generated to better understand the biology of MAF-derived bone metastasis within complete stromal interactions. We designed a transgenic mouse model to express MAF in the mammary gland in an inducible manner. To this end, we generated two constructs; the first contains *rtTA*, *renilla* and *katushka* under MMTV promoter, and the second contains *MAF*, *luciferase* and *tGFP* under Tet-On promoter. We demonstrated the incorporation of several copy numbers of both transgenes in two independent colonies and we detected transgene expression under doxycycline activation by means of luminescent signal. Even though both colonies incorporated several copy number of the transgene, their expression was soft and some relevant leakiness was observed in the non-treated MAF mice. No differences were observed in terms of mammary gland development between transgene-expressing MAF mice and wild-type mice, as well as no tumor initiation was detected in any group. Notably, MAF Tg mouse was crossed with MMTV-PyMT to generate double Tg mice (PyMT-MAF). PyMT-MAF tumor growth presented no significant differences compared to PyMT in terms of time to tumor formation and growth rate. Importantly, no bone metastases were observed at 3-month-old mice of any group. Thus, the generation of this animal model provided new insights to generate a novel bone metastatic mouse model.

Resum

La identificació de gens implicats en el procés de la metàstasis és bàsica per tal d'entendre el mecanisme d'aquest procés, per reconèixer els pacients amb més risc de patir-lo i tractar-los selectivament i finalment pel desenvolupament de nous fàrmacs. Recentment, s'ha identificat el gen MAF com a predictor d'un alt risc de patir metàstasis òssia en pacients de càncer de mama.

En aquesta tesi hem determinat el paper de MAF en diferents contexts. Per una banda, hem demostrat que MAF és un marcador predictiu de les metàstasis òssies també en pacients amb càncer de pròstata. Tot i així, una sobreexpressió de MAF en cèl·lules de càncer de pròstata androgen-independents no va ser suficient per conduir la colonització a l'òs. Per altra banda, hem demostrat que reduir els nivells de MAF en les cèl·lules BoM2, derivades de les cèl·lules de càncer de mama MCF7, redueix la tendència d'aquestes cèl·lules a metastatitzar a l'òs. Cal destacar que aquest efecte és superior al d'altres tractaments com poden ser OPG recombinant o l'antagonista de PTHrP, indicant MAF com a element potencial per a la generació de nous fàrmacs. Finalment, MAF afecta el patró de metàstasis de les cèl·lules ER- de càncer de mama després del tractament preventiu amb àcid Zoledronic, tal com s'observa en pacients.

Per abordar el paper de MAF en el càncer de mama tenint en compte les interaccions amb l'estroma i el sistema immunitari, es va dissenyar un model animal transgènic que sobreexpressava MAF en la glàndula mamària de forma induïble. Es va demostrar la incorporació de vàries còpies del transgèn en el ADN genòmic i també es va detectar, per senyal bioluminiscent, la inducció per doxiciclina de l'expressió del transgèn. Cal destacar que l'expressió era feble i en molts casos inespecífica i independent al tractament amb doxiciclina. El desenvolupament mamari en aquest model no demostrava cap alteració com tampoc es va detectar cap indici de formació de tumor. Aquest model es va creuar amb MMTV-PyMT, i els tumors de les femelles doble transgèniques (PyMT-MAF) no van presentar cap diferència en el temps necessari per a la formació de tumors ni en la velocitat de creixement comparat amb PyMT. De manera destacable, no es van observar metàstasis òssies en el moment del sacrifici. D'aquesta manera, la generació del ratolí MAF transgènic ens va donar noves perspectives per enfocar la generació d'un nou model animal que generi metàstasis òssies.

List of abbreviations

2H2OP	Two-hit by gDNA and two oligos with a targeting plasmid
ADH	Atypical ductal hyperplasia
AI	Aromatase inhibitors
AITL	Angioimmunoblastic T-cell lymphomas
ALH	Lobular hyperplasia
ALPL	Bone alkaline phoshpatase
AMACR	a-methylacyl-CoA racemase
ANGPTL4	Angiopoietin-like 4
AR	Androgen receptor
BBB	Blood-brain barrier
BC	Breast cancer
BLI	Bioluminiscent imaging
BMP	Bone morphogenetic proteins
BMU	Basic multicellular unit
BoM2	Bone metastatic MCF7 derived cell line
bp	Baise pairs
BP	Bisphosphonates
bZIP	Basic leucine zipper
CAB	Combined androgen blockade
cAMP	Cyclic adenosine monophosphate
Cas9	CRISPR associated protein-9 nuclease
CNG	Copy number gain
CRE	cAMP-responsive element
CRISPR	Clustered Regularly Interspaced Short Palindromic Repeats
CSF-1	Colony-stimulating factor 1
CT	Computerized tomography
CTC	Circulating tumor cells
CXCL12	Stromal cell-derived factor 1
CXCR4	C-X-C chemokine receptor type 4
DBM	Dormant bone metastasis cell line
DCIS	Ductal carcinoma in situ
DHT	Dihydrotestosterone
DIG	Digoxigenin
Dlx5	Distal-less homeobox 5
Dox	Doxycycline
DSB	Double strand break
dsDNA	Double stranded DNA
DTC	Disseminated tumor cells
EGF	Epidermal growth factor
EGFR	Epidermal growth factor
EHR	Extended homology region
EMT	Epithelial-to-mesenchymal transition
EpCAM	Epithelial cell adhesion molecule
ER	Estrogen receptor
ERE	Estogen response elements
ET-1	Endothelin-1

ET_A	Endothelin A receptor
F0	Founder mouse
F(n)	(n)th generation of mice
FACS	Fluorescence-activated cell sorting
FGF	Fibroblast growth factor
FISH	Fluorescence in situ hybridization
FOXA1	Hepatocyte nuclear factor 3 alpha
FSH	Follicle-stimulating hormone
GATA3	GATA binding protein 3
gDNA	genomic DNA
GEM	Genetically engineered mouse
GFP	Green fluorescent protein
GH	Growth hormone
GnRH	Gonadotropin-releasing hormone
gRNA	guide RNA
HDR	Homology-directed repair
HER2	Epithermal growth factor receptor 2
HIF1a	Hypoxia-induced growth factor 1 alpha
HSC	Hematopoietic stem cells
H&E	Hematoxylin and eosin
IBC	Invasive Breast cancer
IC	Intracardiac
IDFS	Invasive disease-free survival
IF	Immunofluorescence
IGF-1	Insulin-like growth factor 1
IgH	Immunoglobulin heavy chain
IHC	Immunohistochemistry
IL	Interleukin
IP	Intraperitoneal
IRES	Internal ribosome entry site
IT	Intratibial
K	Cytokeratin
LCIS	Lobular carcinoma in situ
LH	Luteinizing hormone
LOH	Loss of heterozygosity
LOX	Lysyl oxidase
MAF	v-maf avian musculoaponeurotic fibrosarcoma oncogene homolog
MAF L	MAF short isoform
MAF S	MAF short isoform
MARE	Maf-recognition element
MaSC	Mammary stem cell
M-CSF	Macrophage colony stimulating factor
MET	Mesenchymal to epithelial transition
MM	Multiple myeloma
MMP	Matrix metalloproteinase
MMTV	Mouse mammary tumor virus
MRI	Magnetic Resonance Imaging
mRNA	messenger RNA
MSC	Mesenchymal Stem cell
mTOR	Mammalian target of rapamycin

NHEJ	Non-homologous end joining
NTX	Aminoterminal propeptide of type-1 collagen
ODX	Oncotype DX™
OE	Overexpression
O/N	Over-night
OPG	Osteoprotegerin
Opn	Osteopontin
Osx	Osterix
PBS	Phosphate buffered saline
PC	Prostate cancer
PDGF	Platelet derived growth factor
PPi	Pyrophosphate
PR	Progesterone receptor
PSA	Prostate-specific antigen
PTHrP	Parathyroid hormone-related protein
PyMT	Polyoma middle T
qRT-PCR	Quantitative real-time polymerase chain reaction
R26	Rosa26
RANK	Receptor activator of nuclear factor-κB
RANKL	Receptor activator of nuclear factor-κB ligand
RT	Room temperature
rtTA	Reverse Tet repressor controlled transactivator
RUNX2	Runt-related transcription factor 2
SC	Subcutaneous
ssDNA	Single stranded DNA
ssODN	Single-stranded oligodeoxynucleotides
SV40	Simian virus 40
TAM	Tumor-associated macrophages
TBS	Tris-buffered saline
TBS-T	TBS-Tween
TDLU	Terminal duct lobular units
TEB	Terminal end-bud
tetO	Tetracycline operator sequences
Tg	Transgenic
TGF-ß	Transforming growth-factor ß
TN	Triple negative
TNF	Tumor necrosis factor
TNM	Tumor-node-metastasis
TP53	Tumor protein 53
TPA	12-O-tetradecanoyl phorbol 13-acetate
TRE	TPA-responsive element
UGS	Urogenital sinus
UL	Unfolded lobules
uPA	Urokinase-type plasminogen activator
VCAM-1	Vascular cell adhesion molecule-1
VEGF	Vascular endothelial growth factors
VP16	Herpes simplex virus protein 16
WT	Wild-type
ZOL	Zoledronic acid

- I n t r o d u c t i o n -

1. Metastasis, a disease to be tackled

Despite significant advances in diagnosis, surgery, and treatments of primary tumors, metastatic disease is the major cause of cancer-associated deaths. Metastasis is defined as the capability of cancer cells to spread from the primary tumor to distant organs. To accomplish this, cancer cells must overcome various hurdles and acquire multiple abilities during colonization, starting by invading the primary site, surviving in the blood circulation, and finally initiating a secondary tumor in a hostile environment. Simultaneously, cancer cells have to survive systemic conventional therapies, such as chemotherapy, hormonal therapy, and radiation, used to eradicate disseminated diseases. Although it is a complex and highly inefficient process, metastasis remains the invincible hallmark of cancer. Deciphering the rewiring of genetic, molecular, and cellular mechanisms involved in each step of this process is a huge challenge yet an essential requirement if new therapies to cure or prevent metastases are to be developed. Importantly, in metastasis studies, tumor cell properties, as well as interactions with the stroma and the immune system, are factors that should be considered, as they play a key role in the metastatic process.

1.2 The complex invasion-metastasis cascade

In order to succeed, metastatic cells need to overcome a succession of stochastic events to finally disseminate to a distant organ. This process is called the "metastatic cascade" and involves several steps: local invasion, intravasation, dissemination, survival in circulation, arrest at a distant site, extravasation, and colonization (Figure 1) (Massagué and Obenauf, 2016; Valastyan and Weinberg, 2011).

The first step of the metastatic cascade involves **local invasion** of cancer cells from the primary tumor boundaries into the surrounding stroma. To support this movement, cancer cells secrete matrix metalloproteinases (MMPs) that disrupt the basement membrane and remodel the extracellular matrix to pave the way through the peripheral tissue to lymphatic and blood vessels (Kessenbrock et al., 2010). Furthermore, secretion of IL-4 by cancer cells induces cathepsin K activity in tumor-associated macrophages (TAMs), which in turn promotes cancer cell invasiveness (Gocheva et al., 2010). Notoriously, tumor-associated stroma plays a significant role in the metastatic process.

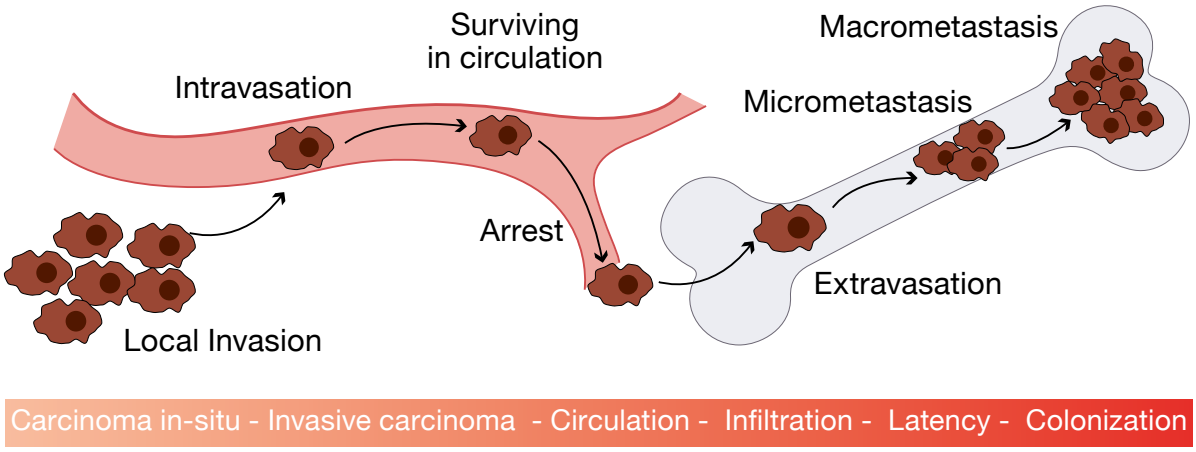

Figure 1. The metastatic process. In order to colonize a distant organ, cancer cells must acquire specific cellular features, including local invasion, intravasation, circulation, extravasation, and colonization, to overcome each barrier encountered in the metastatic process. Modified from Massagué and Obenauf, (2016).

To facilitate access into circulation, cancer cells stimulate the formation of tumor-associated blood vessels in a process termed **angiogenesis**, which is crucial for supporting metastasis progression. Importantly, tumor cells can also secrete factors that induce vascular permeability and intravasation. Mediators of the vascular remodeling program are downstream effectors of vascular endothelial growth factors (VEGFs), such as epidermal growth factor receptor (EGFR), the cyclooxygenase COX2, and matrix-remodeling metalloproteinases MMP1 and MMP2 (Gupta et al., 2007).

Subsequently, metastatic cells are released from the primary tumor and **intravasate** into the lumina of blood and/or lymphatic vessels. This invasion can occur via two mechanisms, namely, single-cell dissemination and collective migration (Friedl et al., 2012). Specifically, *single-cell dissemination* is achieved when single cells dissociate from cohesive lesions through the epithelial-to-mesenchymal transition (EMT), a transient and reversible process in which cancer cells lose their epithelial features, such as cell polarity and adhesion, and gain mesenchymal properties, such as migration, invasiveness, and stemness (Mani et al., 2008; Thiery, 2003). Single-cell dissemination is orchestrated by a set of cell-signaling proteins, including the cytokine TGF-ß (transforming growth factor beta), that are released by stromal cells in tumor margins and blood vessels. TGF-ß signaling is transiently active in a small population of cancer cells, thereby allowing single cell motility (Giampieri et al., 2009) by means of activating E-cadherin repressors and EMT inducers (Seoane and Gomis, 2017). Cell invasion is supported by perivascular

macrophages of the mammary tumor and involves epidermal growth factor (EGF) and colony-stimulating factor (CSF)-1 (Wyckoff et al., 2007). Of note, the Twist and Snail transcription factors induce EMT in epithelial cells (Cano et al., 2000; Kang and Massagué, 2004; Lamouille et al., 2014).

When the invasive unit is a group of heterogeneous cells rather than a single cell, the invasive process is called *collective cell migration*. In this context, cooperation and collective behavior of cells promotes their malignant function. Bulk tumor cells express luminal markers, such as E-cadherin and plakoglobin, which favor cells to remain cohesive (Aceto et al., 2014). In contrast, invasive leader cells develop basal epithelial markers (K14, P-cadherin and K5) through partial or transient EMT. These acquired features pave the way for multicellular strands to migrate into lymph vessels. Of note, leader cells also retained markers of the luminal epithelium, such as K8, K18, and E-cadherin, which contribute to sustaining cohesion between cells (Cheung et al., 2013; Friedl and Gilmour, 2009) and give rise to a "partial EMT" state (Aceto et al., 2014; Grosse-Wilde et al., 2015).

Once tumor single cells or tumor clusters enter the circulation, they must **withstand** the mechanical forces of the bloodstream and the immunologic system. Circulating tumor cells (CTCs) can associate with blood platelets (Labelle et al., 2011), a process that enhances their mesenchymal features and protects them against forceful pressures and clearance by natural killer cells (Gay and Felding-Habermann, 2011; Gupta and Massagué, 2004; Malladi et al., 2016; Palumbo et al., 2005). It is believed that CTCs remain in circulation for brief periods. This circumstance, together with the expression of some oncogenes such as TrkB, allow CTCs to evade death by anoikis (detachment-triggered cell death) (Douma et al., 2004).

CTC **arrest**, in part, is due to the cells being mechanically trapped in capillary beds that have an insufficient diameter to allow them to flow. Thus, the site of attachment is determined mainly by patterns of blood circulation. However, the unusual plasticity of CTCs allows them to bypass these filters and to migrate to distant organs. Platelets help CTC adhesion to the endothelium, thereby supporting extravasation to secondary sites (Gay and Felding-Habermann, 2011; Massagué and Obenauf, 2016).

Tumor cells **extravasate** the bloodstream through vascular walls and enter the parenchyma of distant tissues. Various mechanisms are involved in this process that involve those also active in intravasation (expressing for instance MMP, TGF-ß, and VEGF). However, since each organ presents a particular parenchyma, metastatic cells also need tissue-specific mediators of extravasation. For example, bone and liver contain a fenestrated vasculature with gaps between individual cells, called sinusoids, which facilitate CTC entry and contribute to the high incidence of metastasis in these tissues (Aird, 2007). In contrast, lungs present a physical basement barrier that has to be disrupted to enable tumor cell implantation at the secondary site (Nguyen et al., 2009). In these cases, cancer cells contribute to lung permeability by secreting factors, such as angiopoietin-like-4 (ANGPTL4), which disrupts vascular endothelial cell-cell junctions (Padua et al., 2008), and the cytokine parathyroid hormone-related protein (PTHrP or PTHLH), which triggers caspase-independent death in endothelial cells of the lung microvasculature (Urosevic et al., 2014). *RARRES3* downregulation facilitates breast cancer cell adhesion to the lung parenchyma and maintains cells in an undifferentiated state (Morales et al., 2014). Of note, the brain is the most difficult organ to access because it is surrounded by the blood-brain barrier (BBB). Comprising tight junctions, endothelial cells, astrocytes, and pericytes, the BBB protects neural tissue from fluctuations in blood composition (Aird, 2007; Ballabh et al., 2004; Bos et al., 2009). It also contains brain stromal cells that secrete plasmin, which promotes cancer cell apoptosis. However, specific expression of serpins by CTCs shields them against this process (Valiente et al., 2014).

The microenvironment at the metastatic site differs from that at the primary tumor and compromises the survival of disseminated tumor cells (DTCs). These cells must survive an unfavorable environment in order to form **micrometastasis** and thus further activate their tumor-initiating capacity, leading them to form macrometastatic lesions, which are clinically detectable. The release of systemic factors from the primary tumor can predispose to changes in the stroma of destination organs, creating a pre-metastatic niche—a more favorable and permissible microenvironment for DTC survival. This process involves several factors (Psaila and Lyden, 2009), including for example lysyl oxidase (LOX), a potent mediator of bone pre-metastatic niche formation (Erler et al., 2009). Moreover, recent studies show that tumor-derived exosomes can prime the bone to allow it to support metastatic growth (Peinado et al., 2012). The pre-metastatic niche predisposes DTCs to seeding or extravasation at these sites, generating a tissue tropism of metastatic lesions.

The intrinsic compatibilities of the metastatic cell are also crucial to achieve **macrometastasis**. At the pre-metastatic niches, DTCs return to their epithelial phenotype in a process called the mesenchymal-to-epithelial transition (MET). Whereas some CTCs have advantageous self-renewal and tumor initiation properties and expand rapidly, DTCs are arrested in many tumor types and remain dormant for months or even decades (Sosa et al., 2014). A dormant state is achieved by a balance between proliferation and quiescence, or self-renewal and differentiation (Gomis and Gawrzak, 2017). At some point, interactions with stromal cells activate their tumor-initiating capacity to form macrometastasis, although little is known about the mechanism underlying dormancy (Psaila and Lyden, 2009).

As has been described, metastasis is a highly complex and inefficient process. Only a small percentage of cells released from the primary tumor into the circulation successfully colonize a distant organ (Chambers et al., 2002; Fidler, 2003; Luzzi et al., 1998; Wardley et al., 2005). Cancer cells that reach a secondary organ have to acquire a selection of traits, such as cellular motility, survival, evasion of the immune system, cellular adhesion, and tumor-initiating capacity -usually by genomic instability (Hanahan and Weinberg, 2011)- that enable them to survive in each step (Gupta and Massagué, 2006). Not all cancer cells are able to colonize and grow in any distant organ. In this regard, cell types differ in their propensity to colonize secondary sites.

1.3 Different types of cancer have distinct metastatic patterns

The factors that contribute to the organ tropism of metastasis have been widely discussed in the cancer field. One of the most enduring assumptions was the theory proposed by James Ewing, which proposed circulatory routes as the factor that determines the organ-specific pattern of cancer cell dissemination (Ewing, 1922). However, this theory does not explain clinical and experimental evidence that the anatomically defined patterns of vascular or lymphatic circulation do not correlate with distant metastatic spread. Organs with the highest vascular supply, such as heart, muscle, and kidney, do not correspond to those with highest susceptibility to metastasis. In contrast, organs with less irrigation, such as bone and the adrenal gland, are frequent sites of metastasis for specific types of cancer. Other proposals emerged such the "seed and soil" hypothesis by Stephen Paget (Paget, 1889), who postulated that tumor cells (the "seeds") colonize a distant organ (the

"soil") only when the organ offers favorable conditions in which they can grow (Fidler, 2003). Pre-metastatic niche formation is recent evidence that supports this theory. It is currently believed that lymph and blood vessel direction influence the distribution of cancer cells, while predisposed tissues favor the outgrowth of macrometastases. This postulation certifies that the two theories are not mutually exclusive. In this manner, primary tumor features, genetic alterations developed by tumor cells, blood, and lymphatic circulation, and the microenvironment in the distant organ are factors that together define the pattern of metastasis in each type of cancer.

Table 1: Common sites of metastatic relapse for solid tumors. Typical organs of metastatic incidence are shown for the most common cancer types, excluding lymph nodes. Modified from the National Cancer Institute web (https://www.cancer.gov/types/metastatic-cancer). Modified from Nguyen et al., (2009).

	Main sites of metastasis
Bladder	Bone, liver, lung
Breast	Bone, brain, liver, lung
Colorectal	Liver, lung
Kidney	Adrenal gland, bone, brain, liver, lung
Lung	Adrenal gland, bone, brain, liver other lung
Melanoma	Bone, brain, liver, lung, skin, muscle
Ocular melanoma	Liver
Ovary	Liver, lung, peritoneum
Pancreas	Liver, lung, peritoneum
Prostate	Bone
Sarcoma	Lung
Stomach	Liver, lung
Thyroid	Bone, liver, lung
Uterus	Bone, liver, lung, vagina

In solid tumors, the most frequent secondary sites of metastasis are lymph nodes, followed by liver, lung, and bone (Table 1) (Budczies et al., 2014; Disibio and French, 2008). Some cancers, such as prostate, metastasize mainly to a specific organ, namely the bone (Sturge et al., 2011). In contrast, other types, such as breast and lung cancers, spread to multiple organs (Cummings et al., 2014; Riihimäki et al., 2014). Of note, variation among secondary sites in breast cancer can be seen across cancer subtypes (see section 3.6) (Kennecke et al., 2010; Soni et al., 2015). Curiously, colorectal cancer spreads to the

liver and later to the lung in a sequential manner (Edge et al., 2009, 2010; Urosevic et al., 2014) (Table 1). Furthermore, some types of cancer, such as breast, lung, and kidney cancers, develop numerous metastases, while others, such as liver cancer, present a low frequency. Importantly, once advanced cancer establishes in a distant organ, it becomes almost incurable. In this thesis, we focus on bone metastasis, due to its importance in terms of number of cancer types that metastasize to the bone and consequently the number of current and future patients with this condition.

2. Bone metastasis, an incurable disease

Bone is one of the most common organs affected by metastatic lesions. Thus, the high prevalence of bone metastasis carries heavy clinical and economic costs. Therefore, unraveling the molecular mechanistic bases of metastasis, discovering bone metastasis-specific drugs, and identifying predictive biomarkers are urgently required.

Bone metastasis involves several serious symptoms that reduce the quality of life of the affected persons. Indeed, despite the administration of drugs against bone metastasis, such as bisphosphonates and Denosumab, most persons with bone metastasis present severe bone pain as a result of spinal cord or nerve-compression and an increased resorption of bone (osteolysis). Bone metastasis also results in an increased bone fragility that causes painful fractures and impaired mobility. Hypercalcemia is also a common complication of persons with bone metastasis (Coleman, 1997; Costa et al., 2008; DePuy et al., 2007; Mundy, 2002). Once a secondary lesion is formed in the bone, cancer becomes generally incurable. Of note, to achieve bone metastasis, DTCs must first interact with the bone microenvironment and alter its balance, in order to provide a favorable habitat that enhances their growth.

2.1 The bone microenvironment

Bone has two key functions. First, it has a structural function by providing support and protection of vital organs and sustaining mechanical movement. Second, it stores minerals, maintains plasma calcium homeostasis and hosts hematopoietic cells (Hadjidakis and Androulakis, 2006). The bone matrix is a porous mineralized structure composed basically of crystalline hydroxyapatite $[Ca_3(PO_4)_2]_3Ca(OH)_2$, an inorganic component that accounts for 60% of bone and serves as a reservoir for calcium. It also contains several proteins, such as type I collagen -the major structural component of the matrix, growth factors, and cytokines (Feng, 2009; Robey et al., 1993). Bone can be divided into two types, namely cortical and trabecular (Figure 2). *Cortical* bone is dense and solid, surrounds the bone marrow space, and accounts for most of the total bone mass. In contrast, *trabecular* bone is a porous structure interspersed in the bone marrow compartment (Clarke, 2008). Bone hosts four types of cell: osteoblasts, bone lining cells, osteocytes, and osteoclasts.

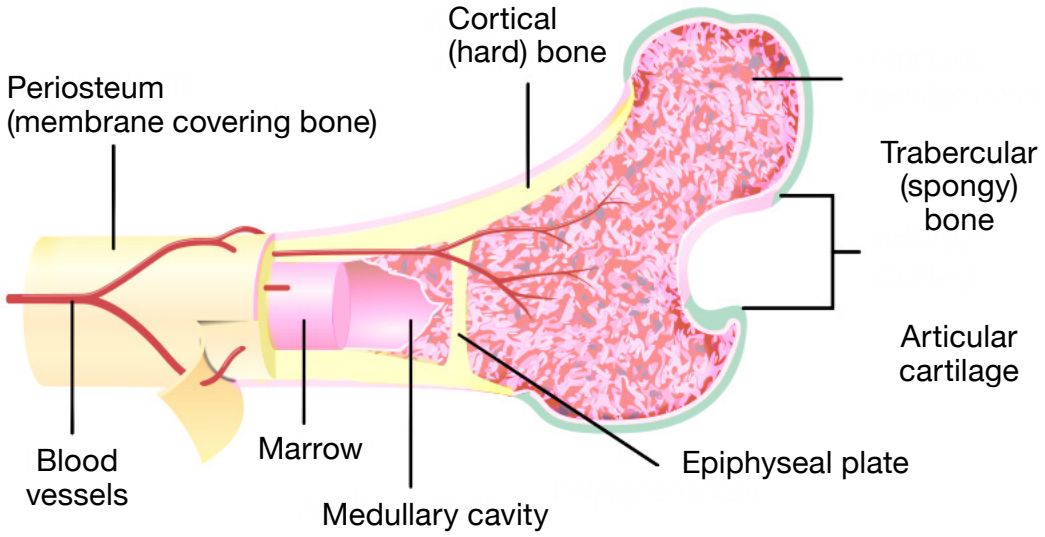

Figure 2. Histology of bone. Cortical bone is compact and dense. It forms the outer layer of almost all bones in the body and strengthens them, thus supporting the whole body and protecting organs. Trabecular bone is a spongy structure located at the end of long bones that contains bone marrow, contributes to bone flexibility, and allows metabolic activities such as calcium ion exchange.

Osteoblasts are bone-forming cells that originate from mesenchymal stem cells (MSCs) located in the bone marrow stroma, like other cells of the connective tissue (adipocytes, myocytes, and chondrocytes). Osteoblast differentiation is a multi-step process in which MSCs differentiate to osteoprogenitors, which further become pre-osteoblasts and finally mature osteoblasts. During differentiation, bone morphogenetic proteins (BMPs) and Wnt signaling are crucial to promote osteoprogenitors from MSCs. Other factors, including TGF-ß, insulin-like growth factor-1 (IGF1), fibroblast growth factors (FGF), and platelet-derived growth factor (PDGF), participate in activating osteoblast function. The pathways of these factors lead to the expression of three key transcriptional regulators that promote osteoblast differentiation: the expression of Runt-related transcription factor 2 (Runx2), its downstream effector osterix (Osx) and distal-less homeobox 5 (Dlx5) (Capulli et al., 2014; Florencio-Silva et al., 2015; Harada and Rodan, 2003). Once activated, osteoblasts synthesize osteoid, the organic compound of the bone matrix formed mainly by collagen. They also contribute to the completion of bone mineralization by releasing bone alkaline phosphatase (ALPL, also known as BALB) (Bussard et al., 2008; Leblond, 1989; Rohde and Mayer, 2007). After the synthesis of new bone, mature and aged osteoblasts undergo apoptosis or give rise to osteocytes or bone-lining cells (Capulli et al., 2014).

Bone lining cells are thought to be quiescent flat osteoblasts that retain the ability to redifferentiate into mature osteoblasts. Lining cells form a layer on the bone surface. After bone resorption by osteoclasts, they clean leftovers from the bone matrix and deposit a layer of fibrillar collagen on the cleaned surfaces, which allows the regulation of mineral ions into and out of the bone matrix (Clarke, 2008; Everts et al., 2002).

Osteocytes are terminally differentiated osteoblasts that act as mechanosensors in the regulation of the bone-remodeling process. They support bone structure, metabolism and intercellular adhesion, as well as providing receptor activator of nuclear factor-κB ligand (RANKL) for osteoclast formation. They are networked to each other, to bone surface lining cells, and to osteoblasts via long cytoplasmatic extensions, allowing direct communication between themselves (Bonewald, 2011; Clarke, 2008).

Osteoclasts are derived from monocytes in the bone marrow in a process regulated by factors provided by osteoblastic cells, including RANKL (also known as TNFSF11) and macrophage-CSF (M-CSF; also known as CSF1). Osteoclasts are multinucleated cells that mediate bone resorption. To this end, they secrete H^+ ions to acidify and dissolve bone mineral, as well as MMP and cathepsin K, which digest the organic matrix of the bone. Bone resorption releases calcium and growth factors deposited in the bone matrix (Clarke, 2008; Garnero et al., 1998; Teitelbaum, 2000).

These cells are interconnected and generate a balance between new bone formation and old bone resorption, thus allowing constant remodeling of bone.

2.2 Bone homeostasis, a dynamic balance

Bone is a highly dynamic tissue that undergoes continuous remodeling throughout life. Bone remodeling was first evidenced by Frost (Frost, 1990). A group of osteoclasts remove the old bone matrix and are followed by a group of osteoblasts that fill it with new bone (Figure 3). This collaboration is called a basic multicellular unit (BMU). Importantly, bone remodeling is constantly active: a balance of old bone replacement by new tissue maintains the bone and repairs damage or adjusts the bone composition to mechanical needs (Parfitt, 1994). Bone remodeling consists of three main steps: resorption, reversal, and formation.

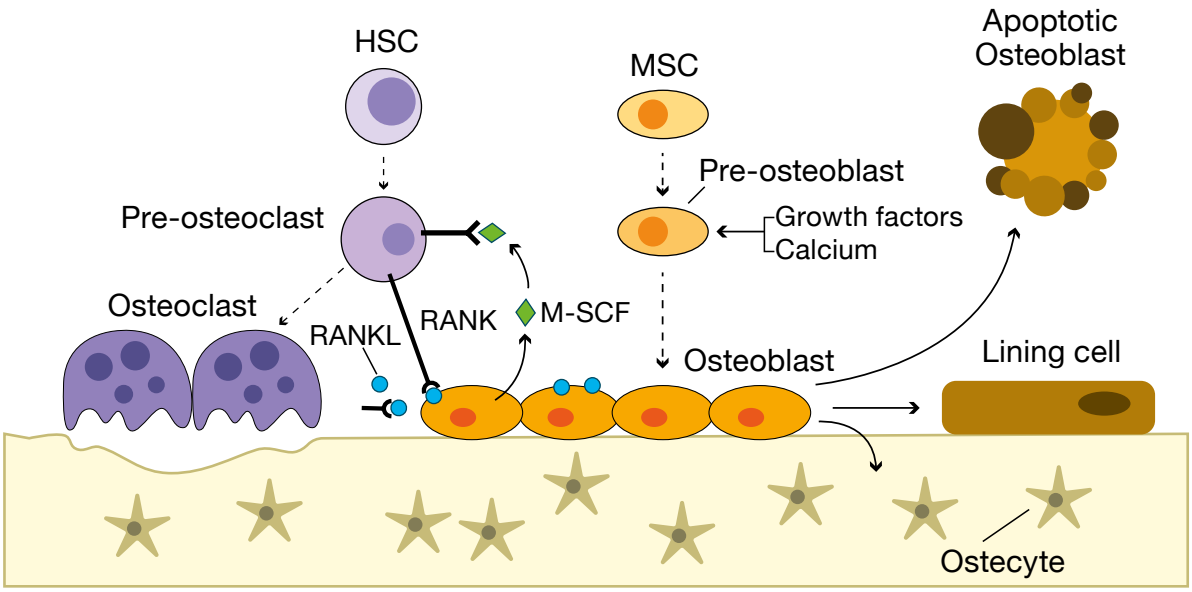

Figure 3. Bone remodeling. Bone pass through continuous cycles of bone degradation and bone formation. This remodeling is balanced and highly regulated: on the one hand, hematopoietic stem cell (HSC)-derived osteoclasts resorb bone, releasing growth factors and calcium into the microenvironment; on the other hand, MSC-derived osteoblasts produce new bone. Once bone has been formed, osteoblasts can overcome apoptosis or can transform into lining cells (which form a layer over bone surfaces) or into osteocytes (terminally differentiated osteoblasts that provide signals for bone remodeling). Abbreviations: M-CSF, Macrophage colony-stimulating factor; RANK, Receptor activator of nuclear factor κB; RANKL, RANK receptor. Modified from Weilbaecher et al., (2011).

Resorption is the phase in which mononuclear pre-osteoclasts migrate to the bone surface to differentiate into mature osteoclasts. Once active, these cells start bone degradation.

RANKL and M-CSF expressed by osteoblastic lineage cells trigger migration of osteoclast precursors and recruitment to a specific bone area (Suda et al., 1999; Teitelbaum, 2000). RANKL is a cytokine member of the tumor necrosis factor (TNF) superfamily that interacts with its receptor RANK localized on the extracellular membrane of osteoclast precursors. The RANK/RANKL interaction causes the activation and differentiation of osteoclasts, thus promoting bone resorption. Noteworthy, the soluble decoy receptor osteoprotegerin (OPG), secreted mainly by osteoblast lineage cells, plays an important role in osteoclast differentiation by competing with RANK for RANKL (Florencio-Silva et al., 2015; Hofbauer and Schoppet, 2004; Simonet et al., 1997; Yasuda et al., 1998). Moreover, the receptor c-fms from osteoclast precursors binds to M-CSF, which provides survival and proliferation signals to osteoclasts (Ross, 2006). Of note, hormones, cytokines and

growth factors (such as PTHrP, interleukin 6 and 1 [IL-6, IL-1], and estrogen) can affect osteoclast differentiation by regulating the expression of RANKL and M-CSF (Kim et al., 2009; Martin, 2005; Shevde et al., 2000; Udagawa et al., 1995). Osteoclasts bind to the bone matrix via podosomes, a multiple F-actin-rich cell-matrix adhesion structure. The Rho family of GTPases and Src family of kinases regulate the assembly and disassembly of podosomes, thus regulating bone resorption (Heckel et al., 2009; Ory et al., 2008).

Reversal is the stage in which mononuclear cells on the bone surface provide signals for osteoblast differentiation and migration, continuing until resorbed bone is completely replaced by new bone. Several studies propose ephrin B2/ephrin B4 binding as responsible for the induction of osteoblast differentiation and inhibition of osteoclastogenesis (Zhao et al., 2006).

Finally, activation of osteoblasts is translated into activation of bone **formation**. Stimulatory factors, such as TGF-ß, IGF, and osteopontin (Opn), are released by osteoclasts from bone matrix into the microenvironment and stimulate osteoblast activity (Canalis et al., 1993; Pfeilschifter and Mundy, 1987).

It is in this scenario that metastatic cells appear and alter the regulatory signals to their own benefit. Cancer cells are able to disrupt the bone remodeling program and take advantage to grow and invade the tissue.

2.3 Bone remodeling by cancer cells

Breast, prostate, and lung cells show preferential colonization of the bone. Various mechanisms of metastasis are activated, depending on the effect of these tumor cells in the bone microenvironment. Breast and lung tumor cells activate osteoclasts, giving rise to osteolytic lesions characterized by an abnormal increase in bone degradation. In contrast, prostate cancer cells activate osteoblasts, thereby generating an unusual mass of new bone. Curiously, in most patients, most bone metastases show cooperation between these two mechanisms; osteolytic and osteoblastic elements are detected at the metastatic site as an attempt to repair bone (Figure 4). Hence, the two processes are linked and modulate bone remodeling, although this link is distorted in cancer.

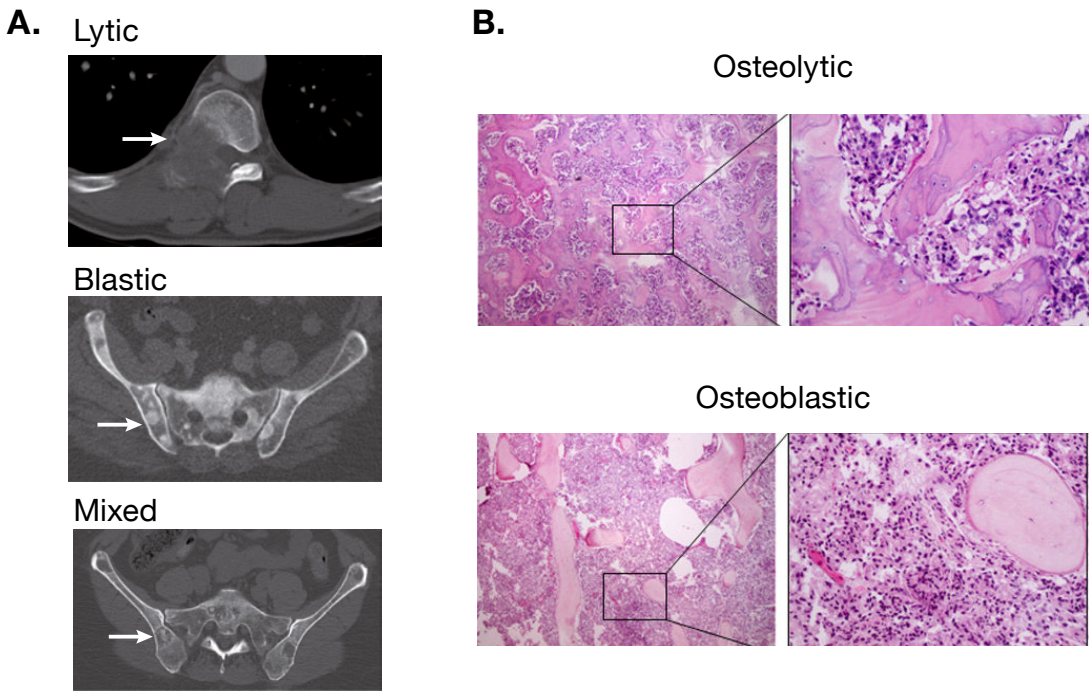

Figure 4. Clinical presentations of osteolytic and osteoblastic lesions. **A.** Computerized tomography (CT) scans that show a vertebral body lytic metastasis (degradation of bone) from a patient with lung cancer bone metastasis, a prostate cancer patient with blastic metastastis (deposition of new bone) in the pelvis, and a patient with mixed breast cancer bone metastasis that shows both lytic and blastic metastasis in the pelvis. **B.** Representative histological images (hematoxylin and eosin [H&E] staining) of osteolytic and osteoblastic bone metastasis. Modified from Larson et al., (2013), and Weilbaecher et al., (2011).

Clinical studies show that metastatic lesions are generally detected in active red marrow of the sternum, ribs, and spine in breast cancer, in spine and pelvis in prostate cancer, and in ribs and spine in lung cancer. Other bones that host metastatic lesions are the femur, scapula, skull, humerus, clavicle, and tibia (Kakhki et al., 2013). Normally, lesions are found in the metaphysis, a highly vascularized structure at the end of long bones, predominantly composed of trabecular bone that undergoes constant remodeling and where, consequently, high concentrations of growth factors are released into the microenvironment. The high vascularization of bone facilitates the arrival of metastatic cells, and the abundance of growth factors activates tumor cell survival and proliferation (Bussard et al., 2008). In addition, preparation of a pre-metastatic niche by the primary tumor contributes to the migration and survival of metastatic cells.

Before the arrival of metastatic CTCs to the bone, primary tumors release systemic factors that condition the bone microenvironment by generating a pre-metastatic niche Heparanase, Opn, LOX and MMP are examples of molecules that benefit tumor cell migration (Cox et al., 2015; Kelly et al., 2005; Lynch et al., 2005; McAllister et al., 2008). Another fact that may facilitate tumor cells migration to the bone is that both osteoblasts and bone stromal cells express high levels of stromal cell-derived factor 1 (SDF1 or CXCL12), while tumor cells express its receptor, C-X-C chemokine receptor type 4 (CXCR4). CXCL12-CXCR4 interaction facilitates establishment and expansion of DTC in the bone (Kang et al., 2003; Lapteva et al., 2005; Müller et al., 2001; Smith et al., 2004; Sun et al., 2005). Additionally, expression of integrin $\alpha_V\beta_3$ lead by CXCR4 in breast and prostate cancer cells is associated with bone adhesion and invasion (Sun et al., 2007). Although the niche is favorable to tumor cells invasion, DTC that have reached the bone have to adapt to the bone microenvironment, connect with stromal cells, and compromise bone homeostasis to finally achieve a successful colonization that gives rise to osteolytic or osteoblastic lesions (Weilbaecher et al., 2011).

2.4 Osteolytic metastasis, a vicious cycle

Osteolytic metastases are caused by several factors -the most important one being PTHrP- that directly or indirectly promote osteoclast activation (Figure 5). PTHrP is overexpressed and secreted by metastatic cells that colonize the bone. Curiously, cells in the primary tumor or those that metastasize to soft tissues do not overexpress this hormone (Guise et al., 1996; Henderson et al., 2006). PTHrP, in turn, stimulates the production and release of cytokine RANKL by osteoblasts. This cytokine binds and activates its receptor, RANK, which is localized at the extracellular membrane of osteoclast precursor cells. Simultaneously, PHTrP inhibits the synthesis of OPG by osteoblasts (Horwood et al., 1998; Thomas et al., 1999a). The balance between OPG and RANKL levels will determine osteoclast activation. In addition to PTHrP hormone, tumor cells secrete other molecules that promote osteoclast differentiation via osteoblast stimulation. This is the case of IL-1, IL-6, IL- 8, and IL-11 (Bendre et al., 2003; Girasole et al., 1994; Kim et al., 2009; Thomas et al., 1999a; Udagawa et al., 1995). To sum up, tumor cells contribute to osteoclast activation via a variety of stimuli. In this regard, tumor cells activate the resorption of the bone, a process that releases growth factors from the bone matrix. Principally, TGF-ß, IGF1, and BMP are released, as well as calcium ions. Specifically,

TGF-ß induces the secretion of PTHrP in metastatic cells by activation of Smad-dependent and -independent signaling pathways, as well as enhance tumor growth (Ikushima and Miyazono, 2010; Kang et al., 2005; Yin et al., 1999). TGF-ß can also modulate many other pro-metastastic and osteolytic factors such as RANK, VEGF and CXCR4. Importantly, IGF is involved in cell proliferation, differentiation and apoptosis (Roddam et al., 2008; Rowlands et al., 2009). BMP promotes invasion and bone metastasis progression (Katsuno et al., 2008; Owens and Naylor, 2013). Moreover, elevated extracellular calcium acts as a chemoattractant for cancer cells, promotes tumor cell proliferation, and enhances PTHrP production (Saidak et al., 2009; Sanders et al., 2000; Yamaguchi et al., 1998).

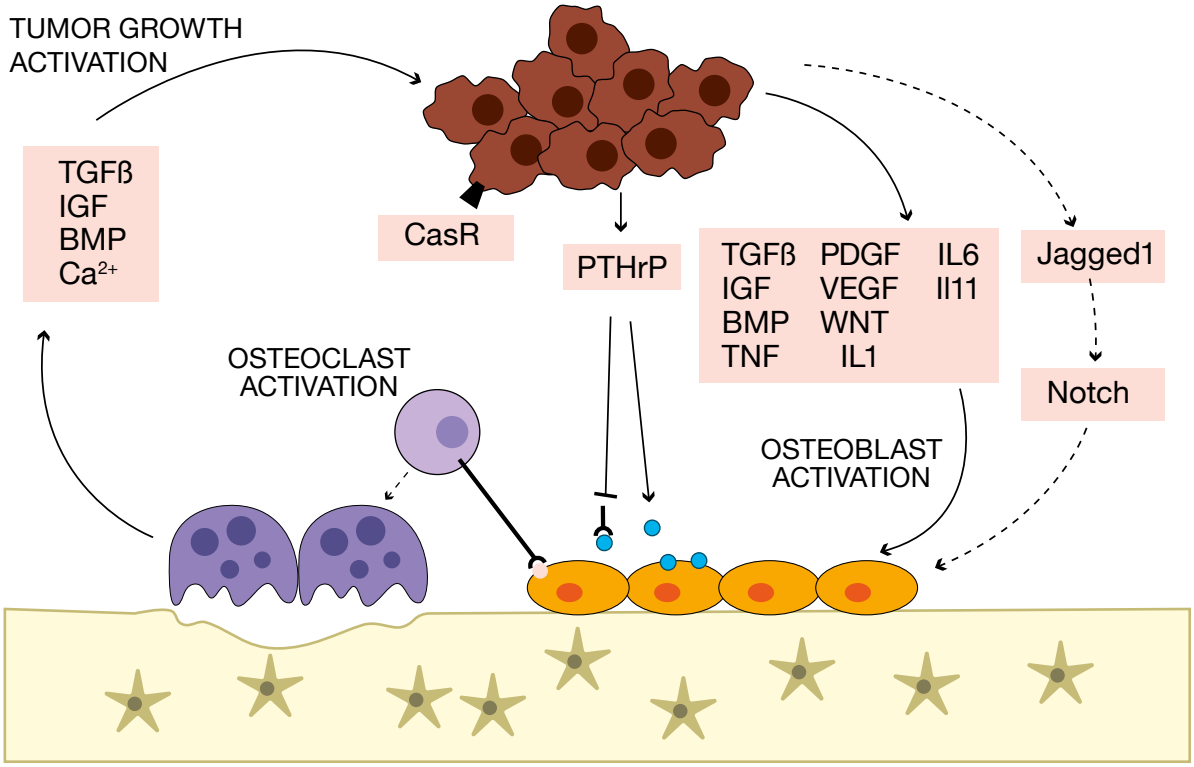

Figure 5. Mechanisms of osteolytic metastasis. Once in the bone microenvironment, tumor cells secrete osteolytic factors (including interleukin-6 and 11), vascular endothelial growth factor (VEGF), tumor necrosis factor (TNF), and parathyroid hormone-related protein (PTHrP or PTHLH), which promote osteoclast bone resorption. Specifically, PTHrP stimulates receptor activator of nuclear factor kappa-B ligand (RANKL) production and inhibits its decoy receptor osteoprotegerin (OPG), thus promoting osteoclast activation. Osteoclast activity causes the release of growth factors (e.g., transforming growth factor β [TGF-β] and insulin-like growth factors [IGFs]) and calcium ions, which in turn promote tumor cell growth. These cells can indirectly activate osteoclast activity through the Jagged1 pathway. Modified from Weilbaecher et al., (2011).

All together, these factors released from the bone matrix stimulate tumor cell maintenance and proliferation. Thus, the "vicious cycle" of bone metastasis consists of the activation of osteoclast activity triggered by tumor cells, and this activity, in turn, promotes tumor cell growth (Kozlow and Guise, 2005; Weilbaecher et al., 2011).

Other tumor cell mechanisms promote bone degradation in a paracrine manner. This is the case of the Jagged1-Notch signaling pathway. Jagged1 is overexpressed in metastatic breast cancer cells. This overexpression activates the Notch pathway in osteoblasts and results in the stimulation of IL-6 secretion. Further on, IL-6 activates osteoclast maturation and finally confers a growth advantage to tumor cells (Sethi et al., 2011). Concurrently, expression of transcription factors, such as GLI2, RUNX2, and hypoxia-induced growth factor 1 α (HIF1α), in tumor cells promotes bone osteolysis as a consequence of the induction of PTHrP expression (Hiraga et al., 2007; Pratap et al., 2009; Sterling et al., 2006). Alternatively, when overexpressed in breast cancer cells, the BMP inhibitor NOG fosters osteoclast differentiation and bone degradation, thereby allowing colonization of bone (Tarragona et al., 2012).

2.5 Osteoblastic metastases, lesions with defective bone formation

Conversely, osteoblastic metastases are caused by factors that stimulate osteoblast differentiation, meaning an increase in new bone production (Figure 6). One of the most widely-studied factors is endothelin-1 (ET-1), a potent vasoconstrictor that is detected in the circulation of patients with osteoblastic metastases and can stimulate osteoblast proliferation via endothelin A receptor (ET_A) (Nelson et al., 1995, 2003; Yin et al., 2003). Expression of proteases such as urokinase-type plasminogen activator (uPA) and prostate-specific antigen (PSA) by prostate cancer cells contributes to the release and activation of osteoblastic factors from the bone matrix (Achbarou et al., 1994; Cramer et al., 1996; Iwamura et al., 1996; Rabbani et al., 1990). Some examples of these growth factors are IGF1, FGF, PDGF, and TGF-ß, which together promote an increase in carcinoma cell growth (Chackal-Roy et al., 1989; Chan et al., 1998; Funa et al., 1991; Gleave et al., 1991; Kim et al., 2003; Logothetis and Lin, 2005; Marcelli et al., 1990; Mundy et al., 2001).

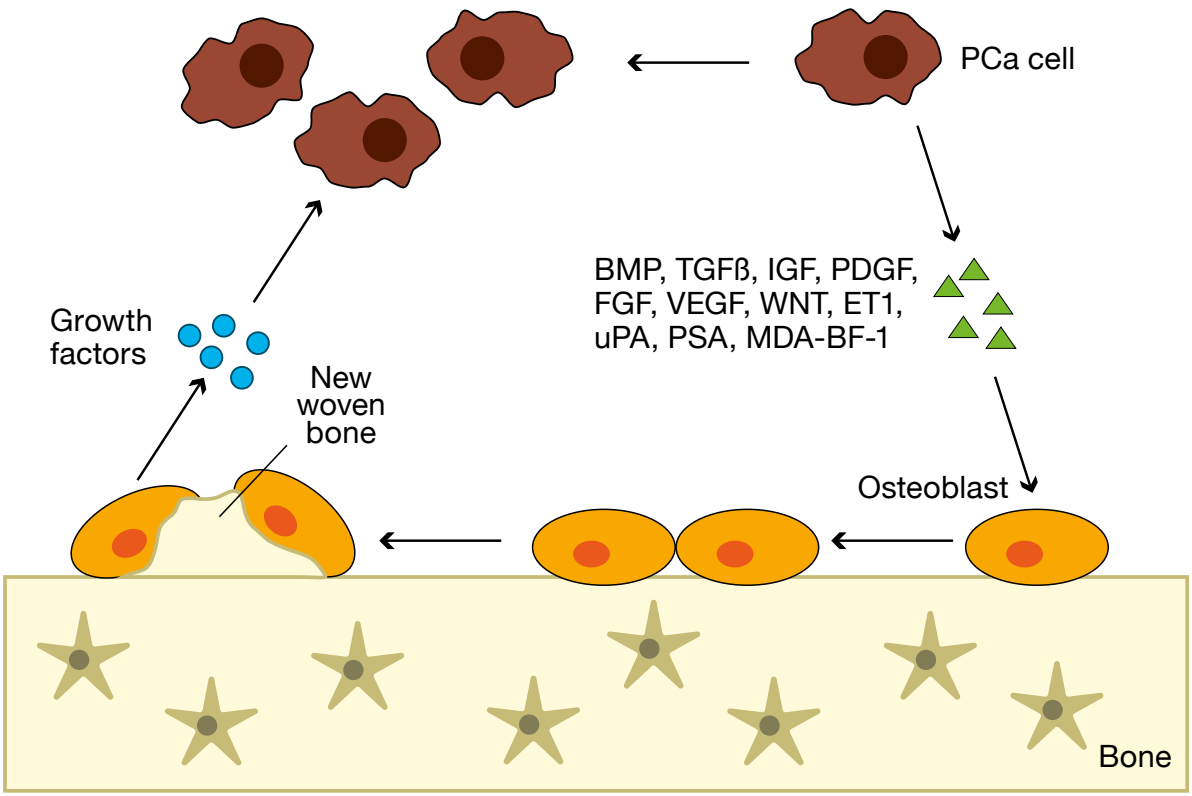

Figure 6. Osteoblastic metastases. Once prostate cancer cells reach the bone, they secrete paracrine factors able to promote osteoblast proliferation and differentiation. These factors include bone morphogenetic protein (BMP), transforming growth factor β (TGF-β), insulin-like growth factor (IGF), platelet-derived growth factor (PDGF), fibroblast growth factor (FGF), vascular endothelial growth factor (VEGF), endothelin-1 (ET-1), urokinase-type plasminogen activator (uPA), prostate-specific antigen (PSA), and bone metastasis factor MDA-BF-1 (a secreted isoform of ErbB3). These factors modulate osteoblast activity and promote new bone formation. Modified from Logothetis and Lin, (2005).

2.6 Importance of stromal cells in bone metastasis

To this extent, bone marrow is a very favorable niche for tumor cell growth, due to its enriched microenvironment in growth factors and the supportive stroma. In addition to osteoclasts and osteoblasts, other stromal cells can favor tumor colonization and growth by preparing the pre-metastatic niche and participating in the "vicious cycle". Stromal and epithelial cells of the bone contribute to bone metastasis by expressing vascular cell adhesion molecule (VCAM-1), which is critical for the production of bone-resorbing factors by cancer cells (Michigami et al., 2000). Endothelial cells, in turn, activate the formation

of new blood vessels by releasing pro-angiogenic factors and their CXCL12 expression promotes the migration of prostate cancer cells (Jahroudi and Greenberger, 1995). On the other hand, fibroblasts secrete syndecan-1, which enhances breast cancer cell proliferation and also stimulates osteoclasts via RANKL pathway (Lau et al., 2006; Maeda et al., 2004). Similarly, adipocytes secrete TNF-α, IL-6, and leptin, which stimulate osteoclasts and inhibit osteoblast at the same time (Gordeladze et al., 2002; Hardaway et al., 2014; Iyengar et al., 2003; Thomas et al., 1999b).

Regarding hematopoietic cells, T cells express RANKL and TNF-α, which activate osteoclast resorption and inhibit osteoblast differentiation (Monteiro et al., 2013; Roato et al., 2005). T cells also release TGF-ß, a potent immunosupressor of T-cell proliferation and natural killer cell function, triggering the survival of cancer cells (Fournier et al., 2006). B cells, in turn, express CXCR4, which enhances tumor cell migration into bone (Burger et al., 1999). Additionally, TAMs can kill tumor cells through interferon and IL-12; alternatively, these macrophages can also promote tumor cell survival through angiogenic growth factors, cytokines, and proteases (Chanmee et al., 2014; Schoppmann et al., 2002). The release of IL-10 by TAMs suppresses the anti-tumor response of cytotoxic T cells (Ng et al., 2013; Noy and Pollard, 2014). Finally, platelets adhere to cancer cells in the blood stream, helping them to evade natural killer cells and to attach to the vascular endothelial cell walls (Menter et al., 2014).

Due to the clinical relevance of metastasis, especially to bone, and to the many scenarios present depending on the disseminated cell type, we will focus in the following sections on the types of cancer that metastasize to bone, starting from their origin and progression and ending with a description of the treatments currently available. Understanding in more detail their mechanism is crucial for bone metastasis research.

3. Breast cancer

Breast cancer (BC) is the most frequent cancer diagnosed in women (although it can also affect men). The National Cancer Institute (www.cancer.gov) estimates that 15% of all new cancer cases diagnosed (252,710 new cases) in 2017 in the United States will be BC, and that this disease will cause 6.8% of all deaths from cancer (40,610 cases) (Siegel et al., 2016). BC is commonly diagnosed between 45 to 65 years old (www.aecc.es) and is a major public health problem. It can be diagnosed by physical examination and medical history, clinical breast examination, mammography, ultrasound, magnetic resonance imaging (MRI), blood chemistry studies, and biopsy. Importantly, 89.7% of women diagnosed with BC will experience long-term disease-free survival, of at least 5 years. This high survival rate is the result of the tremendous advances in early diagnosis and new treatments. Nevertheless, several major unresolved issues remain: How can we prevent BC? Which factors cause aggressive tumor progression? How can we predict, treat, and prevent an aggressive phenotype? Which BC patients will develop therapeutic resistance, and how can it be prevented or overcome?

In this regard, basic scientists and physicians are committed to tackling metastasis, a clinical manifestation of cancer that can appear years or even decades after diagnosis of the primary tumor. To comprehensively assess this disease, a proper understanding of mammary gland development and homeostasis is needed.

3.1 Histology of the mammary gland

To understand the origin of BC, we need to comprehend the structure, function, and homeostasis of the mammary gland. The mammary gland is an exocrine gland that produces and secretes milk to feed offspring. The breast is based on a rudimentary branching duct system lying in a fat pad (Figure 7). Growing ducts end up in a cavity called terminal end buds (TEBs), which consist of the most proliferative part of the ducts (Figure 8). Mammary stem cells (MaSCs) are located in this region, thereby making TEBs a crucial factor for mammary gland development. TEBs consist of two distinct cell types. The first type forms the inner epithelial layer and the second gives rise to an outer layer of undifferentiated cap cells, precursors of myoepithelial cells (Hinck and Silberstein, 2005). Similarly, ducts are surrounded by an inner layer of ductal luminal cells (epithelial cells) and a second layer of myoepithelial cells. Myoepithelial cells form a

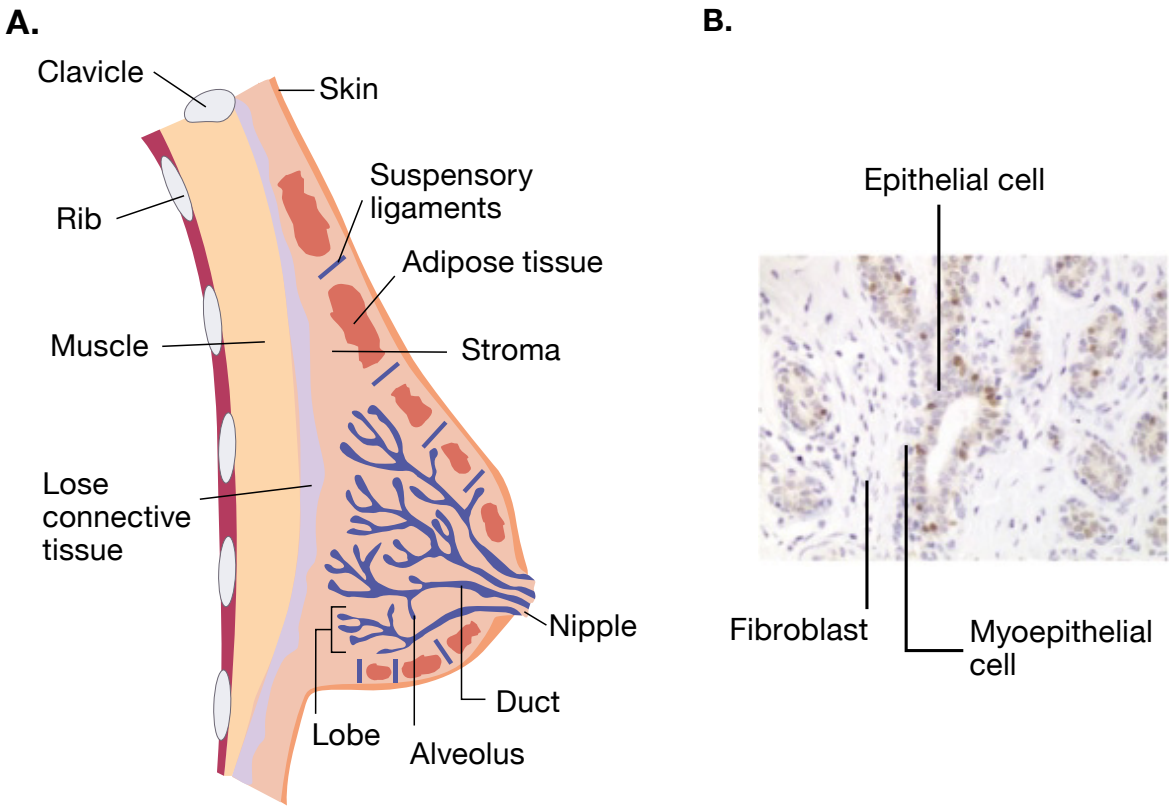

Figure 7. Structure of normal breast tissue. **A.** Anatomy of the normal human mammary gland. The mammary gland contains between 15 and 20 lobes that drains to the nipple through the branched ducts and lies in the fat pad. **B.** Histological image of a duct, composed by a layer of epithelial cells that produce milk and surrounded by a layer of myoepithelial cells with contractile functions. Ducts are embedded in the fibroblast stroma. Modified from Ali and Coombes, (2002).

basement membrane, which is a physical barrier that separates the epithelial and stromal compartments (Gusterson et al., 1982).

After the branching duct system has formed and during pregnancy, the end of the ducts become alveolar buds, which is where milk is produced during lactation (Hennighausen and Robinson, 1998). The outer myoepithelial layer of the ducts and alveoli, which surrounds the luminal layer, exhibits contractile functions to secrete milk during lactation. Multiple alveoli join to form groups called lobes. Each mammary gland contains between 15 and 20 lobes, which drain the milk to the nipple. Mammary stroma is comprised of extracellular matrix and various cell types, such as fibroblasts, adipocytes, immune and hematopoietic cells, and neurons (Hennighausen and Robinson, 1998, 2005; Tiede and Kang, 2011). Importantly, the mammary gland undergoes constant changes throughout life because of the constant development of this organ.

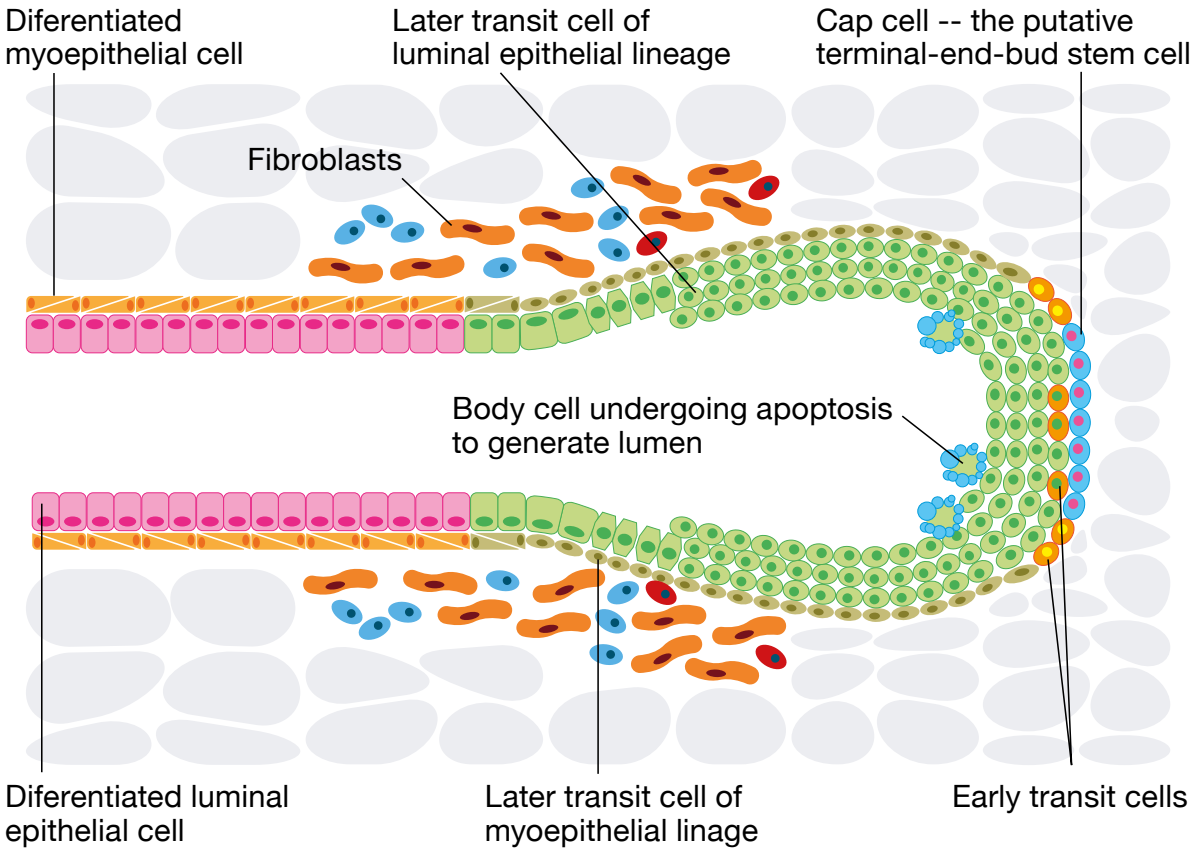

Figure 8. Structure of terminal end bud (TEB). TEBs are the ducts of the developing mammary gland. They are formed by an inner layer of luminal epithelial cells and an outer layer of myoepithelial cells. At the front of the duct, a layer of cap cells generates transit cells of myoepithelial lineage called body cells. Thereafter, body cells undergo apoptosis to generate the lumen, and outer cells differentiate into luminal epithelial cells. Extracellular-matrix enzymes secreted in front of the TEBs enable the degradation of stroma and motility through the fat pad. Modified from Smalley and Ashworth, (2003) and Sternlicht (2005).

3.2 Mammary gland, an organ in constant development

The mammary gland is derived from the ectoderm as a proliferation of basal cells of the epidermis. It undergoes numerous changes during the life of a female. During embryogenesis and birth, males and females have a similar rudimentary mammary gland, and its growth is independent of hormone signaling. Morphological changes in the female breast can be detected from puberty onwards and are triggered by ovarian hormones, mainly estrogen and progesterone. In this period, rudimentary ducts proliferate through the TEBs, which penetrate the fat pad thus leading to the elongation of the ducts. An increased branching of the mammary gland is also observed (Robinson, 2007; Sternlicht, 2005).

During each menstrual cycle, the mammary gland undergoes cycles of growth and involution driven by ovarian hormones. However, the maximum increase in branching and end-bud development is observed during pregnancy and lactation. Ductal structures undergo elongation, bifurcation, and lateral branching until the fat pad is filled and a full epithelial tree is formed. At this time, alveoli increase by about 10-fold per lobule, and new lobules are formed from existing terminal ducts (Russo and Russo, 2004). After weaning, there is massive cell death (apoptosis) and a re-differentiation process to regress to a near pre-pregnancy state. It is this remodeling and dynamic mechanism of epithelial cells that makes the mammary gland more susceptible to acquiring mutations and thus allowing cells to undergo transformation. The ability of the mammary gland to induce angiogenesis, to be protected against involution, and to resist apoptosis during pregnancy and lactation are features reminiscent of the survival abilities of cancer cells (Ali and Coombes, 2002; Potten and Morris, 1988; Smalley and Ashworth, 2003; Sternlicht, 2005; Warburton et al., 1982; Wiseman and Werb, 2002). As mentioned, all of these morphological changes are orchestrated by hormones.

3.3 The big controllers: the hormones

To understand genetic alterations in BC, it is critical to know which mechanisms regulate normal mammary gland development. Ovarian and pituitary hormones are essential for post-pubertal mammary morphogenesis and homeostasis of the adult tissue. The hormones that orchestrate this process are estrogen, progesterone, androgens, glucocorticoids, prolactin, thyroid hormone, insulin, IGF-1 and IGF-2, FGF, EGF, and transforming growth factor α (TGF-α) (Dickson and Lippman, 1995). They are involved in proliferation and the growth of the mammary duct system, as well as massive cell death after weaning. As mentioned above, these pathways are also activated during the tumorigenic process. It is therefore not surprising that malignant cells arising from breast tissue retain hormonal dependence.

During puberty, morphogenetic and proliferation changes are driven by ovarian estrogen and pituitary-derived growth hormone (GH). GH binds to its receptor on mammary stromal cells to induce the local production of IGF-I. Thereby, IGF-1 binds in a paracrine manner to its receptor on IGF-1 receptor-positive epithelial cells and triggers ductal morphogenic changes (Walden et al., 1998). In addition to GH, ovarian secretion

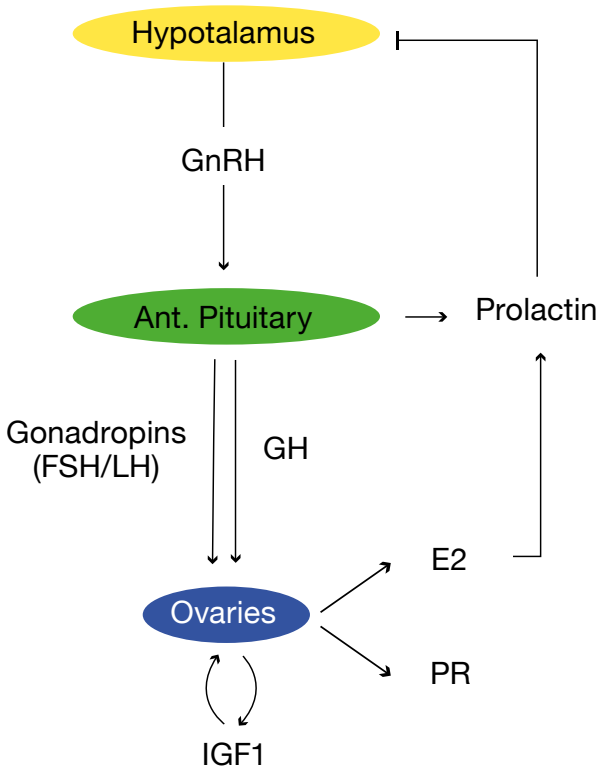

Figure 9. Scheme of hypothalamus-pituitary-ovary axis. Endocrine glands are shown in ovals. Abbreviations: E2, estrogen; FSH, follicle-stimulating hormone; GH, growth hormone; GnRH, Gonadotropin-releasing hormone; IGF1, insulin-like growth factor 1; LH, luteinizing hormone; PR, progesterone. Modified from Brisken and O'Malley, (2010).

of estrogen is crucial for epithelial cell proliferation. Estrogen binds to its receptor ER in epithelial cells and induces the expression of amphiregulin, which binds to and activates EGFR from stromal cells. Amphiregulin is a key intermediary in glandular maturation that can influence early malignant progression (Kenney et al., 1996).

The menstrual cycle in humans, and the estrous cycle in rodents, is controlled by the hypothalamus-pituitary-ovary axis (Figure 9). Gonadotropin-releasing hormone (GnRH) is secreted by the hypothalamus and activates the anterior pituitary to secrete both follicle-stimulating hormone (FSH) and luteinizing hormone (LH) (Hawkins and Matzuk, 2008). These hormones consequently stimulate the ovary to produce estrogen or progesterone.

Secretion of 17beta-estradiol, in turn, triggers an increase in serum progesterone and progesterone receptor (PR) (Beleut et al., 2010). Finally, progesterone and its receptor

(PR) are expressed in both epithelial and stromal compartments. They are required for the side branching of mammary gland during adulthood as well as during pregnancy (Oakes et al., 2006). Furthermore, progesterone is essential for the expansion of basal stem CD24+/CD49high cells (Joshi et al., 2010) and human progenitor cells (Graham et al., 2009). Progesterone can regulate downstream effectors such as RANKL and Wnt4 (Beleut et al., 2010; Brisken et al., 2000; Fernandez-Valdivia and Lydon, 2012). During lactation periods, other endocrine hormones such as prolactin play an important role in lovuloalveolar development and milk secretion. After lactation, PKC, among other factors, induces the apoptosis of epithelial cells during involution (Joshi et al., 2012).

3.3.1 Function of estrogen in breast homeostasis and carcinogenesis

Estrogen (17ß-estradiol or E2) is the most important ovarian steroid hormone in breast development and homeostasis. It promotes branching differentiation, as well as epithelial tumor growth (Yager and Davidson, 2006). Estrogens have other functions in the reproductive tract and gonads, as well as in the skeletal and cardiovascular system.

Estrogen enters the cytoplasm by diffusion and binds to two distinct receptors, ERα and ERß, located in the cytosol. These receptors are encoded for different genes from distinct chromosomes and act as transcription factors (*ESR1* and *ESR2* respectively) (Toft and Gorski, 1966). Estrogen-ER binding promotes a conformational change that allows the receptor to enter the nucleus. Once in the nucleus, ER forms dimers that bind to specific DNA sequences known as Estrogen Response Elements (EREs) located on the promoters of target genes (Björnström and Sjöberg, 2005; Nilsson et al., 2001).

ERα is expressed both in a subset of mammary epithelial cells and in the stroma. Epithelial ERα-positive cells facilitate normal ductal elongation and subsequent side branching and alveologenesis. ERα has also been implicated in uterine and mammary carcinogenesis (Couse and Korach, 1999a; Cunha et al., 1997; Mueller et al., 2002). Myoepithelial cells express ERα and ERß, whereby ERß modulates ERα (Lindberg et al., 2003). Importantly, ER and estrogen are drivers of BC metastasis.

Estrogen is synthesized principally in the ovaries of premenopausal females. Lower levels of estrogen are synthesized by a number of extragonadal sites such as mesenchymal cells of adipose tissue, osteoblasts and chondrocytes of bone, vascular endothelium, aortic

smooth muscle and many regions in the brain. It acts locally at these sites as a paracrine factor. Noteworthy, the synthesis of estrogen in the ovaries ceases at menopause but not in the other secretory organs (Simpson, 2003).

3.4 Breast cancer progression

In most cases, BC development starts in a sporadic mutation or genomic rearrangement of oncogenes or tumor suppressor genes. Markedly, a small but important proportion of BC cases is caused by hereditary mutation in *BRCA1* and/or *BRCA2*. *BRCA1* mutations cause a dysfunction in the BRCA1 pathway, which is important in maintaining genomic stability through DNA repair, homologous recombination and activation of the cell cycle checkpoints. *BRCA1* also orchestrates the differentiation of estrogen receptor negative (ER-) stem or progenitor cells into estrogen receptor positive (ER+) luminal cells. For this reason, *BRCA1* mutation is associated with phenotype of a subtype of BC called basal-like triple negative, characterized by a lack of ER+ cells. In contrast, tumors with a *BRCA2* mutation have an heterogeneous phenotype (Foulkes et al., 2003, 2004; Hedenfalk et al., 2001; Liu et al., 2008; Welcsh et al., 2000).

Ninety-five percent of BCs arise from the luminal epithelial cells of the ducts or lobes. Carcinoma starts with the hyperproliferation of epithelial cells confined in to duct or lobe *in situ*. Later, it presents a preneoplastic phase limited to a basement membrane, then, when the basement membrane is breached, the carcinoma becomes invasive and can invade adjacent tissues and, in the most aggressive cases, it can colonize distant organs (Figure 10).

Before invading distant organs, primary tumor passes through several intermediate premalignant states. Terminal duct lobular units (TDLUs) are the major stem cell compartments that give rise to all types of premalignant breast lesions. TDLUs can expand due to the hyperplasia of their lining epithelium and turn into unfolded lobules (ULs). When small clonal outgrowth starts, ULs become an atypical ductal hyperplasia (ADH), which can become a ductal carcinoma *in situ* (DCIS) when this outgrowth is larger and distends ductal and lobular spaces. At this point, neoplasia varies, from a histological point of view, from low- to high-grade lesions but still remains inside the mammary conduct without invading basal membrane. Finally, DCIS can invade new

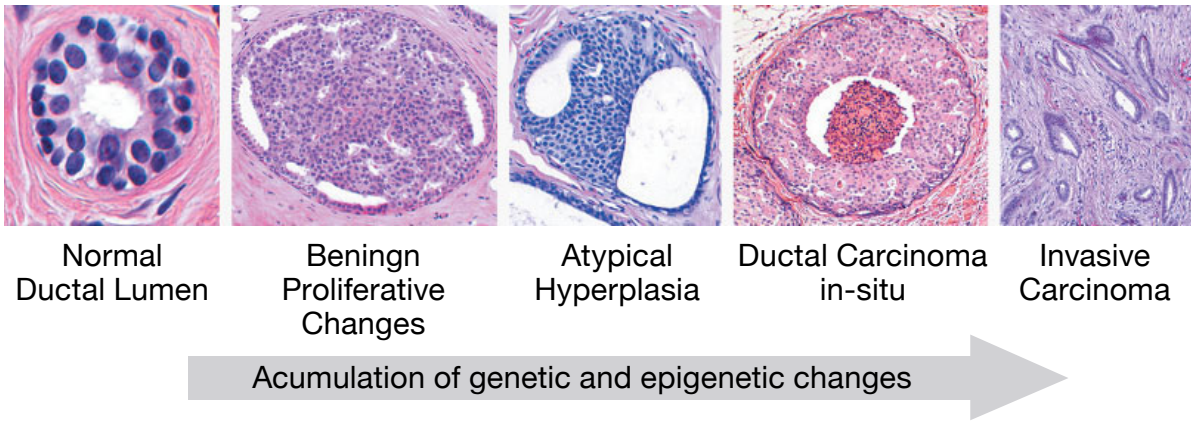

Figure 10. Breast cancer development. Representative images of the transformation process from healthy tissue through ductal carcinoma *in situ* to invasive lesions are shown. Modified from Burstein et al., (2004).

tissues, a process that is called invasive breast cancer (IBC). Although approximately 80% of carcinomas are the ductal subtype, BCs can arise from lobules. In this case, TDLUs become a typical lobular hyperplasia (ALH) and then a lobular carcinoma *in situ* (LCIS), which will similarly result an invasive BC (Figure 11) (Allred et al., 2001; Burstein et al., 2004; Turashvili et al., 2005). Loss of heterozygosity (LOH) is common in more than 70% of high-grade DCIS as compared to an estimated 40% of atypical hyperplasia and non-detectable LOH in specimens of normal breast tissue (Allred et al., 2001; O'Connell et al., 1998; Oesterreich et al., 2001).

Each tumor derived from the mammary gland can be distinguished and classified into subtypes. Classification can be based on molecular or histologic features; in either case, it is useful to determine the behavior of the tumor.

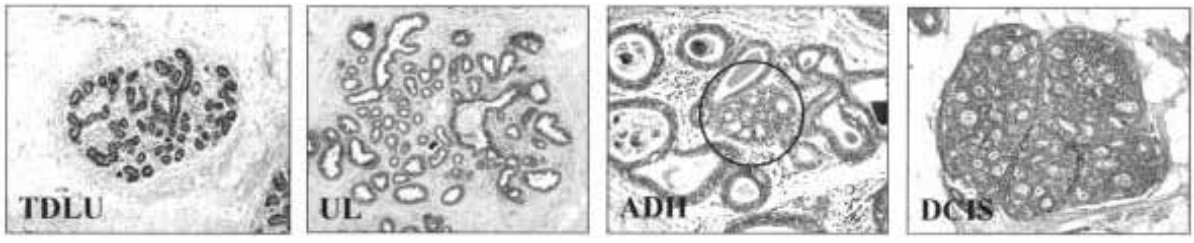

Figure 11. Histological model of breast cancer evolution. Representative photomicrographs images of premalignant lesions are shown. Terminal duct lobular units (TDLUs) give rise to unfolded lobules (ULs) that present a hyperplasia of the lining epithelium. Then, atypical ductal hyperplasias (ADHs) can arise and become ductal carcinoma *in situ* (DCIS). Modified from Allred et al., (2001).

3.5 Molecular classification of breast cancer

BC is characterized by high heterogeneity at the molecular and clinical levels. Each tumor presents distinct specific etiology, molecular features, progression, and response to therapy. In this regard, BC is divided into subtypes depending on its molecular portraits determined by microarray analyses. Some of these classifications give information about the behavior of these tumors before and after treatment. Perou et al. proposed five molecular subtypes of BC distinguished on the basis of their gene expression patterns: luminal A and luminal B, HER2-enriched, basal-like, and normal breast-like; later, a new subtype was added to molecular portraits, Claudin-low (Perou et al., 2000; Prat et al., 2010; Sørlie et al., 2001; Sotiriou and Pusztai, 2009). The six subtypes show distinct physiopathological grades and aggressiveness, and their response to treatment differs, although their clinical utility has yet to be confirmed.

Luminal A BC represent about 50-60% of BC tumors (Yersal and Barutca, 2014). They show enrichment of differentiation genes such as *GATA3* and *FOXA1* and low proliferation index (Ki67). They exhibit expression of ER and luminal markers similar to luminal epithelial cells in the mammary gland such as K7, K8, K18, and K19. They match with good prognosis tumors (Sorlie et al., 2003; Sørlie et al., 2001).

Luminal B BC comprise 15-20% of BC tumors (Yersal and Barutca, 2014). They contain moderate ER and luminal epithelial genes expression. They show greater proliferative capacity (Ki67). Thereby, luminal B BC are aggressive and are associated with a worse prognosis than luminal A (Sorlie et al., 2003).

HER2-enriched BC mostly present the distinctive of *ERBB2* overexpression or amplification (17q21). They are present in 15-20% of all BC (Yersal and Barutca, 2014). They exhibit high proliferative and aggressive phenotype and *TP53* is also frequently mutated in this type of tumors (Rudas et al., 1997; Sorlie et al., 2003; Sørlie et al., 2001).

Basal-like BC represent the 8-37% of all BC (Yersal and Barutca, 2014). They are characterized by the expression of typical genes of normal mammary gland basal myoepithelial cells (i.e. *cytokeratin K5/6, K14*, and *K17*). They are associated with poor clinical outcome, present high proliferation rates, and express poorly differentiation genes. Most basal-like BCs lack ER, PR, and HER2 expression, although some of them can

express low levels of these receptors. Of note, *BRCA1* mutations are strongly associated with a basal tumor phenotype. They also presents high percentage of *tumor protein 53* (*TP53*) gene mutations (Livasy et al., 2006; Montagna et al., 2013; Perou et al., 2000; Rudas et al., 1997).

Normal breast-like BC account for about 5-10% of all BC tumors (Yersal and Barutca, 2014). They are poorly characterized and resemble normal breast tissues (as implied by the name). After luminal A subtype, is the second type of cancer with a better prognosis. They express gene characteristics of adipose tissue and contain low expression of luminal-differentiated genes and high expression of basal-related genes (Perou et al., 2000).

Claudin-low BC represent approximately a 6% of all BC tumors (Sabatier et al., 2014). They exhibit low levels of *claudin* gene expression. Claudins are tight-junction glycoproteins involved in cell-cell adhesion. Tumors present low expression of luminal genes and tumor initiation properties and are consequently highly aggressive and present poor prognosis (Herschkowitz et al., 2007; Prat et al., 2010).

Despite advances in gene pattern classification of breast tumors, these are not currently applied in clinical settings. Clinicians prefer a histopathological categorization, because is cheaper and still gives a better prediction about the response of tumor to treatment. Gene expression signatures do not replace the classical parameters. Nevertheless, in some cases, molecular basis such as MammaPrint and Oncotype DX™ (ODX) as a complement to better define the subtypes and help to adjust the appropriate treatment for patients. Both tests provide predictive information about ER+ and node-negative early-stage BC patients (Marchionni et al., 2008). MammaPrint is a diagnostic test that uses paraffin-embedded or fresh tissues from BC patients to predict the risk of BC recurrence, based on 70 specific genes. It is mainly used to identify young BC patients at low risk for distant metastasis who can avoid systemic treatment (Buyse et al., 2006; Cardoso et al., 2016; Van't Veer et al., 2002; van de Vijver et al., 2002). In contrast, the ODX assay evaluates expression of 21 genes associated with proliferation, invasion, and ER signaling. It predicts those patients who can benefit from chemotherapy after BC surgery and tamoxifen treatment, and it can also determine the patients with DCIS, a non-invasive breast carcinoma, who can benefit from radiation therapy after surgery (Paik et al., 2004, 2006; Sparano and Paik, 2008; Sparano et al., 2015). The PAM50 test (Prosigna) has recently been introduced to

help clinicians to classify patients in the intrinsic basic BC subtypes, with exception of claudin-low, by means of 50 genes (Dowsett et al., 2013; Nielsen et al., 2010; Parker et al., 2009).

3.6 Clinical classification of breast cancer, a predictor to therapy response

Contrary to molecular division of BC tumors, the classification in clinical settings is divided mainly by histopathological types of cancer, as mentioned above. The three principal biological markers used for clinical classification are estrogen receptor (ER), progesterone receptor (PR), and human epithermal growth factor receptor 2 (HER2/Neu). In this regard, BC is classified into triple-negative (TN), luminal A, luminal B, and HER2-positive (Figure 12) (Goldhirsch et al., 2013). These subtypes help clinicians to predict clinical outcome before and after the selected treatment.

ER and PR determine the hormonal status of the tumor and are assessed by immunohistochemistry (IHC). Tumors are defined as ER-positive (ER+) or PR-positive (PR+) if at least 1% of the invasive tumor cells present nuclei positive for ER or PR staining. Classification by these two receptors is fundamental to distinguish those patients who can benefit from endocrine therapy (Hammond et al., 2010). Alternatively, HER2 grade is defined depending on the expression of this receptor by grade 0 (negative), 1+ (low staining), 2+ (medium staining, at least 10% of the cells), or 3+ (high staining, >30% of invasive cells). Grade 0 and 1+ are considered HER2-negative (HER2-), whereas grade 3+ is considered HER2-positive (HER2+). For grade 2+, further analysis of *ERBB2* gene amplification by fluorescent *in situ* hybridization (FISH) should be performed; cells with more than 6 HER2 gene copies per nucleus are considered positive. Identifying patients with ERBB2 amplification allows clinicians to select optimal targeted treatments (Wolff et al., 2007). Thus, based on these parameters, BC is classified, and treatments for BC patients are decided, as follows:

Triple-negative (TN) lack expression of ER, PR, or HER2 (ER-, PR-, HER2-) and in some cases, are termed basal-like because they exhibit significant overlap with basal-like subtype. ER- BC is an aggressive cancer with early relapse in visceral organs, preferably to the lung. Patients are usually treated with chemotherapy, mostly by taxanes or anthracyclines (Couse and Korach, 1999b)

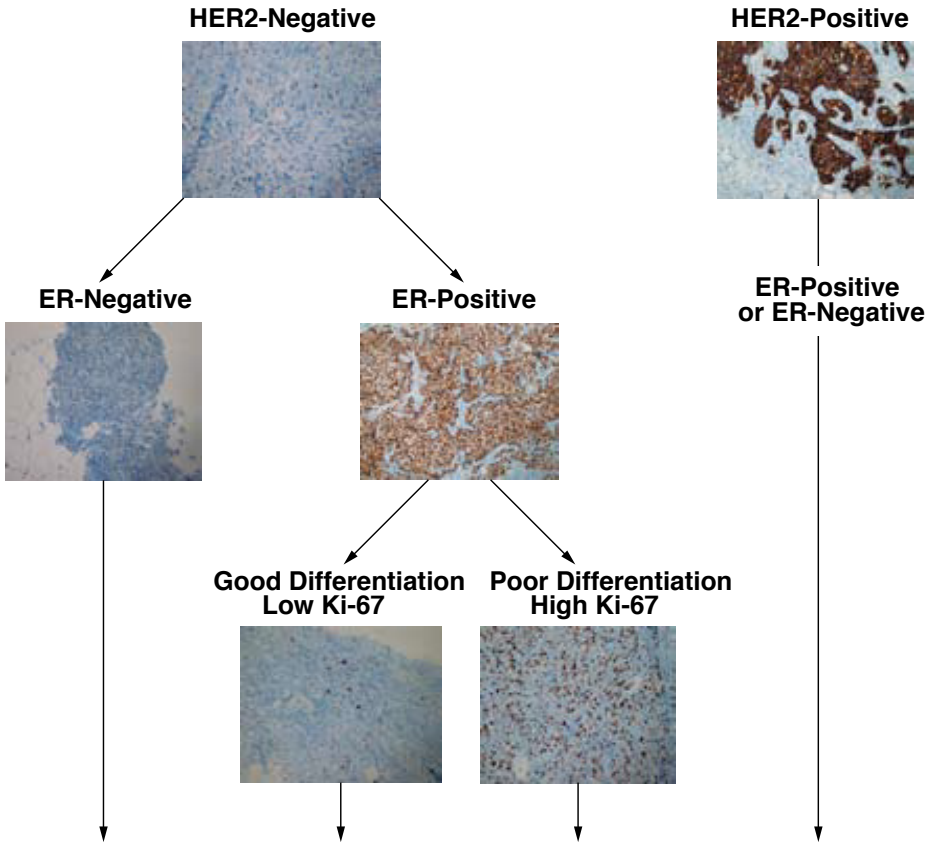

Pathological Variables	Basal-like (%)	Luminal A (%)	Luminal B (%)	HER2-like (%)
HER2-positive (IHC)	10	12	20	100
ER-positive (IHC)	12	96	97	46
Grade III	84	19	53	74
Tumor size >2 cm	75	53	69	74
Node-positive	40	52	65	66

Figure 12. Representative images of clinicopathological features of breast cancer. Breast cancer types are classified in terms of HER2 and estrogen receptor (ER) overexpression and by proliferation rate defined by Ki-67 staining. Modified from Sotiriou and Pusztai, (2009).

Luminal A and B tumors are ER positive and HER2 negative (ER+, HER2-). They differentiate each other by the rate of Ki67: luminal B has higher proliferation status than luminal B. For this reason, the luminal B tumor subtype is associated with poorer outcome. Luminal B also presents lower expression of PR than luminal A. Luminal tumors are more frequently detected in postmenopausal women. ER+ BC exhibits a longer metastatic latency period with tropism to the bone and is always treated with hormone therapy. Additionally, luminal B tumors are complementarily targeted with chemotherapy.

HER2-overexpressing tumors exhibit *ERBB2* gene amplification (HER2+) or *ERBB2* overexpression and are classified independently of hormonal receptor status. HER2 is an EGFR family member and is encoded by *ERBB2* proto-oncogene (Slamon et al., 1987, 1989). HER2 has a highly aggressive phenotype and tropism to the visceral organs, such as liver and brain. Treatments against HER2 have advanced significantly in the last years, improving the overall survival of patients with HER2 overexpression. This treatment consists of monoclonal antibodies against HER2 receptor together with chemotherapy. Hormonal therapy is only administrated if tumors express ER (Burstein, 2005).

Besides histopathological factors, clinicians also treat patients based on tumor-node metastasis (TNM) staging system, which describes the severity of an individual's cancer (Table 2). TNM uses three parameters: T, which describes the extent of the primary tumor;

N, which describes the involvement of regional lymph nodes; and M, which describes the presence or absence of distant metastases (Singletary et al., 2002). These three parameters determine the grade of the cancer at the moment it is detected. The smaller the grade, the better chance the patients have for survival (Table 3).

Table 2: Brief summary of TNM classification in breast cancer patients, American cancer society (www.cancer.org).

T	size	N	LN affection	M	metastasis
T1	0-2 cm	**N0**	0 ganglis	**M0**	no Met
T2	2-5 cm	**N1**	1-3 ganglis	**M1**	Met
T3	>5cm	**N2**	4-9 ganglis		
T4	expanded in skin or thoracic wall	**N3**	>10 ganglis		

Table 3: Brief summary of the grade of breast cancer tumors, American cancer society (www.cancer.org).

Grade		
Grade 0	premalignant, carcinoma *in situ*	
Grade I		T1, N0, M0
Grade II		
	IIA	T0, N1, M0
		T2, N0, M0
	IIB	T2, N1, M0
		T3, N0, M0
Grade III:	ganglis, skin, or thoracic wall (muscle or ribs) affected	
	IIIA	T0-2, N2, M0
		T3, N1-2, M0
	IIIB	T4, N0-2, M0
	IIIC	T0-4, N3, M0
Grade IV:	disseminated cancer and other organs affected	
		M1

Other factors are also decisive for treatment selection, including cellular grade, Ki67 status, localization of the tumor, patient age, general state of well-being, and -most importantly- hormonal state. The differentiation grade of tumors is determined by comparison with normal tissue and is called the cellular grade: grade 1, well-differentiated cells with slow growth; grade 2, medium-differentiated cells; and grade 3, undifferentiated cells with fast growth. In addition, proliferation status by Ki67 IHC is used to assess BC aggressiveness. Tumor localization can be divided into ductal or lobular carcinoma. Finally, the hormonal state distinguishes between premenopausal (reproductive years with menstrual periods), perimenopausal (menopause transition period), and menopausal state (women with amenorrhea from a minimum of 12 months).

Notably, this classification has been a useful guide for searching new target drugs, such as anti-HER2 or ER treatments, and has been believed to be a better prediction of tumor features and response to treatment, and consequently of a great benefit for BC patients.

3.7 Breast cancer treatments, a great breakthrough

BC treatments can be administered by local or systemic approaches and include adjuvant and neoadjuvant therapies. *Local treatment* includes chirurgic intervention and radiation therapy against a localized tumor, while *systemic treatment* involves affectation of the entire organism, usually by chemotherapy or hormonotherapy. An *adjuvant treatment* is a systemic and/or local drug administrated after the first and main treatment, usually surgery, used to reduce the risk of relapse and overall mortality, as a prophylactic treatment, and against primary tumor recurrence and DTC. Alternatively, *neoadjuvant treatment* is a systemic therapy usually used before the local treatment to reduce the tumor volume before surgical intervention. In the next sections, we will expose the most common approaches used to treat BC patients (Table 4).

Table 4. Treatment schematic protocol for BC patients depending on its phenotypic subtype. Modified from Anampa et al., (2015).

Breast cancer subtype/Classification			Adjuvant Systemic therapy		
Phenotypic subtype		Intrinsic subtype	Endocrine therapy	Anti-HER2 Therapy	Chemotherapy
Hormone R	HER2 OE				
+	-	Luminal A or B	Yes	No	Yes (If high risk)
+	+	Luminal A or HER2 Enriched	Yes	Yes	Yes
-	-	Basal	No	No	Yes
-	+	HER2 Enriched	No	Yes	Yes

3.7.1 Surgical treatment

The first approach to beat BC is to resect the tumor by surgery. Conservative surgery covers both tumorectomy, which is extraction of only the tumor, and quadrantectomy, which is extraction of the quadrant in which the tumor is localized. In contrast, conservative surgery aims to extract the whole mammary gland, i.e., mastectomy.

3.7.2 Radiotherapy

Radiation therapy is highly recommended after BC surgery as it reduces by 15% the risk of recurrent cancer in the breast, chest wall, and local lymph nodes (Burstein et al., 2004; Senkus et al., 2015).

3.7.3 Chemotherapy

Chemotherapy should be offered to patients with aggressive tumors such as TN, HER2+, and luminal B. It is always administered in combination of anthracyclines and taxanes (Anampa et al., 2015).

Anthracyclines are drugs with various mechanisms of actions: *i*) they intercalate between base pairs of DNA/RNA strands and inhibit DNA and RNA synthesis on fast growing cancer cells; *ii*) they generate free radicals, leading to DNA damage; and *iii*) they inhibit topoisomerase II, to induce apoptosis. However, they have a relevant side effect of cardiotoxity, which limit their administration. Doxorubicin and cyclophosphamide are the most frequently used anthracyclines in BC (Minotti, 2004).

Taxanes are drugs that disrupt the microtubule function and inhibit mitotic process and consequently cell proliferation. Docetaxel (Taxotere) and paclitaxel (Taxol) are widely used for BC patients with aggressive phenotype. The most common adverse effect is neuropathy (Martin and López-Tarruella, 2015; Rowinsky, 1997; Sparano et al., 2008).

3.7.4 Hormone therapy

Hormone therapy should be offered to patients whose tumors express any level of ER and/or PR. In postmenopausal patients with luminal A tumors, the first-line treatment is the use of aromatase inhibitors (AI). However, AI inhibitors are counterproductive in premenopausal women because they inhibit adipose tissue estrogen secretion, which dramatically stimulates ovarian estrogen production, as this is still active in these women. Consequently, premenopausal women should be offered tamoxifen, an estrogen-competitive inhibitor. In more aggressive cases of BC, such as luminal B, chemotherapy should be co-administrated to the patients. In luminal B postmenopausal women, AI and tamoxifen are the most common drugs administrated. In premenopausal women, ovarian suppression (by GnRHa) or ablation (by surgery) should be used as well as hormone therapy and chemotherapy. Temporary or definitive castration is crucial, as contemporary hormonal agents have been studied and are seen to be functional in women with low levels of estrogen in serum. After metastasis is detected, sequential hormone

therapy should be offered as well as administration of other drugs, such as fulvestrant, palbociclib, everolimus, and exemestrane (Rugo et al., 2016).

Tamoxifen competes with estrogen for binding to cytoplasmatic ER. Tamoxifen/ER binding blocks estrogen activity, consequently avoids growth and division of BC cells (Baum, 1984; Fisher et al., 1998; Jaiyesimi et al., 1995).

Aromatase inhibitors (AI) are the preferred first-line endocrine therapy. AI block aromatase, the enzyme that produces estrogen in the fat pad, which is the principal source of estrogen in postmenopausal women. There are three AI that seem to work equally: anastrozole (Arimidex), letrozole (Femara), and exemestane (Aromasin), all of which produce a superior response than tamoxifen (Baum et al., 2003; Breast International Group (BIG) 1-98 Collaborative Group et al., 2005; Ellis et al., 2001; Goss, 2003; Goss et al., 2003, 2011; van de Velde et al., 2011; Xu et al., 2011).

GnRHa are gonadotropin-releasing hormone (GnRH) analogs that cause chemical ablation of ovarian function. This induction to postmenopausal state is produced by an alteration of LH and FSH and consequently a reduction in blood levels of estrogen. The most common GnRHa is goserelin (Zoladex) (Taylor et al., 1998).

In the metastastic context, in which the primary tumor has spread to other organs, it is recommendable to change the initial treatment and administer other drugs. The most common one is **fulvestrant** that could be administrated with or without **palbociclib**. Fulvestrant (Faslodex) is an ER antagonist that accelerates receptor degradation (Pritchard et al., 2010; Wakeling, 2000). In contrast, palbociclib is a small-molecule inhibitor of cyclin-dependent kinases CDK4/6 (Finn et al., 2015) that inhibits BC cell growth. In BC, resistance to endocrine therapy has been associated with the activation of mammalian target of rapamycin (mTOR). In this regard, **everolimus** (Afinitor), an mTOR inhibitor, is administrated with endocrine therapy to treat advanced metastatic ER+ BC patients (Baselga et al., 2012a).

3.7.5 HER2-directed therapy

The most common drugs used in clinic to target HER2 receptor in those tumors with *ERBB2* amplification are:

Trastuzumab, an anti-human epidermal growth factor 2 (HER2/neu) monoclonal antibody that reduces the risk of disease recurrence by 50%. It is currently administered together with chemotherapy to patients with HER2+ tumors. Due to its cardiotoxicity, concomitant administration with anthracyclines should be avoided (Marty et al., 2005; Piccart-Gebhart et al., 2005; Slamon et al., 2011, 2001; Yin et al., 2011).

Pertuzumab, a monoclonal antibody that targets the extracellular dimerization domain of HER2 protein. Inhibition of signaling pathways causes cell growth arrest and apoptosis. Pertuzumab administration together with trastuzumab increases the median progression-free survival as compared to trastuzumab treatment alone (Baselga et al., 2012b; Swain et al., 2015).

Lapatinib, a small molecule HER1/HER2 tyrosine kinase inhibitor, which can be administered simultaneously with trastuzumab to increase by about 16% the chance disease-free survival as compared to treatment with trastuzumab alone (Blackwell et al., 2010; Geyer et al., 2006; Gomez et al., 2008; Lin et al., 2008; Piccart-Gebhart et al., 2016).

T-DM1 trastuzumab emtansine, an antibody-drug conjugate, which has the HER2 targeted antitumor properties of trastuzumab together with the cytotoxic activity of DM1. DM1 is a microtubule-inhibitory agent (Burris et al., 2011; Verma et al., 2012).

Even though a large amount of effort has advanced cancer therapies, BC is still able to generate treatment resistance and progress to a more aggressive state (Osborne and Schiff, 2011).

4. Prostate cancer

Prostate cancer (PC) is the most common form of cancer in men. The National Cancer Institute (www.cancer.gov) estimates that PC will cause 161,360 new cases (9.6% of all new cancer cases) and 4.4% of all cancer deaths (26,730 cases) only in the United States in 2017 (Siegel et al., 2017). It is believed that 11.6% of men, mainly between 65 and 74 years old, will be diagnosed with PC (www.aecc.es). However, the percentage of 5-year survival rose to about 98.6% over the last years.

PC can be diagnosed early due to the screening of asymptomatic men by the digital rectal exam, and by levels of PSA. Transrectal ultrasound, transrectal magnetic resonance imaging (MRI), and biopsy allow a better diagnosis.

4.1 Histology of the prostate gland

Prostate is a gland that produces and secretes chemical alkaline substances containing PSA that nourish and protect sperm. It is located into the pelvis between the bladder and the penis (Figure 13A). Urethra runs through the center of the prostate gland. Prostate is divided into three zones, termed the peripheral, central, and transitional zones. The peripheral zone surrounds the distal prostatic urethra, the central zone, the ejaculatory ducts, and the transitional zone, the proximal prostatic urethra; this region grows throughout life (Figure 13B) (McNeal, 1988; Timms, 2008).

The prostate gland is an endodermal structure that originates from the urogenital sinus (UGS). In humans, prostate development starts in the second trimester and is almost entirely complete at the time of birth, when buds (epithelial cells) penetrate the

UGS mesenchyme. Branching morphogenesis coordinates epithelial and mesenchymal cell differentiation. Epithelial cells differentiate from progenitor endodermal cells into basal and luminal differentiated cells. Luminal cells express K8 and K18 and secrete prostatic proteins and fluids to the ductal lumen; in contrast, basal cells express K5 and K14 and form a continuous layer between secretory cells and the basement membrane. Mesenchymal cells, on the other hand, condensate around the tip and form a distinctive

pattern of stromal cells along the length of the basement membrane, composed by a layer of smooth muscle cells and a thin surrounding layer of fibroblasts (Figure 14) (Hayward et al., 1996a, 1996b; Marker et al., 2003; Prins and Putz, 2008). The ducts give rise to five lobules: an anterior lobe (localized at the TZ), posterior lobe (in the PZ), right and left lateral lobes, and a median lobe (in the CZ).

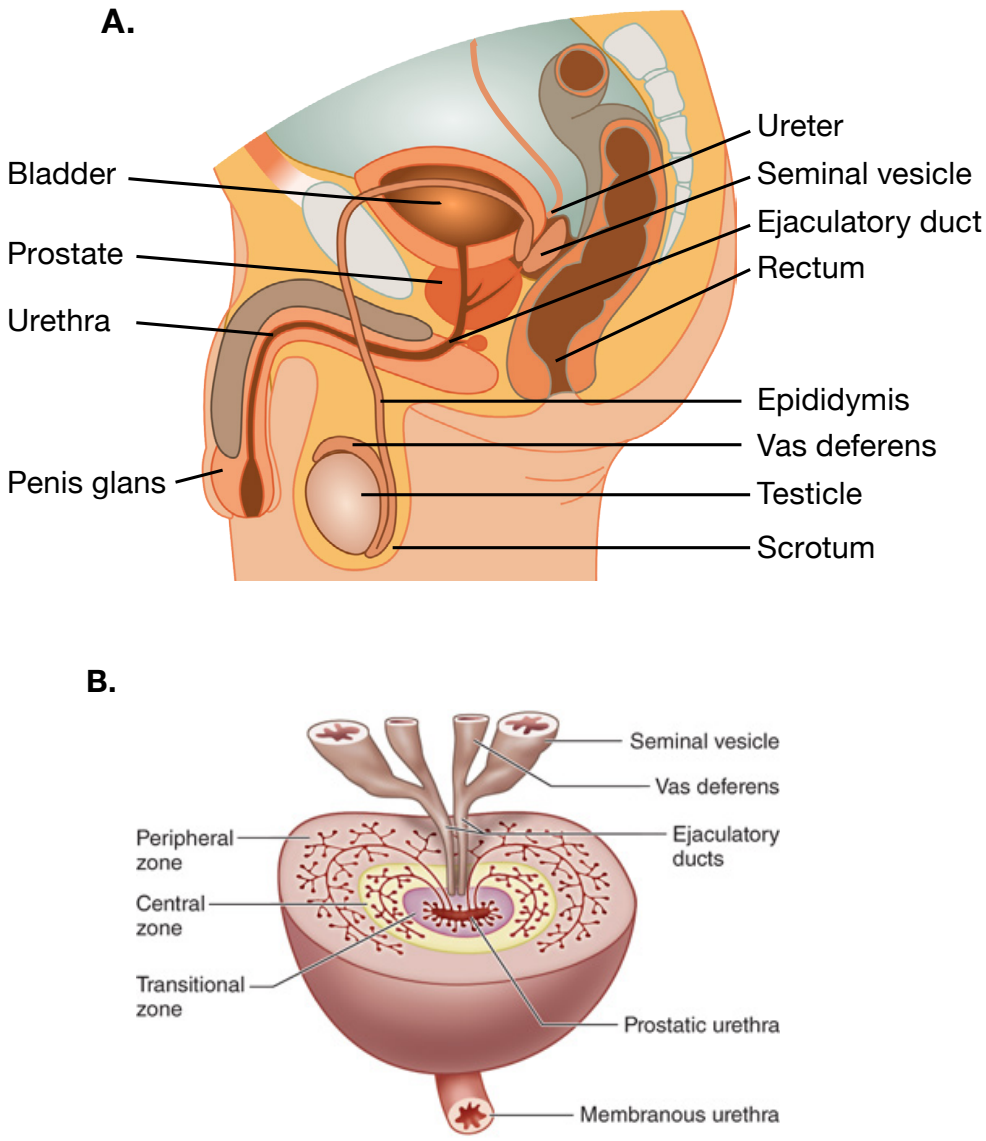

Figure 13. Prostate gland histology. **A.** The prostate gland is located between bladder and the penis. **B.** The prostate gland is structured into three zones: the peripheral zone surrounds the distal urethra, the central zone, the ejaculatory ducts, and the transition zone, the proximal urethra.

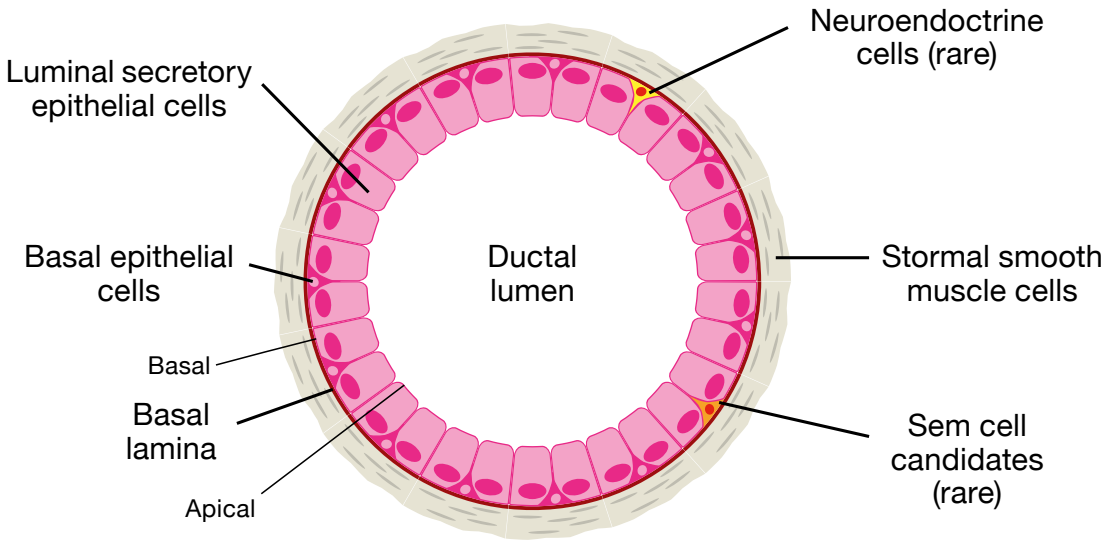

Figure 14. Cellular features of the prostate gland. Prostate gland contains secretory epithelial cells, basal epithelial cells, neuroendocrine cells, stromal smooth muscle cells, and stem cell candidates. Markers commonly used to distinguish these cell types are included in the scheme. Modified from Marker et al., (2003).

4.2 Androgens, the big managers

Prostatic development is entirely dependent upon androgens produced by the fetal testes. Androgens interact with androgen receptor (AR), a member of the transcription factor superfamily that is localized in the nucleus of the cell, and promote cell proliferation and inhibit apoptosis. AR is highly expressed at the urogenital mesenchyme before and during morphogenesis. Alternatively, during budding and branching morphogenesis, it is highly expressed in the epithelial cells. Its activation is essential for prostate determination and for initiation of bud proliferation. Importantly, two hormones can activate AR: testosterone and dihydrotestosterone (DHT). Testosterone is mainly produced by testis and released systemically into the blood stream, and it can directly activate AR or can be converted to DHT by the enzyme 5α-reductase type 2 in the prostate epithelial cells (Marker et al., 2003; Russell and Wilson, 1994). DHT, in turn, is a more potent AR agonist, with a 10-fold higher affinity than testosterone for AR binding (Deslypere et al., 1992). DHT conversion is essential to prostate development, as has been demonstrated by the link between mutations in 5α-reductase and reduced prostatic growth and development (Andersson et al., 1991). In this regard, testosterone is produced by testis due to the activation by gonadotropins including LH and FSH. Moreover, prolactin (also secreted by anterior pituitary) can directly control prostatic growth, function, and integrity. As

mentioned above, release of FSH and LH is activated by releasing factors from the hypothalamus. Alternatively, adrenal cortex can produce steroids that play a minor role in prostate activation (Figure 15) (Sandberg, 1980).

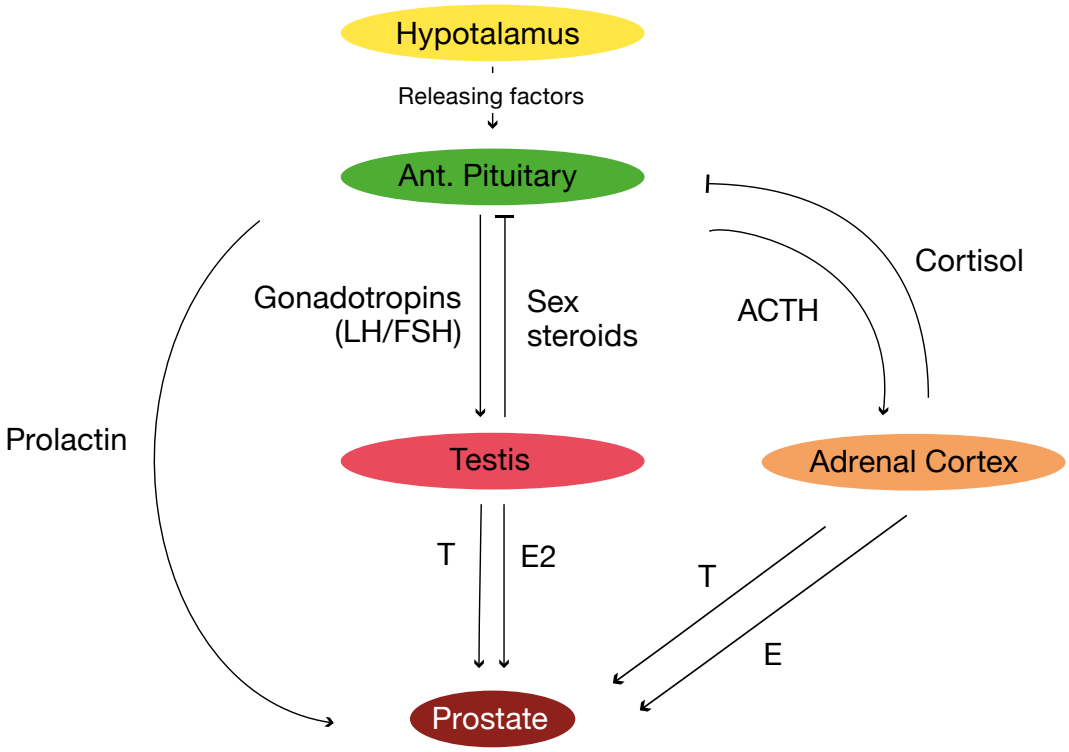

Figure 15. Hormonal regulation of prostate. Hypothalamus release factors that control the synthesis and release of gonadotropins by anterior pituitary and subsequently affect production of testosterone by the testes. Adrenal cortex plays a minor role through steroid production. Modified from Sandberg, (1980).

4.3 Prostate cancer development

PC cell transformation occurs mostly in the peripheral zone (70-80%), less frequently in the transition zone (10-20%), and rarely in the central zone (2-5%). PC begins with a prostatic intraepithelial neoplasia, a hyperplasia in the luminal epithelial cells that leads to a reduction in basal cell number (Figure 16). By contrast, more than a 95% of the human PCs are classified as adenocarcinoma with a strikingly luminal phenotype. To this extent, adenocarcinomas can be confirmed in biopsies by the absence of K5/14 and presence of α-methylacyl-CoA racemase (AMACR), a luminal marker (Humphrey, 2007; Jiang et al., 2005; Luo et al., 2002).

Regarding genetic modifications, it is noteworthy that in more than 90% of PCs lack

expression of glutathione S-transferase π, which is expressed in normal prostatic epithelial cells and catalyzes intracellular detoxification of electrophilic compounds (Lee et al., 1994).

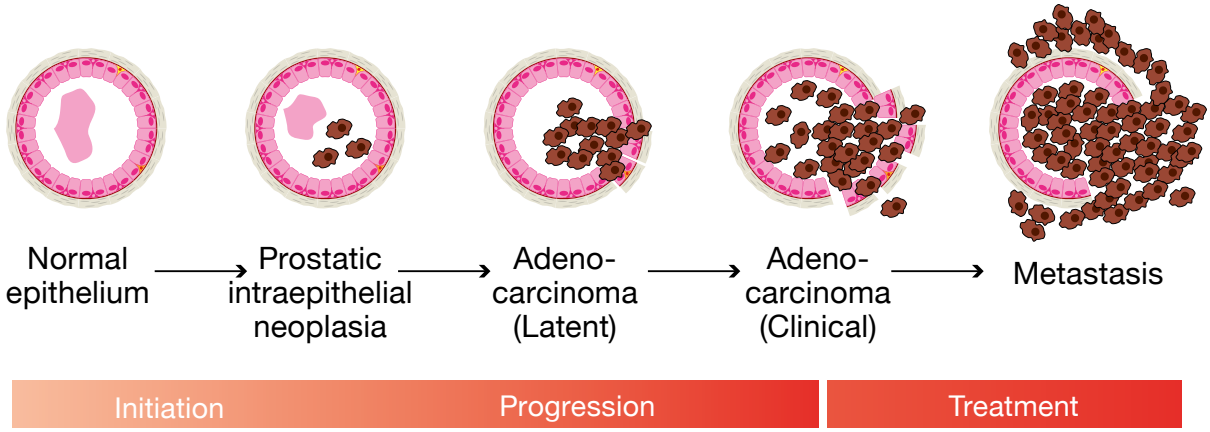

Figure 16. Prostate cancer cell development. Scheme of progression stages in prostate cancer, from normal epithelium to adenocarcinoma to an invasive tumor. Modified from Shen and Abate-Shen, (2010).

4.4 Clinical staging system

In contrast to BC, prostate tumors do not have histopathological subtype classification that predicts tumor aggressiveness and treatment response. Recently, attempts to stage PC into molecular subtypes have been made (Taylor et al., 2010). Nowadays, the most relevant fact in PC is that almost all cancers are adenocarcinomas that are AR-positive (AR+) (Grignon, 2004).

In clinical settings, PC is classified by the TNM status, the Gleason system, and the levels of PSA. **TNM** is a staging system to classify patients according to their tumor severity (also used in BC, as mentioned above) (Table 5). In grade I, tumors are neither palpable nor visible with diagnostic equipment and are usually found incidentally; in grade II, the tumors are palpable and visible but have not invaded outside the prostate, in grade III, tumors have invaded adjacent tissues outside the prostate; and in grade IV, tumors have disseminated to lymphatic nodes or other parts of the organism (Table 6). The **Gleason system** classifies the aggressiveness of the cells from 1 to 5 according to their differentiation state. Finally, **levels of PSA** can be detected in the blood of PC patients as a consequence of normal prostate architecture disruption (Lilja et al., 2008; Shen and Abate-Shen, 2010).

Table 5. Brief summary of TNM classification in prostate cancer patients. Taken from the American Cancer Society (www.cancer.org).

T	size			
	Digital rectal exam	**Transrectal ultrasound**	**Extension outside prostate or seminal vesicles**	**Extension elsewhere**
T1	N	N	N	N
T2	Y	Y	N	N
T3	Y	Y	Y	N
T4	Y	Y	Y	Y

	LN affectation
N0	0 ganglis
N1	>0 ganglis

M	metastasis
M0	no met
M1	
IA	distant LN
IB	bone
IC	lung, liver or brain

Table 6. Brief summary prostate cancer tumor grades. Taken from the American Cancer Society (www.cancer.org).

Grade				
		TNM	**Gleason score**	**PSA**
Grade I		T1, N0, M0	<7	<10
		T2a, N0, M0	<7	<10
Grade II				
	IIA	T1, N0, M0	7	<20
		T1, N0, M0	<7	>10 and <20
		T2a, N0, M0	<8	<20
		T2b, N0, M0	<8	<20
	IIB	T2c, N0, M0	any	any
		T1, N0, M0	any	>20
		T2, N0, M0	any	>20
		T1, N0, M0	>7	any
		T2, N0, M0	>7	any
Grade III		T3, N0, M0	any	any
Grade IV		T4, N0, M0	any	any
		T, N1, M0	any	any
		T, N, M1	any	any

4.5 Prostate cancer treatments and resistance

Once patients are diagnosed and tumor aggressiveness is classified, treatment has to be chosen. Patients with low aggressive tumors (e.g., localized with low growth and progression) have very low risk of progression. In this scenario, the most common option is to continuously observe tumor progression by avoiding oncogenic treatment and its adverse effects as a first approach. On the other hand, patients with an aggressive tumor have to be treated as soon as possible.

The first approach is a surgical excision called radical prostatectomy, which extracts the prostate gland as well as seminal vesicle. Another alternative is the irradiation through external beam therapy or through implantation of radioactive seeds inside the prostate gland (brachytherapy). The second-line treatment is to reduce or eliminate androgen signaling. To address this point, surgical or chemical castration has to be performed. Surgical castration is realized by orchiectomy of the testis, while chemical castration is stimulated by LHRH analog treatment; in both cases, a decrease of serum testosterone is observed. Moreover, to achieve a total androgen ablation in advanced cancer, antiandrogen therapy (usually flutamide) should be offered (Loblaw et al., 2004). Antiandrogen therapy inhibits AR and prevent its activation through androgens, including those produced by the adrenal gland (Labrie et al., 1993). The combination of medical castration and antiandrogen therapy is called combined androgen blockade (CAB) and confers statistically significant clinical improvement of cancer regression. Thereby, this therapy is very effective because inhibition of the AR pathway leads to a reduction in proliferation and an increase in apoptosis of cancer cells. Unfortunately, after androgen deprivation, most PCs recur and became androgen-independent, leading to a metastatic state. In the case of advanced cancer that progresses in solitary lesions to the bone, chemotherapy -and in particular, docetaxel in combination with hormonal therapy and radiotherapy- should be offered. The most frequent type of combination consists of taxane-based chemotherapy (docetaxel) and synthetic corticosteroid analog (prednisone) (Berthold et al., 2008; Sturge et al., 2011; Tannock et al., 2004). However, the conventional use of chemotherapy and radiotherapy to treat the PC bone metastasis nowadays is mainly palliative.

5. Potential treatments of bone metastasis

Bone metastasis causes important complications, such pain, bone fragility, and hyercalcemia. It can be detected by high serum levels of bone-degradation markers, specifically amino terminal propeptide of type-1 collagen (NTX) and/or bone-formation markers, as ALPL. Radiotherapy, surgery, and pain medication can control the symptoms over short periods of time, but they cannot cure bone metastasis. Currently, some specific drugs are used to treat bone metastatic patients together with chemical, HER2-directed and hormonal therapies, if necessary, but better bone-modifying agents to prevent and treat bone metastasis are needed.

The two main drugs that are currently used to treat osteolytic or osteoblastic bone metastases are bisphosphonates and anti-RANKL antibodies. **Bisphosphonates** (BP) are stable synthetic analogues of pyrophosphate (PPi), an inhibitor of calcification. They bind to hydroxyapatite of the exposed mineralized bone matrix by preventing its breakdown by osteoclasts (Drake et al., 2008). Additionally, BP can be released and internalized by the osteoclasts, causing a disruption of the bone resorption process and promoting osteoclast apoptosis (Hughes et al., 1995; Russell and Rogers, 1999). *In vitro* assays have demonstrated the effects of BPs on tumor cells, which include increased apoptosis and reduced capabilities for adhesion, invasion, and proliferation (Denoyelle et al., 2003; Senaratne et al., 2000; Winter et al., 2008). BPs significantly reduce skeletal morbidity and complications (by 30-50%) in BC patients (Coleman, 2008; Paterson et al., 1993; Rosen et al., 2004). Similarly to bone metastasis treatment, BPs have been widely used on other skeletal diseases, such as Paget's disease and osteoporosis (Delmas and Meunier, 1997; Russell, 2006). Zoledronic acid (ZOL) and clodronate are the most frequently used (Coleman, 2001, 2004). They can be administrated as treatment of bone metastasis once lesions have already established or as a prophylactic treatment, although no significant benefit has been shown for the latter (Coleman et al., 2014; Saarto et al., 2001). On the other hand, **denosumab** is a humanized anti-RANKL monoclonal antibody that inhibits osteoclast-mediated bone destruction (Fizazi et al., 2009; Lacey et al., 2012). It has been approved for the treatment of postmenopausal osteoporosis and bone metastasis (Bekker et al., 2004; Dougall and Chaisson, 2006). Clinical trials have demonstrated that it is more efficient than BPs (Fizazi et al., 2011; Stopeck et al., 2010), and it has beneficial effects on both BC and PC patients (Brown and Coleman, 2012; Lipton et al., 2007; Smith et al., 2012).

Regarding experimental treatments on BC bone metastasis, several drugs have been studied as bone-modifying agents, to improve osteolytic lesions (Figure 17), including recombinant osteoprotegerin (OPG-Fc), PTHrP antagonists, and TGF-ß inhibitors. **Recombinant OPG** inhibits osteoclast differentiation, osteolysis, and skeletal tumor burden and increases bone density *in vivo* (Body et al., 2003; Fisher et al., 2006; Morony et al., 2001; Simonet et al., 1997) It is currently in a phase II clinical trial for BC patients. **PTHrP AN** is a neutralizing antibody to PTHrP that inhibits tumor growth in bone and reduces osteolytic lesions (Guise et al., 1996; Saito et al., 2005) which is in a phase II clinical trial for BC patients. **TGF-ß inhibitors** are used to reduce differentiation of osteoclasts in parallel of increasing osteoblast differentiation. Even though TGF-ß is a challenging target due to its divergent roles in tumor and bone microenvironments, preclinical models show the importance of this pathway in promoting osteolytic bone lesions (Ikushima and Miyazono, 2010; Mohammad et al., 2009, 2011). Finally, **radium-223 dichloride (Ra-223)** acts as a calcium mimetic and forms bone mineral complexes in areas with high bone turnover by binding to hydroxyapatite. There, it emits alpha-particles with short penetration. A phase III trial (ALSYMPCA) has demonstrated reduction in overall survival and bone pain with Ra-223 in PC patients (Bruland et al., 2006; Parker et al., 2013; Takalkar et al., 2014; Wenter et al., 2017).

For osteoblastic lesions, other drugs have been studied in pre-clinical trials, such as SRC kinase inhibitors and ET_A inhibitors. SRC kinase has been shown to contribute to PC tumor growth and metastasis as well as to bone metabolism; for this reason, **SRC kinase inhibitors,** including dasatinib, saracatinib, and bosutinib, have recently emerged as potential treatments for bone metastasis (Rabbani et al., 2010; Yang et al., 2010) and are being tested is in a phase II clinical trial. Specifically, dasatinib, a dual Src/Bcr-Abl tyrosine kinase inhibitor, stimulates osteoblast differentiation and downregulates RANKL formation by osteoblasts, thereby activating bone formation and inhibiting osteoclastogenesis (Id Boufker et al., 2010; Koreckij et al., 2009; Lee et al., 2010). On the other hand, **endothelin-A-receptor (ET_A) inhibitor** aims to block activation of osteoblasts and the consequent formation of osteoblastic lesions (Nelson et al., 1995; Yin et al., 2003). In clinical trial phase III showed improvement on PC patients survival.

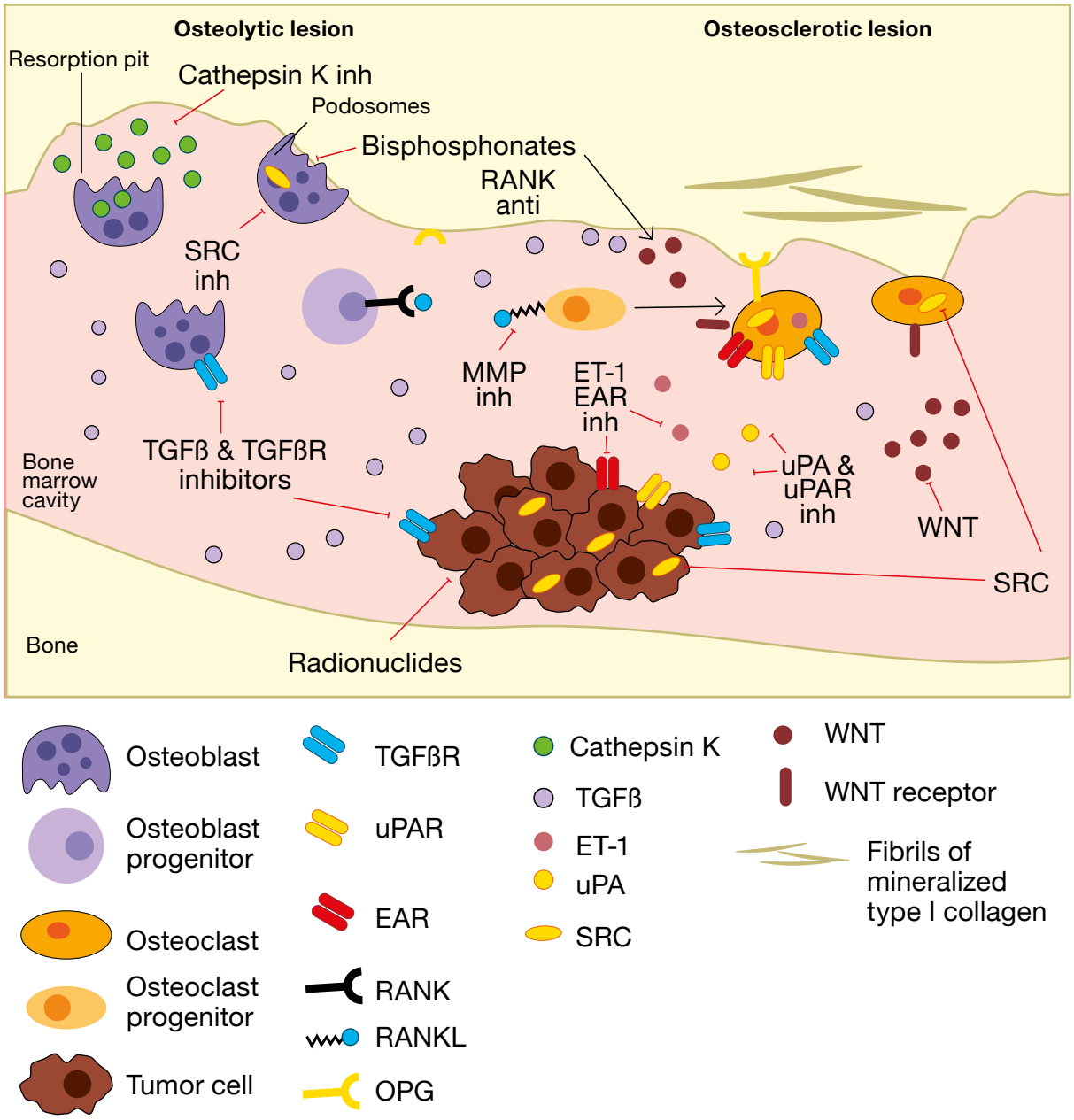

Figure 17. Bone-targeted therapy in PC metastatic lesions. TGF-ß is released from bone matrix due to bone resorption. Matrix metalloproteinases are released from tumor cells and activate RANKL released from osteoblast precursors. Osteoblast also secrete OPG, a decoy receptor that compete with RANKL to bind to RANK on the osteoclast precursors. Cathepsin K mediate bone degradation by forming assembly of podosomes via SRC-dependent and Rho GTPase-dependent pathways. ET-1, Wnt, TGF-ß and uPA are osteoblastic factors that drive formation of woven bone. Therapeutic approaches in ostelytic and osteoclerotic lesions include bisphosphonates, radionuclides, and targeted inhibition of RANKL, cathepsin K, SRC, EAR, TGF-ß and uPA. Abbreviations: ET-1, endothelin-1; EAR, ET-1 receotir; inh, inhibitor; OPG, osteoprotegerin; RANK, receptor activator of nuclear factor-κB; RANKL, RANK ligand; TGF-ß, transforming growth factor ß; uPA, urokinase-type plasminogen activator. Modified from Sturge et al., (2011); Loblaw et al., (2004).

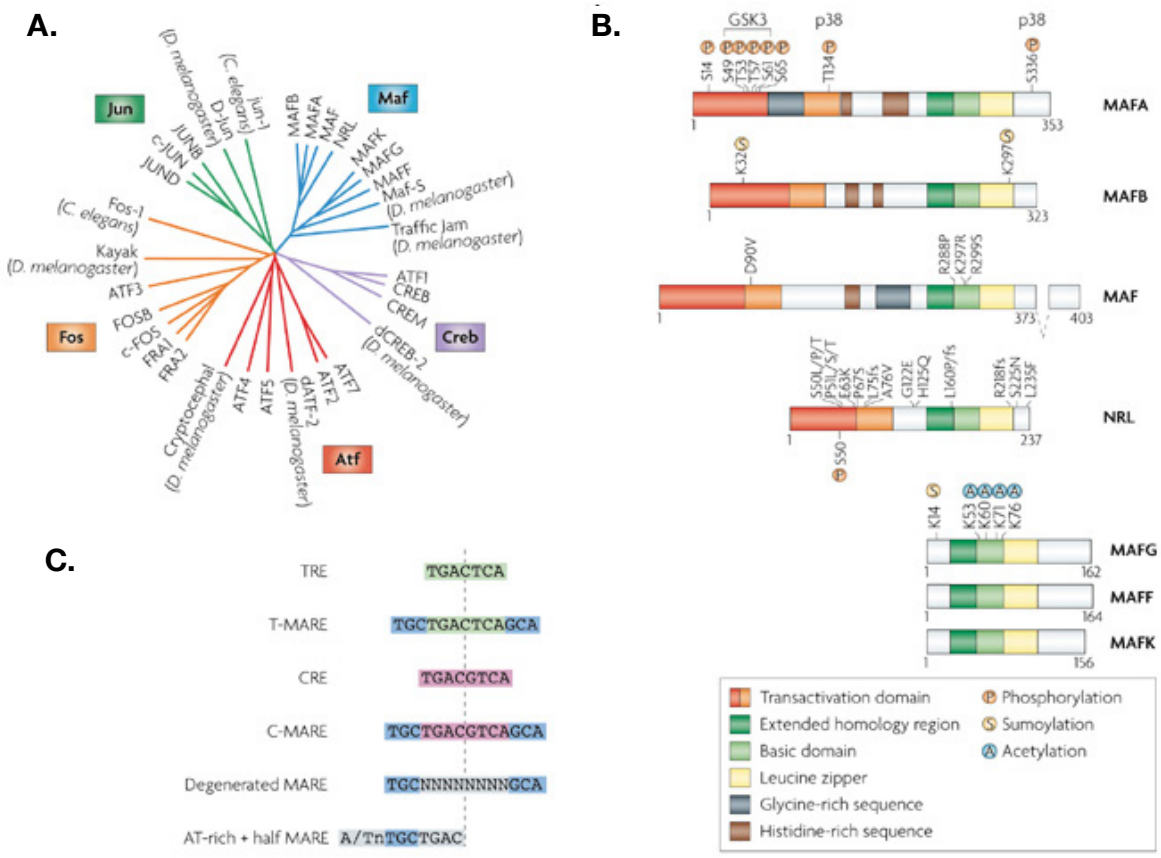

Figure 18. MAF superfamily. **A.** An unrooted phylogenic tree of the AP1 family of proteins. **B.** Schematic representation of human MAF protein structures. *MAF* is alternatively spliced, resulting in two isoforms that differ in their carboxy termini. **C.** Members of the AP1 family have different DNA recognition sequences: TRE (12-O-tetradecanoyl phorbol 13-acetate (TPA)-responsive element, CRE (cAMP-responsive element) and MAREs (Maf recognition elements). Maf proteins can bind to a T-MARE (containing a TRE core), a C-MARE (containing a CRE core), a degenerated MARE or a half MARE flanked by AT-rich sequences. Taken from Eychène et al., (2008).

Currently, bone-modifying agent therapy is recommended for patients with BC or PC with evidence of bone metastases; however, in terms of prevention, a lot of controversy has emerged. Specifically, although treatments seem to reduce skeletal morbidity, no significant improvements have been shown in terms of disease-free survival. In sum, identification of gene predictors for bone metastasis or/and for detection of patients who can potentially benefit from preventive treatment is a basic prerequisite. In this thesis, will focus on MAF, a potential biomarker of bone metastasis in BC patients.

6. MAF, a novel bone metastasis predictor

MAF transcription factors have recently emerged as powerful predictors for identifying patients who are at particularly high risk of developing bone metastasis (Pavlovic et al., 2015). MAF overexpression in the primary tumor of a subset of ER+ patients is associated with a high cumulative risk of metastasis to the bone.

6.1 MAF family of transcription factors

The *MAF* (v-maf avian musculoaponeurotic fibrosarcoma oncogene homolog) gene is located on chromosome 16q22-q23. MAF is a transcription factor member of the AP1 superfamily of basic leucine zipper (bZIP) proteins, which also includes the Fos, Jun, CREC, and ATF families. The MAF family comprises seven members that are classified into both large and small MAF. Large MAF members compromise MAFA (or L-MAF), MAFB, MAF (or c-MAF), and NRL, while MAFF, MAFG, and MAFK comprise the small MAF group. Both groups share extended homology region (EHR), basic domains, and a leucine zipper domain. In contrast, they differ in their transactivation domains, which are only present in the large MAF group (Figure 18) (Eychène et al., 2008).

All MAF family, as well as general AP1 superfamily, can bind to TRE (12-O-tetradecanoyl phorbol 13-acetate (TPA)-responsive element) or CRE (cAMP-responsive element) DNA sequences through their bZIP domain (Vinson et al., 2006). Their bZIP domain concedes the capacity to form heterodimers or homodimers, which is indispensable for DNA binding. However, small and large MAF proteins cannot heterodimerize together. EHR gives the MAF family proteins the capacity to recognize longer palindromic sequences, called MARE (Maf-recognition element) (Figure 18). The basic domain of the protein contacts the TRE or CRE core sequences in the DNA, while the EHR domain contacts the TGC flanking sequences (Kataoka, 2007; Yang and Cvekl, 2007).

In general terms, large MAF proteins can bind to co-activators and activate transcription, while small MAF proteins repress transcription and compete with large MAF proteins for promoter binding (Chen et al., 2002). Therefore, the ratio between small MAF homodimers and large MAF-containing complexes might have important biological consequences (Motohashi et al., 2000). Alternatively, large MAF proteins can positively autoregulate its own expression, as MARE sequences are present in MAF, MAFB, and MAFA promoters (Sakai et al., 2001).

Large MAFs are transcription factors that regulate genes involved early during tissue specification, and later in terminal differentiation in many tissues, such as bone, brain, kidney, lens, pancreas, retina, epidermis, and blood (Cordes and Barsh, 1994; Imaki et al., 2004; Lecoin et al., 2004; Lopez-Pajares et al., 2015; Yang and Cvekl, 2007). Concretely, MAF enforce T helper C cells, lens, and chondrocyte cell differentiation (MacLean et al., 2003). MAF-transforming activity is controlled by post-translational modifications, including GSK-3-dependent phosphorylation, ubiquitylation, and sumoylation (Rocques et al., 2007). Importantly, as described in the following section, MAFs have also been implicated in tumorigenesis.

6.2 MAF and its key role in oncogenesis

Large MAF proteins have been directly involved in carcinogenesis as demonstrated in cell culture, animal models and human cancers. In contrast, small MAF proteins have not shown oncogenic activity to date (Eychène et al., 2008). The first member of the MAF family identified was *v-maf*, discovered as a transforming gene of avian musculoaponeurotic fibrosarcoma virus, AS42 (Kataoka et al., 1993; Nishizawa et al., 1989). It was at this point that *c-maf (MAF)* was described as a proto-oncogene with the capacity to transform cells. *MAF* gene encodes two isoforms generated through alternative splicing: MAF short (MAF S) and MAF long (MAF L). Noteworthy, (Chesi et al., 1998) described a frequent dysregulation involving immunoglobulin heavy chain (IgH) locus and *MAF* gene translocation t(14;16)(q32.3;q23) in 5-10% of all human multiple myeloma (MM) lines. Surprisingly, the percentage of translocation did not correlate with the massive presence of MAF overexpression in 50% of MM patients (Kuehl and Bergsagel, 2002; Seidl et al., 2003). Moreover, MAF overexpression was found in another type of cancer, specifically in 60% of human angioimmunoblastic T-cell lymphomas (AITLs) (Murakami et al., 2007a). Finally, genetically engineered mouse (GEM) with MAF overexpression in T cells are able to develop T-cell lymphomas (Morito et al., 2006).

MAF together with *MAFA* display the strongest oncogenic activity, whereas *MAFB* is less effective in transforming cells, and *NRL* has no transformation capacity. The transforming activity of the MAF proteins depends on their ability to act as transcription factors (Kataoka et al., 2001; Nishizawa et al., 2003; Pouponnot et al., 2006). For instance, some MAF target genes, such as those for cyclin D2, integrin ß7, and ARK5, have deregulated

expression in MM, AITL, and *MAF* transgenic mice (Hurt et al., 2004; Morito et al., 2006; Murakami et al., 2007b; Suzuki et al., 2005; Zhan et al., 2006).

MAF activates expression of *cyclin D2* in MM and AITL that stimulates cell cycle progression and therefore, enhance tumor cell proliferation. Thus, it is believed that MAF promotes cancer cell proliferation by activating cell cycle progression rather than due to any anti-apoptotic activity (Bergsagel et al., 2005; Eychène et al., 2008). MAF also control genes associated with the invasion process, such as *ARK5* and *CXCL12*. ARK5 is an AMP-activated protein kinase (AMPK)-related protein kinase normally regulated by Akt that promotes tumor cell survival. ARK5 has been shown to promote IGF-1 secretion, thus playing an important role in cell invasion, and is highly associated with colon cancer progression (Hurt et al., 2004; Kienast and Berdel, 2004; Suzuki et al., 2004). Adhesion is also modified by MAF overexpression, which promotes the expression of integrin ß7 in MM. Integrinß7 binds to E-cadherin localized on the surface of bone marrow cells and promote myeloma adhesion to the bone. Integrinß7/E-cadherin binding promotes production of the proangiogenic factor VEGF, which in turn enhances cellular proliferation and adhesion (Hurt et al., 2004; Kienast and Berdel, 2004).

6.3 MAF in breast cancer bone metastasis

Since identification of new markers of bone metastasis was one of the main challenges in the field, our laboratory developed an experimental xenograft mouse model to obtain cells with a higher propensity to metastasize to bone. Injection of MCF7, a human ER+ BC cell line, was performed in the left ventricle of BALB/c nude mice, and bone metastatic cells were selected and expanded *in vitro*. After three rounds of injections, a MCF7 derived cell line (called BoM2) with a higher propensity to metastasize to bone than the parental cell line was obtained. A comparative study of copy number alterations (CNA) among these two cell lines, complemented with a study of CNA associated with high risk to bone metastasis in ER+ BC patients, found a common 16q22-24 chromosomal gain that later was associated with *c-Maf* overexpression. We were then able to describe, for the first time, the propensity of the *MAF* gene to serve as a predictor of BC bone metastasis (Pavlovic et al., 2015). Moreover, we found that high MAF protein staining is associated with a cumulative risk of bone metastasis in ER+ patients, but was not associated with other non-visceral and visceral sites (Figure 19).

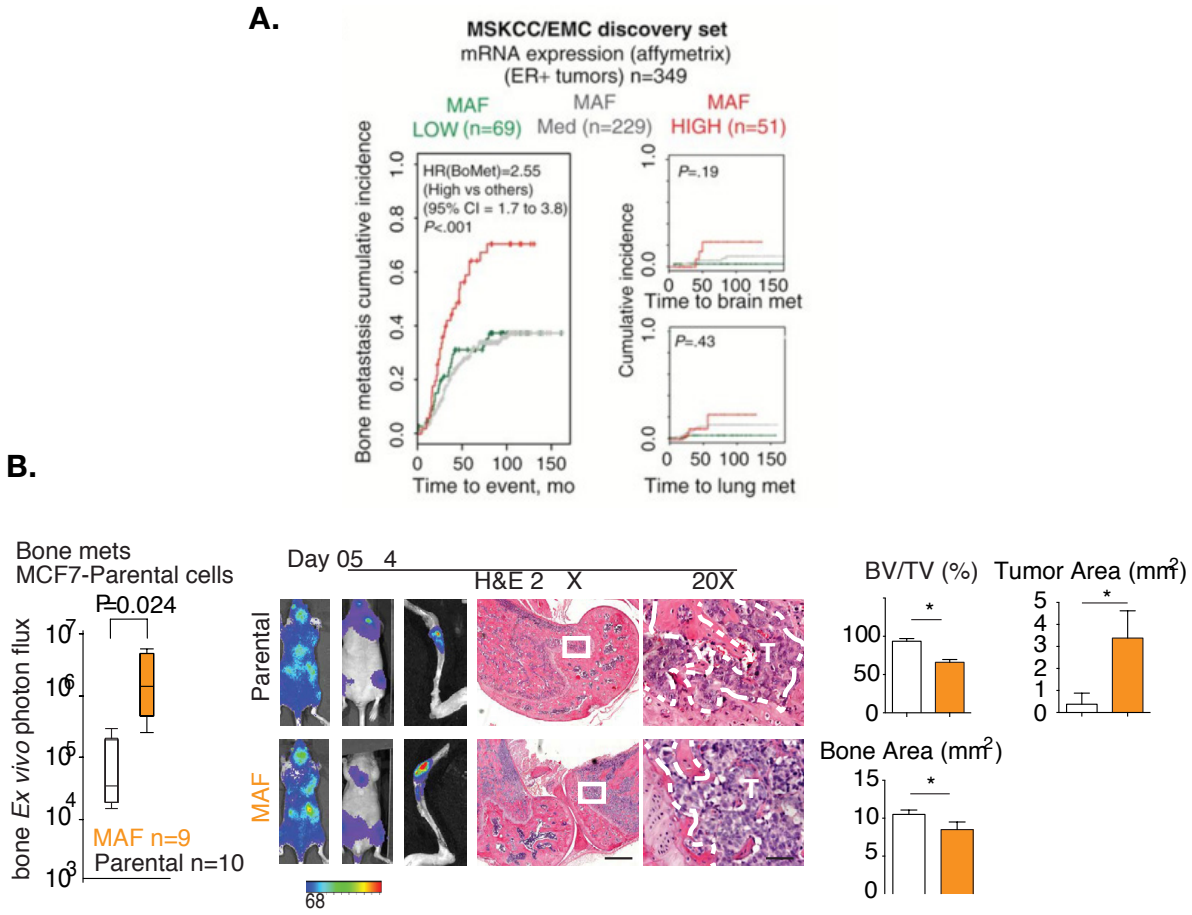

Figure 19. MAF is a predictor gene to bone metastasis. **A.** Cumulative incidence plot of bone, brain, and lung metastasis in ER+ primary BC patients. High MAF expression in the primary tumor is associated with high bone metastatic incidence, but not with brain or lung metastasis. **B.** Quantification of ex vivo bioluminescent signals in hind limbs of mice inoculated with MAF-overexpressing MCF-7 parental cells. Representative bioluminescent images of ex vivo hind limbs at endpoint, with representative CT scans and representative H&E staining of bone metastasis for each group, are shown. Histomorphometric analysis for bone metastasis lesions is depicted (BV/TV, bone area, tumor area). Adapted from Pavlovic et al., 2015.

We performed further xenograft experiments using overexpression or downregulation of *MAF* in a panel of BC cell lines to validate previous results, including orthotopic injection to the mammary gland, left-ventricle injections, and intratibial inoculations. In all cases, *MAF* manifests as a mediator of bone metastasis in all BC cell lines setting. In addition, PTHrP implication downstream of MAF signaling pathway was identified as one of the potential mechanisms driven by MAF transcription factor to colonize the bone.

To better extrapolate these results into a clinical setting, developing a mouse model of BC bone metastasis emerged as a top priority.

On the other hand, MAF has recently been described as a biomarker able to identify patients who may benefit from treatment with and adjuvant bisphosphonate. Tumor samples from the AZURE trial were used; AZURE is a randomized phase III trial that compares tumor evolution from women with stage II/III BC treated with standard adjuvant systemic therapy alone or with ZOL (clinicalTrials.gov identifier: NCT00072020). Patient BC was classified on MAF+ or MAF- tumors through a FISH analysis and a MAFTEST (Inbiomotion), and effects of ZOL were evaluated. ZOL-treated patients with MAF- tumors present better invasive disease-free survival (IDFS) than patients treated with standard therapy. In contrast, patients with MAF+ tumors show no improvement for disease outcome. Strikingly, non-postmenopausal patients with MAF+ tumors treated with ZOL present worse outcomes compared to standard therapy–treated patients. This study suggests MAF as a biomarker able to classify patients who may benefit from ZOL adjuvant treatment (MAF-), and that it can distinguish them from those who may not benefit from ZOL administration (non-postmenopausal MAF+) (Coleman et al, 2017 The lancet oncology).

- O b j e c t i v e s -

Hypothesis

Bone metastasis remains a poorly understood and incurable disease. We hypothesized that different cancer types rely on common mediators to develop bone metastasis. We also hypothesized that as a driver of BC bone metastasis, MAF is a potential therapeutic target to prevent this disease. Moreover, only through proper understanding of MAF molecular contribution to mammary gland development and tumor formation we might comprehensively provide new therapeutic opportunities.

Aims

To test whether MAF drives bone metastasis in prostate cancer.

To validate MAF as a therapeutic target against bone metastasis.

To determine MAF contribution to bone metastasis preventive therapies.

To analyze MAF function during mammary gland development.

To unravel the molecular mechanism responsible for MAF mediated breast cancer bone metastasis.

- R e s u l t s -

Chapter I:
MAF in prostate cancer bone metastasis

Introduction

Previous work in our laboratory identified MAF as a mediator of bone metastasis in breast cancer (BC) patients (Pavlovic et al., 2015). Identification of genes that orchestrate bone colonization would be a great advance for our understanding of metastasis progression as well as an opportunity to develop novel metastatic-specific treatments. Undoubtedly, following this finding, some questions emerged, including whether MAF is a bone metastasis–specific mediator in all cancer types or is specific for BC. To this aim, we focused on prostate cancer (PC), a cancer with high propensity to metastasize to bone and with no evidence of genes that mediate skeletal colonization. Similar to BC, PC is also characterized by the strong influence of hormones on tumor initiation and growing capabilities. To address this unanswered question, we took advantage of the most frequently used PC cell lines in xenograft experiments, summarized in Table 7.

Table 7. PC cell lines used in bone metastasis research. Abbreviations: AR, androgen receptor; IC, intracardiac injection; IF, intrafemoral injection; IT, intratibial injection; IV, intravenous injection into human bone implanted animals; PC, prostate cancer; PSA, prostate-specific antigen. Modified from Dai et al., (2016).

Cell line	Origin	PSA	AR	Bone lesion	Model	References
DU145	Central nerve system met (Stone et al., 1978)	-	-	Osteolytic	IT, IC, IV	(Conley-LaComb et al., 2013; Nemeth et al., 1999; Yin et al., 2007)
PC-3	Vertebral bone met (Kaighn et al., 1979)	-	-	Osteolytic	IT, IF, IC, IV	(Chu et al., 2008; Nemeth et al., 1999; Wu et al., 1998; Zhang et al., 2012)
LNCaP	Lymph node met (Horoszewicz et al., 1980)	-	-	Osteoblastic Osteolytic	IF, IV	(Nemeth et al., 1999; Wu et al., 1998)

Intracardiac (IC) and intratibial (IT) inoculations are the most common models used in the field of bone metastatic research. IC injection introduces the cells into the blood circulation, with a cell distribution that should be throughout the entire organism. Notably, IC inoculation bypasses the early steps in the metastatic process and can be considered as a dissemination assay rather than a true metastatic process. On the other hand, IT injection is the model used to study capacity of specific cells to colonize bone.

Results

Analysis of selected CNG in a discovery training set of PC patients

Regarding the powerful effects of MAF on stratifying BC patients with high risk of developing bone metastasis, and considering the high percentage of bone metastases derived from PC, we hypothesized that MAF could have an analogous role of driving bone metastasis also in PC patients. We analyzed 64 samples of primary PC tumors from patients with annotated clinical follow-up. The copy number gain (CNG) of the 16q23 region has been previously associated with *MAF* gene amplification. From 40 patient samples with ≤2.5 CNG of *MAF*, 92.5% showed no metastasis after 5 years of follow-up. This number is reduced to 21.4% for patients with tumors with >2.5 CNG. Markedly, bone metastasis was present in 64.3% of these patients, and soft tissue colonization, 14.3%; whereas in ≤2.5 CNG of *MAF* was 2.5% and 5%, respectively (Figure 20). Thus, DNA amplification in the 16q23 region was significantly associated with bone metastatic risk in this clinical series.

	CN≤2.5	CN>2.5
No metastasis	37	3
Visceral metastasis	2	2
Bone metastasis	1	9

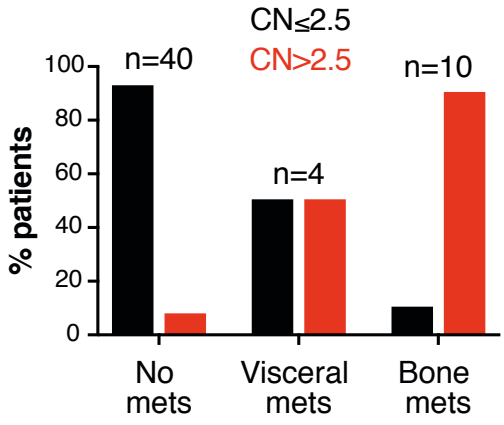

Figure 20. Association between CNG and pattern of metastasis. Analysis of *MAF* CNG from 64 patient tumor samples, and correlation with site of metastasis at 5-year follow-up.

Endogenous expression of *MAF* in PC cell lines

Next, we aimed to validate the importance of MAF in PC tumors by using cell lines such as PC-3, DU-145, and LNCaP in xenograft models. As a first approach, we paraffin-embedded pellets of LNCaP, PC-3, and DU-145 cell lines and analyzed the amplification of 16q23 genomic DNA region by fluorescence *in situ* hybridization (FISH) (Figure 21). We observed that 63.08% of LNCaP cells 28.87% of PC-3 cells, and 34.12% of DU-145 cells had more than 2 copies of the 16q23 region.

As cancer cells have intrinsic genomic instability and are prone to polyploidy, we determined the CNG of another region of the genome, specifically, the 14q chromosome, by means of 14q32 region alteration. Using a MAF gene–specific probe and comparing to 14q32 value, we eliminated the variable of general chromosomes amplification and filtered the gain of 16q23 specific area. LNCaP cells contained the highest gain of 14q32 region (average of 2.23), followed by PC-3 (average of 1.92) and then DU-145 (average of 1.72). Normalization of the 16q23 amplification (MAF) with the FISH 14q32 probe showed a gain of *MAF* of 54.62% of 16q23/14q32 ratio in LNCaP cells, and lower percentages for PC-3 and DU-145 cells, of 38.73% and 42.35%, respectively (Figure 21B). These results suggest that LNCaP cells—the only androgen-dependent PC cell line tested—present higher amplification of 16q23 region than has been associated to an amplification of *MAF* gene.

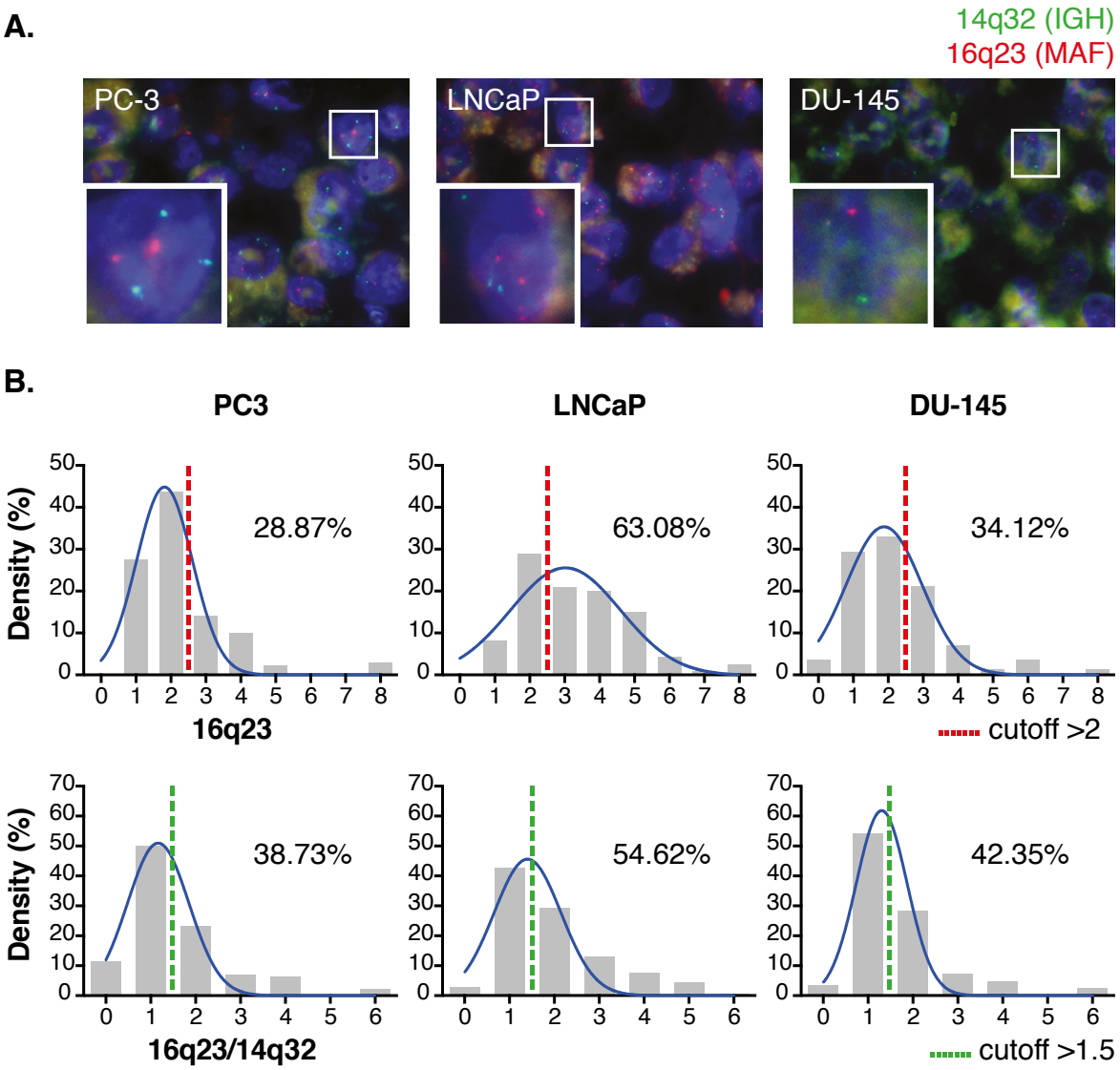

Figure 21. Amplification of the 16q23 genomic DNA region in PC cell lines. **A.** Representative images of stained PC-3, LNCaP, and DU-145 cells by FISH. The 16q23 probe is shown in red, and 14q32 probe, in green. **B.** Top: Kernel density plots representing the density of the various 16q23 genomic region copy number populations. A cutoff of 2 was used to score CNG and is shown as a red dashed line. Bottom: Kernel density plots depicting the ratio between 16q23 region copies and 14q32 region copies. A cutoff of 1.5 was used and is shown with a green dashed line. Percentage of cells above the cutoff is shown. The number of cells scored is 142 PC-3 cells, 260 LNCaP cells, and 85 DU-145 cells.

To confirm an association between 16q23 genomic amplification and MAF expression, we analyzed endogenous *MAF* gene expression in the above-mentioned PC cell lines, both at the mRNA and the protein levels. We determined MAF long (MAF L) isoform mRNA expression by qRT-PCR using a TaqMan probe (Figure 22A). LNCaP showed a higher expression of MAF L than either PC-3 or DU-145 cells. Of note, the mRNA levels of MAF L in LNCaP cells represents 29.3% of those observed in BoM2 cells, a BC cell bone derivative line that highly expresses MAF. In contrast, PC-3 and DU-145 cells presented almost no detectable expression of MAF L mRNA in basal conditions.

Furthermore, we tested whether MAF mRNA expression correlates with MAF protein levels by Western blot. We observed low levels of the MAF L protein in PC-3 and DU-145 PC cell lines, and higher levels in LNCaP cell lines, consistent with mRNA levels (Figure 22B). Nevertheless, all of them presented lower levels of MAF L compared to BoM2 cells. On the other hand, all PC cell lines tested showed similar levels of MAF short (MAF S) expression. These results confirmed the relationship between 16q23 genomic gain with both MAF mRNA and protein expression levels.

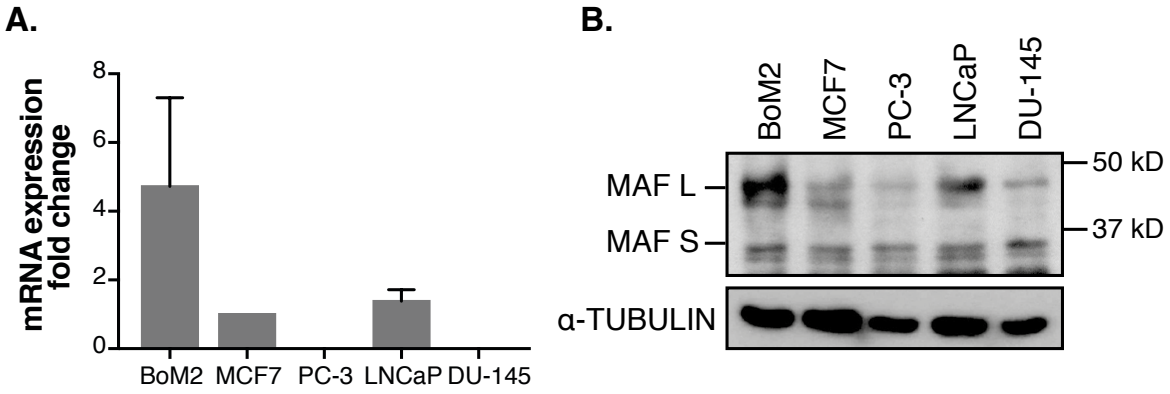

Figure 22. *MAF* expression levels in PC-3, LNCaP and DU-145 PC cell lines as compared to BC BoM2 and MCF7 parental cell lines. **A.** Gene expression levels of MAF L isoform determined by qRT-PCR using TaqMan probe and normalized to B2M levels. *MAF L* levels were referred to MCF7 *MAF* levels. Data are shown as mean ± SD from 3 biological replicates. **B.** Western blot depicting MAF protein levels in BC and PC cells. α-tubulin was used as a loading control.

Overexpression of *MAF* in prostate cancer cell lines

In order to study the effect of MAF in bone metastasis PC, we used a gain- and loss-of-function approach. We overexpressed or downregulated MAF in the PC cell lines, depending on their MAF endogenous levels. Since we showed that DU-145 and PC-3 cells have low basal levels of MAF, we overexpressed MAF S and MAF L isoforms in those cells. We infected cells with pBabe Puro empty plasmid (mock cells) or, alternatively, with pBabe Puro MAF S and pBabe Puro MAF L (MAF cells) plasmids simultaneously. Next, we validated MAF S and MAF L overexpression in terms of protein and mRNA expression (Figure 23A). qRT-PCR data confirmed MAF overexpression by means of mRNA. Accordingly, we could verify a huge overexpression of both MAF protein isoforms in MAF S/L overexpressing (OE) cells as compared to control cells (Figure 23B). In contrast, MAF was downregulated in LNCaP cells, the androgen-dependent cell line that has high levels of endogenous MAF in basal conditions. To this aim, we infected LNCaP cells with pLKO shMAF or alternatively with pLKO empty vector (mock cells). Validation of MAF downregulation of mRNA and protein levels was performed by qRT-PCR and Western blot analyses (data not shown). All cells were infected with the TGL vector and sorted by GFP expression. The TGL vector is a retroviral vector that encodes a triple-fusion protein composed of tyrosine kinase, eGFP, and luciferase. Luciferase expression is used to track cancer cells *in vivo* by quantitative bioluminescence imaging, while eGFP fluorescent protein support cell sorting and *ex vivo* detection of the infected cells.

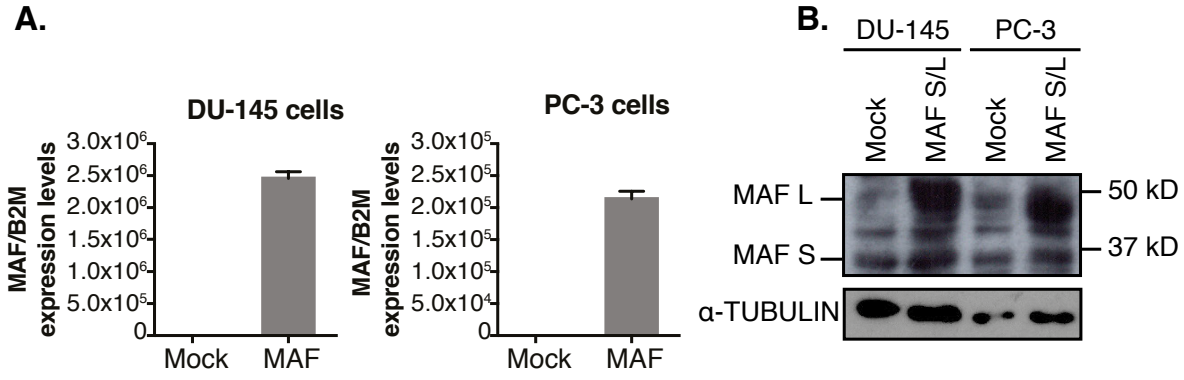

Figure 23. *MAF* expression levels in androgen-independent PC cells co-transfected with MAF S and MAF L spliced isoform expression constructs or, alternatively, with control plasmid (mock). **A.** MAF L expression levels were determined by qRT-PCR using TaqMan probe, normalized to B2M levels and compared to mock levels of DU-145 cells (left panel) and PC-3 cells (right panel). Data are shown as mean ± SD from two biological replicates **B.** Western blot analysis of MAF and α-tubulin proteins in control and overexpressing PC cells lines.

MAF does not mediate bone metastasis in androgen-independent PC cell lines

We next tested the contribution of MAF to bone colonization in genetically-modified PC cells. We injected $5x10^5$ cells into the left ventricle of 10-week-old male BALB/c nude mice. IC inoculation mimics the spread of metastatic cells in the circulation and is used to study extravasation, homing and spontaneous colonization to distant organs. Cells were monitored in terms of bioluminescent imaging (IVIS imaging).

Mice were sacrificed 44 days after inoculation; at this point, LNCaP shC and shMAF cells did not show any metastatic growth (data not shown). However, bone and lung metastatic growth was detected in PC-3 and DU-145 cell inoculations. DU-145 bone metastasis free survival rates did not differ between control and MAF S/L OE cells ($P = 0.5237$) where less than 25% of mice developed symptomatic bone metastasis (Figure 24). Bone metastasis was considered positive when bone BLI signal crossed BLI signal of day of injection (day 0). Even though no differences were observed between groups in the percentage of bone metastatic *ex vivo* lesions, MAF S/L OE group showed a trend towards bigger lesions (Figure 24C). In contrast, less capacity to colonize soft tissues, especially lung, was detected in MAF S/L OE group (Figure 24D). Moreover, after IC injection, neither DU-145 cells nor PC-3 cells showed significant differences in the capacity to initiate bone metastatic lesions (Figure 25), even though PC-3 presented a higher propensity to metastasize than DU-145. BLI quantification showed no significant differences in lung colonization between control and MAF OE groups. These results suggest that overexpression of MAF is not enough to mediate bone metastasis of PC-3 and DU-145 PC cell lines.

Next, we studied the role of MAF-supporting PC cell growth in the bone microenvironment. To this end, we inoculated control and MAF S/L OE cells via IT injection. No metastatic growth was observed in LNCaP cells inoculated into the tibia (data not shown). In contrast, DU-145 and PC-3 cells showed bone metastatic growth capacity. However, MAF S/L OE DU-145 cells showed similar capacity to colonize bone as control cells ($P = 0.5237$). After PC-3 cell inoculation, MAF overexpressing cells showed less capacity to colonize the bone (Figure 26). Altogether, these results suggest that MAF cannot orchestrate bone colonization in the two androgen-independent PC cell lines tested, although in some contexts it may favor metastasis mobilization.

Collectively, although strong association between *MAF* and bone metastasis has been described in a clinical context, no correlation was observed in experimental mouse models.

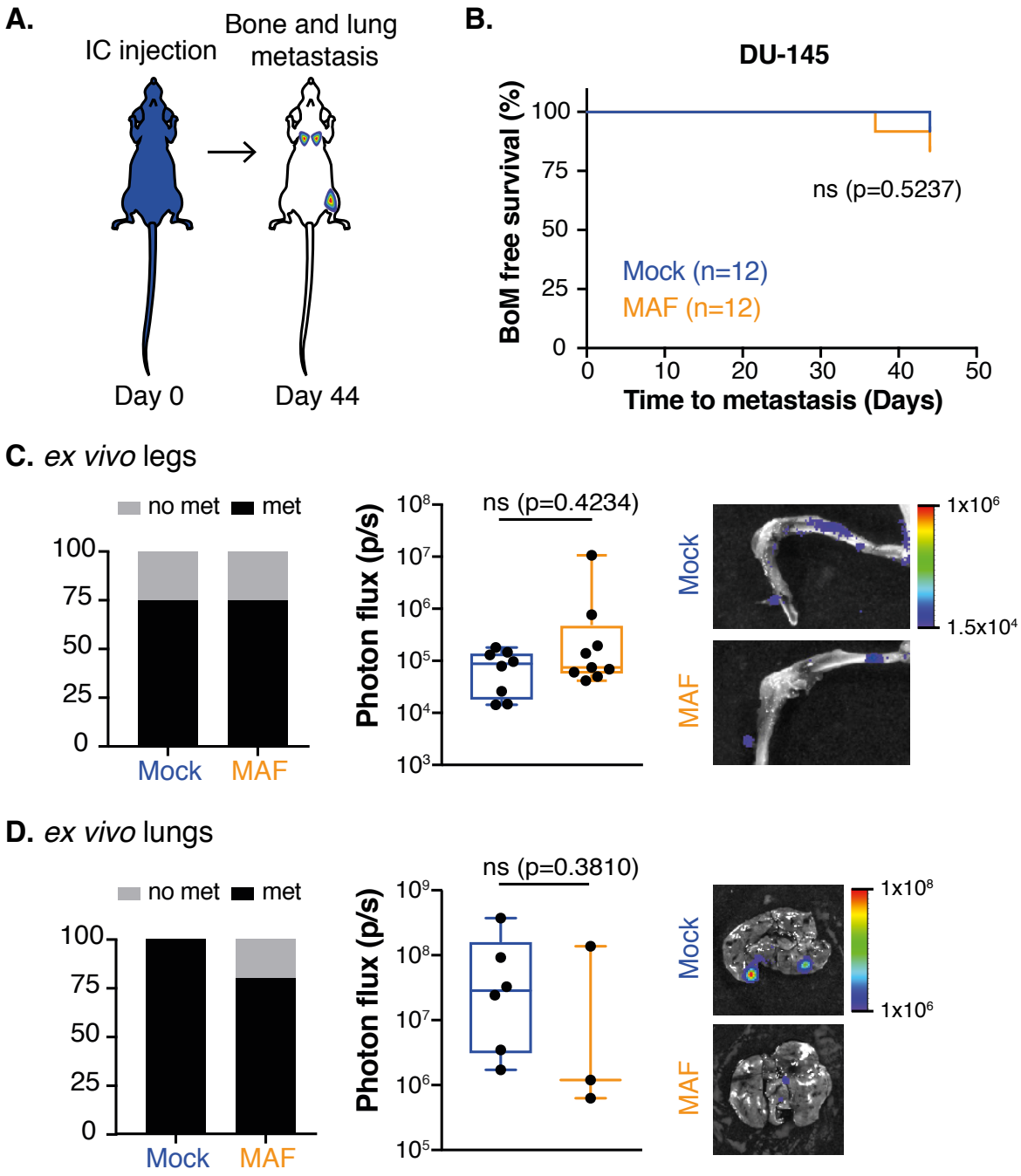

Figure 24. MAF does not mediate bone or lung metastasis in DU-145 cells. **A.** Schematic representation of IC injection and metastasis detection at the sacrifice day. **B.** Kaplan-Meier curve of bone metastasis (BoM)-free survival between control and MAF S/L OE infected cells. *P*-value was obtained using log-rank test. **C.** Comparative analysis of legs with or without *ex vivo* lesions in mice inoculated with control and MAF S/L OE cells. Signal quantification from tibia with metastatic lesion was represented. Representative BLI showing *ex vivo* bone metastasis of control and MAF S/L OE cells at day 44. **D.** Percentage of lungs with BLI signal from mice inoculated with genetically-modified DU-145 cells. Lung metastasis *ex vivo* BL quantification. BLI of representative *ex vivo* lung metastasis of Mock and MAF S/L OE cells. Data are represented by box plot with median, IQR, and min and max values. *P*-value was scored by two-sided Mann-Whitney test.

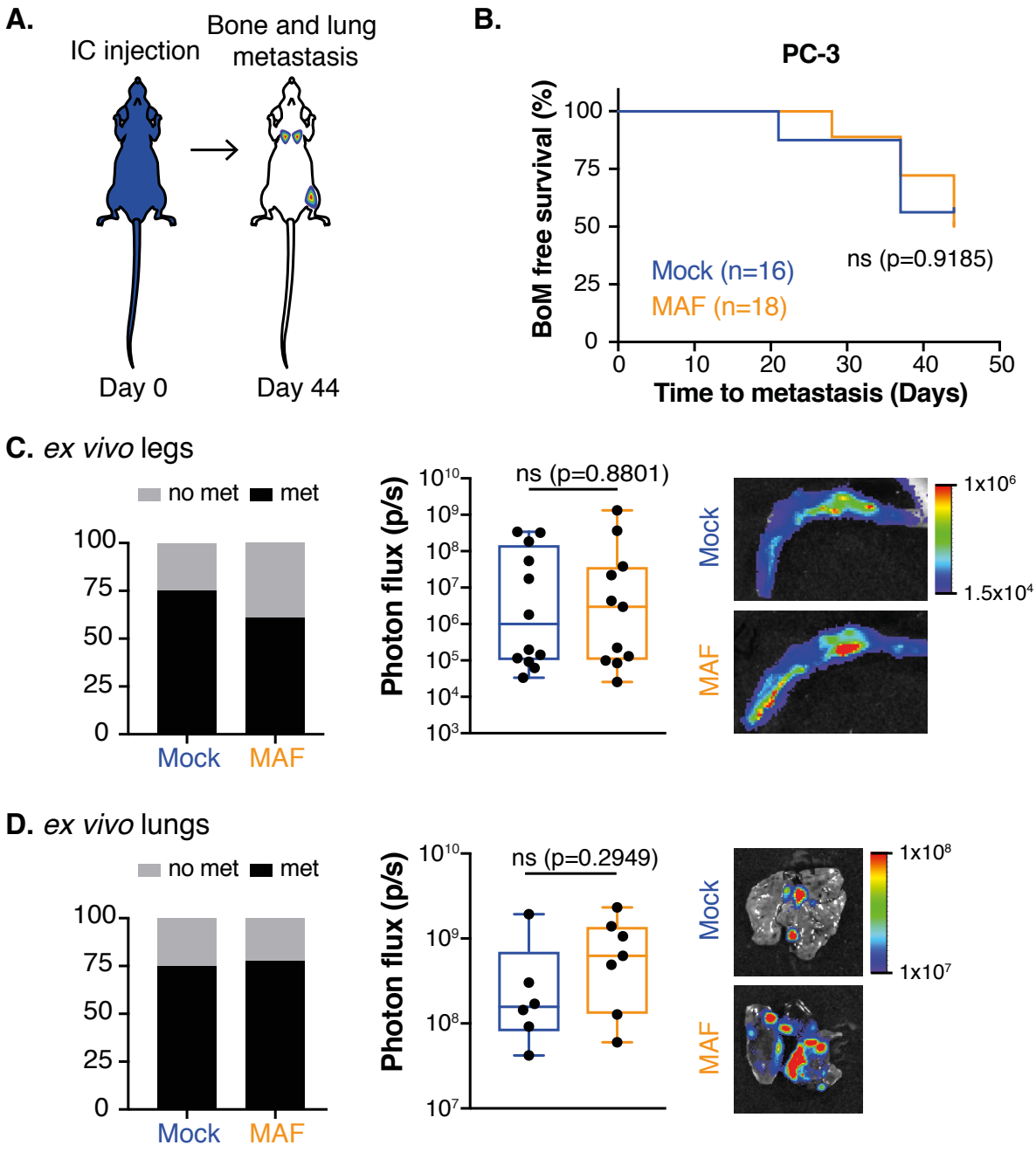

Figure 25. Bone and lung metastasis were not driven by MAF in PC-3 cells. **A.** Schematic of intracardiac injection and metastatic detection. **B.** Kaplan-Meier analysis of bone metastasis-free survival comparing control and MAF S/L OE PC-3 cells. *P*-value was obtained using log-rank test. **C.** Percentage of bone metastatic lesions in mice inoculated with gentetically-modified PC-3 cells. Box plot representing quantification of bone metastatic *ex vivo* lesions of PC-3 cells. Representative BLI pictures of *ex vivo* bone metastasis from control and MAF S/L OE cells. **D.** Percentage of lung metastasis in mice inoculated with control and MAF S/L OE PC-3 cells. *Ex vivo* bioluminescent quantification of lung metastasis. Representative mock and MAF S/L OE cells BLI of *ex vivo* lung metastasis. Data are represented by box plot with median, IQR and min and max values. *P*-value was scored by two-sided Mann-Whitney test.

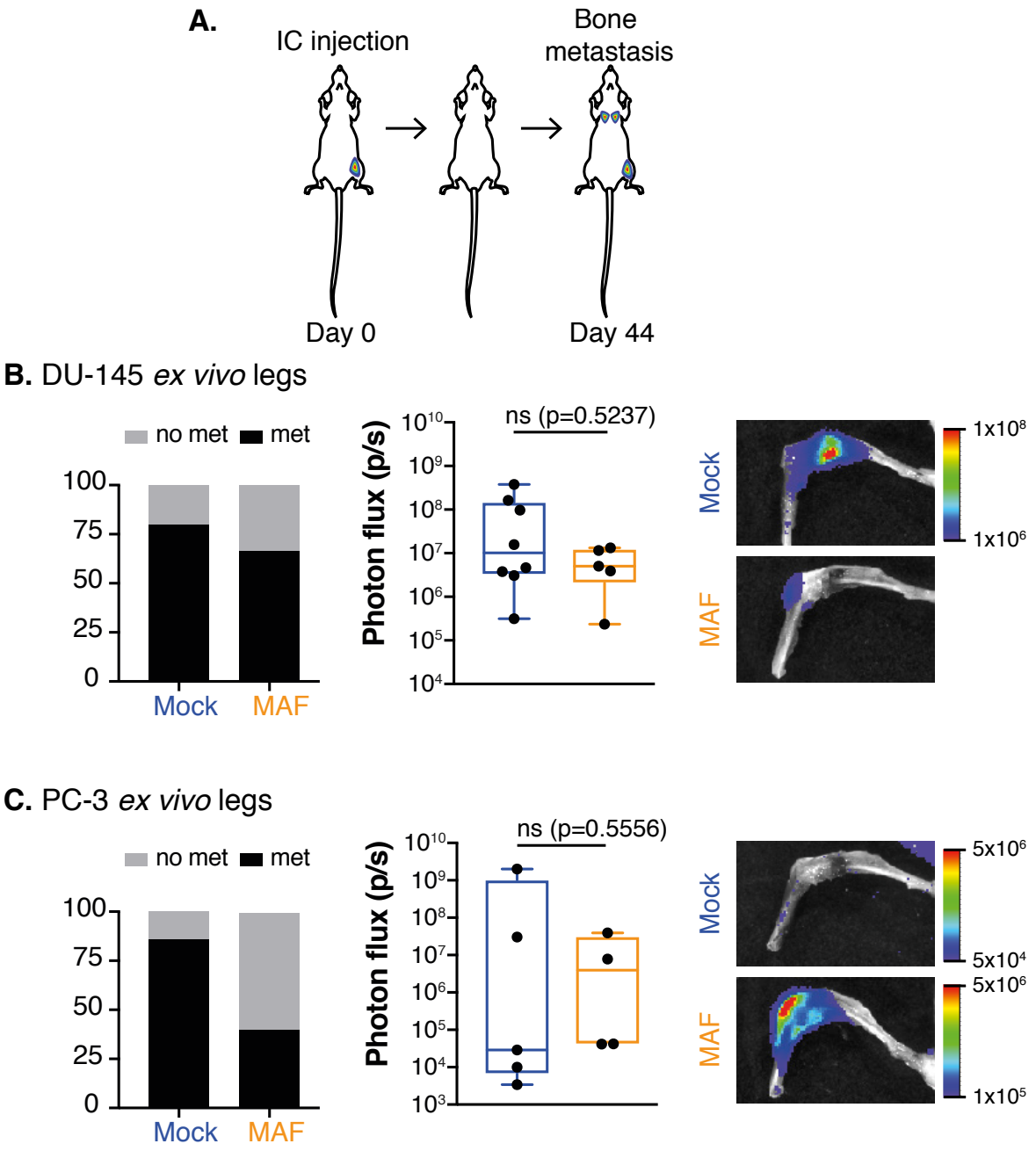

Figure 26. MAF does not promote bone colonization on PC-3 and DU-145 cell lines. **A.** Schematic representation of intratibial injection and metastasis detection. **B.** Percentage of bone metastasis in mice inoculated with DU-145 cells. BLI signal quantification is represented by box plot analysis. Representative images of bone metastasis from control and MAF OE DU-145 cells. **C.** Percentage of bone metastasic lesions in mice inoculated with MAF S/L and control PC-3 cells. Bone metastasis *ex vivo* quantification. Lung representative bioluminescent images obtained by IVIS system. Data are represented by box plot with median, IQR, and min and max values. *P*-value was scored by two-sided Mann-Whitney test.

Chapter II:
MAF in bone metastatic prevention

Introduction

Currently, a handful of drugs are administrated to bone metastatic patients to reduce lesion symptoms such as relieve skeletal pain, and reduce skeletal complications. These drugs cannot cure bone colonization. Once tumor cells reach the bone, BC progression became unstoppable. ZOL is the drug most commonly administrated in bone metastatic treatment, a third-generation of bisphosphonate that reduces bone matrix degradation and promotes osteoclast apoptosis. Its role on preventing bone metastasis is still under consideration.

In this thesis, we aimed to test the effect of MAF on bone metastatic prevention by means of two different experimental approaches. The first approach is to determine the effect of MAF downregulation as a potential new alternative to prevent bone metastasis comparing to the current treatments. The second approach aims to establish a relationship between MAF overexpression tumors and the responsiveness to current preventive treatments.

Results

Modeling early BC adjuvant treatment

A main aim is to validate the importance of MAF in BC bone metastasis, and to determine whether it could be a targetable pathway to generate new drugs. For this, we compared the effect of MAF downregulation in BC cells with treatments used currently in the clinical setting, such as ZOL, or with other potential drugs previously tested in clinical trials, including recombinant OPG and PTHrP antagonist.

We used BoM2, a MCF7-derived cell line generated after three rounds of IC injections and isolated from a bone metastatic clone (Pavlovic et al., 2015). BoM2 cells have a high propensity to metastasize specifically to bone, which has been associated with a high *MAF* gene copy number content. These cells were labeled with a TGL plasmid that drives the

expression of luciferase and eGFP proteins. BoM2 cells were then infected either with a short-hairpin control (shC) lentivirus or with a short-hairpin targeting MAF (shMAF), which caused a 90% reduction of MAF expression by means of mRNA (Figure 27). Next, 9-week-old Balb-c nude female mice were randomized into 5 groups (n = 10 mice/group). Four groups were IC injected with $0.5x10^6$ BoM2 shC cells, and the fifth group, with BoM2 shMAF cells. To evaluate the effect of current treatments versus MAF depletion gene on bone metastasis lesions, mice inoculated with shC BoM2 cells were treated from day 0 with PBS, OPG, ZOL, or a PTHrP antagonist, whereas BoM2 shMAF cells were treated with PBS (injection procedure is summarized in Table 8). In order to ensure the effect of ZOL, we administrated a high-dose (0.5 mg/kg), a concentration that increases bone mineral density (BMD) and bone mineral content (BMC). Metastatic growth was monitored every week by luciferase activity.

Table 8. Summary of cells injected and treatment administrated to each group.

Group	Cells injected	Treatment
PBS	BoM2 shC	PBS
ZOL	BoM2 shC	Zoledronic acid
OPG	BoM2 shC	OPG-Fc
PTHrP AN	BoM2 shC	PTHrP antagonist
shMAF	BoM2 shMAF	PBS

At day 44 after injection, bone metastasis was analyzed *in vivo*, mice were sacrificed, and lesions were analyzed *ex vivo*. Hind limb lesions analyzed *ex vivo* were found to be reduced by more than 90% in the ZOL group, by 78.8% in the MAF-depleted group, by 69.2% in the OPC-Fc group, and by 39.4% in the PTHrP AN group. Taken together, these results suggest that MAF downregulation has a significant inhibition effect on bone metastasis, almost to the same degree as the ZOL treatment. Curiously, inhibiting RANKL with OPG or antagonizing PTHrP had a less protective effect than MAF silencing in this preclinical model. These findings confirm the role of MAF as a driver of bone metastasis in ER+ BC cell lines. MAF is therefore a new potential target for developing novel drugs to treat and/or prevent bone metastasis.

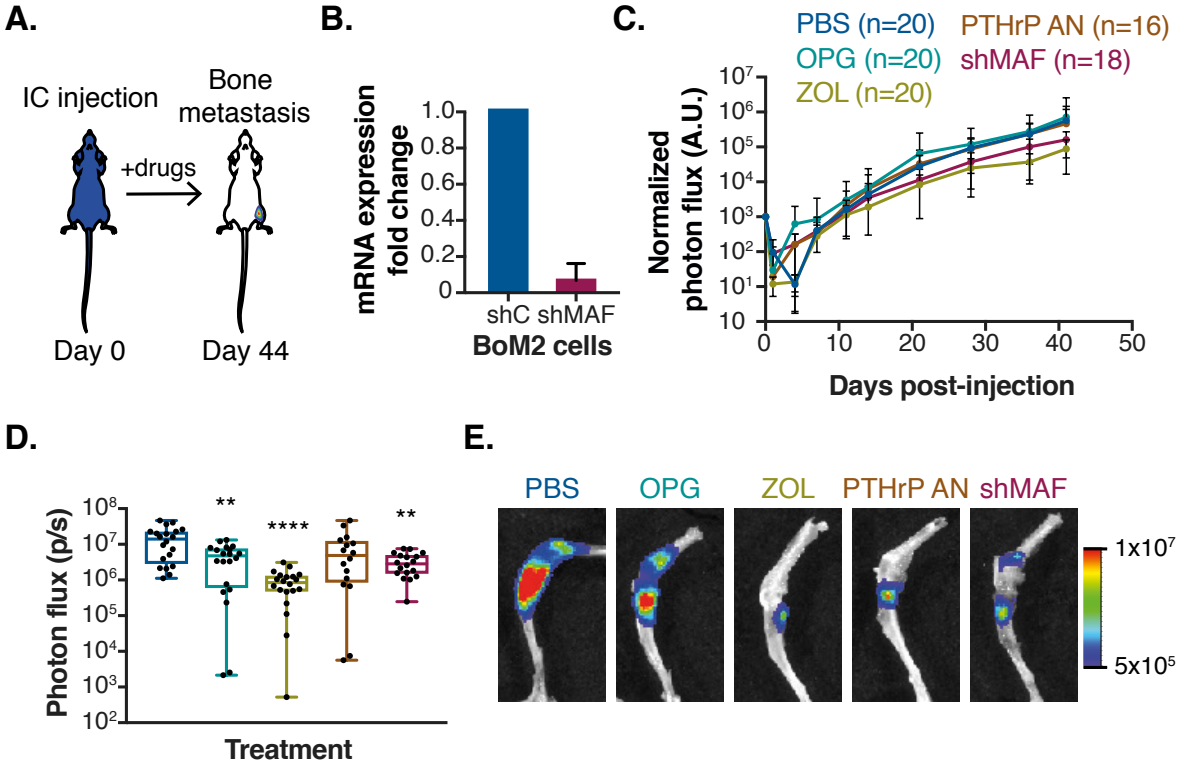

Figure 27. Comparison between MAF downregulation and bone metastatic drugs. **A.** Schematic of intracardiac injection and bone metastasis detection. **B.** MAF mRNA expression levels in control and shMAF-infected BoM2 cells analyzed by qRT-PCR before injections. Values were normalized to B2M expression and compared to the shC group. Data are shown as mean ± SD from 2 biological replicates. **C.** Quantification of BLI signal of bone metastatic lesions *in vivo*. **D.** *Ex vivo* bone metastasis photon flux quantification of all the groups is shown. Data are represented by box plot with median, IQR and min and max values. *P*-values were scored by two-sided Mann-Whitney test. *P*-OPG=0.006 (*), *P*-ZOL<0.0001 (****), *P*-PTHrP AN=0.0565 (ns), *P*-shMAF=0.0015 (**). **E.** Representative bioluminescence images showing *ex vivo* lesions of shMAF cells as well as shC treated with PBS, OPG, ZOL, or PTHrP AN. Abbreviations: OPG, recombinant osteoprotegerin; ZOL, zoledronic acid; PTHrP AN, PTHrP antagonist peptide.

Role of MAF in ZOL treatment

Next, we aimed to analyze the relationship between MAF expression and the effectiveness of potential bone metastatic preventive treatments. In a prospective/retrospective manner, a recent study tested the prognostic value of MAF, and its ability to predict response, for

inclusion of ZOL in the adjuvant setting to prevent bone metastasis in BC patients. ZOL-treated patients with MAF– tumors had improved IDFS, whereas patients with MAF+ tumors did not present any benefit. Indeed, ZOL treatment of non-postmenopausal BC patients with MAF+ tumors is associated with an increase of extraskeletal recurrences and a decrease of IDFS (Coleman et al. 2017). This study is based on the AZURE trial, a phase III trial in which BC patients with grade II/III tumors and lymph node affectation, but without distant metastatic evidence, were randomized to receive standard adjuvant systemic therapy alone or in combination with ZOL (clinical trial number: NCT00072020). Treatment was administrated during 5 years after primary tumor resection. Initial results from the AZURE trial showed no benefits from treating all patients with ZOL. However a benefit with IDFS was observed in postmenopausal patients (Coleman, 2008; Coleman et al., 2014). This fact suggested the need to better classify those women who can benefit from bisphosphonate treatment to prevent bone metastasis, and Coleman et al. (2017) proposed MAF as an indicator of BC responsiveness to ZOL treatment.

In this study, MAF+ tumors were more likely associated with ER-negativity. Thus, to analyze the effect of MAF expression on BC cells treated with ZOL, we took advantage of MDA-MB-231 cells, one of the most commonly used BC ER– cell lines derived from pleural effusion of BC metastatic patient. Cells were infected with pBabe Puro empty vector (mock) or alternatively, with pBabe Puro MAF short or long isoform simultaneously (MAF S/L OE). Cells were infected with TGL virus and sorted for the expression of Luc-GFP, injected into the tibia of 14-week-old Balb-c nude female mice, and tracked *in vivo* by luciferase expression. Mice were divided into two groups, one treated with PBS and the other with ZOL. In this case, we aimed to mimic the doses of ZOL given to the patients (Haider et al., 2014), so we administered 100 µg/kg ZOL once per week by IP injection. Organ colonization was scored weekly by luciferase activity.

No significant differences in terms of site-specific metastasis where observed in control cells with or without ZOL treatment (Figure 28). In contrast, ZOL treatment in mice inoculated with MAF-expressing cells showed a trend towards less bone and liver metastases and more brain and kidney metastases, whereas no differences in lung colonization were confirmed (Figure 28). Collectively, these results suggest that MAF overexpression in the presence of ZOL may revert metastasis to other sites.

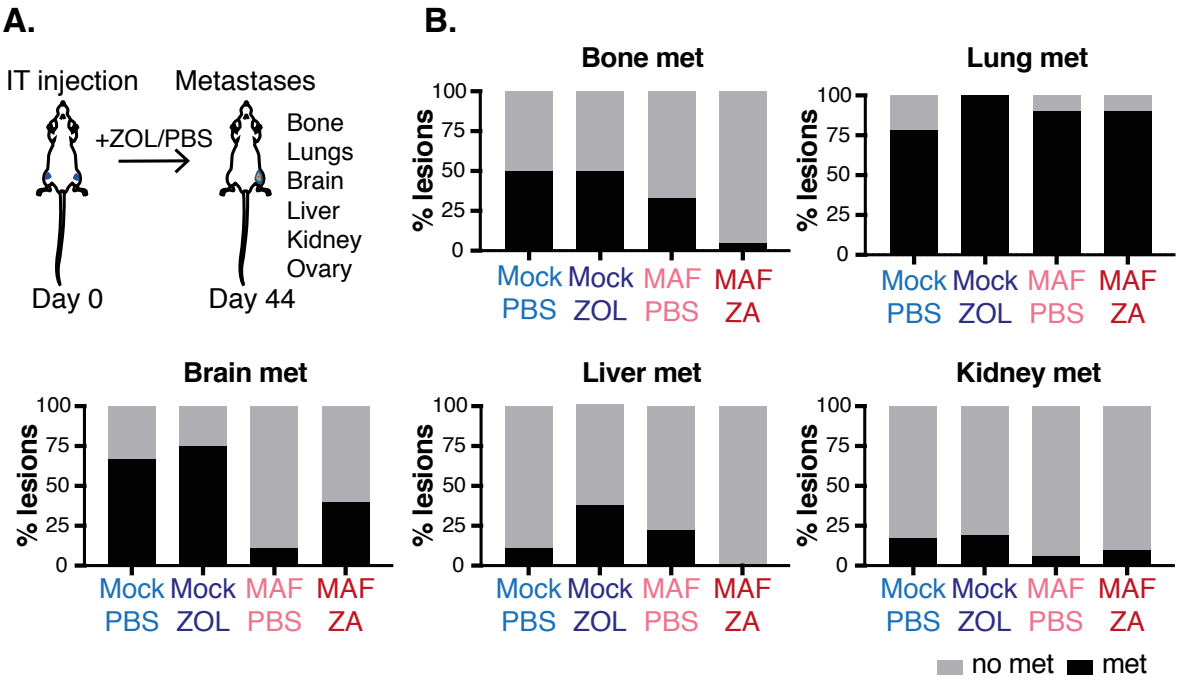

Figure 28. MAF does not affect ZOL treatment effectiveness. **A.** Schematic of intratibial injection, ZOL treatment, and bone metastasis detection. **B.** Quantification of organs with BLI signal *ex vivo* from a panel of metastatic lesions. Bone, lung, brain, liver and kidney metastases are shown. Percentage of organs without metastatic colonization is represented in grey, organs with metastatic lesions are represented in black. Abbreviations: ZOL, zoledronic acid.

Chapter III:
Generation of MAF Tg mouse model

Introduction

Previous reports showed that MAF is a driver of bone metastasis in preclinical models and was associated with bone metastasis in BC patient samples (Pavlovic et al., 2015). However, we aimed to understand the contribution of MAF to early steps of metastasis, with implication of immune system and microenvironment. In addition, we aimed to study the time-dependent contribution of MAF to the metastatic process. To this aim, a genetically engineered mouse (GEM) that mimics the complexity of BC bone metastasis to elucidate MAF mechanism in BC context was generated.

Results

Transgene design

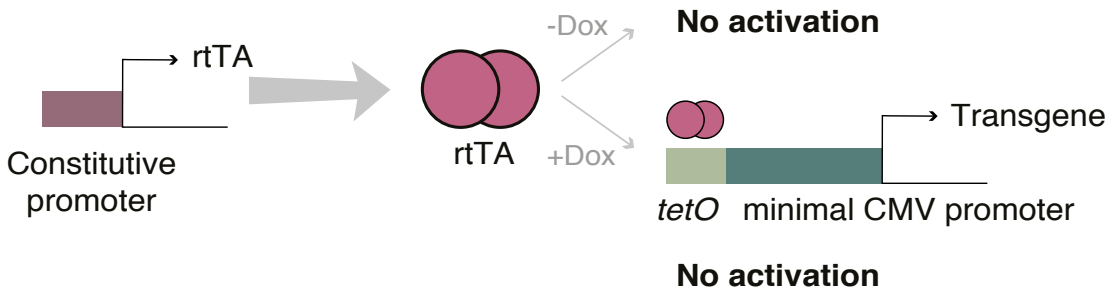

Figure 29. Tet-On system mechanism. Tet-On system requires the presence of doxycyline (Dox) to form a complex with reverse transactivator protein (rtTA), and to allow binding to *tetO* sequences of Tet-On promoter to activate its expression.

We designed a transgenic (Tg) mouse model to overexpress MAF in the mammary gland in an inducible manner based on the Tet-On 3G System (Clontech). The Tet-On system consists of a reverse Tet repressor–controlled transactivator (rtTA) that requires an allosteric effector, in particular doxycycline (Dox), for specific binding to tetracycline operator sequences (*tetO*) and subsequent activation of the Tet-On promoter (Gossen et

al., 1995) (Figure 29). The tetracycline rtTA 3G is the 3rd generation of rtTA, which has higher sensitivity to Dox. The *rtTA* was cloned together with two other genes, *Renilla* and *Katushka*: Renilla (rLuc8) is a bioluminescent enzyme that uses coelenterazine and oxygen as a substrate to generate a photon of light (Czupryna and Tsourkas, 2011; Loening et al., 2006), while Katushka (TurboFP635) is a dimeric far-red fluorescent protein (Shcherbo et al., 2007) useful for non-invasive whole-body optical imaging detection (Diéguez-Hurtado et al., 2011). This construct, called RRK, was inserted downstream of the mouse mammary tumor virus (MMTV) promoter (Ornitz et al., 1991; Sakamoto et al., 2012) (Figure 30A). Importantly, 2A self-cleaving peptides (Kim et al., 2011; Ryan and Drew, 1994) were inserted between the three genes to promote equimolar levels of expression from the three proteins (Trichas et al., 2008). 2A sequences consist of short peptides with the consensus motif Asp-Val/Ile-Glu-X-Asn-Pro-Gly-Pro. The cleavage site is located between the glycine (Gly) and the last proline (Pro), causing ribosome skipping to the next codon, and generating equal levels of protein expression. The sequences with highest cleavage efficiency in mouse are P2A peptide, derived from equine rhinitis A virus, and T2A peptide, derived from the porcine teschovirus-1 (Kim et al., 2011), the ones used in MAF Tg mouse to separate the principal genes.

To promote the overexpression of MAF, we designed an additional plasmid (MLG3G) with the 3rd generation of Tet-On promoter or pTRE3G, that consists of an improved pTRE promoter with seven *tetO* sequences upstream of a minimal CMV promoter. This inducible promoter has lower basal expression and higher maximal expression after induction as compared to pTRE (Loew et al., 2010). We cloned *MAF mouse*-T2A-*Luciferase*-P2A-*turboGFP* downstream of the pTRE3G promoter. Firefly Luciferase (fLuc) generates light through the catalysis of luciferin, ATP, and oxygen (de Wet et al., 1987), and turboGFP (tGFP) is an improved variant of the dimer EGFP with a faster maturation and higher brightness level (Figure 30B).

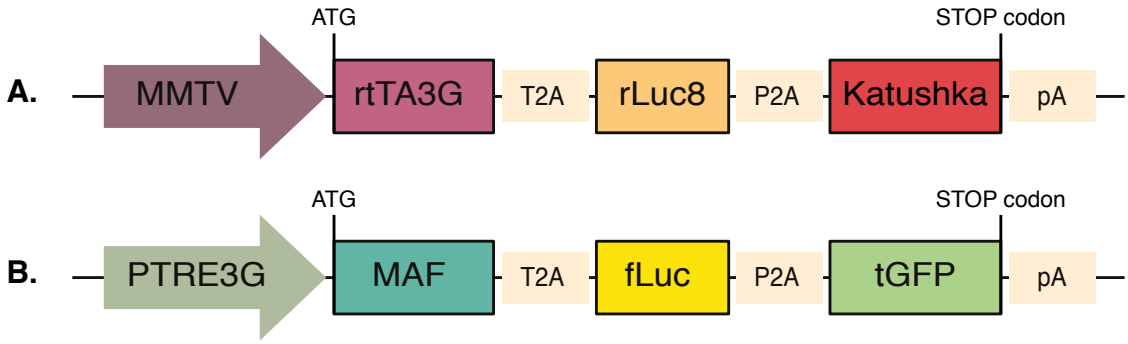

Figure 30. Constructs used to generate the MAF Tg mouse model. ATG and STOP codon sequences are shown. **A.** RRK plasmid, based on rtTA, renilla and Katushka under the MMTV promoter. Genes are separated by T2A and P2A sequences. **B.** MLG3G construct, composed of MAF mouse, luciferase, and tGFP under the TetO promoter and separated by 2A peptide sequences. Abbreviations: MMTV, mouse mammary tumor virus promoter; fLuc, firefly luciferase; pA, poly-A signal; rLuc8, renilla luciferase; rtTA3G, 3rd generation of reverse tetracycline controlled transactivation; PTRE3G, 3rd generation of Tet-On promoter; tGFP, turboGFP.

Founder characterization and colony generation

Both plasmids where co-injected into the pro-nuclei of fertilized FVB oocytes and re-implanted into pseudopregnant females. Littermates were genotyped, and five potential founders were obtained: four males (M5, M15, M28, and M37) and one female (M24). Each founder (F0) was bred with FVB mouse to establish an independent transgenic line. We then studied transgene expression after we had first verified both transmission of the transgenes from founders to offspring (F1), and from the first generation of transgenic mice (F1) to the second generation (F2) by PCR genotyping.

To assess transgene expression *in vivo*, we used bioluminescent imaging (BLI) that detects the activity of luciferase and renilla enzymes, from MLG3G and RRK constructs, respectively. All founders were then injected with luciferine and coelenterazine, followed by BLI, prior to and after 1 week of Dox treatment. Analysis of luciferase expression before Dox treatment was useful to determine the background activity of rtTA in the absence of induction. We observed leakiness luciferase expression in all founders except M15. M5 founder had expression in the eyes, and M28 and M37 had expression in the testis and salivary gland; in contrast, the female M24 had a strong expression distributed throughout the whole body (data not shown). After Dox treatment, we obtained the same

pattern of expression but with higher bioluminescence activity. Noteworthy, the M15 founder presented no luciferase induction after Dox treatment, suggesting a silencing of the transgene in this line due to a positional effect. As has been described (Gunther et al., 2002; Hennighausen et al., 1995), the MMTV promoter is active in the epithelial cells of the mammary gland as well as in other secretory tissues, such as salivary gland and male reproductive organs. We detected this pattern particularly in M28 and M37 founders, suggesting that those founders present a typical MMTV promoter transgene expression. Markedly, renilla expression mimics luciferase activity, with lower intensity (Figure 31A and 31B).

To determine mammary gland transgene expression, we took advantage of the first generation of transgenic females. We could not observe any general evidence of luciferase activity in the mammary glands of virgin females after one week of Dox induction. Of interest, M24 first generation offspring lost the broad expression of the transgene and retained some leakiness expression in the legs and in the tail. Another consideration is that MMTV-expression markedly increases during late pregnancy and lactation. For this reason, we checked luciferase and renilla expression during all the gestation phases under Dox induction (Figure 32). In the lactation state context, we detected specific mammary gland luciferase and renilla BL signal above background level in M24 and M28 transgenic mouse (Figure 31C and 31D). No mammary gland expression was detected in the other transgenic lines (data not shown). Strikingly, luciferase detection was shown in only one female of the M28 F1 after 1 day of Dox induction, independently of lactation period (Figure 31D).

Finally, we generated stable colonies from M24 and M28 founders following those mice that presented a detectable transgene expression. Importantly, we used two different founders because each line has variable copy numbers and unique transgene insertion sites due to the random integration, and this is translated into different MAF protein expression levels. Multiple-line studies also eliminate the possibility that phenotypes arise from the disruption of important genes.

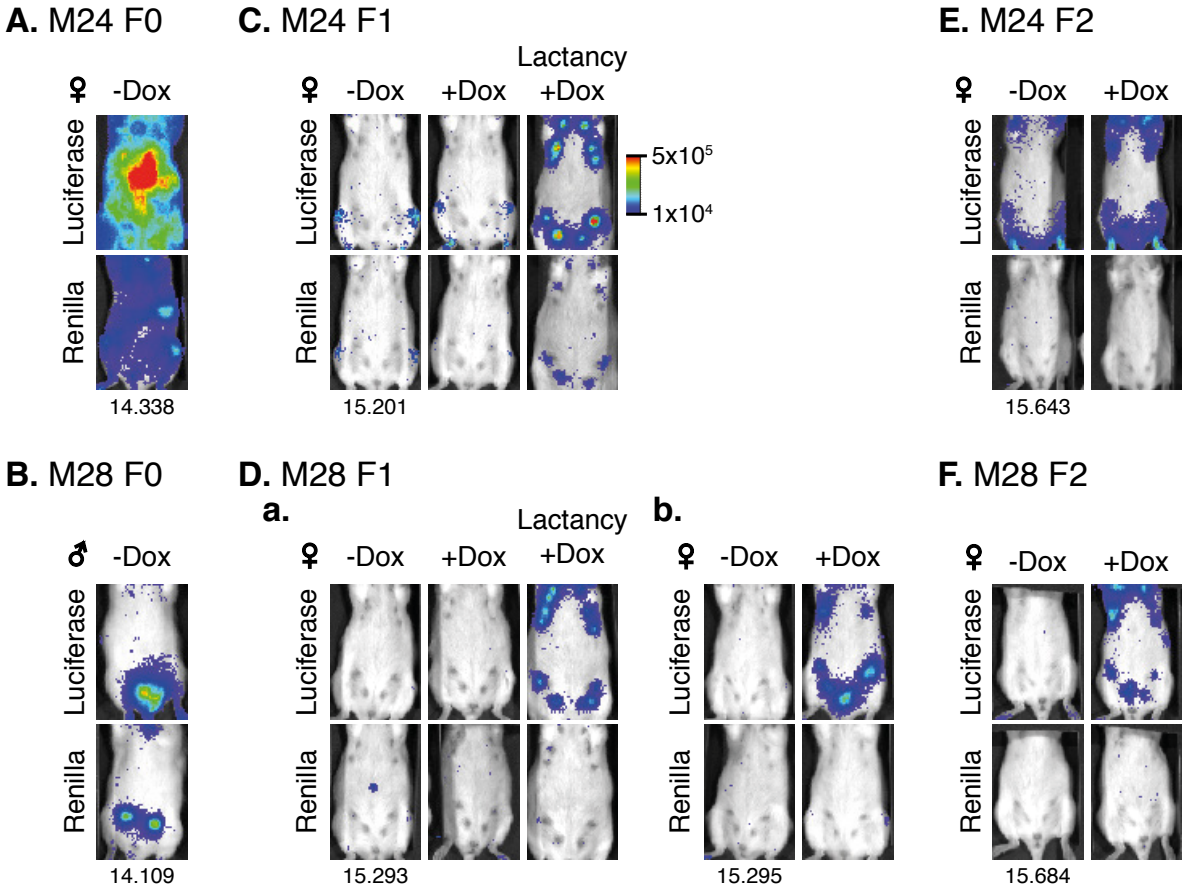

Figure 31. Luciferase and renilla expression in M24 and M28 colonies. **A.** Ventral luciferase and renilla BLI of M24 female founder (F0) without doxycycline (Dox) treatment. **B.** Luciferase and renilla activity in M28 male founder without Dox administration. **C.** Representative image of ventral luciferase and renilla activation before and after Dox induction in M24 first generation (F1) female mouse. BLI during lactancy period is also shown. **D.** Luciferase and renilla BLI image of M28 first generation representative female mouse prior to and after Dox treatment. Representative images show: **a,** lactancy-dependent female after one week of induction and during lactancy induction, and **b,** lactancy-independent transgene expression female after 1 day of Dox treatment. **E.** Representative images of second generation (F2) of M24 females. Bioluminescent enzyme activity before and after Tet-On promoter induction is shown. **F.** Representative BLI of second-generation female mice before and after Dox induction. Abbreviations: Dox, doxycycline.

To determine the induction of gene expression by rtTA activation during pregnancy, a transgenic female BLI was acquired before Dox treatment and mated with FVB males. Dox treatment started at day 0 of gestation (G0) and continued until involution state after lactation. BLI was acquired once per week. Notably, transgene expression was detected in the late pregnancy mammary gland and acquired the maximum peak on the first week of

lactation period in M24 mice. On the other hand, in the M28 colony, maximal induction was achieved during the second week of lactation. Figure 32 shows an increase on renilla expression as for luciferase but at lower intensity, suggesting that the MMTV promoter is distinctly active during pregnancy and lactation periods. In these periods, expression of RRK construct, represented by renilla activation, would consequently activate Tet-On promoter from the MLG3G construct promoting luciferase expression.

One of our concerns was the possible requirement of hormones released during pregnancy or lactation to activate MMTV promoter. Hence, as a first approach, we studied the capacity of steroid hormones, and specifically, progesterone, to activate MMTV promoter during pregnancy and lactation (Di Croce et al., 1999; Truss et al., 1995; Vicent et al., 2009a, 2009b). For this reason, we used 19-week-old females that expressed the transgene in a lactation-dependent manner with Dox induction (example of Figure 31Da). We treated them with progesterone pellets during one week and then added Dox treatment. No changes on luciferase expression were detected with progesterone treatment alone or combined with Dox. Next, we treated other lactancy-dependent transgene expression females with Dox and then progesterone pellets; indeed, no mammary gland signal was observed (Figure 32C). These results, taken together with the proof that one of the mice presented luciferase expression on the mammary gland in a lactation-independent manner, suggested that steroid hormones, such as progesterone, do not cause the maximum activation of MMTV promoter during lactation.

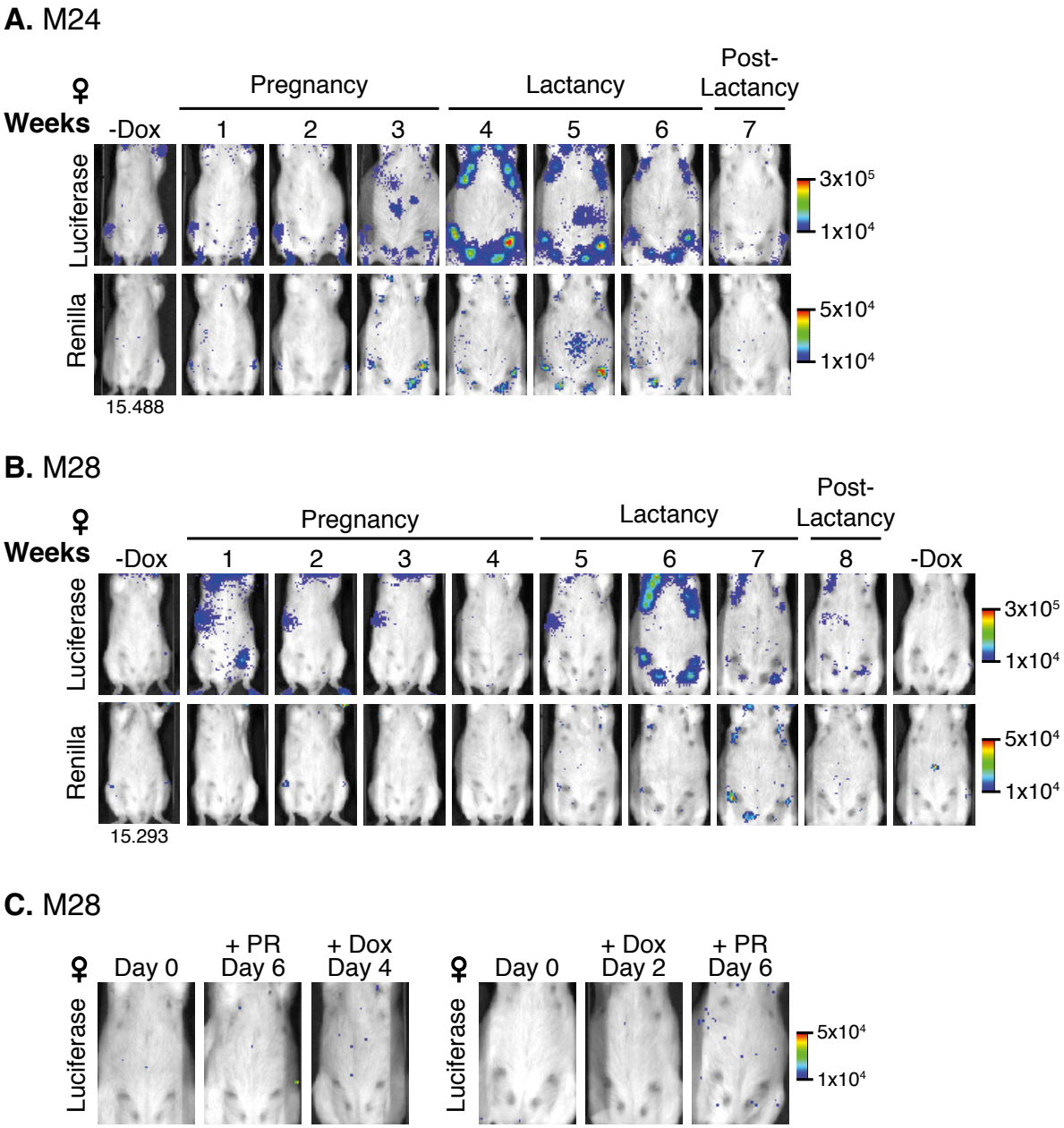

Figure 32. Influence of lactation hormones in transgene induction. **A.** Representative BLI showing transgene induction in the mammary gland of a M24 female mouse. Renilla and luciferase BLI signals of the different gestational periods were shown. **B.** Representative images of transgene activation during pregnancy, lactancy, and post-lactancy periods in M28 female mouse. **C.** BLI images of luciferase activity in M28 female with lactancy-dependent transgene expression. Representative ventral image before and after progesterone (PR) administration and further doxycycline (Dox) treatment were shown (left panel). Luciferase expression before and after Dox treatment and next PR administration were represented (right panel).

Copy number integration of the transgene

Thereafter, in order to assess the copy number integration of the transgene, we performed Southern blot analysis from founders and offspring of both colonies. For this, we generated one probe (P1) to detect RRK construct, and a second probe (P2) to detect the MLG3G construct (Figure 33).

In the M24 colony, a loss of copy number integration of both constructs from the founder to the first generation was detected (Figure 33B). This suggests that the loss of whole body transgene expression was due to a loss of transgene copy number integration. Interestingly, the male that presented lower copy number and integration sites of the transgene (15.195) gave rise to a colony with females that presented lactation-independent transgene expression (Figure 31E). In contrast, mice with higher copy number integration produced a colony with lactation-dependent expression of luciferase. Second and third generations of lactation-independent transgene expression females presented the same copy number integration as its progenitor (Figure 33B). This implies a stable transmission of the transgene to the offspring indicating the generation of a stable transgenic line.

The founder of colony M28 also had lower copy numbers of the transgene in one male of its offspring (15.281), which presented less sites of insertion (Figure 34B). Strikingly, this male produced a colony with lactating-independent expression (Figure 31F). Its copy number integration was maintained during the second generation, confirming a stable transmission to the offspring (Figure 34C).

Taken together, these results suggest that we obtained two founders that presented mosaicism, and that the loss of copy number integrations in the genome benefited the transgene activation in a tissue- and time-specific manner. We created the second generation of M24 and M28 animals from the offspring of lactating-independent transgene expression females. Markedly, second generation of this new branch maintained the same pattern of expression only 1 day after Dox treatment irrespective of hormonal status. Indeed, they also maintained the same copy number as well as number of sites of transgene integration. Therefore, we chose M24 and M28 lines with the lowest transgene copy number integration and best inducible expression to establish lines for further experiments. These lines were stable and did not lose transgene expression during generations. Thus, we succeeded in producing two stable mouse transgenic lines that activate the transgene, by means of luciferase, in a tissue-specific and doxycycline-dependent manner.

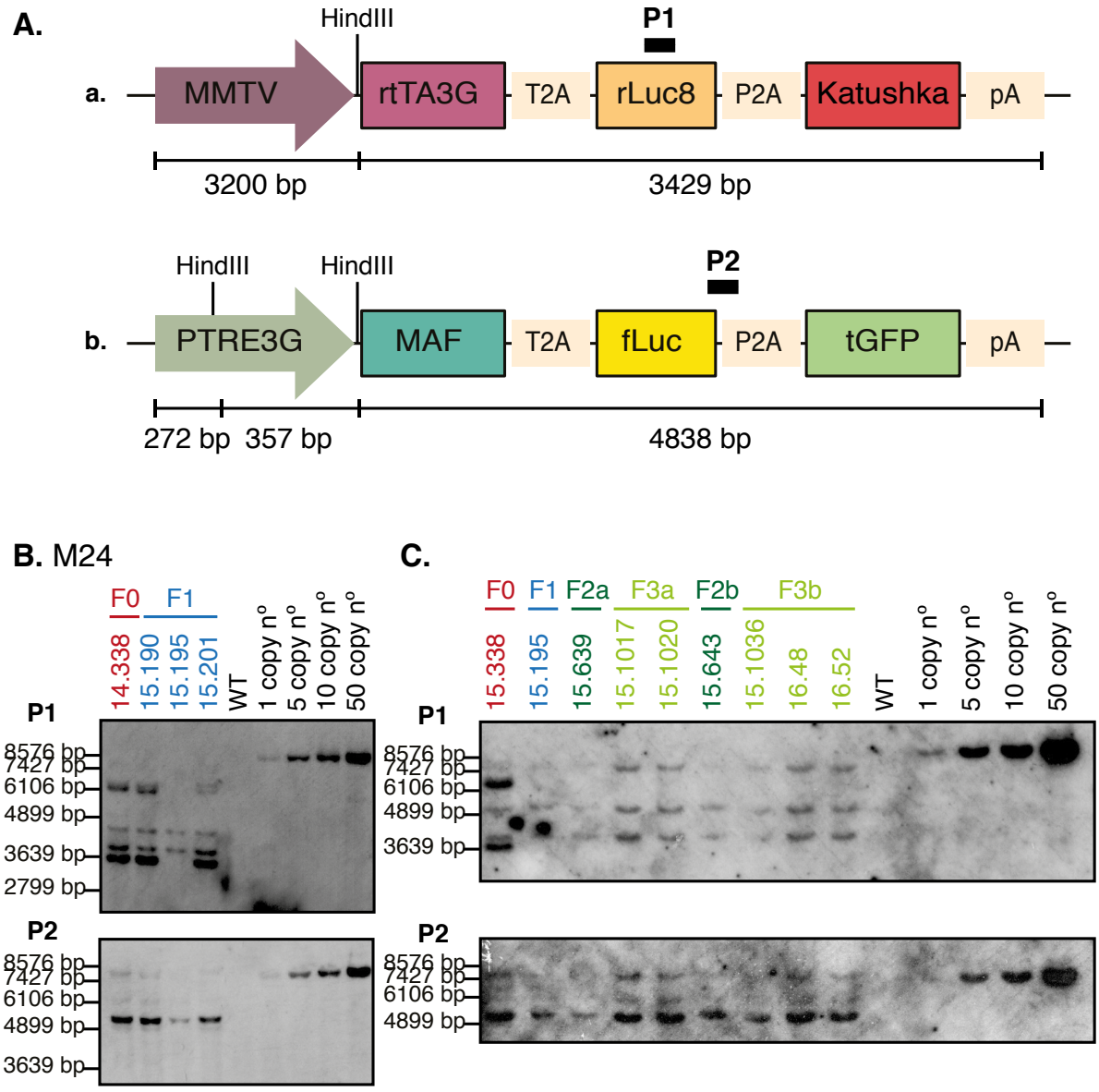

Figure 33. Analysis of transgene copy number integration in M24 colony. **A.** Schematic representation of RRK **(a)** and MLG3G **(b)** constructs. Hind III restriction sites and the size of fragments generated after HindIII digestion are shown. Localization of Southern blot probes for RRK construct (P1) and MLG3G construct (P2) are indicated with a black line. **B.** Southern Blot analyses of founder (F0) and first generation (F1) M24 mice. **C.** Second (F2) and third (F3) generation derived from a first-generation male (15.195) from the M24 colony. Offspring samples are located on the right hand of their parental samples. P1 probe Southern blots are shown at the top, and P2-incubated membranes, at the bottom. F0 number is represented in red, F1 in blue, F2 in dark green and F3 in light green

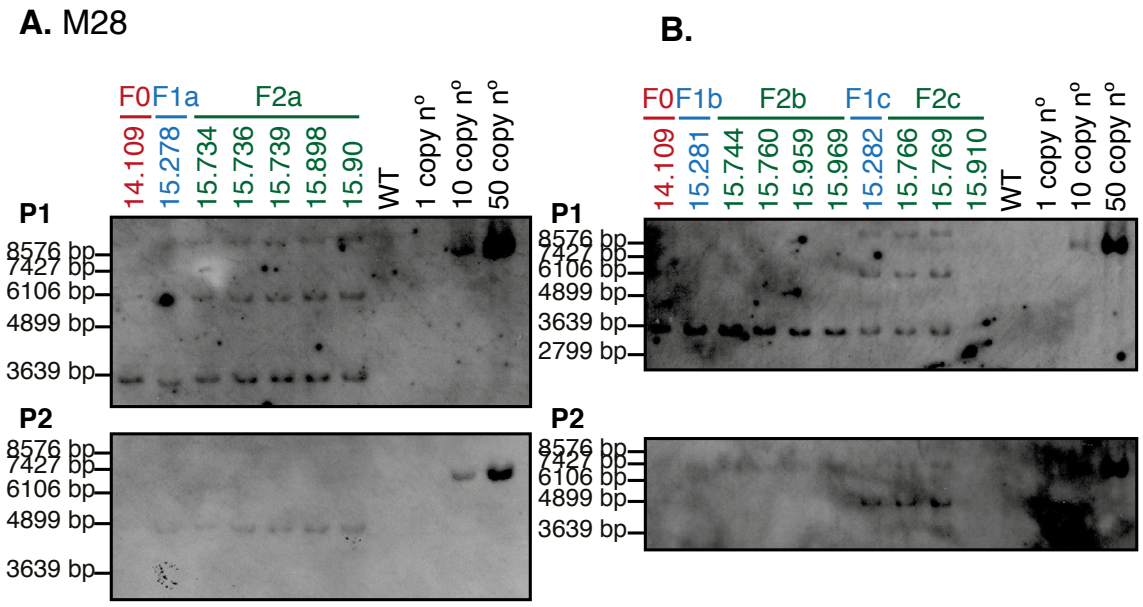

Figure 34. Transgene copy number integration detection in M28 colony. **A.** Southern blot analyses of the M28 founder (F0) and first (F1) and second (F2) generation deriving from mouse 15.278. **B.** Founder, first and second generations derived from mice 15.281 and 15.282. Offspring samples are located on the right hand of their parental samples. Southern blots incubated with a P1 probe are shown at the top, and the P2 probe, at the bottom. Genomic DNA (gDNA) was digested by HindIII restriction enzyme. F0 is represented in red, F1 in blue and F2 in dark green

Transgene induction studies

Once colonies were established, we analyzed the *in vivo* induction of transgene expression by luciferase activity. Five-week-old $MAF^{+/+}$ (termed wild-type [WT]) and $MAF^{Tg/+}$ (namely MAF Tg) females received Dox for 1.5 months through the drinking water, while BLI was acquired once per week. No significant differences of transgene induction were found in colony M24 between treated and non-treated mice ($P = 0.1605$), in part because Tg mouse without Dox treatment presented a high leakiness expression (Figure 35). Markedly, transgene activation was clearly reduced during time ($P < 0.0001$, analyzed with 2-way ANOVA) in MAF Tg treated and non-treated mice (Figure 35B). Contrary, BLI signal analysis in M28 females treated with Dox showed luciferase induction increase of 3-4 folds above non-treated mice ($P = 0.030$) (Figure 36). Noteworthy, low levels of leakiness expression were observed in transgenic mouse without Dox treatment in M28 colony (Figure 36C). M28 females, similar to M24 colony, presented a significant reduction on luciferase activity over time ($P < 0.0001$, calculated with 2-way ANOVA).

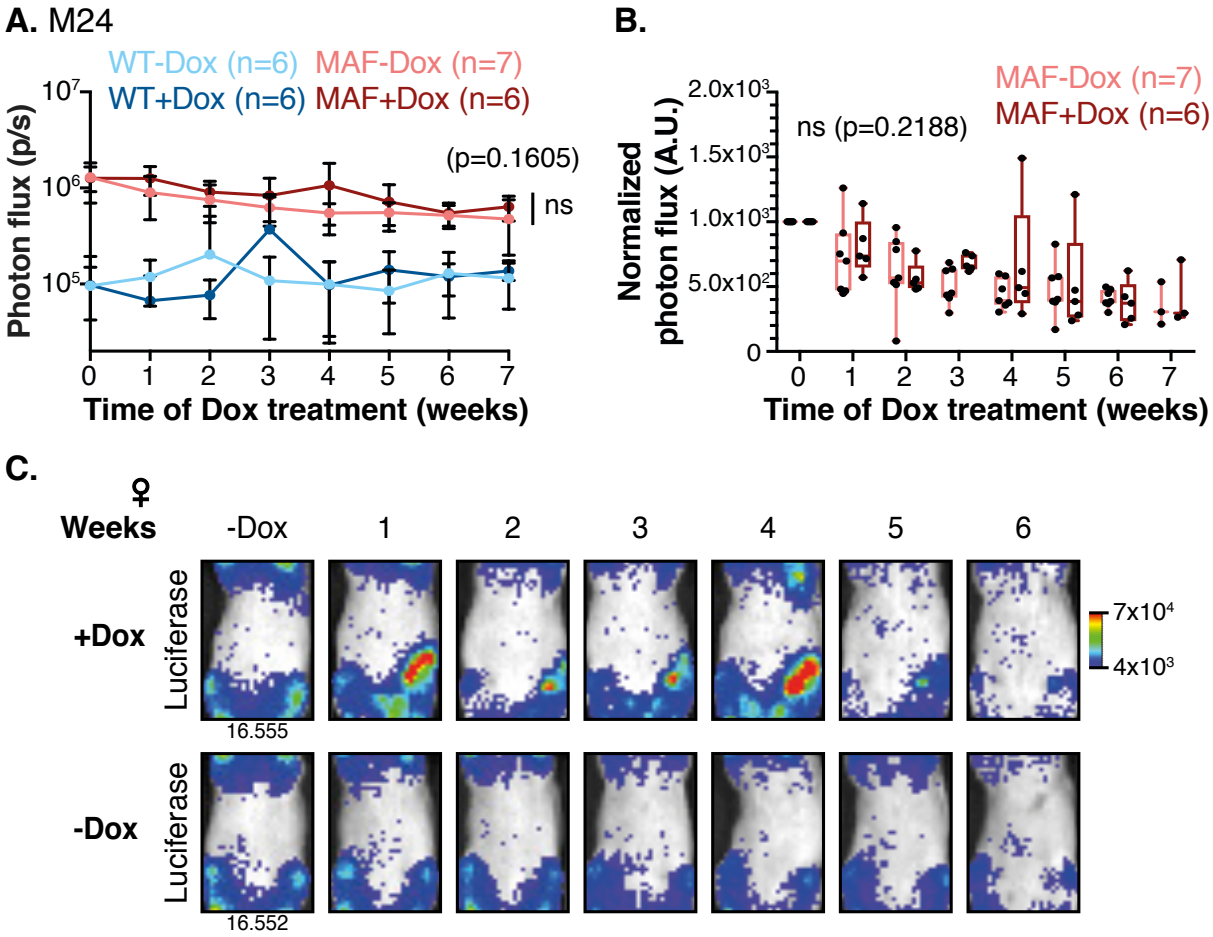

Figure 35. Doxycycline induction of transgene expression in the mammary gland of M24 female mice. **A.** Quantification of luciferase activity *in vivo* in the mammary gland. WT and MAF Tg mice were treated with normal water or Dox-containing water from 5 weeks until 12 weeks of age (n = 6). *P*-values were scored by two-sided Mann-Whitney test. **B.** Box plot representing luciferase activity from M24 MAF Tg females with and without induction of the transgene. Data are normalized to background expression and represented by box plot with median, IQR, and min and max values and normalized to values obtained at day 0 (without Dox). *P*-values were scored by two-sided Mann-Whitney test. **C.** Representative BLI signal of MAF Tg females with or without Dox treatment.

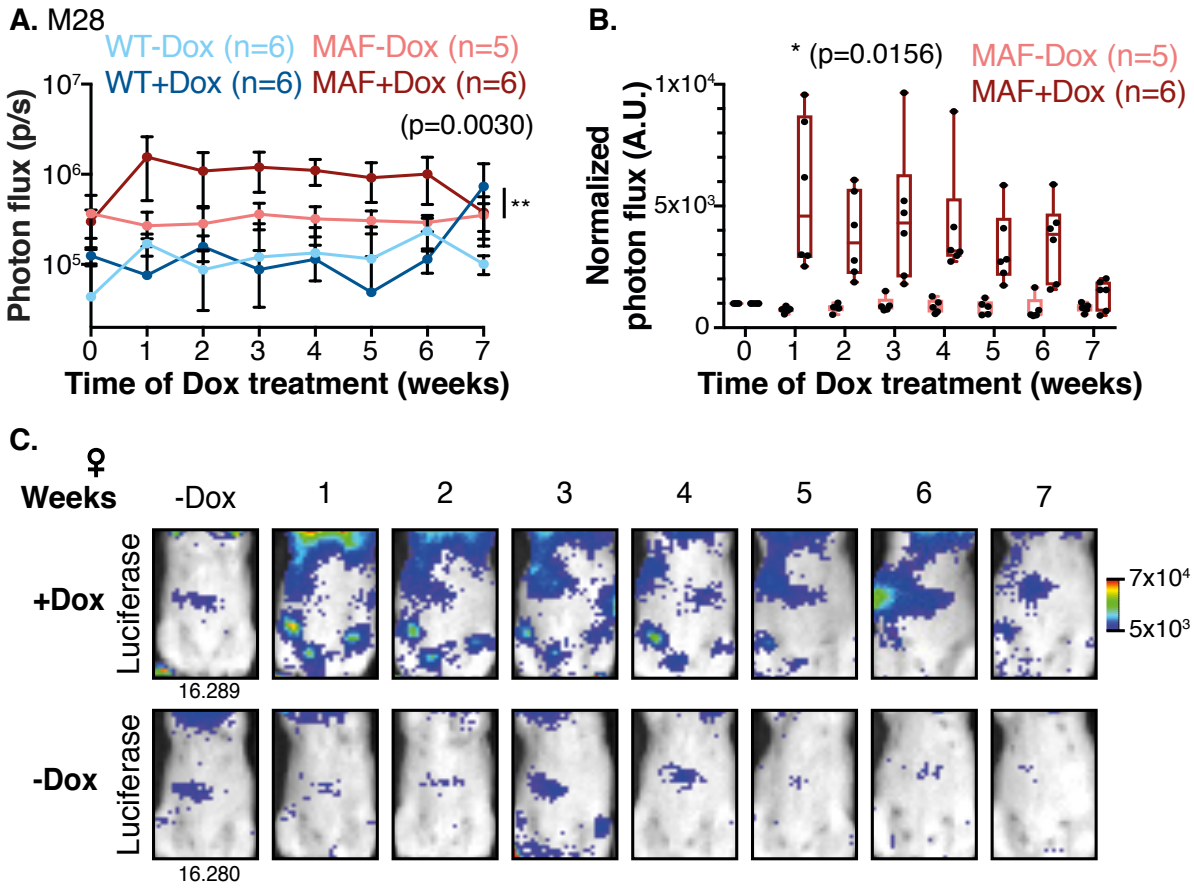

Figure 36. Transgene induction in mammary glands of M28 female mice by Dox treatment. **A.** Quantification of *in vivo* mammary gland luciferase expression from WT and MAF Tg mice treated or non-treated with Dox ($n = 6$). *P*-values were scored by two-sided Mann-Whitney test. **B.** Luciferase activity normalized to day 0 (without treatment). Data are represented by box plot with median, IQR, and min and max values. *P*-values were scored by two-sided Mann-Whitney test. **C.** Representative images of luciferase induction on M28 Tg females with or without Dox treatment are shown.

Next, we studied the kinetics of luciferase induction in the M28 colony during pregnancy and lactation; this colony presented transgene activation independently of the hormonal status. To this end, animals received Dox during pregnancy, lactation, and involution states. During this period, luciferase activity was measured over time by BLI. Intriguingly, in this context, high leakiness expression is observed in M28 non-treated mice, specially during the lactation state. Thus, no differences between Dox-induced and non-induced mice were observed in terms of luciferase activation (Figure 37).

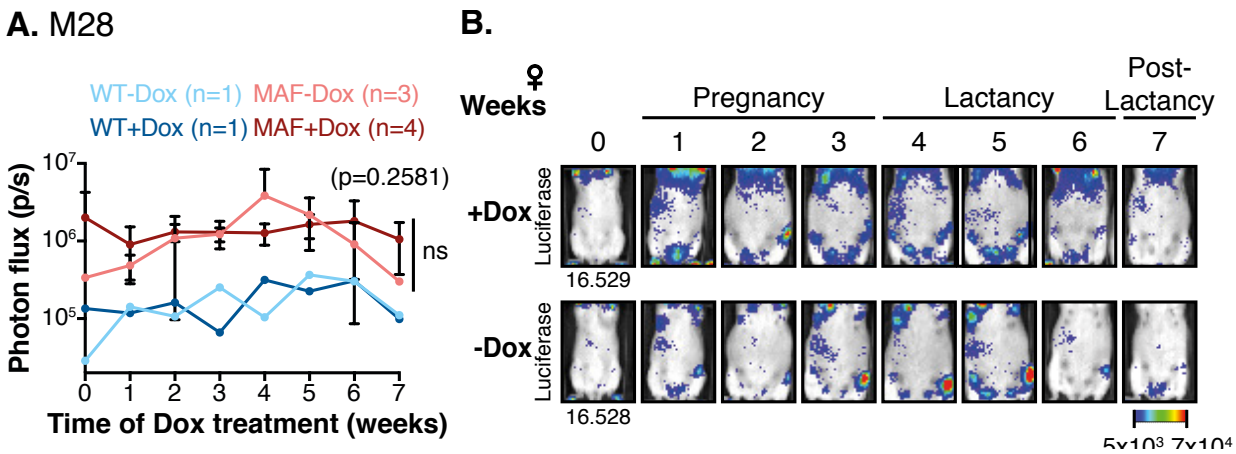

Figure 37. Transgene induction during pregnancy and lactancy of M28 females. **A.** Quantification of *in vivo* luciferase activity in the mammary gland of WT and MAF Tg females with or without Dox treatment. *P*-values were scored by two-sided Mann-Whitney test. **B.** Representative images of MAF Tg females treated or non-treated with Dox during pregnancy and lactancy states.

Ex vivo transgene detection

Our next approach was to detect transgene activation in *ex vivo* organs. First, we detected luciferase activity by means of BLI in the mammary glands. Its expression was heterogeneous in both colonies (Figure 38), as it has previously been described (Hennighausen et al., 1995), due to the heterogeneity expression of MMTV promoter.

After detection of luciferase and renilla activity, we next analyzed transgene expression using tGFP, Katushka or MAF protein. To detect fluorescent proteins, we disaggregate the mammary glands and sorted cells with fluorescence-activated cell sorting (FACS). No tGFP or Katushka expression was detected under these conditions (data not shown). Alternatively, protein expression was analyzed by immunofluorescence (IF), immunohistochemistry (IHC), and Western blot techniques. IF and IHC of non-treated and treated Tg mammary gland sections showed no detectable MAF or GFP protein levels, even though transgene expression was detected through luciferase activity by BLI (Figure 39). Protein levels were also checked by Western Blot and no significant differences on MAF expression were observed between transgenic-treated and WT-treated mouse (data not shown). Unfortunately, GFP, Katushka and rtTA antibodies were not of use in this context due to the presence of several unspecific bands of diverse sizes in the mammary gland extracts. Moreover, luciferase could not be detected with two of the commercially available antibodies tested.

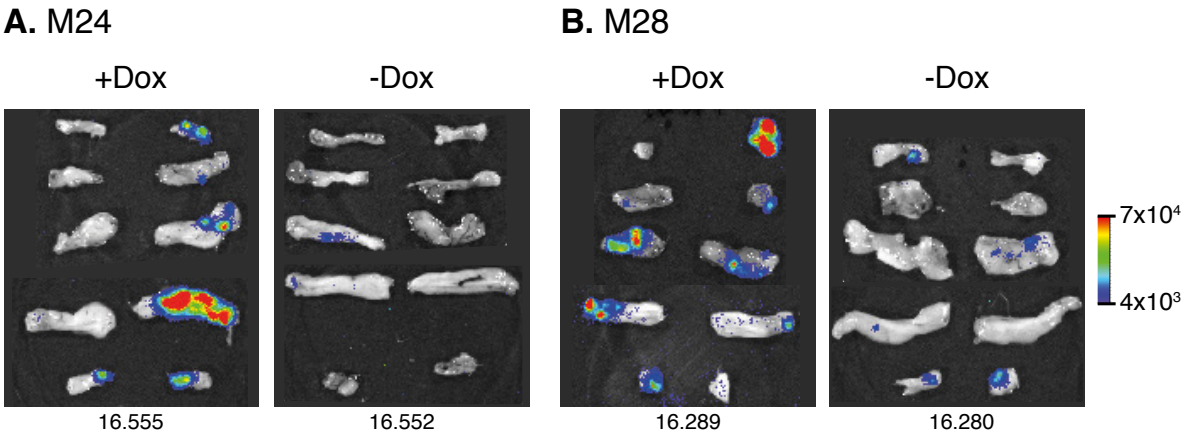

Figure 38. MMTV heterogeneous expression in the mammary gland. **A.** Representative images of *ex vivo* mammary glands from M24 MAF Tg mouse treated and non-treated with Dox. **B.** Representative images of M28 MAF Tg *ex vivo* mammary glands with or without Dox treatment. Mice were treated during 7 weeks and were sacrificed at 12 weeks.

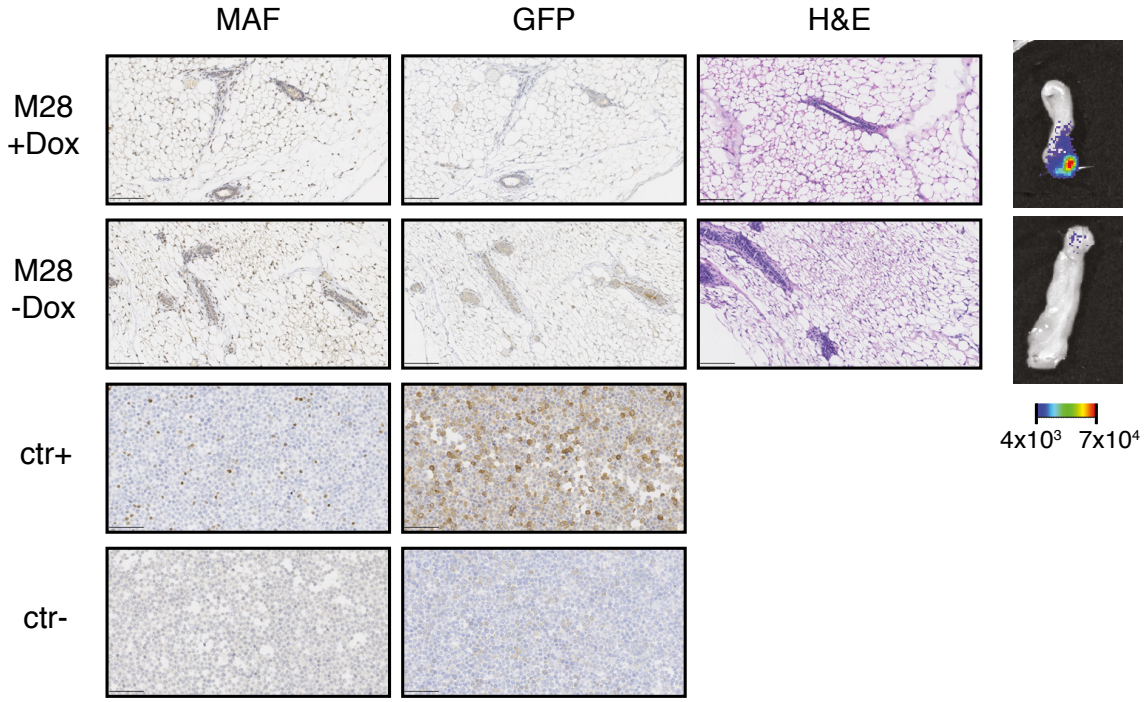

Figure 39. MAF and GFP immunohistochemistry detection. IHC of MAF, GFP and H&E from M28 MAF Tg females with and without transgene induction. On the top are shown representative images of a mammary gland with luciferase activity whereas on the bottom images are from a mammary gland without luciferase activity detection. Cells with MAF and GFP overexpression are represented as control positive and without OE as control negative. Scale bar represents 100μm.

To further analyze mRNA levels of the transgene in epithelial cells of the mammary gland of Tg mice, we first isolated those cells by sorting. Mammary gland is composed mostly by adipose tissue while epithelial cells, the potential expressers of the transgene, represent a low percentage of the whole organ. In this regard and to overcome detection sensitivity limitation, we first separated by sorting epithelial cells and then we performed qRT-PCR on this small group of cells. To perform the sorting, we disaggregated a whole positive mammary gland for BLI and we excluded the events that present Ter119, BP-1 and CD45 (markers of hematopoietic cells) and CD31 (marker of endothelial cells). We then recovered EpCAM^{high} CD49f^{med} cells that represent the epithelial group. Pico profiling extraction of mRNA from approximately 40,000 sorted cells and SyBR Green qRT-PCR was performed and no detectable increase on mRNA from MAF, luciferase, tGFP, rtTA, renilla or Katushka was observed using specific primers of each gene (data not shown). On base of these results, we hypothesized a possible difficulty on protein and mRNA detection due to a detection sensitivity problem even though sorting was performed.

Effect of MAF induction in mammary gland development

Next step was to determine whether the slight expression of the transgene, detected by luciferase expression, was able to promote phenotypic changes on the mammary gland development. To this aim, mammary glands from 12 weeks-old virgin females were extracted. After 7 weeks with or without Dox treatment, percentage of ductal area versus total area was calculated and WT and Tg mammary glands were compared. Results showed no differences in branching or mammary gland development between groups (Figure 40). Moreover, no correlation was found between more luciferase activity *in vivo* and/or *ex vivo* with more branching of the ducts (Figure 40). Additionally, no tumor initiation capabilities were observed after transgene induction by Dox treatment for more than a year (data not shown). These results suggest that MAF transgene expression was not enough to induce morphological changes on the mammary gland, due to its low expression in MAF Tg mouse or because MAF does not have an active role on mammary gland or tumor development.

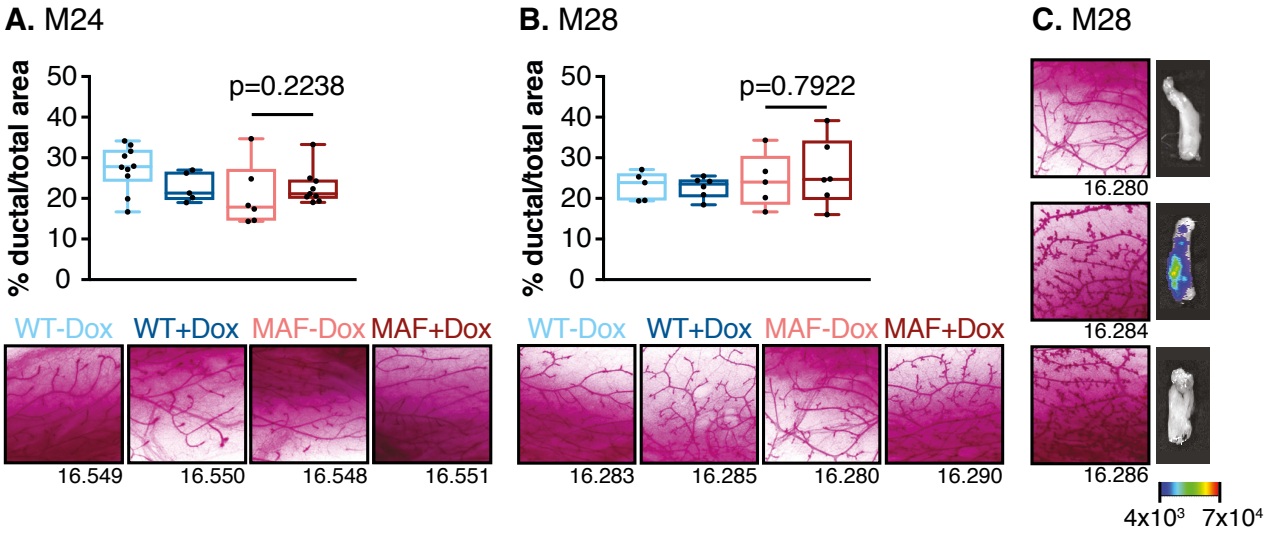

Figure 40. MAF does not cause changes in the mammary gland development. **A.** Quantification of ductal area versus total area from WT and MAF M24 Tg mice with and without Dox treatment. Representative H&E staining are shown at the bottom. **B.** Quantification branching duct percentage in the mammary gland of MAF M28 Tg mice treated and non-treated with Dox. Representative H&E images are shown at the bottom. **C.** Representative BLI images of mammary glands with or without luciferase activity and its corresponding H&E staining. Data are represented by box plot with median, IQR and min and max values. *P*-values were scored by two-sided Mann-Whitney test.

Chapter IV: Generation of double Tg mouse model PyMT-MAF

Introduction

We next aimed to evaluate the effect of MAF overexpression on the tumoral context. To this end, MAF Tg females were crossed with a mouse model that develops spontaneous adenocarcinomas in the mammary gland. Several possible mouse models could be used with various tumor latency periods and differential expression of cancer cell markers. As a first approach, we choose the well-described MMTV-PyMT (FVB/N-Tg(MMTV-PyMT)634Mul) transgenic mouse line because develops tumors in a short latency period, with a 100% penetrance. In this model, hyperplastic lesions arise close to the nipple at a very early age, and when ducts elongate in the prepubertal phase, new lesions arise on the distal end buds. Hyperplasia becomes an adenoma or mammary intraepithelial neoplasia (MIN), then carcinoma *in situ*, and finally an invasive carcinoma. Carcinomas lose the ER and express ErbB2 in time (Fluck and Schaffhausen, 2009).

Results

Double Tg mouse generation and characterization

To determine the effects of MAF on mammary gland tumorigenesis, we crossed MAF Tg female mice with MMTV-PyMT Tg male mice. From the offspring, double transgenic mice MMTV-PyMT$^{Tg/+}$ MAF$^{Tg/+}$ (PyMT-MAF) and MMTV-PyMT$^{Tg/+}$ MAF$^{+/+}$ (PyMT-WT) were selected. PyMT-MAF mice were termed PyMT-M24 or PyMT-M28 depending on the colony of origin. Five-week-old double transgenic mice were treated with Dox for 7 weeks. Transgene induction was analyzed and compared to non-treated mice. In PyMT-M24 colonies tumors reached the maximum induction of luciferase activity, a 14-fold increase, at the first week of Dox treatment (Figure 41). After this maximum, transgene induction decreased during time. In contrast, for the PyMT-M28 colony, tumors presented the same luciferase activity independently of Dox treatment, due to a high leakiness expression in basal conditions rather than a low transgene expression (Figure 42).

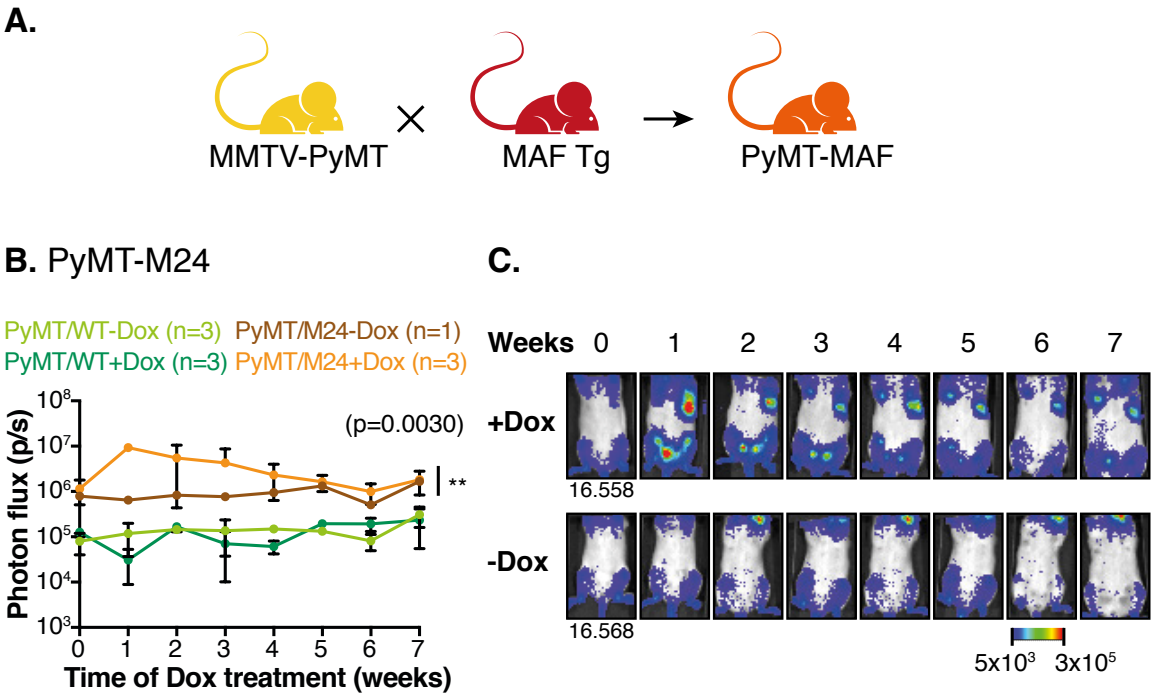

Figure 41. Transgene induction in PyMT-M24 colony during mammary gland tumor development. **A.** Schematic representation of mating between MMTV-PyMT and MAF Tg mice to generate a double transgenic mouse (PyMT-MAF). **B.** Quantification of *in vivo* mammary gland luciferase expression from PyMT-WT and PyMT-M24 Tg mice. Mice were grouped as Dox treated and non-treated mice. *P*-values were scored by two-sided Mann-Whitney test. **C.** Representative images of PyMT-MAF M24 females with Dox treatment (top) or without treatment (bottom).

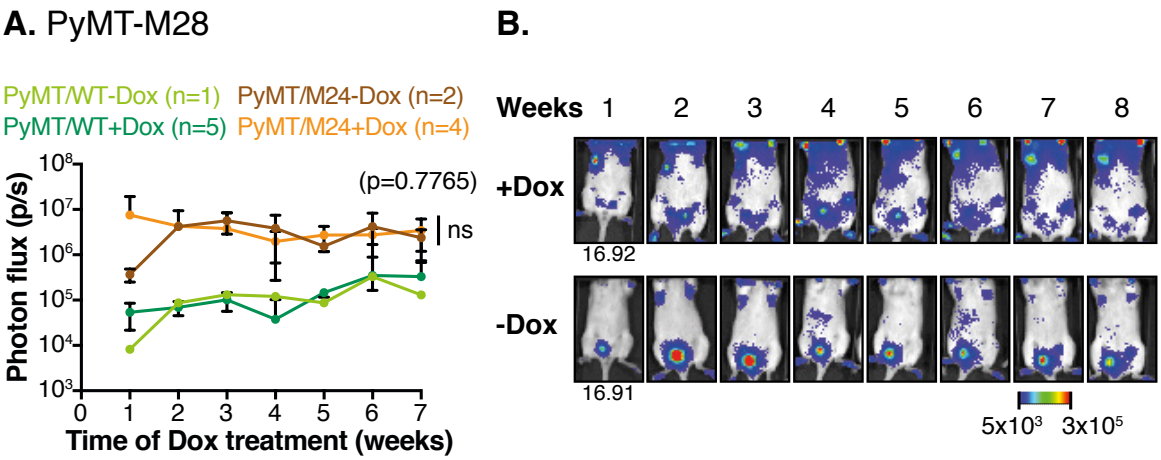

Figure 42. Transgene induction in PyMT-M28 colony during mammary gland tumor development. A. Luciferase expression from PyMT-WT and PyMT-MAF M28 Tg treated and non-treated mice. In vivo mammary gland BLI signal quantification. P-values were scored by two-sided Mann-Whitney test. B. Representative images of PyMT-M28 females with or without Dox induction are shown

Tumors upon transgene induction presented the same capacity to initiate and maintain primary tumor growth as control mice. Tumor initiation was developed without significant differences in PyMT-M24 Tg mice after 1 week of Dox treatment compared to non-treated or WT mice (Figure 43A). Moreover, PyMT-M28 mice showed no significant differences on total tumor size growth over time (Figure 43B).

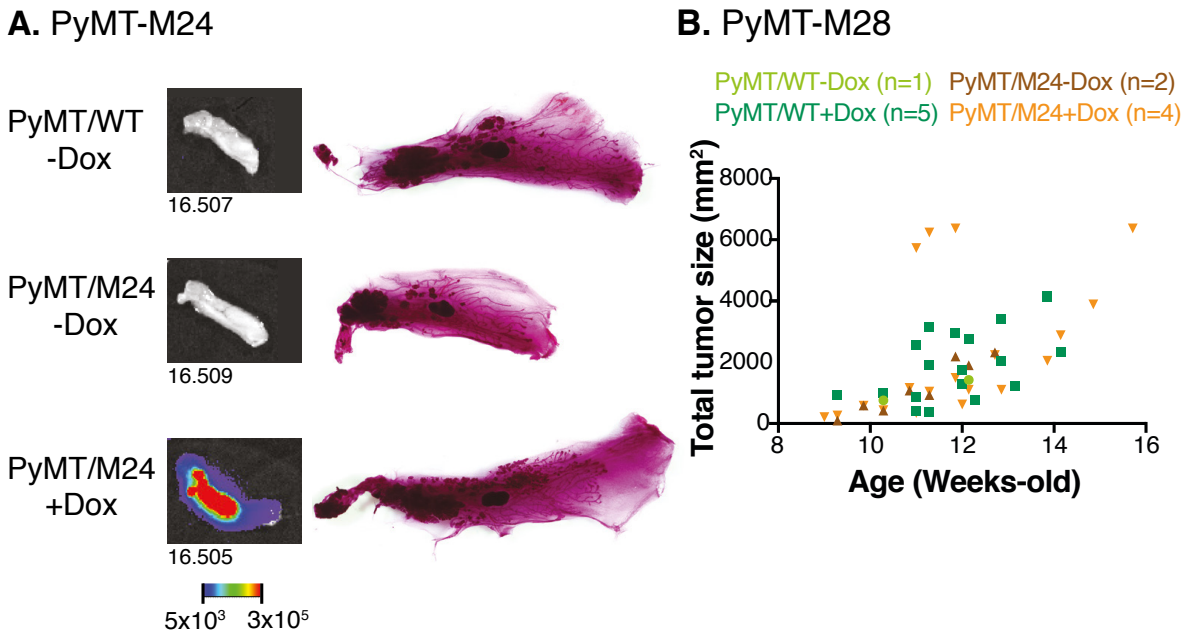

Figure 43. Transgene expression effect on tumor growth. **A.** Representative images of *ex vivo* mammary gland BLI signal from 6-week-old mice. PyMT-WT and PyMT-M24 mice were treated or not for one week with Dox as indicated. Whole mount mammary gland carmine staining shows ductal hyperplastic lesions. **B.** Quantification of total tumor size from the 10 mammary glands of PyMT-WT and PyMT-M28 mice. Females were classified as Dox treated and non-treated mice. Tumor size was measured with caliper and is represented by age.

Transgene detection *ex vivo*

Ex vivo tumors presented the same heterogeneity that we observed in the mammary glands of MAF Tg mice. Transgene expression was activated in several foci on the same tumor, but not in all the cancer cells. This heterogeneity is observed in both colonies (PyMT-M24 and PyMT-M28) (Figure 44). Furthermore, as observed in MAF Tg mouse, a clear loss of expression during tumor growth was detected in both colonies (Figure 45).

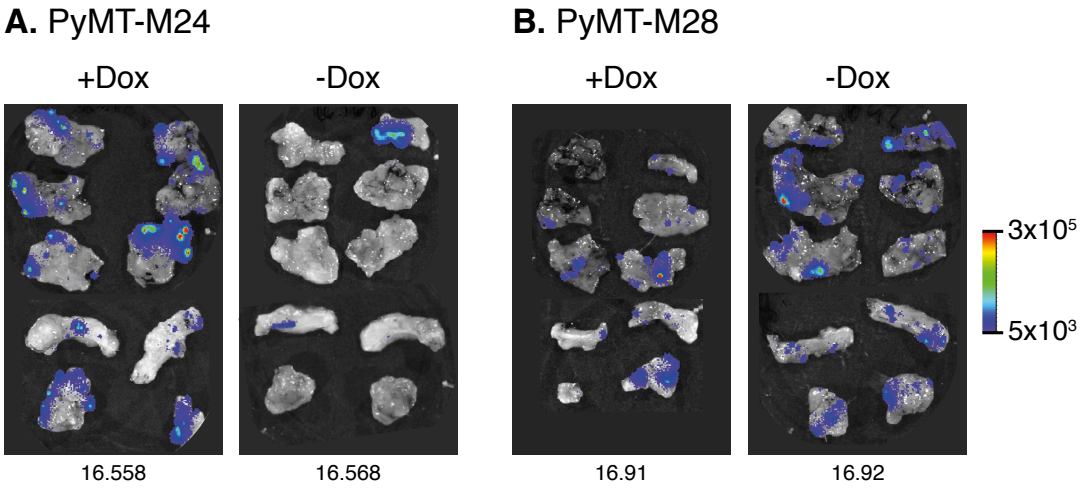

Figure 44. *Ex vivo* tumors from PyMT-MAF mice. **A.** *Ex vivo* tumors from 12-week-old PyMT-M24 females. **B.** *Ex vivo* tumors from 12-week-old PyMT-M28 females. Mice were administrated for 7 weeks with Dox (left panels) or without treatment (right panels).

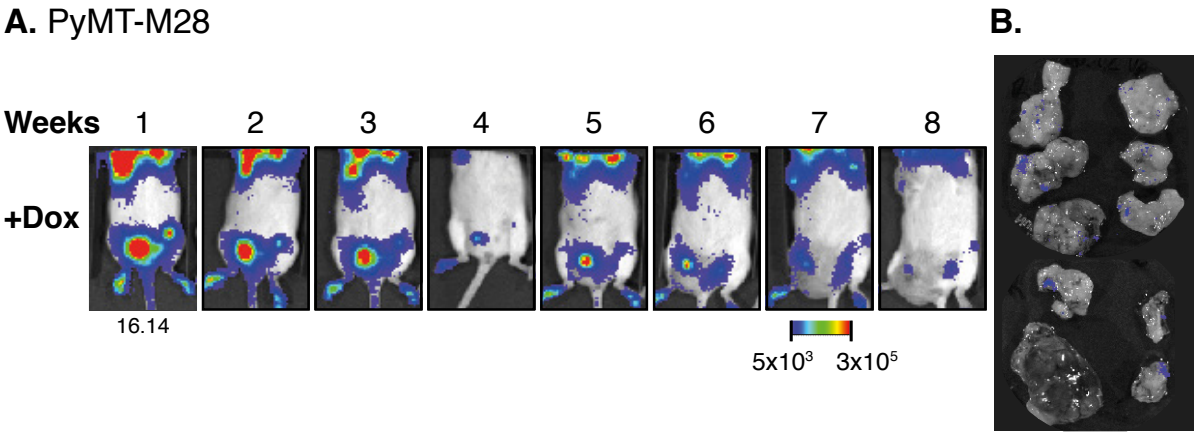

Figure 45. Loss of transgene expression during tumor growth. **A.** Representative *in vivo* ventral BLI images from PyMT-M28 female. Five-week-old mice were treated with Dox for 8 weeks. **B.** *Ex vivo* tumors from 13-week-old female after 8 weeks of Dox treatment.

Next, we assess transgene protein levels in the tumors, whereby a larger mass of epithelial cells with potential capacity to express the transgene was available as compared to normal mammary gland. In disaggregated tumors, no tGFP or Katushka fluorescence was detected by FACS, and MAF, luciferase, tGFP, katushka, and rtTA protein levels were undetectable by Western blot (data not shown). Similarly, no MAF or tGFP expression was detected by IHC or IF of paraffin-embedded sections (Figure 46). After protein analysis, we further analyzed mRNA transgene expression. MAF, GFP, and Luc mRNA were

analyzed by qRT-PCR from small pieces of the tumor with high luciferase signal. Again, expression was undetectable (data not shown).

Finally, no bone metastasis was observed, by means of luciferase activity, in skeleton of PyMT-MAF Tg mice when induced with Dox treatment during 7 weeks (data not shown). These results suggest that MAF expression was not enough to drive tumor cells to the bone and develop bone metastasis in MAF Tg mouse model, due to the need of higher MAF concentrations or longer periods of time.

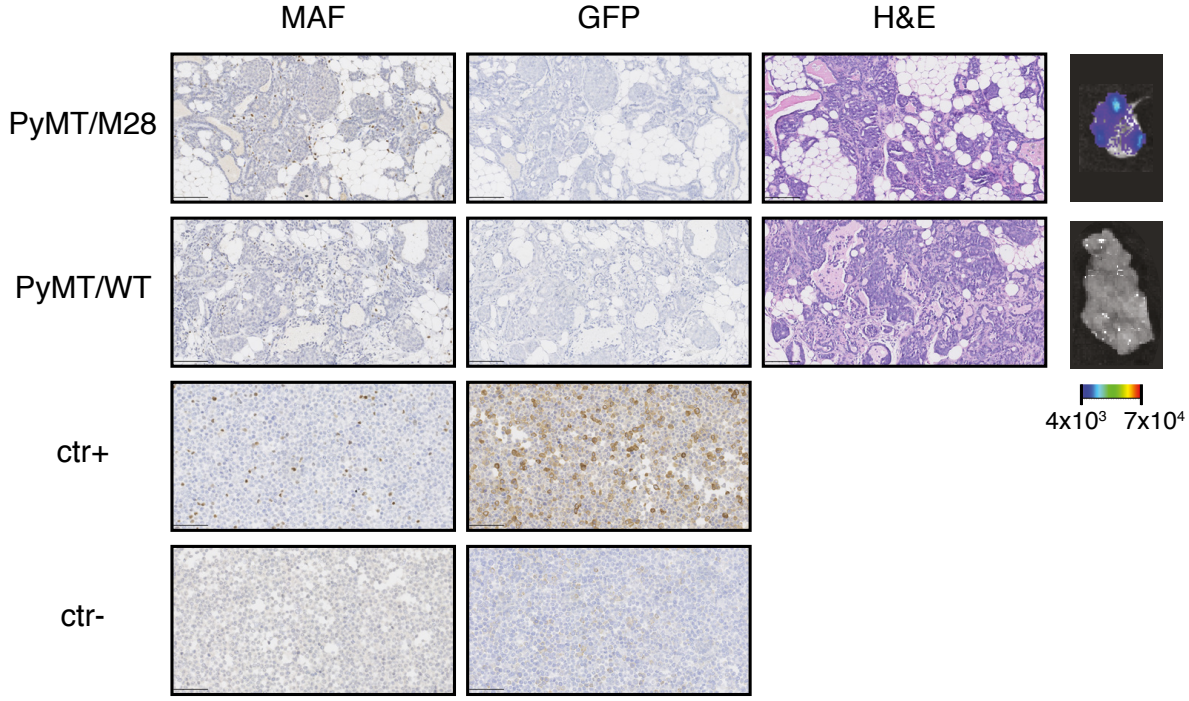

Figure 46. MAF and GFP detection of PyMT-M28 and PyMT-WT tumor sections. IHC of MAF, GFP, and H&E are shown. Pellet of MAF and GFP overexpressing cells is shown as control positive, cells without overexpression is control negative. Scale bar represents 100µm.

Primary culture of mammary epithelial cells

Further assays were performed with immortalized epithelial cells from PyMT-M24 Tg mouse models. We obtained a primary cell culture from PyMT-M24 Tg mouse, called 15.595, and another from PyMT-WT Tg mouse, called 1156. Cells were cultured in the presence or absence of Dox, and after 48 h of treatment, fluorescent protein levels were assessed. No detectable tGFP or Katushka fluorescence was observed by confocal microscopy or FACS (Figure 47A and 47B). Likewise, no differences in MAF protein levels in the PyMT-M24 tumors with luciferase activity were detected, as analyzed by Western blot, and no differences were observed for the mRNA levels of the transgene in

those cells (data not shown). Finally, we measured luciferase and renilla enzymes activity (Figure C). No differences were detected comparing treated and non-treated cells in a renilla assay. In contrast, some luciferase expression was detected in MAF Tg cells treated with 1 µg/ml of Dox.

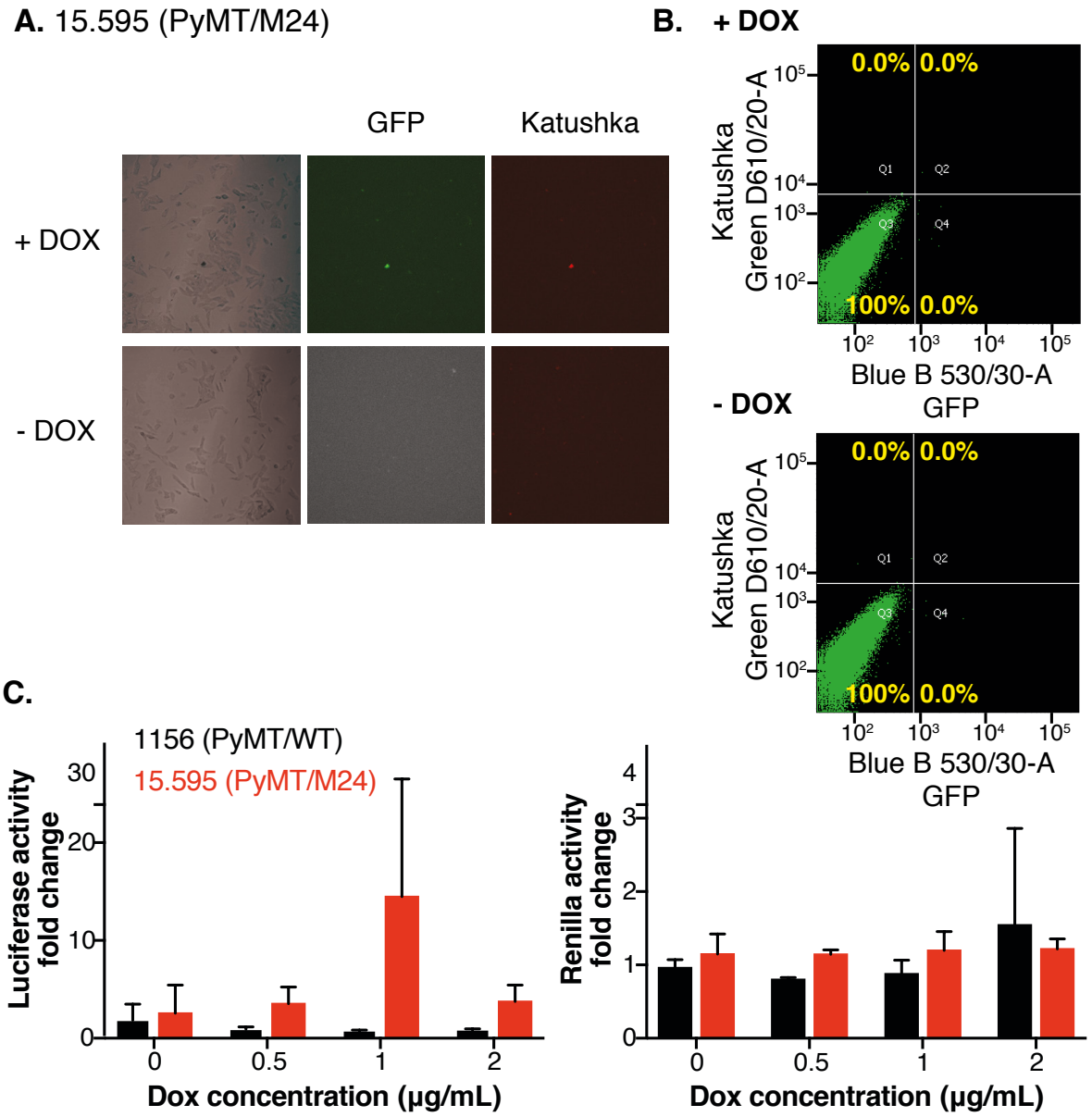

Figure 47. Fluorescent proteins and bioluminescent enzyme detection on primary culture of PyMT-M24 tumor cells. **A.** Confocal microscope images after 48 h of Dox treatment from 15.595 cells derived from a PyMT-M24 tumor. **B.** Flow cytometric analysis of 15.595 cells after Dox treatment (top) or without Dox treatment (bottom). Primary culture cells were analyzed based on GFP and Katushka expression. For all FACS analyses, percentage of gated cells is indicated. **C.** Luciferase and renilla assays of 1156 cells (PyMT-WT) and 15.595 cells (PyMT-M24) after 48 h with 0, 0.5, 1, or 2 µg/ml of Dox treatment. *P*-values were scored by two-sided Mann-Whitney test.

Chapter V:
Knock-in MAF mouse model

Introduction

Generation of transgenic mice is extensively used because it is an easy and fast technique to obtain simple genetically modified mice to perform gain-of-function assays. Transgene construct is injected directly into the pronucleus of fertilized oocytes that, once implanted into pseudopregnant females, give rise to transgenic mice. These mice contain random incorporation of the transgene into the genome causing important limitations, including disruption of important genes or silencing of the transgene as a result of the incorporation into an inactive chromosome region or due to high multiple-tandem copy number integration (Macleod and Jacks, 1999; Porret et al., 2006). To reduce variability and have better control of the transgene insertion, generation of knock-in mouse model was considered. The concept of knock-in mice is the same as for transgenic mouse, with one decisive improvement: the transgene insertion is targeted to a specific locus of the genome. The targeted insertion of a single copy of the transgene is performed by homologous recombination techniques.

Results

Challenges of generating MLG-RKT knock-in mouse

The generation of a knock-in mouse was made in parallel to the Tg mouse experiments. As a first criterion, Rosa26 locus was chosen to integrate the transgene by homologous recombination. The Rosa26 locus is commonly used as insertion site because is a largely known region that lacks essential genes and allows ubiquitous expression of the transgene (Friedrich and Soriano, 1991).

To avoid leakiness of non-treated mice, as we observed for the MAF Tg mouse, we decided to first exchange renilla (which is redundant *in vivo*) for a tTS silencer. tTS is composed of TetR fused to the viral transactivator VP16. It binds to Tet-On promoter in the absence of Dox, inhibiting rtTA unspecific binding. However, in the presence of Dox,

tTS forms a complex with Dox, changing its conformation and losing its affinity to the promoter (Zhu et al., 2001). Importantly, during Dox treatment, both constructs (rtTA and tTS) are co-expressed (Lamartina et al., 2003). To guarantee sufficient amount of rtTA to activate the system, we increased the rtTA/tTS ratio by separating the tTS gene from the rest of the construct using an internal ribosomal entry site (IRES) sequence. IRES facilitates translation initiation complex attachment and allows the expression of more than one gene downstream of a single promoter but in non-equimolar levels. Thus, IRES-dependent second gene is translated to a lower level than the upstream cap-dependent first gene (Mizuguchi et al., 2000).

We generated a large construct containing MAF, luciferase, and tGFP under the TetO promoter (MLG construct), as for the MAF Tg mouse, which was joined with a construct formed by rtTA, Katushka, and tTS under the MMTV promoter (RKT construct). This construct is 14,120 bp long and is flanked by Rosa26 homologous arms of approximately 3,000 bp each (Figure 48). After injection of the dsDNA plasmid into BL/6 ES cells, no homologous recombination was observed.

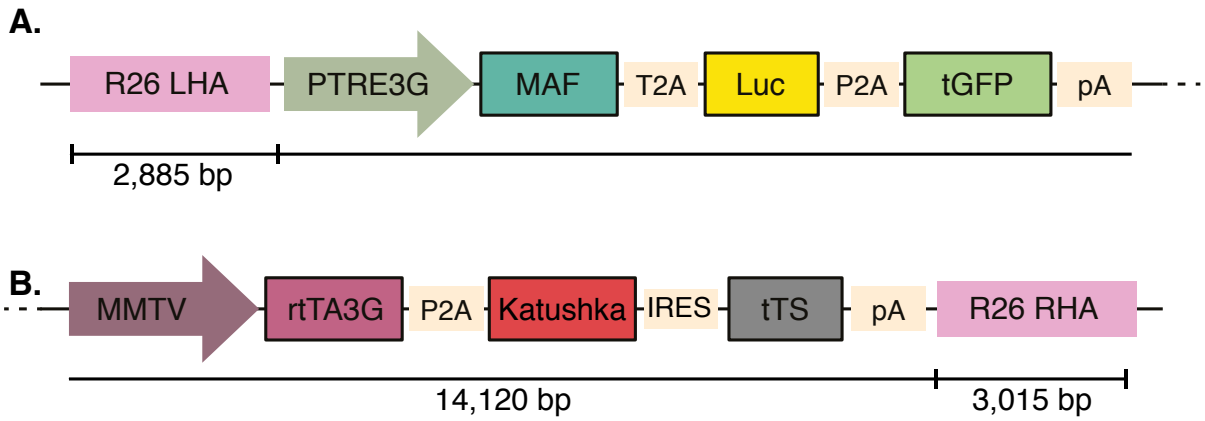

Figure 48. Scheme of MLG-RKT construct flanked by Rosa26 homologous arms. **A.** The MLG construct is formed by Tet-On promoter upstream of MAF, luciferase, and turboGFP genes. This construct has approximately 4,322 bp. **B.** The RKT construct contains rtTA, Katushka, and tTS under the MMTV promoter and is 6,077 bp long. Abbreviations: LHA, left homology arm; R26, Rosa26; RHA, right homology arm.

Alternatively, this construct was injected directly into the pronucleus of fertilized oocytes. To facilitate homologous recombination in the Rosa26 locus, we used CRISPR (Clustered Regularly Interspaced Short Palindromic Repeats)–associated protein-9 nuclease (Cas9).

CRISPR/Cas9 technology was a revolution and has been widely-used to edit the mice genome. The method uses a single guide RNA (gRNA) composed of an RNA duplex: a crRNA and a transactivating crRNA (tracrRNA or trRNA), that not only determines the DNA target site but also binds to the Cas9 endonuclease. Thus, gRNA drives binding of Cas9 to a desired location of the genome (Doudna and Charpentier, 2014; Jinek et al., 2012). There, Cas9 introduces a site-specific double-strand DNA break activating the double-strand break (DSB) repair machinery. It can be repaired either by the cellular non-homologous end joining (NHEJ) pathway, which generates random deletions and/or insertions, or by homology-directed repair (HDR) pathway, if a donor template with homology to the targeted locus is supplied, which would replace the genome in this specific locus (Figure 49). However, when we injected MLG-RKT construct with CRISPR/Cas9, this technology did not undergo homologous recombination, and no knock-in mice were obtained.

To enhance recombination, we next used the 2H2OP technology. The "two-hit by gRNA and two oligonucleotides with a targeting plasmid" technology (2H2OP) consists of the addition of two single-stranded oligodeoxynucleotides (ssODNs) together with two guide RNAs (gRNAs) and the donor plasmid. An advantage of this system compared to basic CRIPSR/Cas9 is that there is no need to add homology arms in the donor vector. One gRNA binds the Rosa26 locus and the other binds to a locus of the donor plasmid, upstream of the construct that will be inserted. They allow the DSB of the genomic DNA and the donor plasmid DNA to be formed. Additionally, ssODNs consists of complementary sequences of the donor plasmid as well as the genome, allowing the ligation of the entire plasmid into the genome (Yoshimi et al., 2016) (Figure 49). However, when we injected the MLG-RKT plasmid into the oocytes using 2H2OP method, no knock-in mice were generated.

The next approach was to isolate the transgene from the total plasmid and use two ssODNs that recognize the transgene and Rosa26 locus. To this aim, only one gRNA to cut the genome was needed (Figure 49). Again, this failed to generate the successful insertion of the transgene, suggesting that one of the biggest limitations that we were confronting was the extremely large size of the construct.

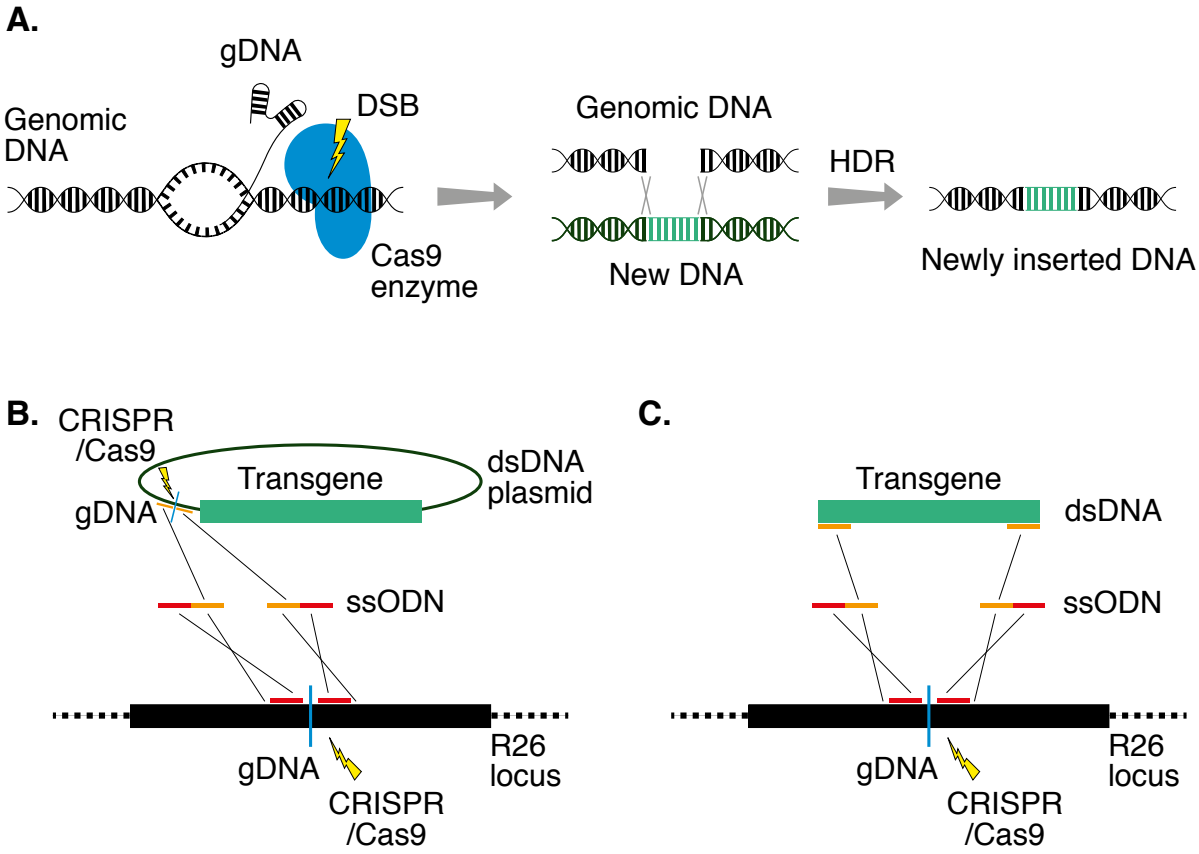

Figure 49. Scheme of CRISPR/Cas9 and 2H2OP technologies. **A.** CRISPR/Cas9 technology. Guide RNA (gRNA) binds to a specific locus of the genome and allows Cas9 nuclease attachment that cuts the target locus by a double-strand break (DSB). Donor DNA is inserted in the DSB by homologous recombination. **B.** 2H2OP technology. Two gRNAs drive Cas9-specific cutting into the genome and donor plasmid. ssODNs allow donor plasmid integration into the genome. **C.** 2H2OP technology. Cas9 cuts the genome, driven by a single gRNA. Two ssODNs drives insertion of the construct to DSB. Abbreviations: CRISPR, Clustered Regularly Interspaced Short Palindromic Repeats; Cas9, CRISPR associated protein-9 nuclease; DSB, double-strand break; dsDNA, double-stranded DNA; gDNA, guide DNA; HDR, Homology-directed repair; R26, Rosa26 locus; ssODN, single-stranded oligodeoxynucleotides.

Generation of MGL knock-in mice

We changed our strategy to generate the knock-in mouse due to the high technical difficulties of inserting a large construct into the genome as well as due to transgene expression limitations of Tet-On system that we had encountered. We therefore generated a new construct based on the Cre system technology (Figure 50). Bacterial Cre is a site-specific recombinase that catalyzes the homologous recombination between specific

sequences, the loxP sites (Branda and Dymecki, 2004). There are two possible methods to use this system: first, by flanking a gene of interest with loxP, which allows recombinase to generate a knock-out by ablation of the gene; and second, generating a knock-in by designing a construct with a flanked stop cassette, a strong translational and transcriptional termination, between the promoter and the transgene (Dragatsis and Zeitlin, 2001; Lakso et al., 1992). In this case, stop cassette blocks transcription, until recombinase removes its presence allowing the expression of the transgene. For our purpose, we chose to use the latter method.

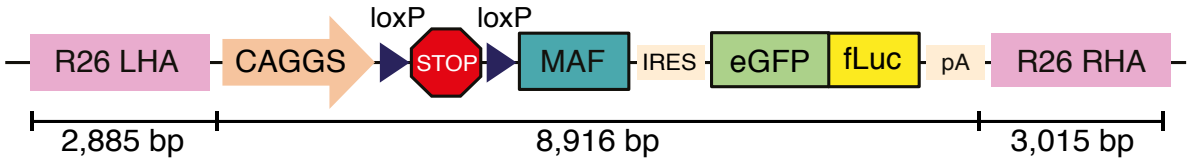

Figure 50. Structure of MGL construct. The CAGGS promoter was cloned upstream of a stop cassette flanked by loxP sites. Downstream *MAF* gene was cloned together with eGFP/luciferase fusion protein. Rosa26 homologous arms flanked MGL construct. Abbreviations: LHA, left homology arm; R26, Rosa26; RHA, right homology arm.

To this end, a stop cassette flanked with loxP sites was cloned downstream of the CAGGS promoter and upstream of MAF, GFP, and Luciferase. The CAAGS promoter comprises the CMV early enhancer element, the chicken β-actin promoter, and the rabbit β-globin polyA signal (Miyazaki et al., 1989), and it drives ubiquitous transgene expression. When inserted in the Rosa26 locus, it gives good results of expression (Alexopoulou et al., 2008). We inserted MAF and eGFP/fLuc fusion genes downstream of the stop cassette; the fusion gene eGFP/fLuc was obtained from the widely-used vector TGL and separated by an IRES sequence. At the end of the construct, we added a polyA sequence. Finally, we cloned recombinant homologous arms of the Rosa26 locus to flank the construct.

New injections were performed in fertilized oocytes with this plasmid by CRISPR/Cas9 technology with the entire construct and by 2H2OP method with the insertion of the dsDNA plasmid donor without homologous recombination arms. No positive knock-in mice were obtained.

On the other hand, homologous recombination on BL/6 ES cells resulted in five positive clones, confirmed by longPCR and Southern blot analysis (Figure 51). Based on these

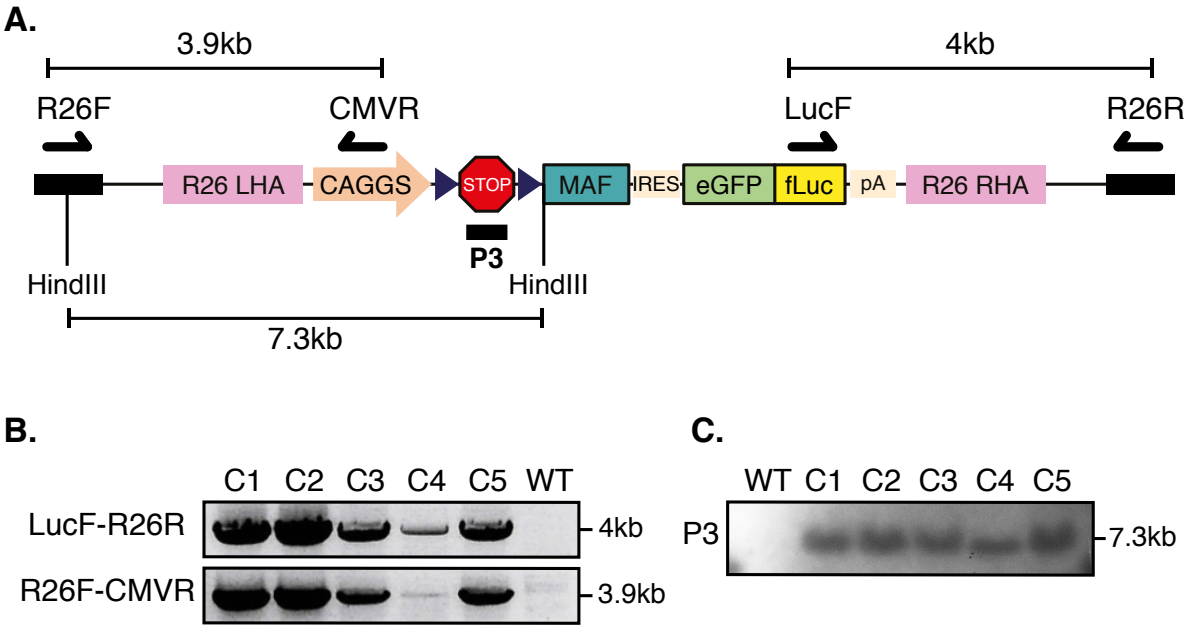

Figure 51. Long PCR and Southern blot confirmation of 5 clones with transgene integration in Rosa26. **A.** Structure of MGL construct. Primers that drive longPCR are represented. HindIII restriction sites and the localization of Southern blot probe (P3) are shown. **B.** LongPCR image of the 5 positive clones and a negative clone. R26F primer is located in the genome, and CMVR primer binds to the CAGGS promoter. The LucF primer recognizes luciferase sequence and amplifies longPCR to R26R primer located on the Rosa26 locus on the mouse genome. **C.** Southern blot analysis using the probe 3 (P3) of the negative and the 5 positive ES cells for the transgene integration.

results, injections of the positive ES cells into early mouse embryos were planned.

Once we obtain the MGL knock-in mouse, we will cross it with a mouse model carrying Cre under a mammary gland specific promoter to activate MAF expression in a tissue-specific manner. To this end, we can benefit from MMTV-Cre or WAP-Cre, the most commonly mouse models used. Alternatively, conditional Cre systems emerged as an improvement in Cre-lox system to control the expression in a time-specific manner. They consist of Cre recombinases, called CreER, composed of the fusion of the Cre recombinase gene to a mutated ligand-binding domain of the human estrogen receptor. Modified CreER can be translocated into the nucleus only after binding of tamoxifen, a ligand of ER, where it performs recombination of loxP sites. Thereby, CRE would only promote recombination under tamoxifen induction (Feil et al., 2009; Sauer and Henderson, 1989; Wagner et al., 1997). For metastatic experiments the cross with breast cancer mouse models will be required.

- Discussion -

Discussion

MAF overexpression on androgen-independent PC cell lines does not promote bone metastasis in xenograft experiments

The National Cancer Institute estimates that prostate cancer will result in 26,730 deaths in 2017 (www.cancer.gov); this high mortality rate is associated to the spread of malignant cells to distant organs, especially to bone. Currently, there are no well-defined bone metastasis mediators in PC patients, making it essential to better understand this process in order to further study potential targets for driving development of new drugs. Given the importance of MAF as a bone metastasis predictor in BC, we hypothesized that MAF could also have a role in PC. To address this, we first analyzed the copy number alteration of MAF in a discovery-training set of patients. Importantly, we have demonstrated an association between MAF expression in primary tumors and bone colonization in PC patients (Figure 20).

We next tested this hypothesis using PC cell lines. For this, we analyzed a panel of three widely-used PC cell lines, of LNCaP, PC-3, and DU-145. PC-3 was derived from a vertebral bone metastasis (Kaighn et al., 1979), and DU-145, from a brain metastasis (Stone et al., 1978). Both of these cell lines lack androgen receptors (AR) and are therefore androgen independent, and they produce poorly differentiated tumors in the mice. However, the majority of PC tumors present AR (Grignon, 2004), such that the PC-3 and DU-145 models do not faithfully mimic human disease. In contrast, the LNCaP cell line was established from a lymph node metastasis and retains androgen sensitivity (Horoszewicz et al., 1980). LNCaP cells have poorly tumorigenic features.

To determine the role of MAF in PC cell lines, we first analyzed *MAF* amplification and endogenous expression. We studied the 16q23 locus amplification in these cell lines and found amplification in all of them, particularly in the LNCaP cell line (Figure 21). This 16q23 locus amplification in LNCaP cells correlated with high endogenous levels of MAF mRNA and MAF protein. Alternatively, both PC-3 and DU-145 presented low levels of MAF expression (Figure 22).

We then aimed to validate this hypothesis with xenograft models using gain- and loss-of-function approaches. We downregulated MAF in LNCaP cells and then injected those cells intracardiacally and intratibially into male mice. No growth was observed in mice inoculated with LNCaP cells into the blood stream or the tibia; this correlates with the previous observation that parental LNCaP cells are not able to colonize the mice skeleton (Wu et al., 1998), although they present capacity to metastasize to human bones (as showed in pre-implanted adult human bone fragments) (Yonou et al., 2004). Alternatively, LNCaP lineage–derived cell lines, such as C4-2, are able to metastasize into mouse bone and could be used in future experiments. First, they are high-expressing endogenous MAF cells for performing knock-down experiments, and second, they mimic the natural course of PC progression in humans by losing androgen dependence and developing bone metastasis. C4-2 cells are an androgen-independent LNCaP subline that acquired point mutations at the androgen receptor (AR), decreasing its steroid specificity (Thalmann et al., 1994). As a second approach, androgen-dependent cells could be inoculated in the presence of dihydrotestosterone (DHT) pellets, even though they are difficult to obtain due to company policy of anabolic steroids exportation.

However, both the MAF short and long isoforms were overexpressed in low-MAF endogenous expressing cell lines (e.g. PC-3 and DU-145). Unexpectedly, no differences were observed in terms of bone or lung colonization by injecting these cells either IC or IT (Figures 24-26). Further proliferation analyses must be done in the injected cells to ensure that the proliferation rate is the same between control and MAF-overexpressing cells, as MAF infection can result in slower growth, with cells needing some time to recover. Xenograft experiments with PC-3 and DU-145 androgen-independent PC cells did not mimic the strong association between MAF and bone metastasis found in PC patients.

The lack of bone metastasis in this context cannot be attributed to bone immaturity at the time of injection, as mice were inoculated between 10 and 12-week-old. Previous studies in our laboratory determined a minimum age of 8 weeks for performing bone metastatic studies. Sexual maturity in mice occurs at 6-8 weeks of age, at which time the longitudinal bone growth is highly reduced (Jilka, 2013). Thus, injections in adult mice is reminiscent of the human adult bone and is the stage at which patients can suffer from bone metastasis. For that reason, all xenograft experiments that aim to study bone metastasis were carried out in sexually mature mice.

MAF as a new potential target to develop novel drugs to prevent or treat bone metastasis

To determine the magnitude of MAF influence in BC bone metastasis, we compared the effect of MAF downregulation (shMAF) in BoM2 MCF7, a high–bone metastasis derivative, together with bone metastatic drugs that target specific pathways in bone, including recombinant osteoprotegerin (OPG), zoledronic acid (ZOL), and antagonist of PTHrP (PTHrP AN). Specifically, OPG competes with RANK for RANKL binding, thereby impinging osteoclast differentiation and bone resorption (Simonet et al., 1997); ZOL is a bisphosphonate that binds to hydroxyapatite of the bone matrix, preventing bone degradation (Drake et al., 2008); and PTHrP AN inhibits PTHrP, resulting in a reduction of osteolytic lesions (Saito et al., 2005). In this thesis, we found that MAF downregulation in BoM2 cells reverts its capacity to colonize bone, in a greater extent than other specialized drugs, and with a similar effectiveness as ZOL (Figure 27).

Currently, the first-line drugs administrated to patients diagnosed with bone metastasis are denosumab and ZOL. Denosumab is a fully human monoclonal antibody that only inhibits human RANKL (Lacey et al., 2012). For this reason, we could not inject this drug in our xenograft experiments in mice. Alternatively, we used the recombinant human OPG-Fc, as it is able to recognize RANKL from multiple species, including mice (Kostenuik et al., 2009). For ZOL treatment, we administrated the maximum dose of ZOL (0.5 mg/kg) to the mice to determine the maximum effect of this drug in terms of bone metastasis reduction and to better compare its effects to the shMAF effect. In contrast, for the experiments in which we directly compared the effects of MAF in ZOL treatment, we reduced the ZOL dose to one that best mimics ZOL administration in patients (0.1 mg/kg) (Ottewell et al., 2008).

MAF is a transcription factor that activates several proteins, such as PTHrP, cyclin D2, integrin β7, CCR1, and ARK5 (Hurt et al., 2004; Suzuki et al., 2005). It has been shown that PTHrP activation by MAF benefits bone colonization but is not enough to predict a high risk of bone metastasis at early stages of BC (Henderson et al., 2006; Takagaki et al., 2012). Consistent with these studies, our results emphasize the hypothesis that MAF has a high potential to promote bone metastasis that does not rely only on PTHrP activation, as the PTHrP antagonist drug has a lower effect on inhibiting bone metastasis than MAF depletion. Thus, upstream players of the MAF pathway emerge as potential targets for developing new drugs against bone colonization.

MAF change BC metastatic pattern in the context of ZOL treatment

The importance of MAF in stratifying BC patients who can benefit from ZOL treatment has recently been reported (Coleman et al., 2017). This study suggests that all patients with MAF- tumors treated with ZOL are likely to have an improved invasive disease-free survival (IDFS) as compared with control patients, independent of their hormone status. In contrast, for BC patients with MAF+ tumors, ZOL treatment is affected by menopause. Importantly, in non-postmenopausal patients, bisphosphonates show adverse effects on IDFS, increasing the extraskeletal metastasis in those patients. To study the behavior of MAF+ cells on colonizing soft tissues *in vivo*, we collected all the metastatic xenograft experiments performed in our laboratory (ER+ and ER– cell lines). In general terms, we observed that MAF expression decreased the ability of cancer cells to metastasize to soft tissues (i.e. lung) (data not shown). It was therefore tempting to speculate that MAF overexpressing cells do not colonize lungs or other soft tissues due to their intrinsic propensity to establish into the bone parenchyma. Notwithstanding, in the context of ZOL treatment, which restricts bone colonization, this propensity can drastically change. As observed in MAF+ tumors from non-postmenopausal women included in the AZURE trial (Coleman et al., 2017), ZOL administration can change MAF+ tumor propensity to metastasize to bone and increase the extraskeletal recurrences.

To further validate this hypothesis in xenograft experiments, we used the ER– cell line MDA-MB-231, to simulate an important subtype of premenopausal BC patient tumors. Cells with or without overexpression of MAF were inoculated intratibialy into mice and treated randomly with ZOL or PBS (as a control) (Figure 28). Surprisingly, MAF OE cells presented less skeletal metastatic incidences than control cells. A low tendency to colonize bone could be due to MAF acting as a mediator of bone metastasis, especially in ER+ tumors, which exhibit a higher propensity to colonize skeleton; indeed, less evidence for this was found in ER– tumors.

For mice treated with ZOL, a trend to decrease bone metastasis incidence and increase brain colonization was observed. Thereby, MAF overexpression showed a trend to change metastatic pattern colonization in the presence of ZOL treatment. Thus, xenograft experiments performed with MDA-MB-231 cells showed a tendency to recapitulate our previous hypothesis that, under ZOL treatment, MAF expression influences BC tumor metastasis mobilization from skeleton to soft tissue. Thus, further experiments are required to fully complete these observations.

One open question was at which time point the first administration of ZOL should be injected into mice, and which BC xenograft model should be used, to mimic in mouse models the results obtained from the AZURE trial. In the AZURE trial, patients were treated with ZOL as an adjuvant systemic treatment after resection of the primary tumor and with no evidence of distant metastases. It is known that CTCs remain in circulation during brief periods of time, and that after primary tumor resection, almost no CTC is found in the bloodstream (Biggers et al., 2009). For this reason, we hypothesized that, at the moment when AZURE randomized patients were treated with preventive ZOL, potential DTCs were already established in the bone microenvironment, even though no evidence of bone colonization was found at that moment. We thus injected MDA-MB-231 cells intratibially and started ZOL injections on the day of cell inoculation, before observing obvious bone lesions.

A second option could have been to inject BC cells by intracardiac injection and to start administration of ZOL treatment some days after BC cell inoculation, once some DTCs are likely to have reached the bone but before acquiring detectable bone lesions.

Alternatively, to mimic the bone metastatic dormant DTCs at the time of ZOL treatment, a T47D-derived cell line developed in our laboratory (dormant bone metastasis, DBM) could be used. DBM cells were isolated from a bone metastatic lesion after two rounds of *in vivo* selection in mice. DBM cells present a long latency and high propensity to metastasize to bone as compared to parental T47D. Kinetics on DBM cells mimic human bone metastasis progression, divided into bone homing, dormant micrometastasis, and (after long periods) macrometastatic lesion. Injection of those cells intracardiacly, and treating with ZOL once dormant micrometastasis are observed, could be an alternative option to validate our hypothesis. As DBM is an ER+ cell line, the majority of ER+ cells present a propensity to metastasize to the bone, and further, it requires external estrogen administration to the mice to mimic the hormonal status of premenopausal patients, making it a good model.

Finally, orthotopic injections and subsequent resection of the primary tumor could also be performed to simulate BC patients included in the AZURE trial.

MAF Tg mouse: Generation and characterization

Genetically-engineered mouse (GEM) models are useful tools to understanding genotype-phenotype relationships underlying disease mechanisms, and have been used as such since the generation of the first GEM through embryos transformation (Gordon et al., 1980). In this thesis, one of our aims was to use this mouse model to decipher the role of MAF in a physiological context, such as in mammary gland development. In addition, we wanted to explore the role of MAF on tumorigenic initiation capabilities and MAF metastatic dependences. For this reason, and due to the importance of MAF OE in BC to mediate bone metastasis, we aimed to generate a transgenic mouse with MAF inducible overexpression in the mammary gland, in an attempt to obtain the first bone metastatic model. This novel Tg mouse would be a tremendously useful tool for studying bone metastasis development and would provide an adequate scenario for screening drug compounds to treat bone metastasis. In addition, it would be an excellent tool to obtain a deep insight into MAF-dependent BC bone metastasis mechanism, and specifically, for understanding when and how MAF is required in this process, and which cells overexpress MAF. Are MAF OE cells those that acquire capabilities to metastasize to the bone, or are they the primary tumor cells that prepare the niche to allow DTC colonization?

When designing a new mouse model, several factors should be considered. The promoter is critical for a spatial-temporal regulation of the transgene. To make a time-inducible expression, we chose a Tet-On system that has a binary system of the Tet-On promoter (PTRE), which is only active in the presence of a transactivation protein rtTA, and Dox (Gossen and Bujard, 1992; Gossen et al., 1995). Tet-On has been successfully used for reversible induction and repression of a variety of genes (Fan et al., 2012; Furth et al., 1994; Xu et al., 2005; Zhu et al., 2002). We took advantage of this system to design two constructs for the generation of an inducible MAF Tg mouse.

The first contains rtTA, renilla, and Katushka under the MMTV promoter. Thus, these genes are transcribed in the mammary gland constitutively. The second construct carries MAF, luciferase, and tGFP under the Tet-On promoter, which is only active in the mammary gland, where rtTA is transcribed, and under Dox treatment (Figure 30). Both constructs were coinjected in the pronucleus of fertilized oocytes, and several founder mice were generated.

We crossed these founders with wild-type mice to generate independent colonies. Finally, we developed the experiments using two independent colonies. We studied the two colonies

in parallel to avoid a phenotype effect due to the site of transgene integration rather than to the transgene itself.

This MAF Tg mouse model was designed to follow transgene expression *in vivo* of both constructs through renilla and luciferase activity. These proteins are enzymes which catalyze a bioluminescent reaction, and their activity can be detected directly by measuring its product formation. Enzyme activity assay is a very sensitive method, because a single enzyme has a high turnover of its numerous substrate molecules, thus amplifying the signal and allowing both single-cell detection and differentiation from biological noise and cellular heterogeneity (Kovarik and Allbritton, 2011; Rabinovich et al., 2008). Indeed, luciferase activity has been reported to detect even a single cancer cell (4T1-luc2) by *in vivo* bioluminescence imaging using the IVIS system (Kim et al., 2010). If we compare luciferase and renilla activity, they have distinctly diverse kinetics of light production. Renilla activity presents a quick peak in the initial 10 s and a further rapid decline in less than 10 min, and has a substrate (coelenterazine) that is instable in plasma, making it an insufficient bioluminescent light yield to monitor *in vivo* (Bhaumik and Gambhir, 2002).

After generating the Tg mouse colonies, we performed *in vivo* renilla and luciferase assays. Importantly, mammary gland bioluminescent luciferase and renilla expression was found in the majority of Dox-treated female mice, but also in an important number of non-treated mice. This leakiness in the system is due to the basal level of affinity that rtTA exhibit to Tet-On promoter even in absence of Dox (Zhu et al., 2001, 2002). Although the system was improved by using a third generation of tetracyclines (Loew et al., 2010; Zhou et al., 2006), which reduced leakiness and increased Dox sensitivity, we still observed a basal transgene expression in the absence of Dox in the MAF Tg mouse model we generated, as well as low doxycycline-dependent induction of the promoter (Figure 31).

The other promoter used in our system was the MMTV promoter taken from MMTV-Sv40-Bssk plasmid (Addgene), which widely used to generate Tg mice and that directs transgene expression in the epithelial cells of the mammary gland and other secretory organs, such as salivary gland (Hennighausen et al., 1995; Muller et al., 1988). This promoter is one of the most frequent promoters used to trigger mammary gland epithelium expression, as is not dependent on the lactation state, such as WAP. The first mouse model generated with the combination of MMTV-rtTA expression and Tet-On promoter was

done by Gunther et al (Gunther et al., 2002). In this case, the MMTV-rtTA mouse model was crossed with a mouse model with a Tet-On reporter gene, and expression was induced and turned off with Dox treatment. Strikingly, in contrast to what we observed in our mouse model, basal activation of the transgene without induction was inappreciable in their experiments.

However, heterogeneous transgene activation in the mammary gland epithelium has been observed in MMTV-based transgenic mice (Gunther et al., 2002; Hennighausen et al., 1995), as we had observed by luciferase activity in MAF Tg mouse model (Figure 38). This fact can imply a low penetrance of transgene-mediated phenotypes, which could make it difficult to study non-aggressive oncogenes. Moreover, heterogeneous expression has been suggested to cause a decrease in transgene expression with age (Gunther et al., 2002), the same phenotype that we observed in MAF Tg old mice (Figures 35-36). It is noteworthy than MAF Tg Dox-treated mice showed transgene expression in other organs besides the mammary gland. Clearly, MMTV expression is also active in the salivary gland of MAF mouse model. However, we observed leakiness expression localized also on the mouse tail and legs. This leakiness must be other secondary sites of MMTV activation, as has been previously shown but which had not been described in a MMTV-tTA/TetO-Luc mouse (Sakamoto et al., 2012).

Next, we determined the copy number integration of the transgene by Southern blot to guarantee that the mouse colony was stable (Figures 33-34). Surprisingly, in the first offspring, a loss of copy number integration was observed, which corresponded to a better transgene expression in the mammary gland. Finally, after three generations of mice, we could verify the stable transmission of the transgene. Importantly, one of the limitations that we confronted in generating a transgenic mouse was the variability of transgene expression, which depended on the locus and the copy number integration of the transgene. Moreover, epigenetic silencing has been shown in old animals with high copy number; this as well as insertion of tandem multiple-copy arrays at single sites may increase chromatin condensation by interaction between repeats, thereby reducing transgene expression (Garrick et al., 1998; Henikoff, 1998). For this reason, the copy number of the transgene needed to promote bone metastasis cannot be predicted. In human patients, three copies of 16q23 (*MAF*) is enough for an association with bone metastasis, although expression of the transgene in mouse models not only depends on the copy number but also on the locus of integration (Haruyama et al., 2009). Integration near a repressed promoter or near an endogenous enhancer or highly active promoter can induce transgene silencing or leaky

expression, respectively. For example, *MAF* overexpression in the T-cell compartment requires a minimum copy number of six transgene to develop T-cell lymphoma. In these studies, the levels of mRNA expression was copy number–dependent (Morito et al., 2006). On the other hand, the MAF Tg mouse model that expresses MAF especially in B cells and that promotes the development of B-cell lymphoma at older ages, resembling to human multiple myeloma (MM), contain between two and four copy numbers of the transgene; this is enough to generate B-cell lymphomas (Morito et al., 2011). This observation is in accordance with the fact that, in human MM, translocation and copy number alteration of the *MAF* gene is found in 5-10% of the patients, but it does not correlate to the 50% of MAF overexpression found in myeloma cells purified from patient samples (Kienast and Berdel, 2004). To sum up, results from Southern blot analysis suggest that we initially generated a Tg with silenced multiple copy number of the transgene localized in tandem, and that loss of some copy number integration after generations allowed a better and more specific transgene expression.

We next performed transgene studies *ex vivo* to detect mRNA by qRT-PCR and proteins by Western blot, FACS, confocal microscopy, IHC, and IF. We analyzed all transcripts involved in this model, including MAF and fluorescent proteins. Unfortunately, we did not detect gene transcription. At this point, we realized the important drawback of our system, namely, while the read-out of the transgene expression and functional activity could be verified by luciferase and renilla signals *in vivo*, the mRNA and proteins could not be observed *ex vivo*. Collectively, these observations suggest that our main difficulty in introducing the MAF mouse model is the detection of transgene expression. It is tempting to postulate that we face low expression of our transgene, undetectable by the limits of our technical resources except for the bioluminescent assays, which is the technique with the lowest detection limits.

One variable that we should consider in these experiments is the concentration of Dox that should be administered to mice. High Dox concentrations may increase Tet-On activation and consequently transgene expression, as we could slightly observe in MAF Tg mouse (data not shown). It is true that some previous studies have observed higher expression of the transgene after treated mice with high concentrations of Dox via the drinking water (2 mg/ml) (Gunther et al., 2002) or via intraperitoneal injections; however, these studies contemplated only short-term exposition. Nonetheless, in long-term experiments high concentrations of Dox must be avoided, as Dox has a bitter taste and

could cause dehydration of mice. We decided to administrate 1 mg/ml of Dox via drinking water with the addition of 5% sucrose to try neutralize its bitter taste (Abad et al., 2013; Mateo et al., 2017). This concentration was enough to observe transgene expression in similar levels as after using higher concentrations.

Irrespective of these limitations, we determined the effect of transgene activation in the mammary gland development (Figure 40). Besides a few individual cases of huge branching development in each group, we did not observe any significant difference in terms of accelerated branching. It should be noted that we assumed that the estrous cycle was synchronized among females in the same cage. The estrous cycle in female mice is a 4-5 days long period composed by four phases: proestrus, estrus, metestrus, and diestrus (Hovey et al., 2002). Estrus is the phase in which ovulation occurs and females can become pregnant. It lasts 15 hours, and ovulation usually occurs during the middle of the dark cycle. As we assumed in our experiments, the estrous cycle could be suppressed by grouping of female mice in the absence of males for 10 to 14 days. This phenomenon is called the Lee-Boot effect (Van der Lee and Boot, 1955). Thereafter, in the presence of either males or male pheromones, the estrous cycle becomes synchronized in females, resulting in a higher percentage of females becoming pregnant, a phenomenon called the Whitten effect (McKinney, 1972).

While grouping females and a Whitten effect can increase the percentage of pregnant mice in a mating, studying development of mammary gland based on a system to track the stage of estrous would be preferable. Even though mice were sacrificed at the same time point, differences on branching could be observed depending of the estrous phase where they were sacrificed. Thus, in future studies, we should perform a vaginal cytology to identify the exact phase of the estrous cycle, and sacrifice females at the same phase instead of the same time point (Byers et al., 2012).

On the other hand, treatment of MAF Tg females for more than a year with Dox did not result in the development of tumors (data not shown), suggesting that the concentration of MAF expressed in the mammary glands of MAF Tg mouse model was not enough to induce tumor initiation capabilities. These data correlate with previous observations of MAF as a predictor of bone metastasis rather than a tumor initiation gene (Pavlovic et al., 2015).

MAF in tumorigenesis

Although much progress has occurred in the past decade on the generation of new preclinical transgenic mouse models that successfully reproduce the initial steps of tumorigenesis, these models still present a limited distribution of metastasis. For instance, brain and bone, organs commonly colonized in patients, are rarely metastatic in transgenic mice due to the lack of key metastasis-driving genes (Eckhardt et al., 2012). After discovering MAF as a mediator of bone metastasis, we had the opportunity and challenge to generate the first bone metastatic BC mouse model. This model could be used to better understand the biology of metastatic disease, and in particular of MAF-derived bone metastasis. Additionally, it could be used to test newly-developed therapies against bone colonization in a context that contains complete stromal and immunologic system interactions. In addition to studying the effect that currently-used drugs, such as bisphosphonates, have on MAF-overexpressing and -non-overexpressing tumors, we would be able to test new drugs, such as MAF-directed target therapies.

Indeed, an important research line in our laboratory is based on identifying new targets against MAF and generating new specific inhibitory drugs, making such a model highly relevant for us. A MAF Tg mouse model with bone metastatic progression could be an ideal tool to test the newly identified drugs and other MAF inhibitors. One example could be the MAF dimerization inhibitor, whose interaction with MAF destabilizes the MAF homodimer that is crucial for binding to DNA, and thereby alters its functions (Pellegrino et al., 2014). An additional, and equally important, new drug could be UBE2O, which is a ubiquitin-conjugating enzyme that mediates MAF polyubiquitiniation and degradation in proteasomes. UBE2O induce apoptosis to a subset of multiple myeloma (MM) cells that express MAF and delays MM tumor growth in mice (Xu et al., 2017). Alternatively, inhibition of USP5, a deubiquitase that stabilizes MAF and prevents its degradation, can also trigger apoptosis in MAF-expressing MM cells (Wang et al., 2017).

To understand the contribution of MAF to metastasis, we first crossed MAF Tg mouse with a BC mouse model. Of the various available mouse models of BC, we chose the MMTV-PyMT mouse model, because it develops mammary tumors with high penetrance. These tumors are, to a certain degree, similar histologically and molecularly to human tumors. They pass through several phases, starting with a premalignant state, converting to a carcinoma *in situ*, and finally acquiring invasive capabilities (Lin et al., 2003). They also present the shortest tumor latency characterized, with a 100% of tumor incidence,

and are able to metastasize to lung and lymph nodes with a 85% and 51% incidence, respectively (Fantozzi and Christofori, 2006). Short tumor latency is beneficial to reducing long-term experiments but could also be a double-edged sword, because shortening the lifetime of the mice can avoid a potential bone metastatic colonization, particularly if longer latency is need to develop such metastasis. Markedly, in BC patients, latency for metastatic disease can occur months or even decades after primary tumor detection. For our experiments, offspring from the cross of MAF Tg mice with MMTV-PyMT were divided into treated and non-treated cages. After 3 months, no bone metastasis was detected. One of the explanations could be the need of longer periods of time to analyze the metastatic disease, or the incapacity to detect small lesions by luminescent activity due to the low transgene expression.

One option for prolonging the development of metastasis could be to resect the primary tumor; however, we discarded this option due to the presence of multiple primary tumors that make this option overly challenging technique (Eckhardt et al., 2012). A further approach to overcoming this problem of short latency would be to resect primary tumors from PyMT-WT or PyMT-MAF mice, divide them into small pieces, and implant them orthotopically in WT or MAF Tg mice (Varticovski et al., 2007). In this context, we could induce MAF in the double Tg mice to promote MAF expression in the tumor, and we could also induce MAF in the receptor mice before and during tumoral growth. This approach could be useful to determine if MAF can prepare the metastatic niche before the arrival of tumor cells, or if only intrinsic MAF expression in the tumor cells is enough to drive metastasis. Moreover, it prolongs the latency time in the mice to allow formation of bone lesions.

Finally, crossing MAF Tg mouse with other mouse models of BC that present longer tumor latency is a strong alternative option. A good candidate could be MMTV-Neu, a mouse that presents multifocal adenocarcinomas with a 6 to 7-month latency and 100% frequency. It metastasizes to the lung after approximately 8 months. MMTV-Neu consists of an amplification of the gene encoding ERBB2. However, this model, as well as MMTV-PyMT, presents a gradual loss of ER and PR receptors. This is similar to BC patients treated with adjuvant therapy, in which metastatic cells present a reduction of 1.65-fold change in ER as compared to tumor cells in the primary tumor (Cejalvo et al., 2017). Given the fact that MAF increases the risk to develop bone metastasis, and that bone metastases are more frequent in ER+ tumors, we can speculate that ER+ mouse models would be more appropriate to perform these experiments. The STAT1

knock-out mouse is the only mouse model that spontaneously develops mammary gland adenocarcinomas, which show remarkable similarities to human ER+ luminal BCs, with the ER presence maintained during tumor growth. Its penetrance is close to 100% in multiparous females, with a latency between 12–20 months (Chen et al., 2015). STAT1$^{-/-}$ mice have been already crossed with a MAF Tg mouse model, and double Tg mice are currently being treated and crossed in our laboratory (data not shown).

One of the big concerns in these experiments is that we found that an increased volume of epithelial cells in tumors does not correlate with higher level of luciferase activity. Two hypotheses emerged to explain this fact: the first one is the heterogeneity of the transgene expression and gradual loss with age (as mentioned above), and the second one is the potential necrotic zones of the tumor that Dox or luciferin cannot reach, thus impinging on transgene expression.

Another important concern is that the Tet-On system has potential limitations, apart from the leakiness expression in mouse models, which could interfere in the planned bone metastatic analysis experiments. For instance, Dox administration cause changes in bone remodeling (Folwarczna et al., 2003). In general, it is believed that tetracyclines, and in particular doxycycline, have the ability to inhibit matrix metalloproteinases (MMPs) including collagenase, which reduces connective tissue breakdown, such as bone resorption (Golub et al., 1998; Klapisz-Wolikow and Saffar, 1996; Williams et al., 1998). Furthermore, tetracycline administration affect both osteoclast and osteoblast function (Bettany et al., 2000; Vernillo and Rifkin, 1998), promoting reduction of bone degradation. In these studies, Dox was presented as a possible therapeutic drug against illnesses that exhibit bone loss, such as osteoporosis. In contrast, some studies suggest the activation of bone resorption by different doses of Dox administration (Folwarczna et al., 1999). Collectively, these studies that describe a bone remodeling alteration by Dox administration should be taken into consideration by incorporating two control groups based on mice lacking MAF transgene and with or without Dox treatment. Thus, monitoring the effect of Dox on the bone of treated-mice as compared to non-treated mice is a crucial next step, considering the importance of bone remodeling on bone metastatic process.

MAF knock-in: The potential bone metastatic mouse model

Given the drawback of the previous MAF Tg mouse model, we aimed to generate a knock-in mouse, to avoid random integration and increase expression of the transgene. In knock-in mouse models, a single copy of the transgene is targeted to a specific locus, such as Rosa26 or Col1α1, mediated by homologous recombination. The Col1α1 promoter has lost the tissue-specificity of the type 1 collagen gene expression, resulting in ubiquitous transgene expression (Beard et al., 2006). However, transgene expression is highly active specially to mature osteoblasts (Elefteriou and Yang, 2011). To avoid leakiness in the bone that could interfere with our results, we decided to use the Rosa26 locus. Several characteristics drive the Rosa26 locus to be the locus of choice for targeting transgenes, including an autosomal location, ubiquitous expression in every single cell of the body, open chromatin structure, and lack of epigenetic inactivation (Soriano, 1999).

To avoid leakiness and low inducible expression, we decided to exchange the Tet-On system for the Cre/loxP system (Figure 50) (Lakso et al., 1992; Sauer and Henderson, 1988, 1989). The Cre/loxP recombination system is among the most widely used and most robust approach to understand the roles of candidate genes. Cre enzyme recognize loxP site and acts as a site-specific recombinase, deleting endogenous genes or activating transgenes. When Cre is expressed under a tissue-specific promoter, loxP recombination would happen only in this tissue.

MMTV-Cre and WAP-Cre are the most commonly used mouse models for expressing Cre specifically in the mammary gland. MMTV-Cre is mostly active in the mammary gland and in other secretory glands, such as the salivary gland, seminal vesicle, and lymphoid cells. Virgin females as well as lactating females express the transgene. We should take into account that MMTV could be active at an early embryonic stage at low levels in many tissues, and this could promote Cre-mediated deletion widespread, something that could affect interpretation of experiments. Another fact that we should consider with this model is that a lactation defect has been described in the widely used MMTV-Cre Tg mice. This fact indicates that we should also use MMTV-Cre mice alone as a control in our experiments to compare mammary gland development (Yuan et al., 2011). On the other hand, WAP-Cre mouse present more tissue-specificity, as it is only expressed in the mammary gland; however, in this model, virgin females lack the transgene expression, and only lactating females present loxP recombination. Thus,

pregnancy should be carried out to realize these experiments (Wagner et al., 1997).

A more sophisticated option would be to use inducible Cre-expressing mouse models to also control transgene expression in a time-specific manner. Cre-inducible recombinase has been developed by the fusion between Cre and hormone-binding domains of the human estrogen receptor (ER). The resulting CreER recombinases are only active in the presence of 4-hydroxytamoxifen (OHT), an ER ligand, which allows it to be transported to the nucleus, where it drives recombination of the DNA inserted within loci containing loxP sites (Metzger et al., 1995). Thus, recombination can be temporally controlled externally by the administration of tamoxifen to the mice, reducing possible side-effects that may result in the recombinase activity in early steps of mouse development.

The latest and widely used CreER recombinase improvement, the $CreER^{T2}$, contains a triple mutation that decreases background activity without tamoxifen induction, and increases tamoxifen-induced sensitivity (Feil et al., 1997; Indra et al., 1999). One of the caveat that should be considered in the context of BC modelling, is that inducible Cre is activated with tamoxifen administration (Bockamp et al., 2008; Metzger and Chambon, 2001). Notably, tamoxifen is currently used to treat ER+ BC patients. This would give a possible double role to the planned knock-in mouse model: on one hand, tamoxifen administration will act as activator of recombination, thus, allowing transgene expression; and on the other hand, it will inhibit ER+ adenocarcinoma growth. However, one administration of tamoxifen is enough to promote removal of floxed DNA and might have only an insignificant effect for tumor growth. In any case, other controls must be incorporated into these studies, including the BC mouse model without MAF transgene with and without tamoxifen treatment, to discard the effects of this drug in the tumor development.

Additionally, when generating a knock-in mouse, we should consider the sequences we insert between genes to separate the different coding regions. There are two main types: the P2A sequences, which promote co-translational cleavage of proteins (Donnelly et al., 2001; Robertson et al., 1985; Trichas et al., 2008), and the internal ribosomal entry site (IRES), a sequence that allows ribosome binding and generation of multiple proteins from a single mRNA transcript (Jang et al., 1988; Martin et al., 2006). In the MAF transgenic mouse model, we decided to use P2A sequences, with multiple genes co-expressed under a single promoter in an equimolar level, as IRES has several limitations that had already described at that moment. The first limitation is that IRES elements

are not small (approximately 600 bp), and this may prove technically challenging for transgene elaboration. The second limitation is that the downstream coding sequence is often translated at lower levels than the upstream sequences, causing non-equivalent levels of expression from genes separated by IRES sequences. These two main limitations made us chose the P2A sequences to generate our MAF Tg mouse model mice.

P2A sequences are short peptides (60 bp approximately) that cause a co-translational ribosome skipping to the next codon and have been used to successfully generate transgenic mouse models (Trichas et al., 2008). But, markedly, part of the P2A peptide remains fused to the C-terminus of the upstream protein, while a proline is added to the N-terminus of the downstream protein. These remaining cleavage peptides themselves can potentially interfere with protein performance, including dimerization processes (Goedhart et al., 2011). As we had encountered serious difficulties on the generation of MAF-tagged proteins in the past, we decided to recap and use IRES sequences in the next knock-in mouse model. Regarding the size of the transgene, while for random integration there is no limit on the length of DNA constructs, for recombinant DNA longer fragments means lower transgene stability and insertion efficiency, which we should also consider (Haruyama et al., 2009).

To insert the transgene into Rosa26 and generate knock-in mice, the CRIPSR/Cas9 technology was used. This system had already been demonstrated by direct injection of 8–11 kb transgenes in zygotes (Chu et al., 2016). However, the possible presence of substantial off-target effects must be taken into account (Cho et al., 2014). Even though the efficiency of CRISPR/Cas9 has improved in the last years, this is still a major concern in the research field. It is noteworthy that delivery of Cas9 protein to the nucleus results in a faster genome editing and reduced off-target cleavage than when it is delivered as DNA or mRNA (Liang et al., 2015; Zuris et al., 2015). Moreover, the insertion of a small single-stranded DNA (ssDNA) donor instead of a double-stranded DNA (dsDNA) leads to a 60% increase in the rate of HDR (Richardson et al., 2016). Furthermore, the guide RNA can be microinjected into the pronucleus by DNA vector or in RNA form, or, alternatively, into the cytoplasm. A high efficiency of transgene integration is acquired when gRNA is injected into the cytoplasm by means of RNA (Horii et al., 2014; Wang et al., 2013). For this reason, we used several strategies to generate the MAF knock-in mice, including injection of high concentrations of gRNA and Cas9 mRNA into the cytoplasm of fertilized oocytes together with dsDNA donor transgene, or injection of the Cas9 protein into the oocyte nucleus. We also performed injections into ES cells with the

CRISPR/Cas9 technology in parallel, which resulted in five positive clones (as confirmed by longPCR and Southern blot) (Figure 51). Consequent injections of positive clones into the early mouse embryos are planned for the near future.

Collectively, we have described the effect of MAF in several contexts. We demonstrated that MAF predicts bone metastasis in PC patients, even though we could not recapitulate this observation in androgen-independent PC cell lines. We also demonstrated the powerful effect of MAF silencing on reducing bone metastasis in BC cell lines, suggesting MAF as a potential target for development of new drugs. Moreover, we determined the contribution of MAF under ZOL treatment in MDA-MB-231 cells by diverting their pattern of metastasis. Finally, we provide new approaches for the development of the first bone metastatic mouse model, a unique tool which will facilitate *in vivo* studies of future new developed bone metastatic treatments. The opportunity to generate this model provides an important step forward in the process of preventing and curing this fatal disease.

- Conclusions -

Conclusions

MAF is a predictor of bone metastasis in prostate cancer patients

MAF does not drive bone metastasis in androgen-independent prostate cancer cells

MAF dowregulation is a potential target to treat breast cancer bone metastasis

MAF expression influences Zoledronic acid responsiveness in BC bone metastasis preclinical models

MAF Tg mouse model, FVB;Tg(TetOn-MAF-Luc-tGFP/MMTV-rtTA-renilla-katushka), generated does not present sufficient MAF levels to promote remarkable phenotypic differences

Third generation of inducible Tet-On system shows low inducible activation and high leakiness expression

PyMT-MAF double Tg mouse does not express useful MAF levels to drive bone metastasis

MMTV promoter drives heterogeneous transgene expression and reduced expression during time in MAF Tg and PyMT-MAF Tg mice

Materials and Methods

Methods

Cell culture

Human embryonic kidney 293T cells, human prostate cancer cell lines DU-145, LNCaP and PC-3 and breast cancer cell line MCF7 were obtained from the American Type Culture Collection (ATCC, USA). BoM2 cells were derived from MCF7 cells as previously described in (Pavlovic et al., 2015). HEK-293, MCF7 and BoM2 cells were cultured with DMEM medium (Gibco) whereas prostate cancer cell lines were cultured in RPMI-1640 medium (Sigma). All cells were maintained in standard conditions (37°C, 5% CO_2) and medium was supplemented with 10% Fetal Bovine Serum (Gibco), Penicillin 100units/mL, Streptomycin 100 µg/mL and L-glutamine (0,29mg/mL). Cells were routinely tested for mycoplasma and found negative.

Stable prostate and breast cancer cell lines expressing MAF overexpression and down-regulation were generated as described in (Pavlovic et al., 2015). Puromycin (4ug/mL) was added for 48h to select the expression of transgenes. All cell lines were stably transduced with TK-GFP-Luciferase construct described in (Minn et al., 2005a) and sorted for GFP expression.

Primary culture mammary epithelial cells

15.595 and 1156 breast cancer cells were derived from 12 weeks-old female mice transgenic for PyMT-WT or double transgenic with PyMT-MAF and MLG mice, respectively (see Generation of MAF Tg mouse model section).

Tumors were extracted individually and minced with a sterile razor blade to generate small pieces. Later, pieces were incubated during 1h at 37°C with a digestion solution, composed by 10 mL DMEM/F12 medium (Gibco), 100µl P/S, 100ul Penicillin/Streptomycin solution, 5µg Amphotericin B (Fungizone, Gibco), 50mg Collagenase A (Roche), 75units Hyluronidase (Sigma Life Science). Subsequently tumor disaggregation was filtered through a 100µm cell stainer (BD Falcon). More DMEM/F12 was added and sample was centrifuged 10 min at 1500rpm. Pellet was resuspended in 5mL DMEM/F12 and centrifuged 4 min at 1500rpm. Consequently, pellet was digested by 50µg DNAse (Sigma-Aldrich) 5min at room temperature (RT). After dilution with 6mL of DMEM/F12 solution was centrifuged 4min at 1500rpm Further 8 spins at 1500rpm were done to

eliminate fibroblasts. Finally, cells were split with DMEM/F12 with double concentration of antibiotic and half amount of FBS (5%). Generation of oncoshperes can be done to favor epithelial cells rather than fibroblasts. After long periods of culture, cells get immortalized and can be sorted with epithelial markers by FACS.

Generation of transgenes

Generation of MAF transgenic mouse model was done at the IRB Barcelona mutant mouse core facility by coinjection of RRK and MLG3G constructs into FVB oocytes.

RRK construct

A cassette bearing rtTA3G-T2A-rLuc-P2A-Katushka sequences was synthesized (GenScript) and inserted into MMTV-Sv40-Bssk vector (Addgene) by HindIII and EcoRV restriction sites.

MLG3G construct

Mouse *MAF* cDNA corresponding to transcript NM_001025577.2 was synthesized together with T2A-Luciferase-P2A-tGFP (GenScript) and inserted into PMM400Sfi plasmid (Addgene) through EcoRV restriction sites. TetOn promoter was changed to TetOn 3G promoter (Clontech) through ClaI and PciI restriction sites.

Transgenic mouse generation

Vectors were verified by restriction enzyme digestion as further sequencing. RRK plasmid was cut by SalI and SpeI; while MLG3G construct was cut by SfiI. Both purified constructs were coinjected into the pronucleus of FVB mouse oocytes and reintroduced into a pseudo pregnant female. Potential founders were genotyped by PCR and positive mice were bred with FVB wild-type (WT) mice to establish separate transgenic lines. Crosses were done within the same strain so no mixed backgrounds will result. Colonies were analyzed by Southern Blot to assure correct and stable genomic integration.

Generation of MAF knock-in mouse model

MAF knock-in mouse model is being generated at the IRB Barcelona mutant mouse core facility (see Knock-in MAF mouse model section).

MGL construct

Mouse *MAF* cDNA was synthesized downstream of a kozak sequence in pOC1 plasmid. Alternatively, *IRES* sequence was synthesized within pOC2 plasmid (Genscript). CAGGS promoter was obtained from plasmid CAGGS-lox-stop-lox-eGFP and inserted upstream of *MAF* mouse cDNA (pOC1) with NheI and KpnI restriction sites. Next, *fLuc* fused with *eGFP* from TGL plasmid (Minn et al., 2005b) was inserted downstream of *IRES* sequence (pOC2) by NcoI and BamHI. We then fused both constructs with ClaI and SalI to obtain the final MLG cassette (Figure 31).

Other mouse models

FVB mice were purchased from Jackson Laboratories. MMTV- PyMT mouse were obtained from Angel Nebreda. All animals were maintained on a pure FVB background.

Mouse models genotyping

Genomic DNA for genotyping was isolated from snipped tail. Digestion was performed overnight (O/N) at 56ºC with 700rpm of agitation employing 750 µL of tail digestion buffer and 0,4mg proteinase K (Sigma-Aldrich). Tail digestion buffer contain 100mM NaCl, 50mM Tris-HCl (pH=8), 100mM EDTA (pH=8) and 1%SDS. Isolation started with addition of 250µL of NaCl 6M during 5min at RT and then centrifugation 10min at RT maximum rpm. Supernatant was then placed in a new eppendorff that contained 500µL of isopropanol. Mixture and 5min centrifugation at 4ºC was performed. Pellet was mixed with 500µL of 70% EtOH and centrifuged during 5min. Finally, pellet was dried and further diluted on 50-100µL of Mili-Q distilled water.

Offspring were tested for integration of the transgene by PCR of genomic DNA using specific primers (see Table 11). All PCR reactions involved in cloning were performed with KOD Hot Start DNA Polymerase (Novagen) following the manufacturer's instructions. LongPCR for EScells were performed with SequalPrep Long PCR Kit (ThermoFisher Scientific) following the manufacturer's instructions.

Southern Blot analysis

Genomic DNA was extracted as mentioned above; 5µg were digested overnight with the appropriate restriction enzyme and separated on a 0.8% agarose gel O/N at 15V. DNA fragments were then transferred to a Hybond-N+ membrane (Amersham) O/N by capillarity of 0.4N NaOH. Next day, membrane was prehybridized with hybridization solution 1h at 42ºC. Then, membrane was hybridized O/N at 42ºC with the specific digoxigenin (DIG) labeled probe. Probes were generated by PCR with specific primers (see Table 11) and labeled with DIG-11-dUTP nucleotides (Roche). The next day, after washing twice the membrane with 2xSSC-0.1%SDS buffer, twice with 0.1xSSC-0.1%SDS and once with washing buffer, incubation with the anti-DIG-AP antibody was carried out for 30min. After washing, probes were detected using a CDP Star solution and by exposition into an Amersham Hyperfilm ECL membrane (GE Healthcare).

Animal studies

All animal work was approved by the Animal Care and Use Committee of Barcelona Science Park (CEEA-PCB) in accordance with applicable legislation of "Generalitat de Catalunya". All efforts were made to minimize use and suffering.

Xenografts

BALB/c Nude females were used for breast cancer bone metastasis experiments while males BALB/c Nude were used for prostate cancer. All the mice were injected at a minimum age of 9 weeks old. Prior to any surgical procedure, mice were anesthetized with a mixture of Ketamine (80mg/Kg body weight) and Xylacine (8mg/Kg body weight) delivered via intraperitoneal injection. Cancer cells were injected via intracardiac (IC) or intratibial (IT) injections. Immediately after injection mice were imaged for luciferase activity by bioluminescent imaging (BLI) and continued to be monitored weekly. For experiments with MCF7 or BoM2 cell lines (ER+), mice were implanted subcutaneously (SC) with 60-day-release estrogen (17β-estradiol 0.18mg/pellet) (Innovative Research of America).

For intra-cardiac injections, cells were resuspended in 100 µl of PBS and inoculated into the left cardiac ventricle using a 25G needle (BS Syringes).

For intra-tibiae injections, cells were resuspended in 5 µl of PBS and injected into the upper half of the tibia medullary cavity using a 28G syringe as described in (Pavlovic et al., 2015).

Treatments

Control: 50µl PBS (Biowest), intraperitoneum injection (IP), 1x week

Osteoprotegerin Human Recombinant /Fc Chimera (OPG-Fc): 3mg/Kg, subcutaneously (SC), 3x week (Canon et al., 2012) (ProSpec – Tany Technogene)

Zoledronic acid: 500µg/Kg, IP, 1x week (Sigma) (Haider et al., 2014; Kato et al., 2016; Pozzi et al., 2009)

PTHrP AN peptide: 0,3mg/Kg, IP, 2x day (Bachem) (Pavlovic et al., 2015)

Induction of TetON expression in mouse models

For GEM experiments, 4-weeks old mice were fed with normal water or doxycycline-containing drinking water exchanged twice a week. Doxycycline drinking water was composed by 1mg/mL of doxycycline (Sigma) and supplemented with 5% sucrose (Sigma).

Bioluminescent imaging (BLI)

For bioluminescent imaging, mice were anesthetized by isofluoran inhalation and injected retro-orbitally with D-luciferin (30mg/Kg). One minute after D-luciferin injection, animals were placed into IVIS Spectrum CT imaging system (Perkin Elmer) to acquire whole body and luminescent image photographs. Exposure time of 60s was done otherwise indicated. Bioluminescent images quantification was performed with LivingImage 4.5 software. Photon flux was calculated using circular measurement ROI enclosing the area of interest and subtracting the background value. For xenograft experiments, all obtained values were normalized to those obtained at the day of xenografting (day 0). Tumor development was followed once a week. Transgenic mouse imaging was also developed once a week otherwise indicated.

IVIS SpectrumCT instrument was used to co-register bioluminescent images with low dose microCT that concede the advantage to detect the organ location of bioluminescent cells. 3D-images were processed using DLIT Reconstruction option in the Living Image software.

Whole mount

Mammary glands were dissected, spread on glass slide and fixed at RT, O/N, in a Carnoy's fixative (60% of EtOH 100%, 30% of chloroform and 10% of glacial acetic acid). Glands were then rehydrated by consecutive 10min washes with 70-50-30-10% EtOH and a last wash of 5min with distilled water. Next, glands were stained O/N at RT by carmine alum stain composed by carmine (2g/L, Sigma) and potassium sulfate (5g/L, Sigma). Next day, clearing of the glands was performed by 15 min-washes with 70-95-100% ETOH and a final xylene step until fat is cleared from the glands. Once glands are prepared, they are mounted with Leica CV Mount media and covered with a glass cover slip.

Multiple photos were taken with an Olympus MVX10 Macroscope and then composite using Mosaic J option of ImageJ software version: 2.0.0-rc-46/1.50g. Images were processed with a custom macro created at the Microscopy Core Facility of IRB Barcelona.

Immunohistochemistry and immunofluorescence

Organs were excised and fixed in neutral-buffered 10% formalin solution (Sigma) O/N at RT. The day after organs were rinsed in 1x phosphate buffered saline (PBS) and pinned flat onto paraffin wax. Alternatively, bones were first washed with PBS and decalcified with Osteosoft buffer (Merck Milipore) for 15 days at RT before embedding in paraffin. Paraffin sections were stained with hematoxylin and eosin (H&E) or subjected to immunostaining. For staining with antibodies, paraffin sections were first deparaffinized and rehydrated through consecutive alcohol dilutions (xylene, 100-96-90-80-70-50-25% EtOH and Mili-Q distilled water). For antigen retrieval two protocols were realized depending on the antibody behavior. The first one was using citrate buffer (pH6) in the autoclave, and the second one was with TRIS-EDTA buffer (pH9) 20min at 97°C.

For immunohistochemistry staining, sections were treated with peroxidase-blocking solution for 10 minutes and washed with PBS. After washing twice with Envision Flex Wash Buffer (DAKO), 100µL of diluted primary antibody was added to cover the sample O/N at 4ºC (see Table 12). After washing three times with PBS secondary HRP-conjugated antibody was applied for 1 hour at RT. Slides were washed 3 times with PBS and incubated with DAB for 10 seconds to 3 minutes. DAB reaction was stopped with water. Hematoxylin was used as counterstaining dye. Stained sections were dehydrated and mounted.

For immunofluorescent staining, sections were directly incubated with 100µL of primary antibody O/N at 4ºC (see Table 12). The day after, sections were washed three times and incubated with secondary antibody dilution. Slides were covered using a drop of DAPI (Life Technologies).

FISH

Cells were processed as described in (Pavlovic et al., 2015). The slides were incubated with 16q23 MAF probe, that covers a 197 kb segment at chr16: 79,460,645-79,657,297, a region that includes the full MAF gene (chr16: 79,625,745 to 79,639,622, 14 kb). In parallel, a 14q32 IGH probe mixture (Abbot) was used to score 14q CNAs (see Table 10). DAPI counterstain was applied and images were acquired with a Leica TCS-SP5 confocal microscope. The quantification was performed with ImageJ software.

Flow cytometry and FACS sorting

Cultured cells were collected by trypsinization. Alternatively, mammary gland cells were obtained by collagenase-hyaluronidase digestion of the mammary glands and further centrifugation of 5 min at 4ºC and 450 x g. Supernatant were suspended in 1mL of cold HF buffer, composed by HBSS solution with 10mM HEPES and 2% FBS. Lyse of red blood cells were performed by addition of 4mL of cold NH_4Cl. After 450xg for 5min at 4ºC centrifugation, pellet was resuspended with 3mL of pre-warmed trypsin. Further dilution with 10mL of cold HF, centrifugation and resuspension with 4mL of pre-warmed dispase solution supplemented with 40µL of 1mg/mL DNAse was performed. Cells were diluted in 10mL cold HF and filtered through a 40µm cell stainer. Cells were pre-blocked

on ice 10min with 1mL of HF buffer and incubated 20 min on ice with the primary antibody. After washing, cells with biotin antibodies were incubated with 2ary antibodies during 15min at 4ºC. Washing and DAPI addition was realized before analyzing them by FACS Aria2.0.

Analysis of mammary gland populations

To analyze the cells, first, cells were gated by FSC/SSC dot plot to exclude debris and FSC/FSC dot plot to exclude cellular aggregates. Second, dead and dying cells were eliminated by exclusion of DAPI negative events. After exclusion of debris, aggregates and death cells, lineage negative cells were eliminated by excluding CD31, CD45, Ter119 and BP-1 positive cells. Finally, luminal cells ($EpCAM^{high}$ $CD49f^{med}$), basal cells ($EpCAM^{med}$ $CD49f^{high}$), and stromal cells ($EpCAM^{-}$ $CD49^{-}$) were separated by EpCAM and CD49 markers (see Table 12).

Protein extraction and Western Blot analysis

For protein expression analysis, cells were scraped from P60 plates and lysed with a buffer composed of 50 mM Tris- HCl (pH 7.5), 150 mM NaCl, 0.5% NP-40, 10mM NaF, 1mM Na_3VO_4, supplemented with protease and phosphatase inhibitors cocktail (Roche). Cells were sonicated 8 minutes on ice with a 30s interval at medium intensity using Bioruptor Standard sonication device (Diagenode). Alternatively, to extract protein from mouse tissue, a piece of $1mm^3$ was lysed by Precellys24 Tissue homogenizer (Bertin instruments) in 300µL of protein lysis buffer.

Tissue and cell extracts were then centrifuged 10 min at 4ºC at 15000rpm and supernatant was kept as protein extract and storage at -80ºC. Protein content was quantified by Protein Assay (BioRad), based on the Bradford method. Equal amount of protein was mixed with sample buffer (45 mM Tris pH 6.8, 10% glycerol, 1% SDS, 52 mM DTT and 1% bromophenol blue) and heated at 99ºC for 5min. Proteins were separated by standard SDS-PAGE and transferred to PVDF membranes (Immobilon-P). Later, unspecific antibody binding was blocked by incubating membranes with Tris-buffered saline (TBS) buffer containing 0.1% tween and 5% of skim milk (Central Lechera Asturiana) for 1h at RT. Primary antibodies were incubated overnight at 4ºC or 1h at RT (see Table 12). Membranes were washed 3 times with TBS-Tween 0.1% (TBS-T) and

incubated for 1h at RT with HRP-conjugated secondary antibodies (1/5000). Membranes were washed with TBST-T and TBS and finally incubated 1 min with ECL WB substrate (Thermo Fisher Scientific). HRP activity from immuno-complexes was visualized by exposure on super RX-N films (Fujifilm) or Amersham Hyperfilm ECL (GE Healthcare).

RNA extraction, cDNA generation and qRT-PCR analysis

RNA extractions from mouse tissue or cultured cells were realized using PureLink RNA Mini Kit (Invitrogen) following manufacturer's instructions. RNA quantity and quality was checked by NanoDrop spectrophotometer. cDNA was generated using 1µg of total RNA and a High capacity cDNA reverse transcriptase kit (Applied biosystems). Quantitative PCR was performed using TaqMan or SYBR Green gene expression assay using specific probes or primers, respectively (see Tables 10-11). Amplification was performed using SYBR Green Select Master Mix or TaqMan Universal PCR Master Mix (Applied Biosystems). All assays were performed in triplicate. The gene expression results were normalized to a housekeeping gene using comparative CT method.

Luciferase and renilla assays

50.000 cells were plated per well in a 12-multiwell plate. The next day, cells were treated with 0, 0.5, 1 or 2µg/mL of Dox during 48h. After Dox treatment, cells were rinsed with PBS and lysed with 1x passive lyses buffer (Promega) during 40min in a shaking platform. 60µL of cell extract was collected along with renilla or luciferase substrate and measured with Lumat LB 9507 luminometer (Berthold Technologies).

Materials

Table 9. List of primers

Name	Type	Description	Selection	Source
TGL	retroviral	luciferase, GFP	GFP	Lab resources
pBABE puro	retroviral	empty	Puromycin	Lab resources
pBABE MAF S	retroviral	MAF isotype 1	Puromycin	Lab resources
pBABE MAF L	retroviral	MAF isotype 2	Puromycin	Lab resources
pLKO	lentiviral	shcontrol	Puromycin	Sigma-Aldrich
pLKO sh MAF	lentiviral	shMAF	Puromycin	Sigma-Aldrich
pCR-Blunt II TOPO vector	Cloning vector	empty	NeoR/KanR	Invitrogenn

Table 10. List of probes

Target	ID	Supplier
qRT-PCR (Taqman)		
B2M	Mm00437762_m1	TermoFisher Scientific
MAF L	Hs00193519_m1	TermoFisher Scientific
FISH		
14q32	05N32-020	Abbot
16q23	05N32-020	Abbot

Table 11. List of primers

Target	primer F	primer F sequence	primer R	primer R sequence	Fragment size
Southern Blot					
Probe1-renilla	AB82	ATGGCTTCCAAGGTGTACGACC	AB83	CCGATCAGATCAGGGATGATGC	239bp
Probe2-Luciferase/ GFP	AB93	TCTTGTCGGTGAAGATCACG	AB94	ACTGGGACGAAGACGAACAC	855bp
Genotyping					
MLG3G (GFP-PolyA)	AB33	GAGTACCAGCACGCCTTCA	AB34	CAAACCACAACTAGAATGCAGTG	798bp
MLG3G (GFP - Luc)	AB93	TCTTGTCGGTGAAGATCACG	AB94	ACTGGGACGAAGACGAACAC	855bp
RRK (renilla)	AB82	ATGGCTTCCAAGGTGTACGACC	AB83	CCGATCAGATCAGGGATGATGC	239bp
RRK (renilla-katushka)	AB78	CAGGAGGACGCTCCAGATGAA	AB79	GGTGATCAGCACGCTATCCTCAC	168bp
PyMT	AB122	GGAAGCAAGTACTTCACAAGGG	AB123	GGAAAGTCACTAGGAGCAGGG	540bp
qRT-PCR (SYBR Green)					
MAF	JUAB5	AAGGAGGAGGTGATCCGACT	JUAB6	TCTCCTGCTTGAGGTGGTCT	154bp
	JUAB7	GAGGAGGTGATCCGACTGAA	JUAB6	TCTCCTGCTTGAGGTGGTCT	151bp
	JUAB5	AAGGAGGAGGTGATCCGACT	JUAB9	TTGCTCACCAGCTTCTCGTA	215bp
	JUAB3	GGCTTCAGAACTGGCAATGAACAAT	JUAB4	CCAGTAGTAGTCTTCCAGGTGC	277bp
	JUAB10	AGACCACCTCAAGCAGGAGA	JUAB11	TGAAAAATTCGGGAGAGGAA	137bp
	JUAB12	GCAATGAACAATTCCGACCT	JUAB13	GTCTCCACCGGTTCCTTTTT	101bp
Luc	AB72	CGATCTTTCCGCCCTTCTTG	AB73	CGCCGTTGTTGTTTTGGAGC	200bp
	AB28	GGTGTTGGAGCAAGATGGAT	AB94	ACTGGGACGAAGACGAACAC	111bp
	AB28	GGTGTTGGAGCAAGATGGAT	AB27	TCAAAGAGGCGAACTGTGTG	230bp
GFP	AB32	GGTGTTGCTGTGATCCTCCT	AB31	AGGACAGCGTGATCTTCACC	245bp
	AB74	TTATTCTTCACCGGCATCTGCA	AB75	TGGGCGATAACGATCTGGATG	245bp

Table 12. List of antibodies

Antigen	Dilution	Source	ID	Supplier	Other details
Western blot					
α-tubulin	1:3000	Mouse		Sigma	5% milk-TBST
MAF	1:50	Rabbit	130(5)	Inbiomotion	5%BSA-TBST
Luciferase	1:1000	Rabbit	ab21176	Abcam	5%BSA-TBST
GFP	1:1000	Rabbit	A11122	Invitrogen	5%BSA-TBST
GFP	1:1000	Rabbit	AB6556	Abcam	5% milk-TBST
tRFP	1:5000	Rabbit	AB233	Evrogen	5%BSA-TBST
rtTA	1:1000	Mouse	631131	Clonetech	5%BSA-TBST
rtTA	1:700	Mouse	Tet02	MoBiTech	5%BSA-TBST
Rabbit IgG HRP-linked	1:5000	Donkey	NA934	GE Healthcare	5%BSA-TBST
Mouse IgG HRP-linked	1:3000	Rabbit	31452	ThermoFisher Scientific	5%BSA-TBST
IHC					
GFP	1:300	Rabbit	A11122	Invitrogen	Polyclonal
	1:600	Chicken	GFP-1020	Aves labs	Polyclonal
MAF	1:200	Rabbit	sc-7866	Santa Cruz Biotechnology	Polyclonal
	1:50	Rabbit	130(5)	Inbiomotion	Monoclonal
IF					
GFP	1:100	Rabbit	A11122	Invitrogen	Polyclonal
	1:100	Goat	ab6673	Abcam	Polyclonal
	1:200	Chicken	GFP-1020	Aves labs	Polyclonal
MAF	1:50	Rabbit	sc-7866	Santa Cruz Biotechnology	Polyclonal
	1:50	Rabbit	130(5)	Inbiomotion	Monoclonal
FACS					
EpCAM - APC	1:1000	Rat	130-102-234	Miltenyi Biotec	Monoclonal
CD49f - PE	1:1000	Rat	130-097-246	Miltenyi Biotec	Monoclonal
CD45 - Biotin	1:1000	Rat	130-101-952	Miltenyi Biotec	Monoclonal
CD31 - Biotin	1:1000	Rat	130-101-955	Miltenyi Biotec	Monoclonal
AntiTer119 - Biotin	1:1000	Rat	130-101-882	Miltenyi Biotec	Monoclonal
Anti BP-1 (Ly-51) - Biotin	1:1000	Rat	130-101-844	Miltenyi Biotec	Monoclonal
Streptavidin - Cy5.5	1:100		45-4317-80	ThermoFisher Scientific	

- B i b l i o g r a p h y -

Abad, M., Mosteiro, L., Pantoja, C., Cañamero, M., Rayon, T., Ors, I., Graña, O., Megías, D., Domínguez, O., Martínez, D., et al. (2013). Reprogramming in vivo produces teratomas and iPS cells with totipotency features. Nature 502, 340–345.

Aceto, N., Bardia, A., Miyamoto, D.T., Donaldson, M.C., Wittner, B.S., Spencer, J.A., Yu, M., Pely, A., Engstrom, A., Zhu, H., et al. (2014). Circulating tumor cell clusters are oligoclonal precursors of breast cancer metastasis. Cell 158, 1110–1122.

Achbarou, A., Kaiser, S., Tremblay, G., Ste-Marie, L.G., Brodt, P., Goltzman, D., and Rabbani, S.A. (1994). Urokinase overproduction results in increased skeletal metastasis by prostate cancer cells in vivo. Cancer Res. 54, 2372–2377.

Aird, W.C. (2007). Phenotypic heterogeneity of the endothelium: I. Structure, function, and mechanisms. Circ. Res. 100, 158–173.

Alexopoulou, A.N., Couchman, J.R., and Whiteford, J.R. (2008). The CMV early enhancer/chicken beta actin (CAG) promoter can be used to drive transgene expression during the differentiation of murine embryonic stem cells into vascular progenitors. BMC Cell Biol. 9, 2.

Ali, S., and Coombes, R.C. (2002). Endocrine-responsive breast cancer and strategies for combating resistance. Nat. Rev. Cancer 2, 101–112.

Allred, D.C., Mohsin, S.K., and Fuqua, S. a (2001). Histological and biological evolution of human premalignant breast disease. Endocr. Relat. Cancer 8, 47–61.

Anampa, J., Makower, D., and Sparano, J.A. (2015). Progress in adjuvant chemotherapy for breast cancer: an overview. BMC Med. 13, 195.

Andersson, S., Berman, D.M., Jenkins, E.P., and Russell, D.W. (1991). Deletion of steroid 5 alpha-reductase 2 gene in male pseudohermaphroditism. Nature 354, 159–161.

Ballabh, P., Braun, A., and Nedergaard, M. (2004). The blood-brain barrier: an overview: structure, regulation, and clinical implications. Neurobiol. Dis. 16, 1–13.

Baselga, J., Campone, M., Piccart, M., Burris, H.A., Rugo, H.S., Sahmoud, T., Noguchi, S., Gnant, M., Pritchard, K.I., Lebrun, F., et al. (2012a). Everolimus in postmenopausal hormone-receptor-positive advanced breast cancer. N. Engl. J. Med. 366, 520–529.

Baselga, J., Cortés, J., Kim, S.-B., Im, S.-A., Hegg, R., Im, Y.-H., Roman, L., Pedrini, J.L., Pienkowski, T., Knott, A., et al. (2012b). Pertuzumab plus Trastuzumab plus Docetaxel for Metastatic Breast Cancer. N. Engl. J. Med. 366, 109–119.

Baum, M. (1984). Prospects for the future in the management of carcinoma of the breast: the biological fall out from clinical trials. Br. J. Cancer 49, 117–122.

Baum, M., Buzdar, A., Cuzick, J., Forbes, J., Houghton, J., Howell, A., Sahmoud, T., and ATAC (Arimidex, T.A. or in C.T.G. (2003). Anastrozole alone or in combination with tamoxifen versus tamoxifen alone for adjuvant treatment of postmenopausal women with early-stage breast cancer: results of the ATAC (Arimidex, Tamoxifen Alone or in Combination) trial efficacy and safety update ana. Cancer 98, 1802–1810.

Beard, C., Hochedlinger, K., Plath, K., Wutz, A., and Jaenisch, R. (2006). Efficient method to generate single-copy transgenic mice by site-specific integration in embryonic stem cells. Genesis 44, 23–28.

Bekker, P.J., Holloway, D.L., Rasmussen, A.S., Murphy, R., Martin, S.W., Leese, P.T., Holmes, G.B., Dunstan, C.R., and DePaoli, A.M. (2004). A single-dose placebo-controlled study of AMG 162, a fully human monoclonal antibody to RANKL, in postmenopausal women. J. Bone Miner. Res. 19, 1059–1066.

Beleut, M., Rajaram, R.D., Caikovski, M., Ayyanan, A., Germano, D., Choi, Y., Schneider, P., and Brisken, C. (2010). Two distinct mechanisms underlie progesterone-induced proliferation in the mammary gland. Proc. Natl. Acad. Sci. U. S. A. 107, 2989–2994.

Bendre, M.S., Montague, D.C., Peery, T., Akel, N.S., Gaddy, D., and Suva, L.J. (2003). Interleukin-8 stimulation of osteoclastogenesis and bone resorption is a mechanism for the increased

osteolysis of metastatic bone disease. Bone 33, 28–37.

Bergsagel, P.L., Kuehl, W.M., Zhan, F., Sawyer, J., Barlogie, B., and Shaughnessy, J. (2005). Cyclin D dysregulation: an early and unifying pathogenic event in multiple myeloma. Blood 106, 296–303.

Berthold, D.R., Pond, G.R., Soban, F., de Wit, R., Eisenberger, M., and Tannock, I.F. (2008). Docetaxel plus prednisone or mitoxantrone plus prednisone for advanced prostate cancer: updated survival in the TAX 327 study. J. Clin. Oncol. 26, 242–245.

Bettany, J.T., Peet, N.M., Wolowacz, R.G., Skerry, T.M., and Grabowski, P.S. (2000). Tetracyclines induce apoptosis in osteoclasts. Bone 27, 75–80.

Bhaumik, S., and Gambhir, S.S. (2002). Optical imaging of Renilla luciferase reporter gene expression in living mice. Proc. Natl. Acad. Sci. U. S. A. 99, 377–382.

Biggers, B., Knox, S., Grant, M., Kuhn, J., Nemunatitis, J., Fisher, T., and Lamont, J. (2009). Circulating Tumor Cells in Patients Undergoing Surgery for Primary Breast Cancer: Preliminary Results of a Pilot Study. Ann. Surg. Oncol. 16, 969–971.

Björnström, L., and Sjöberg, M. (2005). Mechanisms of estrogen receptor signaling: convergence of genomic and nongenomic actions on target genes. Mol. Endocrinol. 19, 833–842.

Blackwell, K.L., Burstein, H.J., Storniolo, A.M., Rugo, H., Sledge, G., Koehler, M., Ellis, C., Casey, M., Vukelja, S., Bischoff, J., et al. (2010). Randomized study of Lapatinib alone or in combination with trastuzumab in women with ErbB2-positive, trastuzumab-refractory metastatic breast cancer. J. Clin. Oncol. 28, 1124–1130.

Bockamp, E., Sprengel, R., Eshkind, L., Lehmann, T., Braun, J.M., Emmrich, F., and Hengstler, J.G. (2008). Conditional transgenic mouse models: from the basics to genome-wide sets of knockouts and current studies of tissue regeneration. Regen. Med. 3, 217–235.

Body, J.-J., Greipp, P., Coleman, R.E., Facon, T., Geurs, F., Fermand, J.-P., Harousseau, J.-L., Lipton, A., Mariette, X., Williams, C.D., et al. (2003). A phase I study of AMGN-0007, a recombinant osteoprotegerin construct, in patients with multiple myeloma or breast carcinoma related bone metastases. Cancer 97, 887–892.

Bonewald, L.F. (2011). The amazing osteocyte. J. Bone Miner. Res. 26, 229–238.

Bos, P.D., Zhang, X.H.-F., Nadal, C., Shu, W., Gomis, R.R., Nguyen, D.X., Minn, A.J., van de Vijver, M.J., Gerald, W.L., Foekens, J.A., et al. (2009). Genes that mediate breast cancer metastasis to the brain. Nature 459, 1005–1009.

Branda, C.S., and Dymecki, S.M. (2004). Talking about a Revolution. Dev. Cell 6, 7–28.

Breast International Group (BIG) 1-98 Collaborative Group, Thürlimann, B., Keshaviah, A., Coates, A.S., Mouridsen, H., Mauriac, L., Forbes, J.F., Paridaens, R., Castiglione-Gertsch, M., Gelber, R.D., et al. (2005). A comparison of letrozole and tamoxifen in postmenopausal women with early breast cancer. N. Engl. J. Med. 353, 2747–2757.

Brisken, C., and O'Malley, B. (2010). Hormone action in the mammary gland. Cold Spring Harb. Perspect. Biol. 2, a003178.

Brisken, C., Heineman, A., Chavarria, T., Elenbaas, B., Tan, J., Dey, S.K., McMahon, J.A., McMahon, A.P., and Weinberg, R.A. (2000). Essential function of Wnt-4 in mammary gland development downstream of progesterone signaling. Genes Dev. 14, 650–654.

Brown, J.E., and Coleman, R.E. (2012). Denosumab in patients with cancer-a surgical strike against the osteoclast. Nat. Rev. Clin. Oncol. 9, 110–118.

Bruland, Ø.S., Nilsson, S., Fisher, D.R., and Larsen, R.H. (2006). High-linear energy transfer irradiation targeted to skeletal metastases by the alpha-emitter 223Ra: adjuvant or alternative to conventional modalities? Clin. Cancer Res. 12, 6250s–6257s.

Budczies, J., Winterfeld, M. Von, Klauschen, F., Dietel, M., Anagnostopoulos, I., and Weichert, W. (2014). The landscape of metastatic progression patterns across major human cancers. Oncotarget 6, 570–583.

Burger, J.A., Burger, M., and Kipps, T.J. (1999). Chronic lymphocytic leukemia B cells express functional CXCR4 chemokine receptors that mediate spontaneous migration beneath bone marrow stromal cells. Blood 94, 3658–3667.

Burris, H.A., Rugo, H.S., Vukelja, S.J., Vogel, C.L., Borson, R.A., Limentani, S., Tan-Chiu, E., Krop, I.E., Michaelson, R.A., Girish, S., et al. (2011). Phase II study of the antibody drug conjugate trastuzumab-DM1 for the treatment of human epidermal growth factor receptor 2 (HER2)-positive breast cancer after prior HER2-directed therapy. J. Clin. Oncol. 29, 398–405.

Burstein, H.J. (2005). The Distinctive Nature of HER2-Positive Breast Cancers. N. Engl. J. Med. 353, 1652–1654.

Burstein, H.J., Polyak, K., Wong, J.S., Lester, S.C., and Kaelin, C.M. (2004). Ductal carcinoma in situ of the breast. N. Engl. J. Med. 350, 1430–1441.

Bussard, K.M., Gay, C. V, and Mastro, A.M. (2008). The bone microenvironment in metastasis; what is special about bone? Cancer Metastasis Rev. 27, 41–55.

Buyse, M., Loi, S., van't Veer, L., Viale, G., Delorenzi, M., Glas, A.M., D'Assignies, M.S., Bergh, J., Lidereau, R., Ellis, P., et al. (2006). Validation and clinical utility of a 70-gene prognostic signature for women with node-negative breast cancer. J. Natl. Cancer Inst. 98, 1183–1192.

Byers, S.L., Wiles, M. V., Dunn, S.L., and Taft, R.A. (2012). Mouse estrous cycle identification tool and images. PLoS One 7, e35538.

Canalis, E., Pash, J., Gabbitas, B., Rydziel, S., and Varghese, S. (1993). Growth factors regulate the synthesis of insulin-like growth factor-I in bone cell cultures. Endocrinology 133, 33–38.

Cano, A., Pérez-Moreno, M.A., Rodrigo, I., Locascio, A., Blanco, M.J., del Barrio, M.G., Portillo, F., and Nieto, M.A. (2000). The transcription factor snail controls epithelial-mesenchymal transitions by repressing E-cadherin expression. Nat. Cell Biol. 2, 76–83.

Canon, J., Bryant, R., Roudier, M., Branstetter, D.G., and Dougall, W.C. (2012). RANKL inhibition combined with tamoxifen treatment increases anti-tumor efficacy and prevents tumor-induced bone destruction in an estrogen receptor-positive breast cancer bone metastasis model. Breast Cancer Res. Treat. 135, 771–780.

Capulli, M., Paone, R., and Rucci, N. (2014). Osteoblast and osteocyte: games without frontiers. Arch. Biochem. Biophys. 561, 3–12.

Cardoso, F., van't Veer, L.J., Bogaerts, J., Slaets, L., Viale, G., Delaloge, S., Pierga, J.-Y., Brain, E., Causeret, S., DeLorenzi, M., et al. (2016). 70-Gene Signature as an Aid to Treatment Decisions in Early-Stage Breast Cancer. N. Engl. J. Med. 375, 717–729.

Cejalvo, J.M., Martínez de Dueñas, E., Galván, P., García-Recio, S., Burgués Gasión, O., Paré, L., Antolín, S., Martinello, R., Blancas, I., Adamo, B., et al. (2017). Intrinsic Subtypes and Gene Expression Profiles in Primary and Metastatic Breast Cancer. Cancer Res. 77, 2213–2221.

Chackal-Roy, M., Niemeyer, C., Moore, M., and Zetter, B.R. (1989). Stimulation of human prostatic carcinoma cell growth by factors present in human bone marrow. J. Clin. Invest. 84, 43–50.

Chambers, A.F., Groom, A.C., and MacDonald, I.C. (2002). Dissemination and growth of cancer cells in metastatic sites. Nat. Rev. Cancer 2, 563–572.

Chan, J.M., Stampfer, M.J., Giovannucci, E., Gann, P.H., Ma, J., Wilkinson, P., Hennekens, C.H., and Pollak, M. (1998). Plasma insulin-like growth factor-I and prostate cancer risk: a prospective study. Science 279, 563–566.

Chanmee, T., Ontong, P., Konno, K., and Itano, N. (2014). Tumor-associated macrophages as major players in the tumor microenvironment. Cancers (Basel). 6, 1670–1690.

Chen, J.Q., Mori, H., Cardiff, R.D., Trott, J.F., Hovey, R.C., Hubbard, N.E., Engelberg, J.A., Tepper, C.G., Willis, B.J., Khan, I.H., et al. (2015). Abnormal Mammary Development in 129:STAT1-Null Mice is Stroma-Dependent. PLoS One 10, e0129895.

Chen, Q., Dowhan, D.H., Liang, D., Moore, D.D., and Overbeek, P.A. (2002). CREB-binding protein/p300 co-activation of crystallin gene expression. J. Biol. Chem. 277, 24081–24089.

Chesi, M., Bergsagel, P.L., Shonukan, O.O., Martelli, M.L., Brents, L. a, Chen, T., Schröck, E., Ried, T., and Kuehl, W.M. (1998). Frequent dysregulation of the c-maf proto-oncogene at 16q23 by translocation to an Ig locus in multiple myeloma. Blood 91, 4457–4463.

Cheung, K.J., Gabrielson, E., Werb, Z., and Ewald, A.J. (2013). Collective invasion in breast cancer requires a conserved basal epithelial program. Cell 155, 1639–1651.

Cho, S.W., Kim, S., Kim, Y., Kweon, J., Kim, H.S., Bae, S., and Kim, J. (2014). Analysis of off-target effects of CRISPR/Cas-derived RNA-guided endonucleases and nickases. Genome Res. 24, 132–141.

Chu, K., Cheng, C.-J., Ye, X., Lee, Y.-C., Zurita, A.J., Chen, D.-T., Yu-Lee, L.-Y., Zhang, S., Yeh, E.T., Hu, M.C.-T., et al. (2008). Cadherin-11 Promotes the Metastasis of Prostate Cancer Cells to Bone. Mol. Cancer Res. 6, 1259–1267.

Chu, V.T., Weber, T., Graf, R., Sommermann, T., Petsch, K., Sack, U., Volchkov, P., Rajewsky, K., and Kühn, R. (2016). Efficient generation of Rosa26 knock-in mice using CRISPR/Cas9 in C57BL/6 zygotes. BMC Biotechnol. 16, 4.

Clarke, B. (2008). Normal bone anatomy and physiology. Clin. J. Am. Soc. Nephrol. 3 Suppl 3, S131-9.

Coleman, R.E. (1997). Skeletal complications of malignancy. Cancer 80, 1588–1594.

Coleman, R.E. (2001). Metastatic bone disease: clinical features, pathophysiology and treatment strategies. Cancer Treat. Rev. 27, 165–176.

Coleman, R.E. (2004). The role of bisphosphonates in breast cancer. Breast 13 Suppl 1, S19-28.

Coleman, R.E. (2008). Risks and benefits of bisphosphonates. Br. J. Cancer 98, 1736–1740.

Coleman, R., Cameron, D., Dodwell, D., Bell, R., Wilson, C., Rathbone, E., Keane, M., Gil, M., Burkinshaw, R., Grieve, R., et al. (2014). Adjuvant zoledronic acid in patients with early breast cancer: final efficacy analysis of the AZURE (BIG 01/04) randomised open-label phase 3 trial. Lancet Oncol. 15, 997–1006.

Coleman, R., Hall, A., Albanell, J., Hanby, A., Bell, R., Cameron, D., Dodwell, D., Marshall, H., Jean-Mairet, J., Tercero, J.-C., et al. (2017). Effect of MAF amplification on treatment outcomes with adjuvant zoledronic acid in early breast cancer: a secondary analysis of the international, open-label, randomised, controlled, phase 3 AZURE (BIG 01/04) trial. Lancet Oncol. 2045, 1–10.

Conley-LaComb, M.K., Saliganan, A., Kandagatla, P., Chen, Y.Q., Cher, M.L., and Chinni, S.R. (2013). PTEN loss mediated Akt activation promotes prostate tumor growth and metastasis via CXCL12/CXCR4 signaling. Mol. Cancer 12, 85.

Cordes, S.P., and Barsh, G.S. (1994). The mouse segmentation gene kr encodes a novel basic domain-leucine zipper transcription factor. Cell 79, 1025–1034.

Costa, L., Badia, X., Chow, E., Lipton, A., and Wardley, A. (2008). Impact of skeletal complications on patients' quality of life, mobility, and functional independence. Support. Care Cancer 16, 879–889.

Couse, J.F., and Korach, K.S. (1999a). Reproductive phenotypes in the estrogen receptor-alpha knockout mouse. Ann. Endocrinol. (Paris). 60, 143–148.

Couse, J.F., and Korach, K.S. (1999b). Estrogen receptor null mice: what have we learned and where will they lead us? Endocr. Rev. 20, 358–417.

Cox, T.R., Rumney, R.M.H., Schoof, E.M., Perryman, L., Høye, A.M., Agrawal, A., Bird, D., Latif, N.A., Forrest, H., Evans, H.R., et al. (2015). The hypoxic cancer secretome induces pre-metastatic bone lesions through lysyl oxidase. Nature 522, 106–110.

Cramer, S.D., Chen, Z., and Peehl, D.M. (1996). Prostate specific antigen cleaves parathyroid hormone-related protein in the PTH-like domain: inactivation of PTHrP-stimulated cAMP

accumulation in mouse osteoblasts. J. Urol. 156, 526–531.

Di Croce, L., Koop, R., Venditti, P., Westphal, H.M., Nightingale, K.P., Corona, D.F., Becker, P.B., and Beato, M. (1999). Two-step synergism between the progesterone receptor and the DNA-binding domain of nuclear factor 1 on MMTV minichromosomes. Mol. Cell 4, 45–54.

Cummings, M.C., Simpson, P.T., Reid, L.E., Jayanthan, J., Skerman, J., Song, S., McCart Reed, A.E., Kutasovic, J.R., Morey, A.L., Marquart, L., et al. (2014). Metastatic progression of breast cancer: insights from 50 years of autopsies. J. Pathol. 232, 23–31.

Cunha, G.R., Young, P., Hom, Y.K., Cooke, P.S., Taylor, J.A., and Lubahn, D.B. (1997). Elucidation of a role for stromal steroid hormone receptors in mammary gland growth and development using tissue recombinants. J. Mammary Gland Biol. Neoplasia 2, 393–402.

Czupryna, J., and Tsourkas, A. (2011). Firefly luciferase and RLuc8 exhibit differential sensitivity to oxidative stress in apoptotic cells. PLoS One 6, e20073.

Dai, J., Hensel, J., Wang, N., Kruithof-de Julio, M., and Shiozawa, Y. (2016). Mouse models for studying prostate cancer bone metastasis. Bonekey Rep. 5, 777.

Delmas, P.D., and Meunier, P.J. (1997). The Management of Paget's Disease of Bone. N. Engl. J. Med. 336, 558–566.

Denoyelle, C., Hong, L., Vannier, J.-P., Soria, J., and Soria, C. (2003). New insights into the actions of bisphosphonate zoledronic acid in breast cancer cells by dual RhoA-dependent and -independent effects. Br. J. Cancer 88, 1631–1640.

DePuy, V., Anstrom, K.J., Castel, L.D., Schulman, K.A., Weinfurt, K.P., and Saad, F. (2007). Effects of skeletal morbidities on longitudinal patient-reported outcomes and survival in patients with metastatic prostate cancer. Support. Care Cancer 15, 869–876.

Deslypere, J.P., Young, M., Wilson, J.D., and McPhaul, M.J. (1992). Testosterone and 5 alpha-dihydrotestosterone interact differently with the androgen receptor to enhance transcription of the MMTV-CAT reporter gene. Mol. Cell. Endocrinol. 88, 15–22.

Dickson, R.B., and Lippman, M.E. (1995). Growth factors in breast cancer. Endocr. Rev. 16, 559–589.

Diéguez-Hurtado, R., Martín, J., Martínez-Corral, I., Martínez, M.D., Megías, D., Olmeda, D., and Ortega, S. (2011). A Cre-reporter transgenic mouse expressing the far-red fluorescent protein Katushka. Genesis 49, 36–45.

Disibio, G., and French, S.W. (2008). Metastatic patterns of cancers: results from a large autopsy study. Arch. Pathol. Lab. Med. 132, 931–939.

Donnelly, M.L., Hughes, L.E., Luke, G., Mendoza, H., ten Dam, E., Gani, D., and Ryan, M.D. (2001). The "cleavage" activities of foot-and-mouth disease virus 2A site-directed mutants and naturally occurring "2A-like" sequences. J. Gen. Virol. 82, 1027–1041.

Doudna, J.A., and Charpentier, E. (2014). Genome editing. The new frontier of genome engineering with CRISPR-Cas9. Science 346, 1258096.

Dougall, W.C., and Chaisson, M. (2006). The RANK/RANKL/OPG triad in cancer-induced bone diseases. Cancer Metastasis Rev. 25, 541–549.

Douma, S., Van Laar, T., Zevenhoven, J., Meuwissen, R., Van Garderen, E., and Peeper, D.S. (2004). Suppression of anoikis and induction of metastasis by the neurotrophic receptor TrkB. Nature 430, 1034–1039.

Dowsett, M., Sestak, I., Lopez-Knowles, E., Sidhu, K., Dunbier, A.K., Cowens, J.W., Ferree, S., Storhoff, J., Schaper, C., and Cuzick, J. (2013). Comparison of PAM50 risk of recurrence score with oncotype DX and IHC4 for predicting risk of distant recurrence after endocrine therapy. J. Clin. Oncol. 31, 2783–2790.

Dragatsis, I., and Zeitlin, S. (2001). A method for the generation of conditional gene repair mutations in mice. Nucleic Acids Res. 29, E10.

Drake, M.T., Clarke, B.L., and Khosla, S. (2008). Bisphosphonates: mechanism of action and role

in clinical practice. Mayo Clin. Proc. 83, 1032–1045.

Eckhardt, B.L., Francis, P.A., Parker, B.S., and Anderson, R.L. (2012). Strategies for the discovery and development of therapies for metastatic breast cancer. Nat. Rev. Drug Discov. 11, 479–497.

Edge, S., Byrd, D.R., Compton, C.C., Fritz, A.G., Greene, F.L., and Trotti, A. (2009). AJCC Cancer Staging Manual, 7th Edition.

Edge, S., Byrd, D.R., Compton, C.C., Fritz, A.G., Greene, F., and Trotti, A. (2010). AJCC cancer staging manual. (Springer).

Elefteriou, F., and Yang, X. (2011). Genetic mouse models for bone studies--strengths and limitations. Bone 49, 1242–1254.

Ellis, M.J., Coop, A., Singh, B., Mauriac, L., Llombert-Cussac, A., Jänicke, F., Miller, W.R., Evans, D.B., Dugan, M., Brady, C., et al. (2001). Letrozole is more effective neoadjuvant endocrine therapy than tamoxifen for ErbB-1- and/or ErbB-2-positive, estrogen receptor-positive primary breast cancer: evidence from a phase III randomized trial. J. Clin. Oncol. 19, 3808–3816.

Erler, J.T., Bennewith, K.L., Cox, T.R., Lang, G., Bird, D., Koong, A., Le, Q.-T., and Giaccia, A.J. (2009). Hypoxia-induced lysyl oxidase is a critical mediator of bone marrow cell recruitment to form the premetastatic niche. Cancer Cell 15, 35–44.

Everts, V., Delaissé, J.M., Korper, W., Jansen, D.C., Tigchelaar-Gutter, W., Saftig, P., and Beertsen, W. (2002). The Bone Lining Cell: Its Role in Cleaning Howship's Lacunae and Initiating Bone Formation. J. Bone Miner. Res. 17, 77–90.

Ewing, J. (1922). Neoplastic diseases: a treatise on tumors. W.B Saunders Co. 2nd edition.

Eychène, A., Rocques, N., and Pouponnot, C. (2008). A new MAFia in cancer. Nat. Rev. Cancer 8, 683–693.

Fan, X., Petitt, M., Gamboa, M., Huang, M., Dhal, S., Druzin, M.L., Wu, J.C., Chen-Tsai, Y., and Nayak, N.R. (2012). Transient, inducible, placenta-specific gene expression in mice. Endocrinology 153, 5637–5644.

Fantozzi, A., and Christofori, G. (2006). Mouse models of breast cancer metastasis. Breast Cancer Res. 8, 212.

Feil, R., Wagner, J., Metzger, D., and Chambon, P. (1997). Regulation of Cre recombinase activity by mutated estrogen receptor ligand-binding domains. Biochem. Biophys. Res. Commun. 237, 752–757.

Feil, S., Valtcheva, N., and Feil, R. (2009). Inducible cre mice.

Feng, X. (2009). Chemical and Biochemical Basis of Cell-Bone Matrix Interaction in Health and Disease. Curr. Chem. Biol. 3, 189–196.

Fernandez-Valdivia, R., and Lydon, J.P. (2012). From the ranks of mammary progesterone mediators, RANKL takes the spotlight. Mol. Cell. Endocrinol. 357, 91–100.

Fidler, I.J. (2003). The pathogenesis of cancer metastasis: the "seed and soil" hypothesis revisited. Nat. Rev. Cancer 3, 453–458.

Finn, R.S., Crown, J.P., Lang, I., Boer, K., Bondarenko, I.M., Kulyk, S.O., Ettl, J., Patel, R., Pinter, T., Schmidt, M., et al. (2015). The cyclin-dependent kinase 4/6 inhibitor palbociclib in combination with letrozole versus letrozole alone as first-line treatment of oestrogen receptor-positive, HER2-negative, advanced breast cancer (PALOMA-1/TRIO-18): a randomised phase 2 study. Lancet. Oncol. 16, 25–35.

Fisher, B., Costantino, J.P., Wickerham, D.L., Redmond, C.K., Kavanah, M., Cronin, W.M., Vogel, V., Robidoux, A., Dimitrov, N., Atkins, J., et al. (1998). Tamoxifen for prevention of breast cancer: report of the National Surgical Adjuvant Breast and Bowel Project P-1 Study. J. Natl. Cancer Inst. 90, 1371–1388.

Fisher, J.L., Thomas-Mudge, R.J., Elliott, J., Hards, D.K., Sims, N.A., Slavin, J., Martin, T.J., and

Gillespie, M.T. (2006). Osteoprotegerin overexpression by breast cancer cells enhances orthotopic and osseous tumor growth and contrasts with that delivered therapeutically. Cancer Res. 66, 3620–3628.

Fizazi, K., Lipton, A., Mariette, X., Body, J.-J., Rahim, Y., Gralow, J.R., Gao, G., Wu, L., Sohn, W., and Jun, S. (2009). Randomized phase II trial of denosumab in patients with bone metastases from prostate cancer, breast cancer, or other neoplasms after intravenous bisphosphonates. J. Clin. Oncol. 27, 1564–1571.

Fizazi, K., Carducci, M., Smith, M., Damião, R., Brown, J., Karsh, L., Milecki, P., Shore, N., Rader, M., Wang, H., et al. (2011). Denosumab versus zoledronic acid for treatment of bone metastases in men with castration-resistant prostate cancer: a randomised, double-blind study. Lancet 377, 813–822.

Florencio-Silva, R., Sasso, G.R.D.S., Sasso-Cerri, E., Simões, M.J., and Cerri, P.S. (2015). Biology of Bone Tissue: Structure, Function, and Factors That Influence Bone Cells. Biomed Res. Int. 2015.

Fluck, M.M., and Schaffhausen, B.S. (2009). Lessons in signaling and tumorigenesis from polyomavirus middle T antigen. Microbiol. Mol. Biol. Rev. 73, 542–63, Table of Contents.

Folwarczna, J., Janiec, W., Firlus, K., and Kaczmarczyk-Sedlak, I. (1999). Effects of doxycycline on the development of bone damage caused by prednisolone in rats. Pol. J. Pharmacol. 51, 243–251.

Folwarczna, J., Pytlik, M., and Janiec, W. (2003). EFFECTS OF DOXYCYCLINE ON DEVELOPMENT OF CHANGES IN HISTOMORPHOMETRIC PARAMETERS OF BONES INDUCED BY BILATERAL OVARIECTOMY IN RATS. Pol. J. Pharmacol. 55, 433–441.

Foulkes, W.D., Stefansson, I.M., Chappuis, P.O., Bégin, L.R., Goffin, J.R., Wong, N., Trudel, M., and Akslen, L.A. (2003). Germline BRCA1 mutations and a basal epithelial phenotype in breast cancer. J. Natl. Cancer Inst. 95, 1482–1485.

Foulkes, W.D., Brunet, J.-S., Stefansson, I.M., Straume, O., Chappuis, P.O., Bégin, L.R., Hamel, N., Goffin, J.R., Wong, N., Trudel, M., et al. (2004). The prognostic implication of the basal-like (cyclin E high/p27 low/p53+/glomeruloid-microvascular-proliferation+) phenotype of BRCA1-related breast cancer. Cancer Res. 64, 830–835.

Fournier, P.G.J., Chirgwin, J.M., and Guise, T. a (2006). New insights into the role of T cells in the vicious cycle of bone metastases. Curr. Opin. Rheumatol. 18, 396–404.

Friedl, P., and Gilmour, D. (2009). Collective cell migration in morphogenesis, regeneration and cancer. Nat. Rev. Mol. Cell Biol. 10, 445–457.

Friedl, P., Locker, J., Sahai, E., and Segall, J.E. (2012). Classifying collective cancer cell invasion. Nat. Cell Biol. 14, 777–783.

Friedrich, G., and Soriano, P. (1991). Promoter traps in embryonic stem cells: a genetic screen to identify and mutate developmental genes in mice. Genes Dev. 5, 1513–1523.

Frost, H.M. (1990). Skeletal structural adaptations to mechanical usage (SATMU): 2. Redefining Wolff's law: the remodeling problem. Anat. Rec. 226, 414–422.

Funa, K., Nordgren, H., and Nilsson, S. (1991). In Situ Expression of mRNA for Proto-Oncogenes in Benign Prostatic Hyperplasia and in Prostatic Carcinoma. Scand. J. Urol. Nephrol. 25, 95–100.

Furth, P.A., St Onge, L., Böger, H., Gruss, P., Gossen, M., Kistner, A., Bujard, H., and Hennighausen, L. (1994). Temporal control of gene expression in transgenic mice by a tetracycline-responsive promoter. Proc. Natl. Acad. Sci. U. S. A. 91, 9302–9306.

Garnero, P., Borel, O., Byrjalsen, I., Ferreras, M., Drake, F.H., McQueney, M.S., Foged, N.T., Delmas, P.D., and Delaissé, J.-M. (1998). The Collagenolytic Activity of Cathepsin K Is Unique among Mammalian Proteinases. J. Biol. Chem. 273, 32347–32352.

Garrick, D., Fiering, S., Martin, D.I., and Whitelaw, E. (1998). Repeat-induced gene silencing in mammals. Nat. Genet. 18, 56–59.

Gay, L.J., and Felding-Habermann, B. (2011). Contribution of platelets to tumour metastasis. Nat. Rev. Cancer 11, 123–134.

Geyer, C.E., Forster, J., Lindquist, D., Chan, S., Romieu, C.G., Pienkowski, T., Jagiello-Gruszfeld, A., Crown, J., Chan, A., Kaufman, B., et al. (2006). Lapatinib plus capecitabine for HER2-positive advanced breast cancer. N. Engl. J. Med. 355, 2733–2743.

Giampieri, S., Manning, C., Hooper, S., Jones, L., Hill, C.S., and Sahai, E. (2009). Localized and reversible TGFbeta signalling switches breast cancer cells from cohesive to single cell motility. Nat. Cell Biol. 11, 1287–1296.

Girasole, G., Passeri, G., Jilka, R.L., and Manolagas, S.C. (1994). Interleukin-11: a new cytokine critical for osteoclast development. J. Clin. Invest. 93, 1516–1524.

Gleave, M., Hsieh, J.T., Gao, C.A., von Eschenbach, A.C., and Chung, L.W. (1991). Acceleration of human prostate cancer growth in vivo by factors produced by prostate and bone fibroblasts. Cancer Res. 51, 3753–3761.

Gocheva, V., Wang, H.-W., Gadea, B.B., Shree, T., Hunter, K.E., Garfall, A.L., Berman, T., and Joyce, J.A. (2010). IL-4 induces cathepsin protease activity in tumor-associated macrophages to promote cancer growth and invasion. Genes Dev. 24, 241–255.

Goedhart, J., van Weeren, L., Adjobo-Hermans, M.J.W., Elzenaar, I., Hink, M.A., and Gadella, T.W.J. (2011). Quantitative co-expression of proteins at the single cell level--application to a multimeric FRET sensor. PLoS One 6, e27321.

Goldhirsch, A., Winer, E.P., Coates, A.S., Gelber, R.D., Piccart-Gebhart, M., Thürlimann, B., Senn, H.-J., and Panel members (2013). Personalizing the treatment of women with early breast cancer: highlights of the St Gallen International Expert Consensus on the Primary Therapy of Early Breast Cancer 2013. Ann. Oncol. Off. J. Eur. Soc. Med. Oncol. 24, 2206–2223.

Golub, L.M., Lee, H.M., Ryan, M.E., Giannobile, W. V., Payne, J., and Sorsa, T. (1998). Tetracyclines inhibit connective tissue breakdown by multiple non-antimicrobial mechanisms. Adv. Dent. Res. 12, 12–26.

Gomez, H.L., Doval, D.C., Chavez, M.A., Ang, P.C.-S., Aziz, Z., Nag, S., Ng, C., Franco, S.X., Chow, L.W.C., Arbushites, M.C., et al. (2008). Efficacy and safety of lapatinib as first-line therapy for ErbB2-amplified locally advanced or metastatic breast cancer. J. Clin. Oncol. 26, 2999–3005.

Gomis, R.R., and Gawrzak, S. (2017). Tumor cell dormancy. Mol. Oncol. 11, 62–78.

Gordeladze, J.O., Drevon, C.A., Syversen, U., and Reseland, J.E. (2002). Leptin stimulates human osteoblastic cell proliferation, de novo collagen synthesis, and mineralization: Impact on differentiation markers, apoptosis, and osteoclastic signaling. J. Cell. Biochem. 85, 825–836.

Gordon, J.W., Scangos, G.A., Plotkin, D.J., Barbosa, J.A., and Ruddle, F.H. (1980). Genetic transformation of mouse embryos by microinjection of purified DNA. Proc. Natl. Acad. Sci. U. S. A. 77, 7380–7384.

Goss, P.E. (2003). Breast cancer prevention--clinical trials strategies involving aromatase inhibitors. J. Steroid Biochem. Mol. Biol. 86, 487–493.

Goss, P.E., Ingle, J.N., Martino, S., Robert, N.J., Muss, H.B., Piccart, M.J., Castiglione, M., Tu, D., Shepherd, L.E., Pritchard, K.I., et al. (2003). A Randomized Trial of Letrozole in Postmenopausal Women after Five Years of Tamoxifen Therapy for Early-Stage Breast Cancer. N. Engl. J. Med. 349, 1793–1802.

Goss, P.E., Ingle, J.N., Alés-Martínez, J.E., Cheung, A.M., Chlebowski, R.T., Wactawski-Wende, J., McTiernan, A., Robbins, J., Johnson, K.C., Martin, L.W., et al. (2011). Exemestane for breast-cancer prevention in postmenopausal women. N. Engl. J. Med. 364, 2381–2391.

Gossen, M., and Bujard, H. (1992). Tight control of gene expression in mammalian cells by tetracycline-responsive promoters. Proc. Natl. Acad. Sci. U. S. A. 89, 5547–5551.

Gossen, M., Freundlieb, S., Bender, G., Müller, G., Hillen, W., and Bujard, H. (1995). Transcriptional activation by tetracyclines in mammalian cells. Science 268, 1766–1769.

Graham, J.D., Mote, P.A., Salagame, U., van Dijk, J.H., Balleine, R.L., Huschtscha, L.I., Reddel, R.R., and Clarke, C.L. (2009). DNA replication licensing and progenitor numbers are increased by progesterone in normal human breast. Endocrinology 150, 3318–3326.

Grignon, D.J. (2004). Unusual subtypes of prostate cancer. Mod. Pathol. 17, 316–327.

Grosse-Wilde, A., Fouquier d'Hérouël, A., McIntosh, E., Ertaylan, G., Skupin, A., Kuestner, R.E., del Sol, A., Walters, K.-A., and Huang, S. (2015). Stemness of the hybrid Epithelial/Mesenchymal State in Breast Cancer and Its Association with Poor Survival. PLoS One 10, e0126522.

Guise, T.A., Yin, J.J., Taylor, S.D., Kumagai, Y., Dallas, M., Boyce, B.F., Yoneda, T., and Mundy, G.R. (1996). Evidence for a causal role of parathyroid hormone-related protein in the pathogenesis of human breast cancer-mediated osteolysis. J. Clin. Invest. 98, 1544–1549.

Gunther, E.J., Belka, G.K., Wertheim, G.B.W., Wang, J., Hartman, J.L., Boxer, R.B., and Chodosh, L.A. (2002). A novel doxycycline-inducible system for the transgenic analysis of mammary gland biology. FASEB J. 16, 283–292.

Gupta, G.P., and Massagué, J. (2004). Platelets and metastasis revisited: a novel fatty link. J. Clin. Invest. 114, 1691–1693.

Gupta, G.P., and Massagué, J. (2006). Cancer Metastasis: Building a Framework. Cell 127, 679–695.

Gupta, G.P., Nguyen, D.X., Chiang, A.C., Bos, P.D., Kim, J.Y., Nadal, C., Gomis, R.R., Manova-Todorova, K., and Massagué, J. (2007). Mediators of vascular remodelling co-opted for sequential steps in lung metastasis. Nature 446, 765–770.

Gusterson, B.A., Warburton, M.J., Mitchell, D., Ellison, M., Neville, A.M., and Rudland, P.S. (1982). Distribution of myoepithelial cells and basement membrane proteins in the normal breast and in benign and malignant breast diseases. Cancer Res. 42, 4763–4770.

Hadjidakis, D.J., and Androulakis, I.I. (2006). Bone remodeling. Ann. N. Y. Acad. Sci. 1092, 385–396.

Haider, M., Holen, I., Dear, T.N., Hunter, K., and Brown, H.K. (2014). Modifying the osteoblastic niche with zoledronic acid in vivo—Potential implications for breast cancer bone metastasis. Bone 66, 240–250.

Hammond, M.E.H., Hayes, D.F., Dowsett, M., Allred, D.C., Hagerty, K.L., Badve, S., Fitzgibbons, P.L., Francis, G., Goldstein, N.S., Hayes, M., et al. (2010). American Society of Clinical Oncology/College of American Pathologists Guideline Recommendations for Immunohistochemical Testing of Estrogen and Progesterone Receptors in Breast Cancer. J. Clin. Oncol. 28, 2784–2795.

Hanahan, D., and Weinberg, R. (2011). Hallmarks of Cancer: The Next Generation. Cell 144, 646–674.

Harada, S., and Rodan, G. a (2003). Control of osteoblast function and regulation of bone mass. Nature 423, 349–355.

Hardaway, A.L., Herroon, M.K., Rajagurubandara, E., and Podgorski, I. (2014). Bone marrow fat: linking adipocyte-induced inflammation with skeletal metastases. Cancer Metastasis Rev. 33, 527–543.

Haruyama, N., Cho, A., and Kulkarni, A.B. (2009). Overview: Engineering Transgenic Constructs and Mice. In Current Protocols in Cell Biology, (Hoboken, NJ, USA: John Wiley & Sons, Inc.), pp. 1–12.

Hawkins, S.M., and Matzuk, M.M. (2008). The menstrual cycle: basic biology. Ann. N. Y. Acad.

Sci. 1135, 10–18.

Hayward, S.W., Baskin, L.S., Haughney, P.C., Foster, B.A., Cunha, A.R., Dahiya, R., Prins, G.S., and Cunha, G.R. (1996a). Stromal development in the ventral prostate, anterior prostate and seminal vesicle of the rat. Acta Anat. (Basel). 155, 94–103.

Hayward, S.W., Baskin, L.S., Haughney, P.C., Cunha, A.R., Foster, B.A., Dahiya, R., Prins, G.S., and Cunha, G.R. (1996b). Epithelial development in the rat ventral prostate, anterior prostate and seminal vesicle. Acta Anat. (Basel). 155, 81–93.

Heckel, T., Czupalla, C., Expirto Santo, A.I., Anitei, M., Arantzazu Sanchez-Fernandez, M., Mosch, K., Krause, E., and Hoflack, B. (2009). Src-dependent repression of ARF6 is required to maintain podosome-rich sealing zones in bone-digesting osteoclasts. Proc. Natl. Acad. Sci. U. S. A. 106, 1451–1456.

Hedenfalk, I., Duggan, D., Chen, Y., Radmacher, M., Bittner, M., Simon, R., Meltzer, P., Gusterson, B., Esteller, M., Kallioniemi, O.P., et al. (2001). Gene-expression profiles in hereditary breast cancer. N. Engl. J. Med. 344, 539–548.

Henderson, M. a., Danks, J.A., Slavin, J.L., Byrnes, G.B., Choong, P.F.M., Spillane, J.B., Hopper, J.L., and Martin, T.J. (2006). Parathyroid hormone-related protein localization in breast cancers predict improved prognosis. Cancer Res. 66, 2250–2256.

Henikoff, S. (1998). Conspiracy of silence among repeated transgenes. Bioessays 20, 532–535.

Hennighausen, L., and Robinson, G.W. (1998). Think globally, act locally: the making of a mouse mammary gland. Genes Dev. 12, 449–455.

Hennighausen, L., and Robinson, G.W. (2005). Information networks in the mammary gland. Nat. Rev. Mol. Cell Biol. 6, 715–725.

Hennighausen, L., Wall, R.J., Tillmann, U., Li, M., and Furth, P.A. (1995). Conditional gene expression in secretory tissues and skin of transgenic mice using the MMTV-LTR and the tetracycline responsive system. J. Cell. Biochem. 59, 463–472.

Herschkowitz, J.I., Simin, K., Weigman, V.J., Mikaelian, I., Usary, J., Hu, Z., Rasmussen, K.E., Jones, L.P., Assefnia, S., Chandrasekharan, S., et al. (2007). Identification of conserved gene expression features between murine mammary carcinoma models and human breast tumors. Genome Biol. 8, R76.

Hinck, L., and Silberstein, G.B. (2005). Key stages in mammary gland development: the mammary end bud as a motile organ. Breast Cancer Res. 7, 245–251.

Hiraga, T., Kizaka-Kondoh, S., Hirota, K., Hiraoka, M., and Yoneda, T. (2007). Hypoxia and hypoxia-inducible factor-1 expression enhance osteolytic bone metastases of breast cancer. Cancer Res. 67, 4157–4163.

Hofbauer, L.C., and Schoppet, M. (2004). Clinical implications of the osteoprotegerin/RANKL/RANK system for bone and vascular diseases. JAMA 292, 490–495.

Horii, T., Arai, Y., Yamazaki, M., Morita, S., Kimura, M., Itoh, M., Abe, Y., and Hatada, I. (2014). Validation of microinjection methods for generating knockout mice by CRISPR/Cas-mediated genome engineering. Sci. Rep. 4, 4513.

Horoszewicz, J.S., Leong, S.S., Chu, T.M., Wajsman, Z.L., Friedman, M., Papsidero, L., Kim, U., Chai, L.S., Kakati, S., Arya, S.K., et al. (1980). The LNCaP cell line--a new model for studies on human prostatic carcinoma. Prog. Clin. Biol. Res. 37, 115–132.

Horwood, N.J., Elliott, J., Martin, T.J., and Gillespie, M.T. (1998). Osteotropic agents regulate the expression of osteoclast differentiation factor and osteoprotegerin in osteoblastic stromal cells. Endocrinology 139, 4743–4746.

Hovey, R.C., Trott, J.F., and Vonderhaar, B.K. (2002). Establishing a framework for the functional mammary gland: from endocrinology to morphology. J. Mammary Gland Biol. Neoplasia 7, 17–38.

Hughes, D.E., Wright, K.R., Uy, H.L., Sasaki, A., Yoneda, T., Roodman, G.D., Mundy, G.R., and

Boyce, B.F. (1995). Bisphosphonates promote apoptosis in murine osteoclasts in vitro and in vivo. J. Bone Miner. Res. 10, 1478–1487.

Humphrey, P.A. (2007). Diagnosis of adenocarcinoma in prostate needle biopsy tissue. J. Clin. Pathol. 60, 35–42.

Hurt, E.M., Wiestner, A., Rosenwald, A., Shaffer, A.L., Campo, E., Grogan, T., Bergsagel, P.L., Kuehl, W.M., and Staudt, L.M. (2004). Overexpression of c-maf is a frequent oncogenic event in multiple myeloma that promotes proliferation and pathological interactions with bone marrow stroma. Cancer Cell 5, 191–199.

Id Boufker, H., Lagneaux, L., Najar, M., Piccart, M., Ghanem, G., Body, J.-J., and Journé, F. (2010). The Src inhibitor dasatinib accelerates the differentiation of human bone marrow-derived mesenchymal stromal cells into osteoblasts. BMC Cancer 10, 298.

Ikushima, H., and Miyazono, K. (2010). TGFβ signalling: a complex web in cancer progression. Nat. Rev. Cancer 10, 415–424.

Imaki, J., Tsuchiya, K., Mishima, T., Onodera, H., Kim, J.I., Yoshida, K., Ikeda, H., and Sakai, M. (2004). Developmental contribution of c-maf in the kidney: distribution and developmental study of c-maf mRNA in normal mice kidney and histological study of c-maf knockout mice kidney and liver. Biochem. Biophys. Res. Commun. 320, 1323–1327.

Indra, A.K., Warot, X., Brocard, J., Bornert, J.M., Xiao, J.H., Chambon, P., and Metzger, D. (1999). Temporally-controlled site-specific mutagenesis in the basal layer of the epidermis: comparison of the recombinase activity of the tamoxifen-inducible Cre-ER(T) and Cre-ER(T2) recombinases. Nucleic Acids Res. 27, 4324–4327.

Iwamura, M., Hellman, J., Cockett, A.T., Lilja, H., and Gershagen, S. (1996). Alteration of the hormonal bioactivity of parathyroid hormone-related protein (PTHrP) as a result of limited proteolysis by prostate-specific antigen. Urology 48, 317–325.

Iyengar, P., Combs, T.P., Shah, S.J., Gouon-Evans, V., Pollard, J.W., Albanese, C., Flanagan, L., Tenniswood, M.P., Guha, C., Lisanti, M.P., et al. (2003). Adipocyte-secreted factors synergistically promote mammary tumorigenesis through induction of anti-apoptotic transcriptional programs and proto-oncogene stabilization. Oncogene 22, 6408–6423.

Jahroudi, N., and Greenberger, J.S. (1995). The role of endothelial cells in tumor invasion and metastasis. J. Neurooncol. 23, 99–108.

Jaiyesimi, I.A., Buzdar, A.U., Decker, D.A., and Hortobagyi, G.N. (1995). Use of tamoxifen for breast cancer: twenty-eight years later. J. Clin. Oncol. 13, 513–529.

Jang, S.K., Kräusslich, H.G., Nicklin, M.J., Duke, G.M., Palmenberg, A.C., and Wimmer, E. (1988). A segment of the 5' nontranslated region of encephalomyocarditis virus RNA directs internal entry of ribosomes during in vitro translation. J. Virol. 62, 2636–2643.

Jiang, Z., Li, C., Fischer, A., Dresser, K., and Woda, B.A. (2005). Using an AMACR (P504S)/34betaE12/p63 cocktail for the detection of small focal prostate carcinoma in needle biopsy specimens. Am. J. Clin. Pathol. 123, 231–236.

Jilka, R.L. (2013). The relevance of mouse models for investigating age-related bone loss in humans. J. Gerontol. A. Biol. Sci. Med. Sci. 68, 1209–1217.

Jinek, M., Chylinski, K., Fonfara, I., Hauer, M., Doudna, J.A., and Charpentier, E. (2012). A Programmable Dual-RNA-Guided DNA Endonuclease in Adaptive Bacterial Immunity. Science (80-.). 337, 816–821.

Joshi, P.A., Jackson, H.W., Beristain, A.G., Di Grappa, M.A., Mote, P.A., Clarke, C.L., Stingl, J., Waterhouse, P.D., and Khokha, R. (2010). Progesterone induces adult mammary stem cell expansion. Nature 465, 803–807.

Joshi, P.A., Di Grappa, M.A., and Khokha, R. (2012). Active allies: hormones, stem cells and the niche in adult mammopoiesis. Trends Endocrinol. Metab. 23, 299–309.

Kaighn, M.E., Narayan, K.S., Ohnuki, Y., Lechner, J.F., and Jones, L.W. (1979). Establishment

and characterization of a human prostatic carcinoma cell line (PC-3). Invest. Urol. 17, 16–23.

Kakhki, V.R.D., Anvari, K., Sadeghi, R., Mahmoudian, A.-S., and Torabian-Kakhki, M. (2013). Pattern and distribution of bone metastases in common malignant tumors. Nucl. Med. Rev. 16, 66–69.

Kang, Y., and Massagué, J. (2004). Epithelial-mesenchymal transitions: twist in development and metastasis. Cell 118, 277–279.

Kang, Y., Siegel, P.M., Shu, W., Drobnjak, M., Kakonen, S.M., Cordón-Cardo, C., Guise, T. a, and Massagué, J. (2003). A multigenic program mediating breast cancer metastasis to bone. Cancer Cell 3, 537–549.

Kang, Y., He, W., Tulley, S., Gupta, G.P., Serganova, I., Chen, C.-R., Manova-Todorova, K., Blasberg, R., Gerald, W.L., and Massagué, J. (2005). Breast cancer bone metastasis mediated by the Smad tumor suppressor pathway. Proc. Natl. Acad. Sci. U. S. A. 102, 13909–13914.

Kataoka, K. (2007). Multiple mechanisms and functions of maf transcription factors in the regulation of tissue-specific genes. J. Biochem. 141, 775–781.

Kataoka, K., Nishizawa, M., and Kawai, S. (1993). Structure-function analysis of the maf oncogene product, a member of the b-Zip protein family. J. Virol. 67, 2133–2141.

Kataoka, K., Shioda, S., Yoshitomo-Nakagawa, K., Handa, H., and Nishizawa, M. (2001). Maf and Jun nuclear oncoproteins share downstream target genes for inducing cell transformation. J. Biol. Chem. 276, 36849–36856.

Kato, J., Futamura, M., Kanematsu, M., Gaowa, S., Mori, R., Tanahashi, T., Matsuhashi, N., and Yoshida, K. (2016). Combination therapy with zoledronic acid and cetuximab effectively suppresses growth of colorectal cancer cells regardless of KRAS status. Int. J. Cancer 138, 1516–1527.

Katsuno, Y., Hanyu, A., Kanda, H., Ishikawa, Y., Akiyama, F., Iwase, T., Ogata, E., Ehata, S., Miyazono, K., and Imamura, T. (2008). Bone morphogenetic protein signaling enhances invasion and bone metastasis of breast cancer cells through Smad pathway. Oncogene 27, 6322–6333.

Kelly, T., Suva, L.J., Huang, Y., Macleod, V., Miao, H.-Q., Walker, R.C., and Sanderson, R.D. (2005). Expression of heparanase by primary breast tumors promotes bone resorption in the absence of detectable bone metastases. Cancer Res. 65, 5778–5784.

Kennecke, H., Yerushalmi, R., Woods, R., Cheang, M.C.U., Voduc, D., Speers, C.H., Nielsen, T.O., and Gelmon, K. (2010). Metastatic behavior of breast cancer subtypes. J. Clin. Oncol. 28, 3271–3277.

Kenney, N.J., Smith, G.H., Rosenberg, K., Cutler, M.L., and Dickson, R.B. (1996). Induction of ductal morphogenesis and lobular hyperplasia by amphiregulin in the mouse mammary gland. Cell Growth Differ. 7, 1769–1781.

Kessenbrock, K., Plaks, V., and Werb, Z. (2010). Matrix metalloproteinases: regulators of the tumor microenvironment. Cell 141, 52–67.

Kienast, J., and Berdel, W.E. (2004). c-maf in multiple myeloma: an oncogene enhancing tumor-stroma interactions. Cancer Cell 5, 109–110.

Kim, H.-J., Kim, J.-H., Bae, S.-C., Choi, J.-Y., Kim, H.-J., and Ryoo, H.-M. (2003). The protein kinase C pathway plays a central role in the fibroblast growth factor-stimulated expression and transactivation activity of Runx2. J. Biol. Chem. 278, 319–326.

Kim, J.-B., Urban, K., Cochran, E., Lee, S., Ang, A., Rice, B., Bata, A., Campbell, K., Coffee, R., Gorodinsky, A., et al. (2010). Non-Invasive Detection of a Small Number of Bioluminescent Cancer Cells In Vivo. PLoS One 5, e9364.

Kim, J.H., Jin, H.M., Kim, K., Song, I., Youn, B.U., Matsuo, K., and Kim, N. (2009). The mechanism of osteoclast differentiation induced by IL-1. J. Immunol. 183, 1862–1870.

Kim, J.H., Lee, S.-R., Li, L., Park, H.-J., Park, J., Lee, K.Y., Kim, M., Shin, B.A., and Choi, S.

(2011). High Cleavage Efficiency of a 2A Peptide Derived from Porcine Teschovirus-1 in Human Cell Lines, Zebrafish and Mice. PLoS One 6, e18556.

Klapisz-Wolikow, M., and Saffar, J.L. (1996). Minocycline impairment of both osteoid tissue removal and osteoclastic resorption in a synchronized model of remodeling in the rat. J. Cell. Physiol. 167, 359–368.

Koreckij, T., Nguyen, H., Brown, L.G., Yu, E.Y., Vessella, R.L., and Corey, E. (2009). Dasatinib inhibits the growth of prostate cancer in bone and provides additional protection from osteolysis. Br. J. Cancer 101, 263–268.

Kostenuik, P.J., Nguyen, H.Q., McCabe, J., Warmington, K.S., Kurahara, C., Sun, N., Chen, C., Li, L., Cattley, R.C., Van, G., et al. (2009). Denosumab, a fully human monoclonal antibody to RANKL, inhibits bone resorption and increases BMD in knock-in mice that express chimeric (murine/human) RANKL. J. Bone Miner. Res. 24, 182–195.

Kovarik, M.L., and Allbritton, N.L. (2011). Measuring enzyme activity in single cells. Trends Biotechnol. 29, 222–230.

Kozlow, W., and Guise, T.A. (2005). Breast cancer metastasis to bone: mechanisms of osteolysis and implications for therapy. J. Mammary Gland Biol. Neoplasia 10, 169–180.

Kuehl, W.M., and Bergsagel, P.L. (2002). Multiple myeloma: evolving genetic events and host interactions. Nat. Rev. Cancer 2, 175–187.

Labelle, M., Begum, S., and Hynes, R.O. (2011). Direct Signaling between Platelets and Cancer Cells Induces an Epithelial-Mesenchymal-Like Transition and Promotes Metastasis. Cancer Cell 20, 576–590.

Labrie, F., Bélanger, A., Dupont, A., Luu-The, V., Simard, J., and Labrie, C. (1993). Science behind total androgen blockade: from gene to combination therapy. Clin. Invest. Med. 16, 475–492.

Lacey, D.L., Boyle, W.J., Simonet, W.S., Kostenuik, P.J., Dougall, W.C., Sullivan, J.K., San Martin, J., and Dansey, R. (2012). Bench to bedside: elucidation of the OPG-RANK-RANKL pathway and the development of denosumab. Nat. Rev. Drug Discov. 11, 401–419.

Lakso, M., Sauer, B., Mosinger, B., Lee, E.J., Manning, R.W., Yu, S.H., Mulder, K.L., and Westphal, H. (1992). Targeted oncogene activation by site-specific recombination in transgenic mice. Proc. Natl. Acad. Sci. U. S. A. 89, 6232–6236.

Lamartina, S., Silvi, L., Roscilli, G., Casimiro, D., Simon, A.J., Davies, M.-E., Shiver, J.W., Rinaudo, C.D., Zampaglione, I., Fattori, E., et al. (2003). Construction of an rtTA2s-m2/ttskid-Based transcription regulatory switch that displays no basal activity, good inducibility, and high responsiveness to doxycycline in mice and Non-Human primates. Mol. Ther. 7, 271–280.

Lamouille, S., Xu, J., and Derynck, R. (2014). Molecular mechanisms of epithelial-mesenchymal transition. Nat. Rev. Mol. Cell Biol. 15, 178–196.

Lapteva, N., Yang, A.-G., Sanders, D.E., Strube, R.W., and Chen, S.-Y. (2005). CXCR4 knockdown by small interfering RNA abrogates breast tumor growth in vivo. Cancer Gene Ther. 12, 84–89.

Larson, S.R., Zhang, X., Dumpit, R., Coleman, I., Lakely, B., Roudier, M., Higano, C.S., True, L.D., Lange, P.H., Montgomery, B., et al. (2013). Characterization of osteoblastic and osteolytic proteins in prostate cancer bone metastases. Prostate 73, 932–940.

Lau, Y.S., Sabokbar, A., Giele, H., Cerundolo, V., Hofstetter, W., and Athanasou, N. a (2006). Malignant melanoma and bone resorption. Br. J. Cancer 94, 1496–1503.

Leblond, C.P. (1989). Synthesis and secretion of collagen by cells of connective tissue, bone, and dentin. Anat. Rec. 224, 123–138.

Lecoin, L., Sii-Felice, K., Pouponnot, C., Eychène, A., and Felder-Schmittbuhl, M.-P. (2004). Comparison of maf gene expression patterns during chick embryo development. Gene Expr. Patterns 4, 35–46.

Lee, W.H., Morton, R.A., Epstein, J.I., Brooks, J.D., Campbell, P.A., Bova, G.S., Hsieh, W.S., Isaacs, W.B., and Nelson, W.G. (1994). Cytidine methylation of regulatory sequences near the pi-class glutathione S-transferase gene accompanies human prostatic carcinogenesis. Proc. Natl. Acad. Sci. U. S. A. 91, 11733–11737.

Lee, Y.-C., Huang, C.-F., Murshed, M., Chu, K., Araujo, J.C., Ye, X., DeCrombrugghe, B., Yu-Lee, L.-Y., Gallick, G.E., and Lin, S.-H. (2010). Src family kinase/abl inhibitor dasatinib suppresses proliferation and enhances differentiation of osteoblasts. Oncogene 29, 3196–3207.

Van der Lee, S., and Boot, L.M. (1955). Spontaneous pseudopregnancy in mice. Acta Physiol. Pharmacol. Neerl. 4, 442–444.

Liang, X., Potter, J., Kumar, S., Zou, Y., Quintanilla, R., Sridharan, M., Carte, J., Chen, W., Roark, N., Ranganathan, S., et al. (2015). Rapid and highly efficient mammalian cell engineering via Cas9 protein transfection. J. Biotechnol. 208, 44–53.

Lilja, H., Ulmert, D., and Vickers, A.J. (2008). Prostate-specific antigen and prostate cancer: prediction, detection and monitoring. Nat. Rev. Cancer 8, 268–278.

Lin, E.Y., Jones, J.G., Li, P., Zhu, L., Whitney, K.D., Muller, W.J., and Pollard, J.W. (2003). Progression to malignancy in the polyoma middle T oncoprotein mouse breast cancer model provides a reliable model for human diseases. Am. J. Pathol. 163, 2113–2126.

Lin, N.U., Carey, L.A., Liu, M.C., Younger, J., Come, S.E., Ewend, M., Harris, G.J., Bullitt, E., Van den Abbeele, A.D., Henson, J.W., et al. (2008). Phase II Trial of Lapatinib for Brain Metastases in Patients With Human Epidermal Growth Factor Receptor 2–Positive Breast Cancer. J. Clin. Oncol. 26, 1993–1999.

Lindberg, M.K., Movérare, S., Skrtic, S., Gao, H., Dahlman-Wright, K., Gustafsson, J.-A., and Ohlsson, C. (2003). Estrogen receptor (ER)-beta reduces ERalpha-regulated gene transcription, supporting a "ying yang" relationship between ERalpha and ERbeta in mice. Mol. Endocrinol. 17, 203–208.

Lipton, A., Steger, G.G., Figueroa, J., Alvarado, C., Solal-Celigny, P., Body, J.-J., de Boer, R., Berardi, R., Gascon, P., Tonkin, K.S., et al. (2007). Randomized active-controlled phase II study of denosumab efficacy and safety in patients with breast cancer-related bone metastases. J. Clin. Oncol. 25, 4431–4437.

Liu, S., Ginestier, C., Charafe-Jauffret, E., Foco, H., Kleer, C.G., Merajver, S.D., Dontu, G., and Wicha, M.S. (2008). BRCA1 regulates human mammary stem/progenitor cell fate. Proc. Natl. Acad. Sci. U. S. A. 105, 1680–1685.

Livasy, C.A., Karaca, G., Nanda, R., Tretiakova, M.S., Olopade, O.I., Moore, D.T., and Perou, C.M. (2006). Phenotypic evaluation of the basal-like subtype of invasive breast carcinoma. Mod. Pathol. 19, 264–271.

Loblaw, D.A., Mendelson, D.S., Talcott, J.A., Virgo, K.S., Somerfield, M.R., Ben-Josef, E., Middleton, R., Porterfield, H., Sharp, S.A., Smith, T.J., et al. (2004). American Society of Clinical Oncology recommendations for the initial hormonal management of androgen-sensitive metastatic, recurrent, or progressive prostate cancer. J. Clin. Oncol. 22, 2927–2941.

Loening, A.M., Fenn, T.D., Wu, A.M., and Gambhir, S.S. (2006). Consensus guided mutagenesis of Renilla luciferase yields enhanced stability and light output. Protein Eng. Des. Sel. 19, 391–400.

Loew, R., Heinz, N., Hampf, M., Bujard, H., and Gossen, M. (2010). Improved Tet-responsive promoters with minimized background expression. BMC Biotechnol. 10, 81.

Logothetis, C.J., and Lin, S.-H. (2005). Osteoblasts in prostate cancer metastasis to bone. Nat. Rev. Cancer 5, 21–28.

Lopez-Pajares, V., Qu, K., Zhang, J., Webster, D., Barajas, B., Siprashvili, Z., Zarnegar, B., Boxer, L., Rios, E., Tao, S., et al. (2015). A LncRNA-MAF:MAFB Transcription Factor Network Regulates Epidermal Differentiation. Dev. Cell 32, 693–706.

Luo, J.-H., Yu, Y.P., Cieply, K., Lin, F., Deflavia, P., Dhir, R., Finkelstein, S., Michalopoulos, G., and Becich, M. (2002). Gene expression analysis of prostate cancers. Mol. Carcinog. 33, 25–35.

Luzzi, K.J., MacDonald, I.C., Schmidt, E.E., Kerkvliet, N., Morris, V.L., Chambers, A.F., and Groom, A.C. (1998). Multistep nature of metastatic inefficiency: dormancy of solitary cells after successful extravasation and limited survival of early micrometastases. Am. J. Pathol. 153, 865–873.

Lynch, C.C., Hikosaka, A., Acuff, H.B., Martin, M.D., Kawai, N., Singh, R.K., Vargo-Gogola, T.C., Begtrup, J.L., Peterson, T.E., Fingleton, B., et al. (2005). MMP-7 promotes prostate cancer-induced osteolysis via the solubilization of RANKL. Cancer Cell 7, 485–496.

MacLean, H.E., Kim, J.I., Glimcher, M.J., Wang, J., Kronenberg, H.M., and Glimcher, L.H. (2003). Absence of transcription factor c-maf causes abnormal terminal differentiation of hypertrophic chondrocytes during endochondral bone development. Dev. Biol. 262, 51–63.

Macleod, K.F., and Jacks, T. (1999). Insights into cancer from transgenic mouse models. J. Pathol. 187, 43–60.

Maeda, T., Alexander, C.M., and Friedl, A. (2004). Induction of Syndecan-1 Expression in Stromal Fibroblasts Promotes Proliferation of Human Breast Cancer Cells. Cancer Res. 64, 612–621.

Malladi, S., Macalinao, D.G., Jin, X., He, L., Basnet, H., Zou, Y., de Stanchina, E., and Massagué, J. (2016). Metastatic Latency and Immune Evasion through Autocrine Inhibition of WNT. Cell 165, 45–60.

Mani, S. a, Guo, W., Liao, M., Eaton, E.N., Ayyanan, A., Zhou, A.Y., Brooks, M., Reinhard, F., Zhang, C.C., Shipitsin, M., et al. (2008). The epithelial-mesenchymal transition generates cells with properties of stem cells. Cell 133, 704–715.

Marcelli, C., Yates, A.J., and Mundy, G.R. (1990). In vivo effects of human recombinant transforming growth factor β on bone turnover in normal mice. J. Bone Miner. Res. 5, 1087–1096.

Marchionni, L., Wilson, R.F., Wolff, A.C., Marinopoulos, S., Parmigiani, G., Bass, E.B., and Goodman, S.N. (2008). Systematic Review: Gene Expression Profiling Assays in Early-Stage Breast Cancer. Ann. Intern. Med. 148, 358.

Marker, P.C., Donjacour, A.A., Dahiya, R., and Cunha, G.R. (2003). Hormonal, cellular, and molecular control of prostatic development. Dev. Biol. 253, 165–174.

Martin, T.J. (2005). Osteoblast-derived PTHrP is a physiological regulator of bone formation. J. Clin. Invest. 115, 2322–2324.

Martin, M., and López-Tarruella, S. (2015). Optimizing Adjuvant Taxanes in Early Breast Cancer. J. Clin. Oncol. 33, 2334–2336.

Martin, P., Albagli, O., Poggi, M.C., Boulukos, K.E., and Pognonec, P. (2006). Development of a new bicistronic retroviral vector with strong IRES activity. BMC Biotechnol. 6, 4.

Marty, M., Cognetti, F., Maraninchi, D., Snyder, R., Mauriac, L., Tubiana-Hulin, M., Chan, S., Grimes, D., Antón, A., Lluch, A., et al. (2005). Randomized phase II trial of the efficacy and safety of trastuzumab combined with docetaxel in patients with human epidermal growth factor receptor 2-positive metastatic breast cancer administered as first-line treatment: the M77001 study group. J. Clin. Oncol. 23, 4265–4274.

Massagué, J., and Obenauf, A.C. (2016). Metastatic colonization by circulating tumour cells. Nature 529, 298–306.

Mateo, F., Arenas, E.J., Aguilar, H., Serra-Musach, J., de Garibay, G.R., Boni, J., Maicas, M., Du, S., Iorio, F., Herranz-Ors, C., et al. (2017). Stem cell-like transcriptional reprogramming mediates metastatic resistance to mTOR inhibition. Oncogene 36, 2737–2749.

McAllister, S.S., Gifford, A.M., Greiner, A.L., Kelleher, S.P., Saelzler, M.P., Ince, T.A., Reinhardt, F., Harris, L.N., Hylander, B.L., Repasky, E.A., et al. (2008). Systemic endocrine instigation

of indolent tumor growth requires osteopontin. Cell 133, 994–1005.
McKinney, T.D. (1972). Estrous Cycle in House Mice: Effects of Grouping, Preputial Gland Odors, and Handling. J. Mammal. 53, 391–393.
McNeal, J.E. (1988). Normal histology of the prostate. Am. J. Surg. Pathol. 12, 619–633.
Menter, D.G., Tucker, S.C., Kopetz, S., Sood, A.K., Crissman, J.D., and Honn, K. V. (2014). Platelets and cancer: a casual or causal relationship: revisited. Cancer Metastasis Rev. 33, 231–269.
Metzger, D., and Chambon, P. (2001). Site- and Time-Specific Gene Targeting in the Mouse. Methods 24, 71–80.
Metzger, D., Clifford, J., Chiba, H., and Chambon, P. (1995). Conditional site-specific recombination in mammalian cells using a ligand-dependent chimeric Cre recombinase. Proc. Natl. Acad. Sci. U. S. A. 92, 6991–6995.
Michigami, T., Shimizu, N., Williams, P.J., Niewolna, M., Dallas, S.L., Mundy, G.R., and Yoneda, T. (2000). Cell-cell contact between marrow stromal cells and myeloma cells via VCAM-1 and alpha(4)beta(1)-integrin enhances production of osteoclast-stimulating activity. Blood 96, 1953–1960.
Minn, A.J., Kang, Y., Serganova, I., Gupta, G.P., Giri, D.D., Doubrovin, M., Ponomarev, V., Gerald, W.L., Blasberg, R., and Massagué, J. (2005a). Distinct organ-specific metastatic potential of individual breast cancer cells and primary tumors. J. Clin. Invest. 115, 44–55.
Minn, A.J., Gupta, G.P., Siegel, P.M., Bos, P.D., Shu, W., Giri, D.D., Viale, A., Olshen, A.B., Gerald, W.L., and Massagué, J. (2005b). Genes that mediate breast cancer metastasis to lung. Nature 436, 518–524.
Minotti, G. (2004). Anthracyclines: Molecular Advances and Pharmacologic Developments in Antitumor Activity and Cardiotoxicity. Pharmacol. Rev. 56, 185–229.
Miyazaki, J., Takaki, S., Araki, K., Tashiro, F., Tominaga, A., Takatsu, K., and Yamamura, K. (1989). Expression vector system based on the chicken beta-actin promoter directs efficient production of interleukin-5. Gene 79, 269–277.
Mizuguchi, H., Xu, Z., Ishii-Watabe, A., Uchida, E., and Hayakawa, T. (2000). IRES-dependent second gene expression is significantly lower than cap-dependent first gene expression in a bicistronic vector. Mol. Ther. 1, 376–382.
Mohammad, K.S., Chen, C.G., Balooch, G., Stebbins, E., McKenna, C.R., Davis, H., Niewolna, M., Peng, X.H., Nguyen, D.H.N., Ionova-Martin, S.S., et al. (2009). Pharmacologic inhibition of the TGF-beta type I receptor kinase has anabolic and anti-catabolic effects on bone. PLoS One 4, e5275.
Mohammad, K.S., Javelaud, D., Fournier, P.G.J., Niewolna, M., McKenna, C.R., Peng, X.H., Duong, V., Dunn, L.K., Mauviel, A., and Guise, T.A. (2011). TGF-beta-RI kinase inhibitor SD-208 reduces the development and progression of melanoma bone metastases. Cancer Res. 71, 175–184.
Montagna, E., Maisonneuve, P., Rotmensz, N., Cancello, G., Iorfida, M., Balduzzi, A., Galimberti, V., Veronesi, P., Luini, A., Pruneri, G., et al. (2013). Heterogeneity of triple-negative breast cancer: histologic subtyping to inform the outcome. Clin. Breast Cancer 13, 31–39.
Monteiro, A.C., Leal, A.C., Gonçalves-Silva, T., Mercadante, A.C.T., Kestelman, F., Chaves, S.B., Azevedo, R.B., Monteiro, J.P., and Bonomo, A. (2013). T cells induce pre-metastatic osteolytic disease and help bone metastases establishment in a mouse model of metastatic breast cancer. PLoS One 8, e68171.
Morales, M., Arenas, E.J., Urosevic, J., Guiu, M., Fernández, E., Planet, E., Fenwick, R.B., Fernández-Ruiz, S., Salvatella, X., Reverter, D., et al. (2014). RARRES3 suppresses breast cancer lung metastasis by regulating adhesion and differentiation. EMBO Mol. Med. 6, 1–17.
Morito, N., Yoh, K., Fujioka, Y., Nakano, T., Shimohata, H., Hashimoto, Y., Yamada, A., Maeda,

A., Matsuno, F., Hata, H., et al. (2006). Overexpression of c-Maf contributes to T-cell lymphoma in both mice and human. Cancer Res. 66, 812–819.

Morito, N., Yoh, K., Maeda, A., Nakano, T., Fujita, A., Kusakabe, M., Hamada, M., Kudo, T., Yamagata, K., and Takahashi, S. (2011). A novel transgenic mouse model of the human multiple myeloma chromosomal translocation t(14;16)(q32;q23). Cancer Res. 71, 339–348.

Morony, S., Capparelli, C., Sarosi, I., Lacey, D.L., Dunstan, C.R., and Kostenuik, P.J. (2001). Osteoprotegerin inhibits osteolysis and decreases skeletal tumor burden in syngeneic and nude mouse models of experimental bone metastasis. Cancer Res. 61, 4432–4436.

Motohashi, H., Katsuoka, F., Shavit, J. a, Engel, J.D., and Yamamoto, M. (2000). Positive or negative MARE-dependent transcriptional regulation is determined by the abundance of small Maf proteins. Cell 103, 865–875.

Mueller, S.O., Clark, J.A., Myers, P.H., and Korach, K.S. (2002). Mammary gland development in adult mice requires epithelial and stromal estrogen receptor alpha. Endocrinology 143, 2357–2365.

Muller, W.J., Sinn, E., Pattengale, P.K., Wallace, R., and Leder, P. (1988). Single-step induction of mammary adenocarcinoma in transgenic mice bearing the activated c-neu oncogene. Cell 54, 105–115.

Müller, A., Homey, B., Soto, H., Ge, N., Catron, D., Buchanan, M.E., McClanahan, T., Murphy, E., Yuan, W., Wagner, S.N., et al. (2001). Involvement of chemokine receptors in breast cancer metastasis. Nature 410, 50–56.

Mundy, G.R. (2002). Metastasis to bone: causes, consequences and therapeutic opportunities. Nat. Rev. Cancer 2, 584–593.

Mundy, G.R., Chen, D., Zhao, M., Dallas, S., Xu, C., and Harris, S. (2001). Growth regulatory factors and bone. Rev. Endocr. Metab. Disord. 2, 105–115.

Murakami, Y.I., Yatabe, Y., Sakaguchi, T., Sasaki, E., Yamashita, Y., Morito, N., Yoh, K., Fujioka, Y., Matsuno, F., Hata, H., et al. (2007a). c-Maf Expression in Angioimmunoblastic T-cell Lymphoma. Am. J. Surg. Pathol. 31, 1695–1702.

Murakami, Y.I., Yatabe, Y., Sakaguchi, T., Sasaki, E., Yamashita, Y., Morito, N., Yoh, K., Fujioka, Y., Matsuno, F., Hata, H., et al. (2007b). c-Maf Expression in Angioimmunoblastic T-cell Lymphoma. Am. J. Surg. Pathol. 31, 1695–1702.

Nelson, J.B., Hedican, S.P., George, D.J., Reddi, A.H., Piantadosi, S., Eisenberger, M.A., and Simons, J.W. (1995). Identification of endothelin-1 in the pathophysiology of metastatic adenocarcinoma of the prostate. Nat. Med. 1, 944–949.

Nelson, J.B., Nabulsi, A.A., Vogelzang, N.J., Breul, J., Zonnenberg, B.A., Daliani, D.D., Schulman, C.C., and Carducci, M.A. (2003). Suppression of prostate cancer induced bone remodeling by the endothelin receptor A antagonist atrasentan. J. Urol. 169, 1143–1149.

Nemeth, J.A., Harb, J.F., Barroso, U., He, Z., Grignon, D.J., and Cher, M.L. (1999). Severe combined immunodeficient-hu model of human prostate cancer metastasis to human bone. Cancer Res. 59, 1987–1993.

Ng, T.H.S., Britton, G.J., Hill, E. V., Verhagen, J., Burton, B.R., and Wraith, D.C. (2013). Regulation of adaptive immunity; the role of interleukin-10. Front. Immunol. 4, 129.

Nguyen, D.X., Bos, P.D., and Massagué, J. (2009). Metastasis: from dissemination to organ-specific colonization. Nat. Rev. Cancer 9, 274–284.

Nielsen, T.O., Parker, J.S., Leung, S., Voduc, D., Ebbert, M., Vickery, T., Davies, S.R., Snider, J., Stijleman, I.J., Reed, J., et al. (2010). A Comparison of PAM50 Intrinsic Subtyping with Immunohistochemistry and Clinical Prognostic Factors in Tamoxifen-Treated Estrogen Receptor-Positive Breast Cancer. Clin. Cancer Res. 16, 5222–5232.

Nilsson, S., Mäkelä, S., Treuter, E., Tujague, M., Thomsen, J., Andersson, G., Enmark, E., Pettersson, K., Warner, M., and Gustafsson, J.A. (2001). Mechanisms of estrogen action. Physiol.

Rev. 81, 1535–1565.
Nishizawa, M., Kataoka, K., Goto, N., Fujiwara, K.T., and Kawai, S. (1989). v-maf, a viral oncogene that encodes a "leucine zipper" motif. Proc. Natl. Acad. Sci. U. S. A. 86, 7711–7715.
Nishizawa, M., Kataoka, K., and Vogt, P.K. (2003). MafA has strong cell transforming ability but is a weak transactivator. Oncogene 22, 7882–7890.
Noy, R., and Pollard, J.W. (2014). Tumor-Associated Macrophages: From Mechanisms to Therapy. Immunity 41, 49–61.
O'Connell, P., Pekkel, V., Fuqua, S. a, Osborne, C.K., Clark, G.M., and Allred, D.C. (1998). Analysis of loss of heterozygosity in 399 premalignant breast lesions at 15 genetic loci. J. Natl. Cancer Inst. 90, 697–703.
Oakes, S.R., Hilton, H.N., and Ormandy, C.J. (2006). The alveolar switch: coordinating the proliferative cues and cell fate decisions that drive the formation of lobuloalveoli from ductal epithelium. Breast Cancer Res. 8, 207.
Oesterreich, S., Allredl, D.C., Mohsin, S.K., Zhang, Q., Wong, H., Lee, a V, Osborne, C.K., and O'Connell, P. (2001). High rates of loss of heterozygosity on chromosome 19p13 in human breast cancer. Br. J. Cancer 84, 493–498.
Ornitz, D.M., Moreadith, R.W., and Leder, P. (1991). Binary system for regulating transgene expression in mice: targeting int-2 gene expression with yeast GAL4/UAS control elements. Proc. Natl. Acad. Sci. U. S. A. 88, 698–702.
Ory, S., Brazier, H., Pawlak, G., and Blangy, A. (2008). Rho GTPases in osteoclasts: orchestrators of podosome arrangement. Eur. J. Cell Biol. 87, 469–477.
Osborne, C.K., and Schiff, R. (2011). Mechanisms of Endocrine Resistance in Breast Cancer. Annu. Rev. Med. 62, 233–247.
Ottewell, P.D., Monkkonen, H., Jones, M., Lefley, D. V, Coleman, R.E., and Holen, I. (2008). Antitumor Effects of Doxorubicin Followed by Zoledronic Acid in a Mouse Model of Breast Cancer. JNCI J. Natl. Cancer Inst. 100, 1167–1178.
Owens, T.W., and Naylor, M.J. (2013). Breast cancer stem cells. Front. Physiol. 4 AUG, 1–10.
Padua, D., Zhang, X.H.-F., Wang, Q., Nadal, C., Gerald, W.L., Gomis, R.R., and Massagué, J. (2008). TGFbeta primes breast tumors for lung metastasis seeding through angiopoietin-like 4. Cell 133, 66–77.
Paget, S. (1889). THE DISTRIBUTION OF SECONDARY GROWTHS IN CANCER OF THE BREAST. Lancet 133, 571–573.
Paik, S., Shak, S., Tang, G., Kim, C., Baker, J., Cronin, M., Baehner, F.L., Walker, M.G., Watson, D., Park, T., et al. (2004). A multigene assay to predict recurrence of tamoxifen-treated, node-negative breast cancer. N. Engl. J. Med. 351, 2817–2826.
Paik, S., Tang, G., Shak, S., Kim, C., Baker, J., Kim, W., Cronin, M., Baehner, F.L., Watson, D., Bryant, J., et al. (2006). Gene expression and benefit of chemotherapy in women with node-negative, estrogen receptor-positive breast cancer. J. Clin. Oncol. 24, 3726–3734.
Palumbo, J.S., Talmage, K.E., Massari, J. V, La Jeunesse, C.M., Flick, M.J., Kombrinck, K.W., Jirousková, M., and Degen, J.L. (2005). Platelets and fibrin(ogen) increase metastatic potential by impeding natural killer cell-mediated elimination of tumor cells. Blood 105, 178–185.
Parfitt, A.M. (1994). Osteonal and hemi-osteonal remodeling: the spatial and temporal framework for signal traffic in adult human bone. J. Cell. Biochem. 55, 273–286.
Parker, C., Nilsson, S., Heinrich, D., Helle, S.I., O'Sullivan, J.M., Fosså, S.D., Chodacki, A., Wiechno, P., Logue, J., Seke, M., et al. (2013). Alpha emitter radium-223 and survival in metastatic prostate cancer. N. Engl. J. Med. 369, 213–223.
Parker, J.S., Mullins, M., Cheang, M.C.U., Leung, S., Voduc, D., Vickery, T., Davies, S., Fauron, C., He, X., Hu, Z., et al. (2009). Supervised risk predictor of breast cancer based on intrinsic subtypes. J. Clin. Oncol. 27, 1160–1167.

Paterson, A.H., Powles, T.J., Kanis, J.A., McCloskey, E., Hanson, J., and Ashley, S. (1993). Double-blind controlled trial of oral clodronate in patients with bone metastases from breast cancer. J. Clin. Oncol. 11, 59–65.

Pavlovic, M., Arnal-Estapé, A., Rojo, F., Bellmunt, A., Tarragona, M., Guiu, M., Planet, E., Garcia-Albéniz, X., Morales, M., Urosevic, J., et al. (2015). Enhanced MAF Oncogene Expression and Breast Cancer Bone Metastasis. J. Natl. Cancer Inst. 107, djv256.

Peinado, H., Alečković, M., Lavotshkin, S., Matei, I., Costa-Silva, B., Moreno-Bueno, G., Hergueta-Redondo, M., Williams, C., García-Santos, G., Ghajar, C., et al. (2012). Melanoma exosomes educate bone marrow progenitor cells toward a pro-metastatic phenotype through MET. Nat. Med. 18, 883–891.

Pellegrino, S., Ronda, L., Annoni, C., Contini, A., Erba, E., Gelmi, M.L., Piano, R., Paredi, G., Mozzarelli, A., and Bettati, S. (2014). Molecular insights into dimerization inhibition of c-Maf transcription factor. Biochim. Biophys. Acta - Proteins Proteomics 1844, 2108–2115.

Perou, C.M., Sørlie, T., Eisen, M.B., van de Rijn, M., Jeffrey, S.S., Rees, C. a, Pollack, J.R., Ross, D.T., Johnsen, H., Akslen, L. a, et al. (2000). Molecular portraits of human breast tumours. Nature 406, 747–752.

Pfeilschifter, J., and Mundy, G.R. (1987). Modulation of type beta transforming growth factor activity in bone cultures by osteotropic hormones. Proc. Natl. Acad. Sci. U. S. A. 84, 2024–2028.

Piccart-Gebhart, M., Holmes, E., Baselga, J., de Azambuja, E., Dueck, A.C., Viale, G., Zujewski, J.A., Goldhirsch, A., Armour, A., Pritchard, K.I., et al. (2016). Adjuvant Lapatinib and Trastuzumab for Early Human Epidermal Growth Factor Receptor 2-Positive Breast Cancer: Results From the Randomized Phase III Adjuvant Lapatinib and/or Trastuzumab Treatment Optimization Trial. J. Clin. Oncol. 34, 1034–1042.

Piccart-Gebhart, M.J., Procter, M., Leyland-Jones, B., Goldhirsch, A., Untch, M., Smith, I., Gianni, L., Baselga, J., Bell, R., Jackisch, C., et al. (2005). Trastuzumab after adjuvant chemotherapy in HER2-positive breast cancer. N. Engl. J. Med. 353, 1659–1672.

Porret, A., Mérillat, A.-M., Guichard, S., Beermann, F., and Hummler, E. (2006). Tissue-specific transgenic and knockout mice. Methods Mol. Biol. 337, 185–205.

Potten, C.S., and Morris, R.J. (1988). Epithelial stem cells in vivo. J. Cell Sci. Suppl. 10, 45–62.

Pouponnot, C., Sii-Felice, K., Hmitou, I., Rocques, N., Lecoin, L., Druillennec, S., Felder-Schmittbuhl, M.-P., and Eychène, A. (2006). Cell context reveals a dual role for Maf in oncogenesis. Oncogene 25, 1299–1310.

Pozzi, S., Vallet, S., Mukherjee, S., Cirstea, D., Vaghela, N., Santo, L., Rosen, E., Ikeda, H., Okawa, Y., Kiziltepe, T., et al. (2009). High-Dose Zoledronic Acid Impacts Bone Remodeling with Effects on Osteoblastic Lineage and Bone Mechanical Properties. Clin. Cancer Res. 15, 5829–5839.

Prat, A., Parker, J.S., Karginova, O., Fan, C., Livasy, C., Herschkowitz, J.I., He, X., and Perou, C.M. (2010). Phenotypic and molecular characterization of the claudin-low intrinsic subtype of breast cancer. Breast Cancer Res. 12, R68.

Pratap, J., Imbalzano, K.M., Underwood, J.M., Cohet, N., Gokul, K., Akech, J., van Wijnen, A.J., Stein, J.L., Imbalzano, A.N., Nickerson, J.A., et al. (2009). Ectopic runx2 expression in mammary epithelial cells disrupts formation of normal acini structure: implications for breast cancer progression. Cancer Res. 69, 6807–6814.

Prins, G.S., and Putz, O. (2008). Molecular signaling pathways that regulate prostate gland development. Differentiation. 76, 641–659.

Pritchard, K.I., Rolski, J., Papai, Z., Mauriac, L., Cardoso, F., Chang, J., Panasci, L., Ianuli, C., Kahan, Z., Fukase, K., et al. (2010). Results of a phase II study comparing three dosing regimens of fulvestrant in postmenopausal women with advanced breast cancer (FINDER2). Breast Cancer Res. Treat. 123, 453–461.

Psaila, B., and Lyden, D. (2009). The metastatic niche: adapting the foreign soil. Nat. Rev. Cancer 9, 285–293.

Rabbani, S.A., Desjardins, J., Bell, A.W., Banville, D., Mazar, A., Henkin, J., and Goltzman, D. (1990). An amino-terminal fragment of urokinase isolated from a prostate cancer cell line (PC-3) is mitogenic for osteoblast-like cells. Biochem. Biophys. Res. Commun. 173, 1058–1064.

Rabbani, S.A., Valentino, M.-L., Arakelian, A., Ali, S., and Boschelli, F. (2010). SKI-606 (Bosutinib) blocks prostate cancer invasion, growth, and metastasis in vitro and in vivo through regulation of genes involved in cancer growth and skeletal metastasis. Mol. Cancer Ther. 9, 1147–1157.

Rabinovich, B. a, Ye, Y., Etto, T., Chen, J.Q., Levitsky, H.I., Overwijk, W.W., Cooper, L.J.N., Gelovani, J., and Hwu, P. (2008). Visualizing fewer than 10 mouse T cells with an enhanced firefly luciferase in immunocompetent mouse models of cancer. Proc. Natl. Acad. Sci. U. S. A. 105, 14342–14346.

Richardson, C.D., Ray, G.J., DeWitt, M.A., Curie, G.L., and Corn, J.E. (2016). Enhancing homology-directed genome editing by catalytically active and inactive CRISPR-Cas9 using asymmetric donor DNA. Nat. Biotechnol. 34, 339–344.

Riihimäki, M., Hemminki, A., Fallah, M., Thomsen, H., Sundquist, K., Sundquist, J., and Hemminki, K. (2014). Metastatic sites and survival in lung cancer. Lung Cancer 86, 78–84.

Roato, I., Grano, M., Brunetti, G., Colucci, S., Mussa, A., Bertetto, O., and Ferracini, R. (2005). Mechanisms of spontaneous osteoclastogenesis in cancer with bone involvement. FASEB J. 19, 228–230.

Robertson, B.H., Grubman, M.J., Weddell, G.N., Moore, D.M., Welsh, J.D., Fischer, T., Dowbenko, D.J., Yansura, D.G., Small, B., and Kleid, D.G. (1985). Nucleotide and amino acid sequence coding for polypeptides of foot-and-mouth disease virus type A12. J. Virol. 54, 651–660.

Robey, P.G., Fedarko, N.S., Hefferan, T.E., Bianco, P., Vetter, U.K., Grzesik, W., Friedenstein, A., Van der Pluijm, G., Mintz, K.P., and Young, M.F. (1993). Structure and molecular regulation of bone matrix proteins. J. Bone Miner. Res. 8 Suppl 2, S483-7.

Robinson, G.W. (2007). Cooperation of signalling pathways in embryonic mammary gland development. Nat. Rev. Genet. 8, 963–972.

Rocques, N., Abou Zeid, N., Sii-Felice, K., Lecoin, L., Felder-Schmittbuhl, M.-P., Eychène, A., and Pouponnot, C. (2007). GSK-3-mediated phosphorylation enhances Maf-transforming activity. Mol. Cell 28, 584–597.

Roddam, A.W., Allen, N.E., Appleby, P., Key, T.J., Ferrucci, L., Carter, H.B., Metter, E.J., Chen, C., Weiss, N.S., Fitzpatrick, A., et al. (2008). Insulin-like growth factors, their binding proteins, and prostate cancer risk: analysis of individual patient data from 12 prospective studies. Ann. Intern. Med. 149, 461–471, W83-8.

Rohde, M., and Mayer, H. (2007). Exocytotic process as a novel model for mineralization by osteoblasts in vitro and in vivo determined by electron microscopic analysis. Calcif. Tissue Int. 80, 323–336.

Rosen, L.S., Gordon, D.H., Dugan, W., Major, P., Eisenberg, P.D., Provencher, L., Kaminski, M., Simeone, J., Seaman, J., Chen, B.-L., et al. (2004). Zoledronic acid is superior to pamidronate for the treatment of bone metastases in breast carcinoma patients with at least one osteolytic lesion. Cancer 100, 36–43.

Ross, F.P. (2006). M-CSF, c-Fms, and signaling in osteoclasts and their precursors. Ann. N. Y. Acad. Sci. 1068, 110–116.

Rowinsky, E.K. (1997). The development and clinical utility of the taxane class of antimicrotubule chemotherapy agents. Annu. Rev. Med. 48, 353–374.

Rowlands, M., Gunnell, D., Harris, R., Vatten, L.J., Holly, J.M.P., and Martin, R.M. (2009). Circulating insulin-like growth factor peptides and prostate cancer risk: A systematic review and meta-analysis. Int. J. Cancer 124, 2416–2429.

Rudas, M., Neumayer, R., Gnant, M.F.X., Mittelböck, M., Jakesz, R., and Reiner, A. (1997). p53 Protein expression, cell proliferation and steroid hormone receptors in ductal and lobular in situ carcinomas of the breast. Eur. J. Cancer Part A 33, 39–44.

Rugo, H.S., Rumble, R.B., Macrae, E., Barton, D.L., Connolly, H.K., Dickler, M.N., Fallowfield, L., Fowble, B., Ingle, J.N., Jahanzeb, M., et al. (2016). Endocrine Therapy for Hormone Receptor-Positive Metastatic Breast Cancer: American Society of Clinical Oncology Guideline. J. Clin. Oncol. 34, 3069–3103.

Russell, R.G.G. (2006). Bisphosphonates: from bench to bedside. Ann. N. Y. Acad. Sci. 1068, 367–401.

Russell, D.W., and Wilson, J.D. (1994). Steroid 5 alpha-reductase: two genes/two enzymes. Annu. Rev. Biochem. 63, 25–61.

Russell, R.G.G., and Rogers, M.J. (1999). Bisphosphonates: from the laboratory to the clinic and back again. Bone 25, 97–106.

Russo, J., and Russo, I.H. (2004). Development of the human breast. Maturitas 49, 2–15.

Ryan, M.D., and Drew, J. (1994). Foot-and-mouth disease virus 2A oligopeptide mediated cleavage of an artificial polyprotein. EMBO J. 13, 928–933.

Saarto, T., Blomqvist, C., Virkkunen, P., and Elomaa, I. (2001). Adjuvant Clodronate Treatment Does Not Reduce the Frequency of Skeletal Metastases in Node-Positive Breast Cancer Patients: 5-Year Results of a Randomized Controlled Trial. J. Clin. Oncol. 19, 10–17.

Sabatier, R., Finetti, P., Guille, A., Adelaide, J., Chaffanet, M., Viens, P., Birnbaum, D., and Bertucci, F. (2014). Claudin-low breast cancers: clinical, pathological, molecular and prognostic characterization. Mol. Cancer 13, 228.

Saidak, Z., Boudot, C., Abdoune, R., Petit, L., Brazier, M., Mentaverri, R., and Kamel, S. (2009). Extracellular calcium promotes the migration of breast cancer cells through the activation of the calcium sensing receptor. Exp. Cell Res. 315, 2072–2080.

Saito, H., Tsunenari, T., Onuma, E., Sato, K., Ogata, E., and Yamada-Okabe, H. (2005). Humanized monoclonal antibody against parathyroid hormone-related protein suppresses osteolytic bone metastasis of human breast cancer cells derived from MDA-MB-231. Anticancer Res. 25, 3817–3823.

Sakai, M., Serria, M.S., Ikeda, H., Yoshida, K., Imaki, J., and Nishi, S. (2001). Regulation of c-maf gene expression by Pax6 in cultured cells. Nucleic Acids Res. 29, 1228–1237.

Sakamoto, K., Schmidt, J.W., and Wagner, K.-U. (2012). Generation of a novel MMTV-tTA transgenic mouse strain for the targeted expression of genes in the embryonic and postnatal mammary gland. PLoS One 7, e43778.

Sandberg, A.A. (1980). Endocrine control and physiology of the prostate. Prostate 1, 169–184.

Sanders, J.L., Chattopadhyay, N., Kifor, O., Yamaguchi, T., Butters, R.R., and Brown, E.M. (2000). Extracellular calcium-sensing receptor expression and its potential role in regulating parathyroid hormone-related peptide secretion in human breast cancer cell lines. Endocrinology 141, 4357–4364.

Sauer, B., and Henderson, N. (1988). Site-specific DNA recombination in mammalian cells by the Cre recombinase of bacteriophage P1. Proc. Natl. Acad. Sci. 85, 5166–5170.

Sauer, B., and Henderson, N. (1989). Cre-stimulated recombination at loxP-containing DNA sequences placed into the mammalian genome. Nucleic Acids Res. 17, 147–161.

Schoppmann, S.F., Birner, P., Stöckl, J., Kalt, R., Ullrich, R., Caucig, C., Kriehuber, E., Nagy, K., Alitalo, K., and Kerjaschki, D. (2002). Tumor-associated macrophages express lymphatic endothelial growth factors and are related to peritumoral lymphangiogenesis. Am. J. Pathol.

161, 947–956.
Seidl, S., Kaufmann, H., and Drach, J. (2003). New insights into the pathophysiology of multiple myeloma. Lancet. Oncol. 4, 557–564.
Senaratne, S.G., Pirianov, G., Mansi, J.L., Arnett, T.R., and Colston, K.W. (2000). Bisphosphonates induce apoptosis in human breast cancer cell lines. Br. J. Cancer 82, 1459–1468.
Senkus, E., Kyriakides, S., Ohno, S., Penault-Llorca, F., Poortmans, P., Rutgers, E., Zackrisson, S., Cardoso, F., and ESMO Guidelines Committee (2015). Primary breast cancer: ESMO Clinical Practice Guidelines for diagnosis, treatment and follow-up. Ann. Oncol. Off. J. Eur. Soc. Med. Oncol. 26 Suppl 5, v8-30.
Seoane, J., and Gomis, R.R. (2017). TGF-β Family Signaling in Tumor Suppression and Cancer Progression. Cold Spring Harb. Perspect. Biol. a022277.
Sethi, N., Dai, X., Winter, C.G., and Kang, Y. (2011). Tumor-derived JAGGED1 promotes osteolytic bone metastasis of breast cancer by engaging notch signaling in bone cells. Cancer Cell 19, 192–205.
Shcherbo, D., Merzlyak, E.M., Chepurnykh, T. V, Fradkov, A.F., Ermakova, G. V, Solovieva, E.A., Lukyanov, K.A., Bogdanova, E.A., Zaraisky, A.G., Lukyanov, S., et al. (2007). Bright far-red fluorescent protein for whole-body imaging. Nat. Methods 4, 741–746.
Shen, M.M., and Abate-Shen, C. (2010). Molecular genetics of prostate cancer: new prospects for old challenges. Genes Dev. 24, 1967–2000.
Shevde, N.K., Bendixen, A.C., Dienger, K.M., and Pike, J.W. (2000). Estrogens suppress RANK ligand-induced osteoclast differentiation via a stromal cell independent mechanism involving c-Jun repression. Proc. Natl. Acad. Sci. 97, 7829–7834.
Siegel, R.L., Miller, K.D., and Jemal, A. (2016). Cancer Statistics , 2016. 66, 7–30.
Siegel, R.L., Miller, K.D., and Jemal, A. (2017). Cancer statistics, 2015. CA. Cancer J. Clin. 65, 5–29.
Simonet, W.S., Lacey, D.L., Dunstan, C.R., Kelley, M., Chang, M.S., Lüthy, R., Nguyen, H.Q., Wooden, S., Bennett, L., Boone, T., et al. (1997). Osteoprotegerin: a novel secreted protein involved in the regulation of bone density. Cell 89, 309–319.
Simpson, E.R. (2003). Sources of estrogen and their importance. J. Steroid Biochem. Mol. Biol. 86, 225–230.
Singletary, S.E., Allred, C., Ashley, P., Bassett, L.W., Berry, D., Bland, K.I., Borgen, P.I., Clark, G., Edge, S.B., Hayes, D.F., et al. (2002). Revision of the American Joint Committee on Cancer staging system for breast cancer. J. Clin. Oncol. 20, 3628–3636.
Slamon, D., Eiermann, W., Robert, N., Pienkowski, T., Martin, M., Press, M., Mackey, J., Glaspy, J., Chan, A., Pawlicki, M., et al. (2011). Adjuvant trastuzumab in HER2-positive breast cancer. N. Engl. J. Med. 365, 1273–1283.
Slamon, D.J., Clark, G.M., Wong, S.G., Levin, W.J., Ullrich, A., and McGuire, W.L. (1987). Human breast cancer: correlation of relapse and survival with amplification of the HER-2/neu oncogene. Science 235, 177–182.
Slamon, D.J., Godolphin, W., Jones, L.A., Holt, J.A., Wong, S.G., Keith, D.E., Levin, W.J., Stuart, S.G., Udove, J., and Ullrich, A. (1989). Studies of the HER-2/neu proto-oncogene in human breast and ovarian cancer. Science 244, 707–712.
Slamon, D.J., Leyland-Jones, B., Shak, S., Fuchs, H., Paton, V., Bajamonde, A., Fleming, T., Eiermann, W., Wolter, J., Pegram, M., et al. (2001). Use of chemotherapy plus a monoclonal antibody against HER2 for metastatic breast cancer that overexpresses HER2. N. Engl. J. Med. 344, 783–792.
Smalley, M., and Ashworth, A. (2003). Stem cells and breast cancer: A field in transit. Nat. Rev. Cancer 3, 832–844.
Smith, M.C.P., Luker, K.E., Garbow, J.R., Prior, J.L., Jackson, E., Piwnica-Worms, D., and Luker,

G.D. (2004). CXCR4 regulates growth of both primary and metastatic breast cancer. Cancer Res. 64, 8604–8612.

Smith, M.R., Saad, F., Coleman, R., Shore, N., Fizazi, K., Tombal, B., Miller, K., Sieber, P., Karsh, L., Damião, R., et al. (2012). Denosumab and bone-metastasis-free survival in men with castration-resistant prostate cancer: results of a phase 3, randomised, placebo-controlled trial. Lancet 379, 39–46.

Soni, A., Ren, Z., Hameed, O., Chanda, D., Morgan, C.J., Siegal, G.P., and Wei, S. (2015). Breast cancer subtypes predispose the site of distant metastases. Am. J. Clin. Pathol. 143, 471–478.

Soriano, P. (1999). Generalized lacZ expression with the ROSA26 Cre reporter strain. Nat. Genet. 21, 70–71.

Sorlie, T., Tibshirani, R., Parker, J., Hastie, T., Marron, J.S., Nobel, A., Deng, S., Johnsen, H., Pesich, R., Geisler, S., et al. (2003). Repeated observation of breast tumor subtypes in independent gene expression data sets. Proc. Natl. Acad. Sci. U. S. A. 100, 8418–8423.

Sørlie, T., Perou, C.M., Tibshirani, R., Aas, T., Geisler, S., Johnsen, H., Hastie, T., Eisen, M.B., van de Rijn, M., Jeffrey, S.S., et al. (2001). Gene expression patterns of breast carcinomas distinguish tumor subclasses with clinical implications. Proc. Natl. Acad. Sci. U. S. A. 98, 10869–10874.

Sosa, M.S., Bragado, P., and Aguirre-Ghiso, J.A. (2014). Mechanisms of disseminated cancer cell dormancy: an awakening field. Nat. Rev. Cancer 14, 611–622.

Sotiriou, C., and Pusztai, L. (2009). Gene-Expression Signatures in Breast Cancer. N. Engl. J. Med. 360, 790–800.

Sparano, J.A., and Paik, S. (2008). Development of the 21-gene assay and its application in clinical practice and clinical trials. J. Clin. Oncol. 26, 721–728.

Sparano, J.A., Wang, M., Martino, S., Jones, V., Perez, E.A., Saphner, T., Wolff, A.C., Sledge, G.W., Wood, W.C., and Davidson, N.E. (2008). Weekly Paclitaxel in the Adjuvant Treatment of Breast Cancer. N. Engl. J. Med. 358, 1663–1671.

Sparano, J.A., Gray, R.J., Makower, D.F., Pritchard, K.I., Albain, K.S., Hayes, D.F., Geyer, C.E., Dees, E.C., Perez, E.A., Olson, J.A., et al. (2015). Prospective Validation of a 21-Gene Expression Assay in Breast Cancer. N. Engl. J. Med. 373, 2005–2014.

Sterling, J.A., Oyajobi, B.O., Grubbs, B., Padalecki, S.S., Munoz, S.A., Gupta, A., Story, B., Zhao, M., and Mundy, G.R. (2006). The hedgehog signaling molecule Gli2 induces parathyroid hormone-related peptide expression and osteolysis in metastatic human breast cancer cells. Cancer Res. 66, 7548–7553.

Sternlicht, M.D. (2005). Key stages in mammary gland development: The cues that regulate ductal branching morphogenesis. Breast Cancer Res. 8, 201.

Stone, K.R., Mickey, D.D., Wunderli, H., Mickey, G.H., and Paulson, D.F. (1978). Isolation of a human prostate carcinoma cell line (DU 145). Int. J. Cancer 21, 274–281.

Stopeck, A.T., Lipton, A., Body, J.-J., Steger, G.G., Tonkin, K., de Boer, R.H., Lichinitser, M., Fujiwara, Y., Yardley, D.A., Viniegra, M., et al. (2010). Denosumab compared with zoledronic acid for the treatment of bone metastases in patients with advanced breast cancer: a randomized, double-blind study. J. Clin. Oncol. 28, 5132–5139.

Sturge, J., Caley, M.P., and Waxman, J. (2011). Bone metastasis in prostate cancer: emerging therapeutic strategies. Nat. Rev. Clin. Oncol. 8, 357–368.

Suda, T., Takahashi, N., Udagawa, N., Jimi, E., Gillespie, M.T., and Martin, T.J. (1999). Modulation of osteoclast differentiation and function by the new members of the tumor necrosis factor receptor and ligand families. Endocr. Rev. 20, 345–357.

Sun, Y.-X., Schneider, A., Jung, Y., Wang, J., Dai, J., Wang, J., Cook, K., Osman, N.I., Koh-Paige, A.J., Shim, H., et al. (2005). Skeletal localization and neutralization of the SDF-1(CXCL12)/CXCR4 axis blocks prostate cancer metastasis and growth in osseous sites in vivo. J. Bone

Miner. Res. 20, 318–329.

Sun, Y.-X., Fang, M., Wang, J., Cooper, C.R., Pienta, K.J., and Taichman, R.S. (2007). Expression and activation of alpha v beta 3 integrins by SDF-1/CXC12 increases the aggressiveness of prostate cancer cells. Prostate 67, 61–73.

Suzuki, A., Lu, J., Kusakai, G., Kishimoto, A., Ogura, T., and Esumi, H. (2004). ARK5 is a tumor invasion-associated factor downstream of Akt signaling. Mol. Cell. Biol. 24, 3526–3535.

Suzuki, A., Iida, S., Kato-Uranishi, M., Tajima, E., Zhan, F., Hanamura, I., Huang, Y., Ogura, T., Takahashi, S., Ueda, R., et al. (2005). ARK5 is transcriptionally regulated by the Large-MAF family and mediates IGF-1-induced cell invasion in multiple myeloma: ARK5 as a new molecular determinant of malignant multiple myeloma. Oncogene 24, 6936–6944.

Swain, S.M., Baselga, J., Kim, S.-B., Ro, J., Semiglazov, V., Campone, M., Ciruelos, E., Ferrero, J.-M., Schneeweiss, A., Heeson, S., et al. (2015). Pertuzumab, trastuzumab, and docetaxel in HER2-positive metastatic breast cancer. N. Engl. J. Med. 372, 724–734.

Takagaki, K., Takashima, T., Onoda, N., Tezuka, K., Noda, E., Kawajiri, H., Ishikawa, T., and Hirakawa, K. (2012). Parathyroid hormone-related protein expression, in combination with nodal status, predicts bone metastasis and prognosis of breast cancer patients. Exp. Ther. Med. 3, 963–968.

Takalkar, A., Adams, S., and Subbiah, V. (2014). Radium-223 dichloride bone-targeted alpha particle therapy for hormone-refractory breast cancer metastatic to bone. Exp. Hematol. Oncol. 3, 23.

Tannock, I.F., de Wit, R., Berry, W.R., Horti, J., Pluzanska, A., Chi, K.N., Oudard, S., Théodore, C., James, N.D., Turesson, I., et al. (2004). Docetaxel plus Prednisone or Mitoxantrone plus Prednisone for Advanced Prostate Cancer. N. Engl. J. Med. 351, 1502–1512.

Tarragona, M., Pavlovic, M., Arnal-Estapé, A., Urosevic, J., Morales, M., Guiu, M., Planet, E., González-Suárez, E., and Gomis, R.R. (2012). Identification of NOG as a Specific Breast Cancer Bone Metastasis-supporting Gene. J. Biol. Chem. 287, 21346–21355.

Taylor, B.S., Schultz, N., Hieronymus, H., Gopalan, A., Xiao, Y., Carver, B.S., Arora, V.K., Kaushik, P., Cerami, E., Reva, B., et al. (2010). Integrative Genomic Profiling of Human Prostate Cancer. Cancer Cell 18, 11–22.

Taylor, C.W., Green, S., Dalton, W.S., Martino, S., Rector, D., Ingle, J.N., Robert, N.J., Budd, G.T., Paradelo, J.C., Natale, R.B., et al. (1998). Multicenter randomized clinical trial of goserelin versus surgical ovariectomy in premenopausal patients with receptor-positive metastatic breast cancer: an intergroup study. J. Clin. Oncol. 16, 994–999.

Teitelbaum, S.L. (2000). Bone resorption by osteoclasts. Science 289, 1504–1508.

Thalmann, G.N., Anezinis, P.E., Chang, S.M., Zhau, H.E., Kim, E.E., Hopwood, V.L., Pathak, S., von Eschenbach, A.C., and Chung, L.W. (1994). Androgen-independent cancer progression and bone metastasis in the LNCaP model of human prostate cancer. Cancer Res. 54, 2577–2581.

Thiery, J.P. (2003). Epithelial-mesenchymal transitions in development and pathologies. Curr. Opin. Cell Biol. 15, 740–746.

Thomas, R.J., Guise, T.A., Yin, J.J., Elliott, J., Horwood, N.J., Martin, T.J., and Gillespie, M.T. (1999a). Breast cancer cells interact with osteoblasts to support osteoclast formation. Endocrinology 140, 4451–4458.

Thomas, T., Gori, F., Khosla, S., Jensen, M.D., Burguera, B., and Riggs, B.L. (1999b). Leptin acts on human marrow stromal cells to enhance differentiation to osteoblasts and to inhibit differentiation to adipocytes. Endocrinology 140, 1630–1638.

Tiede, B., and Kang, Y. (2011). From milk to malignancy: the role of mammary stem cells in development, pregnancy and breast cancer. Cell Res. 21, 245–257.

Timms, B.G. (2008). Prostate development: a historical perspective. Differentiation. 76, 565–577.

Toft, D., and Gorski, J. (1966). A receptor molecule for estrogens: isolation from the rat uterus and preliminary characterization. Proc. Natl. Acad. Sci. U. S. A. 55, 1574–1581.

Trichas, G., Begbie, J., and Srinivas, S. (2008). Use of the viral 2A peptide for bicistronic expression in transgenic mice. BMC Biol. 6, 40.

Truss, M., Bartsch, J., Schelbert, A., Haché, R.J., and Beato, M. (1995). Hormone induces binding of receptors and transcription factors to a rearranged nucleosome on the MMTV promoter in vivo. EMBO J. 14, 1737–1751.

Turashvili, G., Bouchal, J., Burkadze, G., and Kolár, Z. (2005). Differentiation of tumours of ductal and lobular origin: I. Proteomics of invasive ductal and lobular breast carcinomas. Biomed. Pap. Med. Fac. Univ. Palacky. Olomouc. Czech. Repub. 149, 57–62.

Udagawa, N., Takahashi, N., Katagiri, T., Tamura, T., Wada, S., Findlay, D.M., Martin, T.J., Hirota, H., Taga, T., Kishimoto, T., et al. (1995). Interleukin (IL)-6 induction of osteoclast differentiation depends on IL-6 receptors expressed on osteoblastic cells but not on osteoclast progenitors. J. Exp. Med. 182, 1461–1468.

Urosevic, J., Garcia-Albéniz, X., Planet, E., Real, S., Céspedes, M.V., Guiu, M., Fernandez, E., Bellmunt, A., Gawrzak, S., Pavlovic, M., et al. (2014). Colon cancer cells colonize the lung from established liver metastases through p38 MAPK signalling and PTHLH. Nat. Cell Biol. 16, 685–694.

Valastyan, S., and Weinberg, R.A. (2011). Tumor metastasis: molecular insights and evolving paradigms. Cell 147, 275–292.

Valiente, M., Obenauf, A.C., Jin, X., Chen, Q., Zhang, X.H.-F., Lee, D.J., Chaft, J.E., Kris, M.G., Huse, J.T., Brogi, E., et al. (2014). Serpins Promote Cancer Cell Survival and Vascular Co-Option in Brain Metastasis. Cell 156, 1002–1016.

Van't Veer, L.J., Dai, H., Van de Vijver, M.J., He, Y.D., Hart, A.A.M., Mao, M., Peterse, H.L., van der Kooy, K., Marton, M.J., Witteveen, A.T., et al. (2002). Gene expression profiling predicts clinical outcome of breast cancer. Nature 415, 530–536.

Varticovski, L., Hollingshead, M.G., Robles, A.I., Wu, X., Cherry, J., Munroe, D.J., Lukes, L., Anver, M.R., Carter, J.P., Borgel, S.D., et al. (2007). Accelerated preclinical testing using transplanted tumors from genetically engineered mouse breast cancer models. Clin. Cancer Res. 13, 2168–2177.

van de Velde, C.J.H., Rea, D., Seynaeve, C., Putter, H., Hasenburg, A., Vannetzel, J.-M., Paridaens, R., Markopoulos, C., Hozumi, Y., Hille, E.T.M., et al. (2011). Adjuvant tamoxifen and exemestane in early breast cancer (TEAM): a randomised phase 3 trial. Lancet (London, England) 377, 321–331.

Verma, S., Miles, D., Gianni, L., Krop, I.E., Welslau, M., Baselga, J., Pegram, M., Oh, D.-Y., Diéras, V., Guardino, E., et al. (2012). Trastuzumab emtansine for HER2-positive advanced breast cancer. N. Engl. J. Med. 367, 1783–1791.

Vernillo, A.T., and Rifkin, B.R. (1998). Effects of tetracyclines on bone metabolism. Adv. Dent. Res. 12, 56–62.

Vicent, G.P., Zaurin, R., Ballaré, C., Nacht, A.S., and Beato, M. (2009a). Erk signaling and chromatin remodeling in MMTV promoter activation by progestins. Nucl. Recept. Signal. 7, e008.

Vicent, G.P., Zaurin, R., Nacht, A.S., Li, A., Font-Mateu, J., Le Dily, F., Vermeulen, M., Mann, M., and Beato, M. (2009b). Two chromatin remodeling activities cooperate during activation of hormone responsive promoters. PLoS Genet. 5, e1000567.

van de Vijver, M.J., He, Y.D., van 't Veer, L.J., Dai, H., Hart, A.A.M., Voskuil, D.W., Schreiber, G.J., Peterse, J.L., Roberts, C., Marton, M.J., et al. (2002). A Gene-Expression Signature as a Predictor of Survival in Breast Cancer. N. Engl. J. Med. 347, 1999–2009.

Vinson, C., Acharya, A., and Taparowsky, E.J. (2006). Deciphering B-ZIP transcription factor

interactions in vitro and in vivo. Biochim. Biophys. Acta 1759, 4–12.

Wagner, K.U., Wall, R.J., St-Onge, L., Gruss, P., Wynshaw-Boris, A., Garrett, L., Li, M., Furth, P. a, and Hennighausen, L. (1997). Cre-mediated gene deletion in the mammary gland. Nucleic Acids Res. 25, 4323–4330.

Wakeling, A. (2000). Similarities and distinctions in the mode of action of different classes of antioestrogens. Endocr. Relat. Cancer 7, 17–28.

Walden, P.D., Ruan, W., Feldman, M., and Kleinberg, D.L. (1998). Evidence That the Mammary Fat Pad Mediates the Action of Growth Hormone in Mammary Gland Development. Endocrinology 139, 659–662.

Wang, H., Yang, H., Shivalila, C.S., Dawlaty, M.M., Cheng, A.W., Zhang, F., and Jaenisch, R. (2013). One-step generation of mice carrying mutations in multiple genes by CRISPR/Cas-mediated genome engineering. Cell 153, 910–918.

Wang, S., Juan, J., Zhang, Z., Du, Y., Xu, Y., Tong, J., Cao, B., Moran, M.F., Zeng, Y., and Mao, X. (2017). Inhibition of the deubiquitinase USP5 leads to c-Maf protein degradation and myeloma cell apoptosis. Cell Death Dis. 8, e3058.

Warburton, M.J., Mitchell, D., Ormerod, E.J., and Rudland, P. (1982). Distribution of myoepithelial cells and basement membrane proteins in the resting, pregnant, lactating, and involuting rat mammary gland. J. Histochem. Cytochem. 30, 667–676.

Wardley, A., Davidson, N., Barrett-Lee, P., Hong, A., Mansi, J., Dodwell, D., Murphy, R., Mason, T., and Cameron, D. (2005). Zoledronic acid significantly improves pain scores and quality of life in breast cancer patients with bone metastases: a randomised, crossover study of community vs hospital bisphosphonate administration. Br. J. Cancer 92, 1869–1876.

Weilbaecher, K.N., Guise, T.A., and McCauley, L.K. (2011). Cancer to bone: a fatal attraction. Nat. Rev. Cancer 11, 411–425.

Welcsh, P.L., Owens, K.N., and King, M.C. (2000). Insights into the functions of BRCA1 and BRCA2. Trends Genet. 16, 69–74.

Wenter, V., Herlemann, A., Fendler, W.P., Ilhan, H., Tirichter, N., Bartenstein, P., Stief, C.G., la Fougère, C., Albert, N.L., Rominger, A., et al. (2017). Radium-223 for primary bone metastases in patients with hormone-sensitive prostate cancer after radical prostatectomy. Oncotarget 8, 44131–44140.

de Wet, J.R., Wood, K. V, DeLuca, M., Helinski, D.R., and Subramani, S. (1987). Firefly luciferase gene: structure and expression in mammalian cells. Mol. Cell. Biol. 7, 725–737.

Williams, S., Wakisaka, A., Zeng, Q.Q., Barnes, J., Seyedin, S., Martin, G., Wechter, W.J., and Liang, C.T. (1998). Effect of minocycline on osteoporosis. Adv. Dent. Res. 12, 71–75.

Winter, M.C., Holen, I., and Coleman, R.E. (2008). Exploring the anti-tumour activity of bisphosphonates in early breast cancer. Cancer Treat. Rev. 34, 453–475.

Wiseman, B.S., and Werb, Z. (2002). Stromal effects on mammary gland development and breast cancer. Science 296, 1046–1049.

Wolff, A.C., Hammond, M.E.H., Schwartz, J.N., Hagerty, K.L., Allred, D.C., Cote, R.J., Dowsett, M., Fitzgibbons, P.L., Hanna, W.M., Langer, A., et al. (2007). American Society of Clinical Oncology/College of American Pathologists guideline recommendations for human epidermal growth factor receptor 2 testing in breast cancer. Arch. Pathol. Lab. Med. 131, 18–43.

Wu, T.T., Sikes, R.A., Cui, Q., Thalmann, G.N., Kao, C., Murphy, C.F., Yang, H., Zhau, H.E., Balian, G., and Chung, L.W. (1998). Establishing human prostate cancer cell xenografts in bone: induction of osteoblastic reaction by prostate-specific antigen-producing tumors in athymic and SCID/bg mice using LNCaP and lineage-derived metastatic sublines. Int. J. Cancer 77, 887–894.

Wyckoff, J.B., Wang, Y., Lin, E.Y., Li, J., Goswami, S., Stanley, E.R., Segall, J.E., Pollard, J.W., and Condeelis, J. (2007). Direct visualization of macrophage-assisted tumor cell intravasation in

mammary tumors. Cancer Res. 67, 2649–2656.

Xu, H. Bin, Liu, Y.J., and Li, L. (2011). Aromatase inhibitor versus tamoxifen in postmenopausal woman with advanced breast cancer: A literature-based meta-analysis. Clin. Breast Cancer 11, 246–251.

Xu, K., Deng, X.-Y., Yue, Y., Guo, Z.-M., Huang, B., Hong, X., Xiao, D., and Chen, X.-G. (2005). Generation of the regulatory protein rtTA transgenic mice. World J. Gastroenterol. 11, 2885–2891.

Xu, Y., Zhang, Z., Li, J., Tong, J., Cao, B., Taylor, P., Tang, X., Wu, D., Moran, M.F., Zeng, Y., et al. (2017). The ubiquitin-conjugating enzyme UBE2O modulates c-Maf stability and induces myeloma cell apoptosis. J. Hematol. Oncol. 10, 132.

Yager, J.D., and Davidson, N.E. (2006). Estrogen carcinogenesis in breast cancer. N. Engl. J. Med. 354, 270–282.

Yamaguchi, T., Chattopadhyay, N., Kifor, O., Butters, R.R., Sugimoto, T., and Brown, E.M. (1998). Mouse osteoblastic cell line (MC3T3-E1) expresses extracellular calcium (Ca2+o)-sensing receptor and its agonists stimulate chemotaxis and proliferation of MC3T3-E1 cells. J. Bone Miner. Res. 13, 1530–1538.

Yang, Y., and Cvekl, A. (2007). Large Maf Transcription Factors: Cousins of AP-1 Proteins and Important Regulators of Cellular Differentiation. Einstein J. Biol. Med. 23, 2–11.

Yang, J.C., Bai, L., Yap, S., Gao, A.C., Kung, H.-J., and Evans, C.P. (2010). Effect of the specific Src family kinase inhibitor saracatinib on osteolytic lesions using the PC-3 bone model. Mol. Cancer Ther. 9, 1629–1637.

Yasuda, H., Shima, N., Nakagawa, N., Mochizuki, S.I., Yano, K., Fujise, N., Sato, Y., Goto, M., Yamaguchi, K., Kuriyama, M., et al. (1998). Identity of osteoclastogenesis inhibitory factor (OCIF) and osteoprotegerin (OPG): a mechanism by which OPG/OCIF inhibits osteoclastogenesis in vitro. Endocrinology 139, 1329–1337.

Yersal, O., and Barutca, S. (2014). Biological subtypes of breast cancer: Prognostic and therapeutic implications. World J. Clin. Oncol. 5, 412–424.

Yin, J., Pollock, C., Tracy, K., Chock, M., Martin, P., Oberst, M., and Kelly, K. (2007). Activation of the RalGEF/Ral pathway promotes prostate cancer metastasis to bone. Mol. Cell. Biol. 27, 7538–7550.

Yin, J.J., Selander, K., Chirgwin, J.M., Dallas, M., Grubbs, B.G., Wieser, R., Massagué, J., Mundy, G.R., and Guise, T. a (1999). TGF-beta signaling blockade inhibits PTHrP secretion by breast cancer cells and bone metastases development. J. Clin. Invest. 103, 197–206.

Yin, J.J., Mohammad, K.S., Käkönen, S.M., Harris, S., Wu-Wong, J.R., Wessale, J.L., Padley, R.J., Garrett, I.R., Chirgwin, J.M., and Guise, T.A. (2003). A causal role for endothelin-1 in the pathogenesis of osteoblastic bone metastases. Proc. Natl. Acad. Sci. U. S. A. 100, 10954–10959.

Yin, W., Jiang, Y., Shen, Z., Shao, Z., and Lu, J. (2011). Trastuzumab in the adjuvant treatment of HER2-positive early breast cancer patients: a meta-analysis of published randomized controlled trials. PLoS One 6, e21030.

Yonou, H., Ochiai, A., Goya, M., Kanomata, N., Hokama, S., Morozumi, M., Sugaya, K., Hatano, T., and Ogawa, Y. (2004). Intraosseous growth of human prostate cancer in implanted adult human bone: relationship of prostate cancer cells to osteoclasts in osteoblastic metastatic lesions. Prostate 58, 406–413.

Yoshimi, K., Kunihiro, Y., Kaneko, T., Nagahora, H., Voigt, B., and Mashimo, T. (2016). ssODN-mediated knock-in with CRISPR-Cas for large genomic regions in zygotes. Nat. Commun. 7, 10431.

Yuan, T., Wang, Y., Pao, L., Anderson, S.M., and Gu, H. (2011). Lactation Defect in a Widely Used MMTV-Cre Transgenic Line of Mice. PLoS One 6, e19233.

Zhan, F., Huang, Y., Colla, S., Stewart, J.P., Hanamura, I., Gupta, S., Epstein, J., Yaccoby, S.,

Sawyer, J., Burington, B., et al. (2006). The molecular classification of multiple myeloma. Blood 108, 2020–2028.

Zhang, Z., Li, K., Zhang, X., Fang, Z., Xiong, W., Chen, Q., Chen, W., and Li, F. (2012). Effect of Id1 knockdown on formation of osteolytic bone lesions by prostate cancer PC3 cells in vivo. J. Huazhong Univ. Sci. Technolog. Med. Sci. 32, 364–369.

Zhao, C., Irie, N., Takada, Y., Shimoda, K., Miyamoto, T., Nishiwaki, T., Suda, T., and Matsuo, K. (2006). Bidirectional ephrinB2-EphB4 signaling controls bone homeostasis. Cell Metab. 4, 111–121.

Zhou, X., Vink, M., Klaver, B., Berkhout, B., and Das, A.T. (2006). Optimization of the Tet-On system for regulated gene expression through viral evolution. Gene Ther. 13, 1382–1390.

Zhu, Z., Ma, B., Homer, R.J., Zheng, T., and Elias, J. a. (2001). Use of the tetracycline-controlled transcriptional silencer (tTS) to eliminate transgene leak in inducible overexpression transgenic mice. J. Biol. Chem. 276, 25222–25229.

Zhu, Z., Zheng, T., Lee, C.G., Homer, R.J., and Elias, J.A. (2002). Tetracycline-controlled transcriptional regulation systems: advances and application in transgenic animal modeling. Semin. Cell Dev. Biol. 13, 121–128.

Zuris, J.A., Thompson, D.B., Shu, Y., Guilinger, J.P., Bessen, J.L., Hu, J.H., Maeder, M.L., Joung, J.K., Chen, Z.-Y., and Liu, D.R. (2015). Cationic lipid-mediated delivery of proteins enables efficient protein-based genome editing in vitro and in vivo. Nat. Biotechnol. 33, 73–80.